UNIVERSIDAD AUTÓNOMA DE MADRID

DOCTORAL THESIS

Applications and Developments of Density Functional Theory to Complex Systems

Author: *Diego* SOLER POLO

Supervisor: *José* ORTEGA MATEO

Facultad de Ciencias

Departamento de Física Teórica de la Materia Condensada

Programa de Doctorado en Física de la Materia Condensada, Nanociencia y Biofísica

Resumen de la Tesis Doctoral

Título: Applications and Developments of Density Functional Theory to Complex Systems
Doctorando: Diego Soler Polo
Director: José Ortega Mateo

Resumen:

La presente tesis doctoral trata diversos desarrollos y aplicaciones en el ámbito de la Teoría del Funcional de la Densidad (DFT, por sus siglas en ingles). Antes de detallar los contenidos, conviene mencionar que en ella se tratan diversos temas que, a nivel superficial, pueden parecer poco relacionados entre sí. Si bien esto refleja de cierto modo la propia naturaleza de la labor científica, donde se tratan aquellos problemas que van surgiendo de modo orgánico en el curso de la investigación, resulta interesante destacar dos aspectos unificadores que están presentes en todos los contenidos de este trabajo:

1)En primer lugar, toda la tesis trata del estudio atomístico de sistemas complejos donde muchas partículas están interaccionando entre ellas. En este tipo de problemas es siempre necesario desarrollar métodos y aproximaciones que nos permitan superar las limitaciones de los recursos computacionales.

2)En segundo lugar, como ya ha sido comentado, y a un nivel más concreto y metodológico, toda la tesis tiene que ver -de un modo u otro- con la DFT.

La presente memoria de tesis, si bien absolutamente teórica, tiene un carácter dual: una parte concierne a aplicaciones de la DFT a simulaciones de sistemas concretos, y otra se ocupa del desarrollo e implementación de modelos o procedimientos que pueden ser luego aplicados en nuevos cálculos concretos.

En cuanto a los contenidos, la tesis está organizada como sigue:

El primer capítulo es una breve introducción teórica a la DFT y otras herramientas relevantes para las simulaciones moleculares, como son el integrador de Verlet o el termostato de Langevin. Además, se presenta en detalle una formulación poco común y alternativa de la DFT, la llamada OO-DFT (*Orbital Occupancy* DFT), que tiene interés en un capítulo posterior del trabajo. Hasta donde sabemos, se presenta aquí por primera vez los teoremas fundacionales de la DFT en el formalismo OO-DFT. Se describen además, en una sección aparte, los rudimentos del software Fireball, con el que se ha trabajado de modo continuo, tanto para su desarrollo como en la práctica de aplicaciones a simulaciones de sistemas concretos (que se tratan en capítulos posteriores).

El segundo capítulo describe varias adiciones incorporadas a Fireball con todos los detalles teóricos pertinentes descritos. En particular, se describen ahí la inclusión de términos dipolares de largo alcance en un cálculo DFT de orbitales localizados, se discuten dos métodos nuevos de proyección de cargas y se detalla un nuevo esquema para introducir los funcionales de canje y correlación en los cálculos. Como ejemplo de las aplicaciones de estos desarrollos teóricos, se muestra aquí con detalle cómo uno de los nuevos métodos de proyección de carga desarrollado, junto al nuevo esquema mencionado para el canje-correlación, es capaz de proveer un método de cálculo preciso para las fuerzas en una simulación de DFT basado en la versión auto-consistente del

funcional de Harris-Foulkes (lo cual resulta una aplicación crucial en el contexto del software Fireball).

El tercer capítulo retoma el tema de las simulaciones moleculares y trata en profundidad diversos métodos de cálculo de la energía libre que han sido empleados y comparados en varios problemas de interés. Se discute aquí la hipótesis ergódica, el *umbrela sampling*, el método WHAM o el método Jarzynski, basado en una identidad para promedios sobre trayectorias fuera del equilibrio termodinámico (un ejemplo de los teoremas de fluctuación de entropía). Se describe asimismo un método novedoso para el cálculo de perfiles de energía libre que mezcla la integración termodinámica con el *umbrella sampling* y se da un resumen de algunas de las aplicaciones realizadas con todos estos métodos: el estudio de las fluctuaciones dinámicas en una superficie, el impacto de una mutación en una proteína, y la transferencia de protones en el ADN (tratado en detalle en el capítulo 4 y una de las contribuciones centrales de la tesis).

El cuarto capítulo está consagrado a una descripción detallada de ciertas transferencias de protones en ADN en pares de base de guanina y citosina. Este problema resulta ser de gran interés debido al hecho de que las transferencias espontáneas de protones dan lugar a formas tautoméricas anómalas que, a su vez, pueden ser responsables de mutaciones de substitución en el código genético. A pesar de que este problema ha recibido una gran atención, la cuestión no ha sido del todo dilucidada. Las limitaciones de las técnicas de femto-láseres *in vivo* hacen que los estudios teóricos sobre este sistema aún resulten de gran interes, pero, debido a las altas exigencias computacionales del problema, resulta muy difícil llegar a conclusiones fuertes. En efecto, se trata de un sistema dinámico a temperatura ambiente (con las correspondientes fluctuaciones estadísticas) y con miles de átomos, por lo que, por lo común, los estudios previos consisten en cálculos estáticos o investigaciones de sistemas pequeños que sirvan de modelo. En nuestro trabajo, el empleo de un método QM/MM reciente basado en Fireball nos permite tratar el problema teniendo en cuenta por primera vez la naturaleza dinámica de un ambiente biomolecular que incluye explícitamente miles de átomos. El resultado más interesante de este trabajo es el hallazgo de cómo el ambiente molecular desestabiliza de forma crucial el tautómero anómalo (que resultaría mutagénico y que sí posee una vida media no despreciable *in vacuo*), protegiendo así la estabilidad del código genético.

El quinto capítulo está dedicado al estudio de un modelo para sistemas de electrones fuertemente correlacionados, como los que se encuentran en los orbitales *d* de los metales de transición. El modelo parte de una versión del conocido como hamiltoniano de Kanamori conectado a cadenas de niveles sin términos de muchos cuerpos (que pretenden modelar cadenas metálicas) y, por medio de un método de construcción de las matrices y su diagonalización exacta, se calculan las energías y potenciales de correlación. Después, los resultados se emplean para definir un potencial DFT+U, que queda, además, completamente formalizado en el contexto de la OO-DFT y que, en este caso, incluye también la interacción de intercambio y puede usarse para entender la relación entre la regla de Hund y la aparición de soluciones magnéticas. A continuación, presentamos brevemente un esquema de interpolación para calcular la Densidad de Estados de muchos cuerpos de un hamiltoniano de este tipo más allá del régimen perturbativo.

El sexto capítulo es una breve descripción de una aplicación de la DFT, a través de Fireball, para diseñar modelos *tight-Binding* fiables en el que sólo un mínimo de parámetros han de ser ajustados para reproducir ciertas propiedades experimentales (en este caso, la aparición de estados de borde como consecuencia del alto *hopping* de unos puentes de hidrógeno a temperaturas extremadamente bajas, T ~ 5K). Este trabajo, parte de una colaboración realizada durante la estancia doctoral, donde

se estudian cadenas de quinonas enlazadas por puentes de hidrógeno y depositadas sobre oro, muestra la importancia de los efectos cuánticos nucleares en los átomos de hidrógeno a muy bajas temperaturas, y fusiona dos elementos, a saber, la modelización y parametrización con un cálculo DFT, y la explicación modelística de los estados de borde y la estabilidad mecánica de una cadena de moléculas de la que no puede dar cuenta el DFT por sí mismo (debido a la importancia de la naturaleza cuántica de los núcleos atómicos a temperaturas tan bajas).

"Illud in his rebus non est mirabile, quare, omnia cum rerum primordia sint in motu, summa tamen summa uideatur stare quiete [...] Omnis enim longe nostris ab sensibus infra primorum natura iacet; quapropter, ubi ipsa cernere iam nequeas, motus quoque surpere debent." [1]

Lucretius, *De Rerum Natura*, Liber Secundus, 310

[1] "On this regard, it is no surprise that, while all atoms are in motion, the universe seems to be still [...] For the atoms lie beyond our senses, and so, since you cannot perceive them, their motion elude you"

Contents

A Cristina Usaola Sánchez y Macario Polo Hervás

Acknowledgments

Al dar por concluida mi tesis doctoral y recapitular sobre todo lo que ha supuesto, enseguida me di cuenta de que tengo la inmensa suerte -o la difícil tarea- de tener una plétora de personas a las que agradecer todo tipo de cosas.

En primer lugar, y sobre todo, quiero agradecer a mi director José Ortega Mateo la oportunidad ofrecida y todo el proyecto compartido a lo largo de estos cuatro años. Con él, que aúna calidad científica y humana, he podido aprender y trabajar en temas apasionantes, descubriendo en el camino lo que es la investigación de primera línea, y siempre en un ambiente amable. Le agradezco profundamente, pues, no sólo por lo conveniente de estudiar y trabajar con él, por el científico que es, sino también por lo disfrutable de hacerlo, por la persona que es.

Estoy también muy especialmente agradecido a Fernando Flores, por su guía, sus ideas, su inteligencia rápida, su reservorio intimidante de conocimientos y su facilidad para motivarme. Su paciencia para aguantar mis preguntas me ha resultado extremadamente útil, como también lo han sido las ya docenas de conversaciones enriquecedoras con él y con José. Espero -creo que así será- que en el futuro haya muchas más.

Por otra parte, quiero agradecer a Jesús I. Mendieta-Moreno, Daniel G. Trabada y César González su apoyo y compañerismo en todo este tiempo, particularmente cuando estaba empezando a adentrarme en un mundo nuevo y, sin su ayuda, habría estado vagando entre scripts con la desesperación de quien se pierde por entre los anaqueles de la Biblioteca de Babel. Los tres han sido mentores y compañeros que han hecho disfrutables y amistosos unos retos que, de otro modo, habrían sido dificultades solitarias.

Gracias también a Jesús Mendieta, de la Universidad Francisco de Vitoria, por numerosas valiosas conversaciones y por facilitarme mis discretas inmersiones en el gigantesco mundo de la bioquímica con paciencia y pasión. Agradezco también a él y a Guy Novoa la colaboración sobre un proyecto inacabado con la papaína que, basándome en sus cálculos y simulaciones, he usado para un ejemplo interesante al final del capítulo 3.

En cuanto a otra gente del Departamento (Física Teórica de la Materia Condensada), quiero agradecer todo lo compartido a Javier Cuerda y a Eduardo Zubizarreta -primero compañeros del despacho 513, luego buenos amigos- y a Mónica Sánchez Barquillo. Gracias por los intereses compartidos y por todo lo que me han enseñado -pero no les pido perdón por las innumerables veces que no les he dejado trabajar en paz.

Fuera del Departamento, agradezco también sus bioenseñanzas, útiles conversaciones acerca de la energía libre o temas relacionados, y ayuda con los scripts en

mis comienzos con la tesis a Íñigo Marcos Alcalde, del Centro de Biología Molecular Severo Ochoa.

Por otra parte, y en relación a mi estancia doctoral en el Instituto de Física de la Academia Checa de Ciencias, en Praga, quiero agradecer fuertemente a Pavel Jelínek no sólo la oportunidad de trabajar y crecer en un magnífico entorno científico, sino, además, la diligencia con la que me ayudó cuando, debido a los efectos de la pandemia, acabé pasando en Praga casi dos meses más del tiempo previsto.

Fuera de este círculo de personas estrechamente vinculadas al desarrollo de mi tesis, debo uno de mis más afectuosos agradecimientos a Cristóbal Meroño Moreno y a Nikita Simonov, que acaso me disculpan por no ser matemático. No podría imaginar una amistad más profunda o más polifacética, y juntos hemos hablado o discutido de absolutamente todo lo que nos apasiona o nos preocupa en la vida -y en particular, en lo concerniente a esta tesis, la física, desde los electrones hasta la entropía, ha ocupado no pocas de nuestras horas comunes- Gracias por hacer de las matemáticas, de la física y de todo lo demás algo de lo que me apetece seguir siendo parte.

A David Rus, tantas conversaciones, tantos paseos y, en relación a la tesis, gracias por su agilísima ayuda diseñando y ejecutando una figura especialmente artística en el capítulo 1, tomando como base un boceto mío ajeno a la noción de perspectiva.

Gracias también a Andrea Navas Olivé, por tantas conversaciones e intercambios fascinantes y, en relación a la tesis, gracias en especial por el diseño y elaboración de la fantástica portada artístico-científica que la cubre.

A mi Grupo Poco Común, Bea, Carles, Miquel, Sergio, sólo me cabe agradecerle desde el amor su contribución a que mi cabeza no haya acabado en un cesto lleno de escorpiones, el haberme rescatado tantas veces y el compartir conmigo todo un mundo que, por increíble que resulte, parece existir fuera de la universidad y de la física.

Gracias a Hana, děkuji, že jsi mi ukázala, že *Prag lässt nicht los*, por lo compartido y por todo lo que hay por compartir.

A mi familia le agradezco el apoyo, el amor y la diversión compartida. Un agradecimiento especial para mi madre, que me ha ayudado de modo crucial con la edición y maquetación de las figuras en las tesis, ha realizado varios dibujos, y sin cuyas habilidades con el GIMP me habría desesperado (más). Gracias a mi padre por su apoyo, sus influencias, todas las pasiones y conversaciones compartidas y por escuchar mis emocionadas charlas sobre el tema, parece que con verdadero interés. A mis hermanas, Cristina y María, a y a mi maravillosa familia en su conjunto, a Merche y Paula por los años de convivencia, solapados de forma casi exacta con los años de la tesis, y a Maco y a Dani, entre otras cosas, por las conversaciones sobre combinatoria y programación que me ayudaron cuando estaba empezando a trabajar con mis hamiltonianos, así como por muchísimas otras cosas y a muchas otras personas (no cabría todo en la extensión de una tesis).

Introduction

This Doctoral Thesis deals with a number of topics which, on the surface, appear to bear little relation to one another. Although this partly reflects the organic nature of scientific research, where problems are addressed in a natural way as they arise, I feel the urge to point out that two fundamentals concepts connect all the contents of the present work:

1) First of all, the atomistic study of complex systems where many particles are interacting with each other and the limitations of finite computational resources must be overcome by appropriate approximations

2) More concretely, regarding the methodology, the so-called Density Functional Theory (DFT) pervades all the research efforts undertaken during the realization of the doctoral work.

The thesis, although absolutely theoretical, has a dual nature: one part concerns applications of DFT and other methods for computer simulations; while the other part is dedicated to the development and implementation of new models and methodologies, always with the goal in mind of applying them further to new contexts.

As for the contents, the thesis has been organized as follows: The first chapter is a brief theoretical introduction to DFT and some relevant tools for molecular simulations. Besides, in this introductory chapter we discuss an alternative and unusual formulation of DFT, the so-called OO-DFT, of further interest in the thesis, and the basic ideas behind the software Fireball, which has been used extensively in our research.

The second chapter deals with several improvements or new features that have been implemented in the software Fireball. More details about Fireball can be found there and all the details concerning the theory of the new features added are explicitly shown. In particular, we discuss the inclusion of correct long-range interaction terms in the Hartree part of the hamiltonian, the investigation around new methods for projecting the charges in a DFT simulation, and a new scheme to calculate the exchange-correlation energy which has special relevance for the Fireball code.

The third chapter comes back to the topic of molecular simulations to discuss Free Energy (FE) methods, which are essential when studying processes whose timescales are larger than those accessible by ordinary simulations. In this chapter we analyze a selection of FE methods which have been tested, compared, programmed and employed successfully in several problems of interest. We also show a novel FE method which can be potentially of interest for some and, lastly, summarize some of the applications that we have found for these methods.

The fourth chapter discusses in-depth our study of proton transfer reactions in DNA. This is a problem of the greatest interest since spontaneous proton transfer

reactions yield anomalous tautomeric forms which might be potentially responsible for substitution mutations in the genetic code. Furthermore, although extensive work has been done on this problem, the topic has not as yet been completely solved. Due to the complex biomolecular environment with thousands of atoms, dynamical simulations are very demanding and the studies usually concern static calculations or simulations of (relatively) small systems. In our study, we applied a novel QM/MM method based on Fireball and different Free Energy techniques to study the problem taking into account the dynamic nature of the environment.

The fifth chapter deals with a many-body model for highly correlated systems of electrons. For this problem, a Hubbard-Kanamori hamiltonian including the exchange interaction, an atom is connected to metallic chains and we calculate the exact exchange-correlation energy and potential. This is used to define a LDA+U type of approach. DFT+U is an important method to correct the limitations of DFT calculations for highly correlated electrons, such as the d electrons in transition metal, and in the context of OO-DFT we can formalize it and use it to see how the Hund's rule may explain the appearance of magnetic solutions.

The sixth chapter explores another application of DFT calculations: the construction of a reliable Tight-Binding model in which only the very few parameters not estimated with DFT are tuned to reproduce certain experimental features (in this case, related to hydrogen bonds where the protons, due to extremely low temperatures, present a deep tunneling regime accounting for edge states).

Resumen en Español

La presente tesis doctoral trata diversos temas que, a nivel superficial, pueden parecer poco relacionados entre sí. Si bien esto refleja de cierto modo la propia naturaleza de la labor científica, donde se tratan aquellos problemas que van surgiendo de modo orgánico en el curso de la investigación, resulta interesante destacar dos aspectos unificadores que están presentes en todos los contenidos de este trabajo:

1) En primer lugar, conviene destacar que toda la tesis trata del estudio atomístico de sistemas complejos donde muchas partículas están interaccionando entre ellas. En este tipo de problemas es siempre necesario desarrollar métodos y aproximaciones que nos permitan superar las limitaciones de los recursos computacionales.

2) En segundo lugar, y a un nivel más concreto y metodológico, toda la tesis tiene que ver -de un modo u otro- con la así llamada Teoría del Funcional de la Densidad (DFT por sus siglas en inglés).

La presente memoria de tesis, si bien absolutamente teórica, tiene un carácter dual: una parte concierne a aplicaciones de la DFT a simulaciones de sistemas concretos, y otra se ocupa del desarrollo e implementación de modelos o procedimientos que pueden ser luego aplicados en nuevos cálculos concretos.

En cuanto a los contenidos, la tesis está organizada como sigue:

El primer capítulo es una breve introducción teórica a la DFT y otras herramientas relevantes para las simulaciones moleculares, como son el integrador de Verlet o el termostato de Langevin. Además, se introduce una formulación poco común y alternativa de la DFT, la llamada OO-DFT, que tiene interés en un capítulo posterior del trabajo. Se describen además los rudimentos del software Fireball, con el que se ha trabajado de modo continuo.

El segundo capítulo describe varias adiciones incorporadas a Fireball con todos los detalles teóricos pertinentes descritos. En particular, se describen ahí la inclusión de términos dipolares de largo alcance en un cálculo DFT de orbitales localizados, se discuten dos métodos nuevos de proyección de cargas y se detalla un nuevo esquema para introducir los funcionales de canje y correlación en los cálculos.

El tercer capítulo retoma el tema de las simulaciones moleculares y trata en profundidad diversos métodos de cálculo de la energía libre que han sido empleados y comparados en varios problemas de interés. Se describe asimismo un método novedoso para el cálculo de perfiles de energía libre y se da un resumen de algunas de las aplicaciones.

El cuarto capítulo está consagrado a una descripción detallada de ciertas transferencias de protones en ADN. Este problema resulta ser de gran interés debido al hecho de que las transferencias espontáneas de protones dan lugar a formas tautoméricas anómalas que, a su vez, pueden ser responsables de mutaciones de substitución en el código genético. A pesar de que este problema ha recibido una gran atención, la cuestión no ha sido del todo dilucidada, debido a las altas exigencias computacionales del problema. En efecto, se trata de un sistema dinámico a temperatura ambiente (con las correspondientes fluctuaciones estadísticas) y con miles de átomos, por lo que, por lo común, los estudios previos consisten en cálculos estáticos o investigaciones de sistemas pequeños que sirvan de modelo. En nuestro trabajo, el empleo de un método QM/MM reciente basado en Fireball nos permite tratar el problema teniendo en cuenta la naturaleza dinámica de un ambiente biomolecular que incluye explícitamente miles de átomos.

El quinto capítulo está dedicado al estudio de un modelo para sistemas de electrones fuertemente correlacionados, como los que se encuentran en los orbitales *d* de los metales de transición. El modelo parte de una versión del conocido como hamiltoniano de Kanamori conectado a cadenas metálicas y, por medio de un método de construcción de las matrices y su diagonalización exacta, se calculan las energías y potenciales de correlación. Después, los resultados se emplean para definir un potencial LDA+U, que queda formalizado en el contexto de la OO-DFT y que, en este caso, incluye también la interacción de intercambio y puede usarse para entender la relación entre la regla de Hund y la aparición de soluciones magnéticas.

El sexto capítulo es una breve descripción de una aplicación de la DFT, a través de Fireball, para diseñar modelos *Tight-Binding* fiables en el que sólo un mínimo de parámetros han de ser ajustados para reproducir ciertas propiedades experimentales (en este caso, la aparición de estados de borde como consecuencia del alto *hopping* de unos puentes de hidrógeno a temperaturas extremadamente bajas, $T \approx 5$).

Chapter 1

Density Functional Theory

Why, there's a chap on Saturn -he looks something like a mushroom on stilts- who solves partial differential equations mentally; and even he's given up.

The Devil and Simon Flagg, Arthur Porges

1.1 Why DFT?

In 1929, amidst the justified triumphalism of the early founders of Quantum Mechanics, the British physicist (and future Nobel laureate) Paul Dirac warned [1] that the fundamental laws of physics, albeit known, were far too complex to be employed in any practical calculation for complex systems. The emergence of Density Functional Theory in the mid 60's, [2, 3], addressed directly these shortcomings and became extremely popular among chemists and physicists of different areas. DFT was not, however, the first such attempt. In the 20's, the Thomas-Fermi theory [4, 5], attempted to solve the Schrödinger equation for complex systems by expressing all the physical observables explicitly in terms of the density, and thus is a fundamental historical precedent of modern DFT. However, several limitations of this approach were found. In particular, this theory could not describe molecular bonding [6], since the sum of the energies of the components is always less than the energy of the compound, a pitfall which could not be overcome by further work on the subject [7].

Another famous approach to treat complex interacting systems is Hartree-Fock theory [8–10], based on approximating the wave-function by a Slater determinant (which amounts to a one-electron approximation in which the interactions are accounted for in the form of a single-particle non-local potential). The Hartree-Fock method can be systematically improved to account for electronic correlation with the use of perturbative methods [11, 12], the Interaction of Configurations, the Coupled Cluster approach [13] . These methods, which make explicit use of the molecular Wave-function, yield highly accurate results but have a huge computational cost. DFT is frequently the choice (and many times the only option available) for the balance it offers between accuracy and efficiency.

In this Chapter we start by discussing the approximations allowing us to treat the electrons and the nuclei in separated calculations. The nuclei are much bigger, energetic and slow than the electrons, so it is intuitive that their dynamics can be decoupled to some degree from that of the electrons. The adiabatic theorem and the Born-Oppenheimer separation formalize and quantify this fact. Next, we begin our study of Density Functional Theory, prove the Hohenberg-Kohn theorems,

the Kohn-Sham equations, and make some comments about the functionals. In the next section we summarize two basic techniques of Molecular Dynamics Simulations which have been used extensively. Then we give an introduction to the Fireball software, a local-orbital molecular dynamics DFT code also used extensively in our work. We finish by looking briefly at an alternative formulation of DFT which is also relevant in our work.

1.2 Born-Oppenheimer

Before entering the realm of DFT, we discuss first the adiabatic theorem (due to Max Born and Vladimir Fock in 1928) and the Born-Oppenheimer separation. The former essentially states that *if a given system is in an eigenstate, the system remains at the corresponding instantaneous eigenstate at any moment if a perturbation is introduced, provided that the hamiltonian varies slowly enough.*

This result will allow us to understand in simple terms the foundations of a key strategy in quantum simulations: For every position of the nuclei, the electronic ground state is calculated. From such calculation, the forces experienced by the nuclei are obtained. The nuclei are then moved for a very brief time step δt, and the electronic calculation is recalculated assuming that the system, in the new geometry, is still on the ground state.

We will give a sketch of proof, without entering the details of the exact asymptotics, in the particular case where the hamiltonian depends explicitly and directly on time. Suppose we have a Hamiltonian $\hat{\mathcal{H}}$ with a basis of eigenstates and eigenenergies $\{\psi^n, E^n\}$. Now we consider a time-dependent hamiltonian $\hat{\mathcal{H}}(t)$, with instantaneous eigenstates and eigenenergies $\{\psi^n(t), E^n(t)\}$. We suppose that $\hat{\mathcal{H}}(0) = \hat{\mathcal{H}}$. We will make the Ansatz $\Psi(t) = \sum_n c_n(t)\psi^n(t)\exp(i\theta_n(t))$ for the Schrodinger equation $\hat{\mathcal{H}}(t)\Psi = i\hbar\frac{\partial\Psi}{\partial t}$. We can thus compute:

$$\hat{\mathcal{H}}(t)\Psi = \sum_n c_n(t)E^n(t)\Psi^n(t)\exp(i\theta_n(t)) = i\hbar\frac{\partial\Psi}{\partial t} =$$
$$i\hbar\sum_n \dot{c}_n(t)\psi^n(t)\exp(i\theta_n(t)) + i\hbar\sum_n c_n(t)\dot{\psi}^n(t)\exp(i\theta_n(t))$$
$$-\hbar\sum_n c_n(t)\psi^n(t)\dot{\theta}_n(t)\exp(i\theta_n(t)),$$

so, by setting $\theta_n(t) = -\hbar^{-1}\int_0^t E^n(\tau)d\tau$, we have:

$$\sum_n c_n(t)\dot{\psi}^n(t)\exp(i\theta_n(t)) =$$
$$-\sum_n \dot{c}_n\psi^n(t)\exp(i\theta_n(t)).$$

By taking spatial inner product with $\psi^m(t)$ we further derive:

$$-\sum_n c_n(t)\langle\psi^m(t)|\dot{\psi}^n(t)\rangle\exp(i\theta_n(t) - i\theta_m(t)) = \dot{c}_m(t). \tag{1.1}$$

Next we derive with respect to time the instantaneous eigenstate equation $\hat{\mathcal{H}}(t)\psi^n(t) = E^n(t)\psi^n(t)$, thus getting:

$$\dot{\hat{\mathcal{H}}}(t)\psi^n(t) + \hat{\mathcal{H}}(t)\dot{\psi}^n(t) = \dot{E}^n(t)\psi^n(t) + E^n(t)\dot{\psi}^n(t).$$

By taking again products with $\psi^m(t)$ we have:

$$\langle\psi^m(t)|\dot{\hat{\mathcal{H}}}(t)|\psi^n(t)\rangle + \langle\psi^m(t)|\hat{\mathcal{H}}(t)|\dot{\psi}^n(t)\rangle = E^n(t)\langle\psi^m(t)|\dot{\psi}^n(t)\rangle + \dot{E}^n(t)\langle\psi^m(t)|\psi^n(t)\rangle.$$

From this and noticing that $\langle\psi^m(t)|\hat{\mathcal{H}}(t)|\dot{\psi}^n(t)\rangle = E^m(t)\langle\psi^m(t)|\dot{\psi}^n(t)\rangle$ and $\langle\psi^m(t)|\psi^n(t)\rangle = \delta_{nm}$, we finally get:

$$\dot{c}_m(t) = -c_m(t)\langle\psi^m(t)|\dot{\psi}^m(t)\rangle + \sum_{n\neq m} c_m(t)\frac{-\langle\psi^m(t)|\dot{\hat{\mathcal{H}}}(t)|\psi^n(t)\rangle}{E^n(t) - E^m(t)}\exp\left(i\theta_n(t) - i\theta_m(t)\right). \tag{1.2}$$

Therefore, if we assume very slowly varying hamiltonians, we have $\dot{\hat{\mathcal{H}}}(t) \approx 0$ and we then have $c_m(t) = c_m(0)\exp\left(i\gamma_m(t)\right)$, where $\gamma_m(t) = i\int_0^t \langle\psi^m(\tau)|\dot{\psi}^m(\tau)\rangle d\tau$.

Note that γ is a real number, which is key to the whole argument.

We conclude that Ψ is given by:

$$\Psi = \sum_n c_n(0)\exp\left(i(\theta_n(t) + \gamma_n(t)\right)\psi^n(t).$$

So we can clearly see that for slowly varying hamiltonian the time evolution consists in adding phases to each of the eigenstates, which in particular proves the adiabatic theorem stated at the beginning of the section.

Now we are ready to study the so-called Born-Oppenheimer approximation, also widely known as the adiabatic approximation. It is the starting point for most electronic structure computations. The idea of the Born-Oppenheimer approximation is that, due to the fact that the nuclei are much heavier than the electrons, we can try to "factorize" the wave function into a nuclear and a electronic part. This is conceptually identical to the Adiabatic Theorem, since, for a fixed configuration of nuclei, we can write a specific electronic hamiltonian and try to solve that problem. If the nuclei move, our electronic hamiltonian varies as well, but since the protons and neutrons are much slower that the electron, we can assume that this is a slowly time-varying electronic hamiltonian, and therefore use the previous theorem to conclude that if we are in a electronic configuration which is an electronic eigenstate, we will remain in the same eigenstate when the nuclei move a little bit. From the previous discussion (see the complete differential equation, eq. 1.2, for $c_m(t)$), it is clear that this kind of reasoning breaks down when there are two energies which are very close. In the case of the Born-Oppenheimer approximation, this means that if for a certain nuclei configuration there is an excited electronic eigenstate close in energy to the Ground state , then the approximation won't be very good, and more sophisticated ideas, involving transitions between electronic levels, are needed.

Let us consider a molecule, and let us denote in this section, to simplify the notation, by r the electronic degrees of freedom and by R the nuclear degrees of freedom. r is actually a collection of vectors $\mathbf{r}_1, \cdots, \mathbf{r}_M$, with M the number of electrons, and

R is a collection of vectors, $\mathbf{R}_1, \cdots, \mathbf{R}_N$, with N the number of atoms. Consider a molecular eigenwavefunction $\Psi(r;R)$. This must satisfy the stationary Schrodinger equation:

$$\left(\hat{T}_{el} + \hat{T}_{nuc} + \hat{V}_{ee} + \hat{V}_{eN} + \hat{V}_{NN}\right)\Psi(r;R) = E\Psi(r;R),$$

where:

$$\begin{aligned}
\hat{T}_{el} &= \frac{-\hbar^2}{2m}\sum_j \Delta_{r_j}, \\
\hat{T}_{nuc} &= \sum_\alpha \frac{-\hbar^2}{2M_\alpha}\Delta_{R_\alpha}, \\
\hat{V}_{ee} &= \frac{e^2}{8\pi\epsilon_0}\sum_{j\neq k}\frac{1}{|r_j - r_k|}, \\
\hat{V}_{eN} &= \frac{-e^2}{4\pi\epsilon_0}\sum_{j,\alpha}\frac{Z_\alpha}{|r_j - R_\alpha|}, \\
\hat{V}_{NN} &= \frac{e^2}{8\pi\epsilon_0}\sum_{\alpha\neq\beta}\frac{Z_\alpha Z_\beta}{|R_\alpha - R_\beta|}.
\end{aligned} \tag{1.3}$$

The Born-Oppenheimer approximation starts by assuming that we can find particular solutions to this equation of the form $\Psi(r,R) = \phi(R)\psi(r;R)$, and proceeds afterwards by taking the solution to be a combination:

$$\Psi(r,R) = \sum_n \phi^n(R)\psi^n(r,R).$$

For a fixed configuration of nuclei, define the "clamped" electronic hamiltonian $\hat{\mathcal{H}}_{el} := \hat{\mathcal{H}} - \hat{T}_{nuc}$, and suppose we can solve the stationary Schrödinger equation for it (this is what is achieved approximately by means of electronic structure methods such as Hartree-Fock or DFT, that we shall study in future sections). Let us call the eigenstates and eigenenergies of H_{el} $\psi^n(r;R)$ and $\epsilon^n(R)$ respectively, where R, the position of the nuclei, is here treated as a parameter. We assume orthonormalization of the states. With this knowledge, we will try to solve the complete equation by making the above-mentioned Ansatz.We have:

$$\begin{aligned}
&\left(\hat{T}_{nuc} + \hat{\mathcal{H}}_{el}\right)\sum_n \phi^n(R)\psi^n(r;R) = E\sum_n \phi^n(R)\psi^n(r;R); \\
&\sum_n \hat{T}_{nuc}\phi^n(R)\psi^n(r,R) + \sum_n \epsilon^n(R)\phi^n(R)\psi^n(r;R) = E\sum_n \phi^n(R)\psi^n(r;R).
\end{aligned}$$

By the product rule for the derivatives:

$$\begin{aligned}
&\Delta_{R_\alpha}\left(\phi^n(R)\psi^n(r;R)\right) = \psi^n(r;R)\Delta_{R_\alpha}\phi^n(R) + \phi^n(R)\Delta_{R_\alpha}\psi^n(r;R) + \\
&2\nabla_{R_\alpha}\psi^n(r,R)\cdot\nabla_{R_\alpha}\phi^n(R).
\end{aligned}$$

we are going to multiply by $\psi^m(r,R)^*$ the Schrodinger equation and integrate over electronic coordinates.

Note now that, due to the normalization of the electronic eigenstates, it holds that $\langle\psi^n|\nabla_{R_\alpha}|\psi^n\rangle = 0$, where the $\langle\rangle$ denote scalar product with respect to the electronic degrees of freedom.

Also, let us introduce the notation

$$\Delta^m(R) := \langle \psi^m | \hat{T}_{nuc} | \psi^m \rangle$$
$$\hat{C}_{nm}(R) = \langle \psi^m | \hat{T}_{nuc} | \psi^n \rangle + \sum_\alpha \frac{\hbar^2}{M_\alpha} \langle \psi^m | \nabla_{R_\alpha} | \psi^n \rangle \nabla_{R_\alpha}.$$

Then a straight-forward computation, using the identity

$$\langle \psi^m | \nabla_{R_\alpha} | \psi^n \rangle = \frac{1}{\epsilon^m - \epsilon^n} \sum_j \langle \psi^m | \frac{r_j - R_\alpha}{|r_j - R_\alpha|^3} | \psi^m \rangle,$$

which is easily proved by computing the commutator $[\hat{\mathcal{H}}_{el}, \nabla_{R_\alpha}]$ [1] yields:

$$\begin{cases} \left(\hat{T}_{nuc} + \Delta^m(R) + \epsilon^m(R) - E\right) \phi^m(R) = \sum_{n \neq m} \hat{C}_{nm}(R) \phi^n(R), \\ \hat{\mathcal{H}}_{el} \phi^n(r, R) = \epsilon^m(R) \phi^n(r, R). \end{cases} \tag{1.4}$$

The adiabatic Born-Oppenheimer approximation consists in neglecting all those coupling terms $\Delta^m(R)$ and $\hat{C}_{nm}\phi^m(R)$.

As seen above, this separation allows us to focus on the Hamiltonian for the electrons and treat the nuclei separately. Furthermore, in most practical applications the nuclei are treated at the classical level, since their characteristic action is typically much bigger that $\hbar$ (the nuclei have relatively large energies, compared to the electrons, and larger time scales associated to their movements). Three extensions, however, are worth mentioning. On the one hand, approaches to include quantum corrections to the dynamics of the nuclei have also been developed [14–16], mostly based on the Path Integral formulation [17]. These effects, though usually negligible, become relevant, and sometimes even crucial, in hydrogen atoms at very low temperatures [18]. Also, it is worth mentioning that in recent years a Multi-component DFT has been proposed, which allows to treat systems of different species of fermions [19, 20]. On the other hand, methods to go beyond the Born-Oppenheimer have also been developed. In molecular simulations, this is relevant when the eigenstates are very close in energy and electronic transitions may take place. To treat this problem, several methods have been developed, like Ehrenfest's method [21] and Tully's fewest switches algorithm [22]. The second one has been implemented in the code Fireball [23], has been used to explore, for example, photo-damage in thymine dimers in DNA [24], and we have used it to investigate the dynamics of proton transfer in DNA in an excited state (see chapter 4).

1.3 Hohenberg-Kohn Theorem

After making the Born-Oppenheimer separation, we are still left with a difficult problem; namely, solving the many-body electronic hamiltonian. This hamiltonian is of the form

$$\hat{H} = \hat{T} + \hat{V}_{ee} + \hat{v}, \tag{1.5}$$

[1] This identity is very useful and essentially tells us the same thing the differential equation for the coefficients c's told us: If two energetic levels are very similar for some set of R, the approximation breaks down because these so-called vibronic and coupling terms cannot be neglected.

where $\hat{V}_{ee}$ is the electron-electron (Coulomb) interaction operator and $\hat{v} = \sum_{j=1}^{N} \hat{v}^j$, with N the number of electrons in the system, is the external one-particle potential. Each $\hat{v}^j$ is a one-particle potential which in the position representation is just the multiplication operator $v(\mathbf{r_j})$, and the $\mathbf{r}_j$ is the position vector of the $j-$th electron. $\sum_j \hat{v}^j$ in principle will be the potential generated by the nuclei, but, in the context of the foundations of DFT, is very general. Notice that the last term, the external potential, can also be written in terms of the density operator $\hat{n}(\mathbf{r})$, which in the position representation has the form $\sum_{j=1}^{N} \delta(\mathbf{r} - \mathbf{r}_j)$, as

$$\sum_j \hat{v}^j = \int\!\!\!\int v(\mathbf{r})\hat{n}(\mathbf{r})d\mathbf{r}.$$

The foundational theorem of DFT, the first Hohenberg-Kohn theorem, guarantees that the ground state electronic density determines the external potential $v(\mathbf{r})$ (and, thus, shockingly, every property of the system, including also the excited states), and has a remarkably simple proof which was published in the year 1964 in the seminal work by Hohenberg and Kohn [2]. We recall here that the electronic density associated to a wave-function $|\Psi\rangle$ is:

$$n(\mathbf{r}) = \langle\Psi|\hat{n}(\mathbf{r})|\Psi\rangle = N \int\!\!\!\int |\Psi(\mathbf{r}, \mathbf{r}_2, \cdots, \mathbf{r}_N)|^2 d\mathbf{r}_2 \cdots d\mathbf{r}_N, \tag{1.6}$$

Theorem 1. ***First Hohenberg-Kohn Theorem*** *The ground state electronic density, $n(\mathbf{r})$, of a system of interacting electrons determines the external potential $v(\mathbf{r})$ up to a constant*

Proof. We will proceed by *reductio ad absurdum*. Assume we have two different potentials, $v_1(\mathbf{r})$ and $v_2(\mathbf{r})$, giving rise to the same ground state density, $n(\mathbf{r})$. We call their associated Hamiltonians $\hat{H}_1 = \hat{T} + \hat{V}_{ee} + \hat{v}_1$ and $\hat{H}_2 = \hat{T} + \hat{V}_{ee} + \hat{v}_2$, with each $\hat{v}_i$ represented as before as a sum of one-particle operators; $\hat{v}_i = \sum_j \hat{v}_i^j$, with each $\hat{v}_i^j$ defined in the position representation as the multiplication operator by $v_i(\mathbf{r}_j)$. Call their respective Ground state wavefunctions $|\Psi_1\rangle$ and $|\Psi_2\rangle$ and the respective ground state energies E_1 and E_2. First, let us notice that $|\Psi_1\rangle$ and $|\Psi_2\rangle$ cannot be equal, for, if that was the case, then we would have $(\hat{v}_1 - \hat{v}_2)\Psi\rangle = (E_1 - E_2)|\Psi\rangle$, which in the position representation yields

$$\sum_{j=1}^{N} v_1(\mathbf{r}_j) - v_2(\mathbf{r}_j) = E_1 - E_2$$

for all $\mathbf{r}_1, \cdots, \mathbf{r}_N$ at which $\Psi(\mathbf{r}_1, \cdots, \mathbf{r}_N) \neq 0$. Keeping $N-1$ constant and letting $\mathbf{r}_j$ vary (we can do this for every j) would lead to the fact that the potentials differ by only a constant (since $E_1 - E_2$ is, of course, a constant).

Now the variational principle allows us to write:

$$\begin{aligned} E_1 =& \langle\Psi_1|\hat{H}_1|\Psi_1\rangle < \langle\Psi_2|\hat{H}_1|\Psi_2\rangle = \\ & \langle\Psi_2|\hat{H}_2|\Psi_2\rangle + \langle\Psi_2|\hat{H}_1 - \hat{H}_2|\Psi_2\rangle = \\ & E_2 + \int\!\!\!\int n(\mathbf{r})\left(v_1(\mathbf{r}) - v_2(\mathbf{r})\right)d\mathbf{r}. \end{aligned}$$

However, starting with E_2 and applying the same reasoning, we reach exactly the same result with the indices 1 and 2 reverted:

$$E_2 < E_1 + \int\!\!\!\int n(\mathbf{r})\left(v_2(\mathbf{r}) - v_1(\mathbf{r})\right)d\mathbf{r}.$$

Adding both relations, we get the contradiction $E_1 + E_2 < E_2 + E_1$, which proves the theorem. □

It is worth mentioning, however, that the above proof assumes non-degeneracy of the working Hamiltonian. An easy extension for the degenerate case can be found, for example, in [25] and [26]. The correspondence of n with $|\Psi\rangle$ must be substituted by a correspondence of n with every possible Ground State. If $\{|\Psi_{0,j}\rangle\}$ denote the (orthogonalized) set of Ground states, any combination $|\Psi_{\{a_j\}}\rangle = \sum_j a_j|\Psi_{0,j}\rangle$ is a Ground state with associated density $n_{\{a_j\}}(\mathbf{r}) = \sum_j |a_j|^2\langle\Psi_{0,j}|\hat{n}(\mathbf{r})|\Psi_{0,j}\rangle$. What we first do, in this case, is to establish a one to one correspondence of the set of potentials, v, up to an additive constant, and the set of $\{n_{\{a_j\}}\}$ (that is, we need all the possible $\{n_{\{a_j\}}\}$ in order to determine the external potential v). The proof above then applies in the same way: If two potentials v_1 and v_2 differ by more than a constant, then a fundamental state of $\hat{H}_1$ cannot be fundamental state of $\hat{H}_2$, for in that case we would equally get $\sum_j v_1(\mathbf{r}_j) - v_2(\mathbf{r}_j) = E_1 - E_2$. Even though the Ground state of $\hat{H}_1$ is degenerate, none of the Ground states of $\hat{H}_2$ can be Ground state of $\hat{H}_1$, and thus we can apply the same argument to reach the contradiction $E_1 + E_2 < E_2 + E_1$. Therefore, even in the degenerate case a density $n(\mathbf{r})$ can only emerge from one potential $v(\mathbf{r})$. Notice that, in this case, there is not a correspondence between n and $|\Psi\rangle$ (such a notion does not make sense in the degenerate case). However, this is irrelevant, since the only important conclusion of the theorem is the possibility to define the energy as a functional of the electron density, $E[n]$.

The correspondence $n \to v$ suggests that we should be able to define an energy functional in terms of the density; i.e, that given any density, n, we can calculate the energy $E[n]$ of a system described by a hamiltonian 1.5.

The next key result, which in part follows easily from the theorem above, is the fact the the Ground State energy and density can be calculated by minimizing the energy functional, $E[n]$, which indeed attains its minimum at the ground state density. The subtle point, of course, is the domain of the functional $E[n]$, which must be conveniently extended, as we show after the next proof.

With the definitions given in eq. 1.3, let us now define:

$$\hat{H}_v = \hat{T}_{el} + \hat{V}_{ee} + \int v(\mathbf{r})\hat{n}(\mathbf{r})d\mathbf{r},$$

with $\hat{n}(\mathbf{r})$ equal to $\sum_{j=1}^{N}\delta(\mathbf{r} - \mathbf{r}_j)$ in the position representation, with N the number of electrons in the systems and the $\mathbf{r}_j$ the position vector of each one. We can then formulate the:

Theorem 2. ***Second Hohenberg-Kohn Theorem*** *For every external potential, v, it is possible to define an energy functional depending on the density such that its minimum equals the Ground State energy of the system and is attained by the ground state density, n_v, linked to v in virtue of Theorem 1.*

Proof. Given an external potential v, call n_v to the density of the Ground State of the hamiltonian $\hat{H}_v$. We know, from the first Hohenberg-Kohn theorem, that T_{el} and V_{ee} are determined by the density, so the Ground State energy E_v can be written as $E_v = T_{el}[n_v] + V_{ee}[n_v] + \int v(\mathbf{r})n_v(\mathbf{r})d\mathbf{r}$. Skipping for a moment the subtlety of the domain of the functional, this should allow us to define, for each v, a functional:

$$E_v[n] := \underbrace{T_{el}[n] + V_{ee}[n]}_{F[n]} + \int v(\mathbf{r})n(\mathbf{r})d\mathbf{r}, \tag{1.7}$$

where we have implicitly defined a new functional, $F[n]$, as $F[n] = E_v[n] - \int v(\mathbf{r})n(\mathbf{r})d\mathbf{r}$, or, equivalently, we can define it explicitly -and, more importantly, in a form appropriate for its extension- as in 1.8 below, that is, as $F[n] = \min_{|\Psi\rangle\to n}\langle\Psi|\hat{T}_{el} + \hat{V}_{ee}|\Psi\rangle$. However, at this point, this functional only makes sense on the set of ground states densities arising from solving the Schrödinger equation for hamiltonians of the form in eq. 1.5, the so called $v-$representable densities. It is obvious from the definition that $E_v[n_v] = E_v$ and, reasoning in the same spirit as in the Hohenberg-Kohn theorem above, which is nothing but to invoke the variational theorem, we see that for any $n_{v'} \neq n_v$ it holds that $E_v(n_v) < E_v[n_{v'}]$. The comments below about the Levy-Lieb formalism, which allow to extend the functional to a wider domain, show that this inequality holds for generic n, without restricting ourselves to the narrow space of $v-$representable densities, which in turn proves the theorem □

The functional defined in the proof is, in principle, only defined for densities which arise as the densities of Ground States of hamiltonians $\hat{H}_v$. These are called $v-$representable densities. These densities do not form an appropriate functional space (many reasonable functions cannot be obtained as a ground state density) [2], and in such a setting it does not even make sense to take functional derivatives. We must, therefore, extend this functional to a larger and complete vector space, where it makes sense to find its minimum.

In order to do this, let us briefly look at another formulation of DFT, due independently to Levy and Lieb [5, 27, 28]: The Constrained Search approach , in which we define the functional

$$F_{LL}(n) = \min_{|\Psi\rangle\to n}\langle\Psi|\hat{T}_{el} + \hat{V}_{ee}|\Psi\rangle, \tag{1.8}$$

where, as before, $\hat{V}$ is the many-body interaction and the $|\Psi\rangle \to n$ means that the minimum is searched in the set of all antisymmetric wave-functions yielding the density n,

$$n(\mathbf{r}) = N\int|\Psi(\mathbf{r},\mathbf{r}_2,\cdots,\mathbf{r}_N)|^2 d\mathbf{r}_2\cdots d\mathbf{r}_N, \tag{1.9}$$

where N is the total number of electrons in the system.

This allows us to define an extended functional

$$E[n] = F_{LL}[n] + \int v(\mathbf{r})n(\mathbf{r})d\mathbf{r}, \tag{1.10}$$

where the definition of $F_{LL}[n]$ involves, as seen above, looking for a minimizer Ψ_n in an appropriate functional space. The functional in 1.10 admits now functions n which are not restricted to Ground State densities, which is an important step towards our goal: defining the energy functional in a space big enough so that taking functional derivatives makes sense.

Notice next that the Ground state energy can be written in terms of this density functional as

$$\begin{aligned} E = &\min_{|\Psi\rangle}\langle\Psi|\hat{T}_{el} + \hat{V}_{ee} + \hat{v}||\Psi\rangle = \min_{n}\min_{|\Psi\rangle\to n}\langle\Psi|\hat{T}_{el} + \hat{V}_{ee} + \hat{v}||\Psi\rangle = \\ &\min_{n}\{F_{LL}[n] + \int v(\mathbf{r})n(\mathbf{r})d\mathbf{r}\}. \end{aligned} \tag{1.11}$$

[2] For example, without the need to go into detailed computations, it is clear that in a problem with spherical symmetry, the Ground State does not have nodes, so any function that vanishes at some points will be not $v-$representable in such a case

It is crucial to understand that, due to the variational principle for the Schrödinger equation, the extension of the energy functional, 1.10, has the same minimizer, n_v, than the original functional defined for $v-$representable densities. The final step to appropriately extend the domain of these functional is to show that, actually, any "reasonable" density is $\Psi-$representable; i.e, can be obtained from a Ψ by the relation 1.9. Actually, it is interesting to note that it is enough to search Ψ in the subset of Slater determinants. The result is actually quite intuitive and it is possible to give an explicit construction. Given a density $n(\mathbf{r})$, let us construct a Slater determinant $|\Phi\rangle = \text{Alt}\left(\bigotimes_{j=1}^{N} |\phi_j\rangle\right)$ yielding n through relation 1.9, which in the case of Slater determinants reduces to

$$n(\mathbf{r}) = \sum_{j=1}^{N} |\phi_j(\mathbf{r})|^2. \tag{1.12}$$

Intuitively, we need the wave-function to behave as $\approx \sqrt{\frac{n(\mathbf{r})}{N}}$. The relation 1.12 will be satisfied if we define (let us ignore spin here for simplicity, which is irrelevant) the ϕ_j to be of the form:

$$\phi_j(\mathbf{r}) = \sqrt{\frac{n(\mathbf{r})}{N}} e^{iG_j(\mathbf{r})},$$

but, also, the ϕ_j have to be orthogonal and be part of a complete basis set. To achieve this, change the integer index j by a 3-tuple $\mathbf{k} \in \mathbb{Z}^3$ and define (we can always find an isomorphism between the indices j and the $\mathbf{k}$):

$$\phi_{\mathbf{k}}(\mathbf{r}) = \sqrt{\frac{n(\mathbf{r})}{N}} e^{i\mathbf{k}\cdot\mathbf{f}(\mathbf{r})}.$$

It is easy to see that

$$\int \phi^*_{\mathbf{k}}(\mathbf{r})\phi_{\mathbf{k}'}(\mathbf{r})d\mathbf{r}' = \frac{1}{N}\int n(\mathbf{r}) e^{i(\mathbf{k}-\mathbf{k}')\cdot\mathbf{f}(\mathbf{r})} d\mathbf{r},$$

so that, in order for the orbitals to be orthonormal, we would like to find a vector-function $\mathbf{f}(\mathbf{r})$ such that

$$\int n(\mathbf{r})d\mathbf{r} = \frac{N}{(2\pi)^3}\int_{[0,2\pi]^3} d\mathbf{f},$$

which would immediately imply orthonormality. It can be shown by a straight computation (see, for example, [25]) that this can attained by defining:

$$\begin{aligned}
f_1(\mathbf{r}) =& 2\pi \frac{\int_{-\infty}^{x} n(x',y,z)dx'}{\int_{-\infty}^{\infty} n(x',y,z)dx'},\\
f_2(\mathbf{r}) =& 2\pi \frac{\int_{-\infty}^{y}\int_{-\infty}^{\infty} n(x',y',z)dx'dy'}{\int_{-\infty}^{\infty}\int_{-\infty}^{\infty} n(x',y',z),dx'dy'},\\
f_3(\mathbf{r}) =& 2\pi \frac{\int_{-\infty}^{z}\int_{-\infty}^{\infty}\int_{-\infty}^{\infty} n(x',y',z')dx'dy'}{\int_{-\infty}^{\infty}\int_{-\infty}^{\infty}\int_{-\infty}^{\infty} n(x',y',z),dx'dy'dz'},
\end{aligned}$$

Similarly, using these definitions, it can be shown that, including all $\mathbf{k} \in \mathbb{Z}^3$, this set is complete, i.e, $\sum_{\mathbf{k}\in\mathbb{Z}^3} |\phi_{\mathbf{k}}\rangle\langle\phi_{\mathbf{k}}| = 1$. Next, take any set of different $\mathbf{k}_1, \cdots, \mathbf{k}_N$ and define

$$\Phi(\mathbf{r}_1, \cdots, \mathbf{r}_N) = \frac{1}{\sqrt{N}} \det\left(\phi_{\mathbf{k}_j}(\mathbf{r}_i)\right)_{ij},$$

which clearly yields the density $n(\mathbf{r})$. Notice that is possible to construct infinitely many wave-functions yielding this density, since an arbitrary phase (not dependent on $\mathbf{k}$) can be added to the spin-orbitals.

As shown by Gilbert [29], the only requirement for this procedure to be possible on the formal level is that the density, other than being positive and integrate the number of electrons, N, fulfills the integrability condition

$$\int\!\!\!\int |\nabla n^{1/2}(\mathbf{r})|^2 d\mathbf{r} < \infty.$$

This condition, which may look abstract at first sight, is actually very natural: The wave-function, $|\Psi\rangle$, which is a solution of the Schrödinger equation, must have a well-defined kinetic energy, $\langle\Psi|\hat{T}|\Psi\rangle$. Roughly speaking, the kinetic energy gives terms such as (let us now write just one spatial index to lighten the notation; the idea is the same in the general case):

$$\langle\hat{T}\rangle \approx \int\!\!\!\int \Psi(\mathbf{r})\Delta\Psi(\mathbf{r})d\mathbf{r}.$$

By integrating by parts, assumming a good decaying of Ψ, this equals

$$\langle\hat{T}\rangle \approx \int\!\!\!\int \nabla\Psi(\mathbf{r})\cdot\nabla\Psi(\mathbf{r})d\mathbf{r},$$

so that the key assumption for the solution to have sense in a formal sense is that the wave-function has a integrable gradient. This is a well-known instance of the so-called weak formulation of Partial Differential Equations, see for example [30]. Since the density is extracted, roughly speaking, from integrating the square of the wave-function, posing the condition $\int\!\!\!\int |\nabla n^{1/2}(\mathbf{r})|^2 d\mathbf{r} < \infty$ becomes natural. A mathematically rigorous account of how this technical conditions grants the existence of minimizers and functional derivatives can be found in [26].

All of this would be helpless were it not for the existence of informed guesses for the functional $F[n]$. A first attempt to create a Hohenberg-Kohn functional is based in the Thomas-Fermi theory, mentioned before, which actually predates DFT as a theory and thus has a big historical significance. In this approximation, the kinetic energy is proportional to the integral of a power of the density. Specifically, in the most basic Thomas-Fermi scheme, we make the guess:

$$F^{TF}[n] = C_{TF}\int\!\!\!\int n^{5/3}(\mathbf{r})d^3\mathbf{r} + \frac{1}{2}\int\!\!\!\int \frac{n(\mathbf{r}')n(\mathbf{r})}{|\mathbf{r}-\mathbf{r}'|}d^3\mathbf{r}d^3\mathbf{r}', \tag{1.13}$$

where the first term is the kinectic energy obtained for the electron gass (which suggests, by extrapolation, precisely that very simple density functional for the kinetic energy), with C_{TF} a constant, and the second term is just the Hartree part of the electron-electron coloumbian interaction, to which exchange-correlation corrections could of course be added. This is actually capable of reproducing several interesting features, but suffers from crucial shortcomings, as mentioned in the introduction.

The failure of the Thomas-Fermi model was a consequence of its poor treatment of kinetic energy. Density Functional Theory took over this approximation when it managed to overcome this weakness by means of the so-called Kohn-Sham equations.

1.4 Kohn-Sham equations

1.4.1 Summary of the method

Merely a year after the publication of the Hohenberg-Kohn theorems, a second work appeared, by Kohn and Sham [3], in which the authors define a scheme which goes beyond Thomas-Fermi, not writing explicitly the kinetic energy in terms of the density, but as the kinetic energy of a set of non-interacting electrons whose density reproduces that of the real interacting system. While in Hartree-Fock also the electrostatic potential and energy are written in terms of the orbitals of a system of non-interacting electrons [8, 10], in DFT these are (formally) written solely in terms of the density, and only the kinetic energy makes explicit use of one-particle orbitals. In the Kohn-Sham approach we construct spin-orbitals $|\phi_j\rangle$ such that the associated density, $\sum f_j|\phi(\mathbf{r})|^2$, with f_j the occupation numbers, coincides with that of the interacting system. For that, an effective potential, $v_{\text{eff}}(\mathbf{r})$, is needed to solve the following one-electron problem:

$$\left(-\frac{\hbar^2}{2m}\Delta + v_{\text{eff}}(\mathbf{r})\right)\phi_i(\mathbf{r}) = \varepsilon_i\phi_i(\mathbf{r}). \tag{1.14}$$

This effective potential is split as $v_{\text{eff}}(\mathbf{r}) = v_{\text{ext}}(\mathbf{r}) + v_H(\mathbf{r}) + v_{xc}(\mathbf{r})$, where $v_{\text{ext}}(\mathbf{r})$ is the external potential, $v_H(\mathbf{r})$ is the Hartree potential, $v_H(\mathbf{r}) = \int \frac{n(\mathbf{r}')}{|\mathbf{r}-\mathbf{r}'|}d\mathbf{r}'$ and $v_{xc}(\mathbf{r})$ is the so-called exchange-correlation potential, which we will discuss in detail later on. This potential $v_{\text{eff}}(\mathbf{r})$ is written on terms of the density, so that we will write, with a slight abuse of notation, $v_{\text{eff}}(n)$, and, since we are looking for the condition $n(\mathbf{r}) = \sum f_j|\phi(\mathbf{r})|^2$, this yields a set of self-consistent equations that must be solved by iterative procedure. Once the solution for the one-electron problem has been reached, the energy of the interacting system can calculated. The sum of occupied eigenvalues, $\sum_{j\in\text{occupied}} \varepsilon_j$ includes the kinetic energy of the non-interacting system, T_s, but also the energy due to the Hartree potential, $\int v_H(n)n(\mathbf{r})d\mathbf{r}$, and due to the exchange-correlation potential, $\int v_{xc}(n)n(\mathbf{r})d\mathbf{r}$. To get the total energy, we must therefore substract these two terms from the sum of occupied eigenvalues and add the correct Hartree energy, $\frac{1}{2}\int\int n(\mathbf{r})n(\mathbf{r}')d\mathbf{r}d\mathbf{r}' = \frac{1}{2}\int v_H(n)n(\mathbf{r})d\mathbf{r}$ and the correct exchange-correlation energy, $E_{xc}[n]$, thus getting:

$$E[n] = \sum_{j\in\text{occupied}} \varepsilon_j - \frac{1}{2}\int v_{\text{H}}[n]n(\mathbf{r})\,\mathrm{d}r - \int v_{\text{xc}}[n]n(\mathbf{r})\,\mathrm{d}r + E_{\text{xc}}[n]. \tag{1.15}$$

To derive the Kohn-Sham equations 1.14 with the prescribed form for the effective potential, two possibilities can be considered, and both are common in the literature. One possible approach is to take the functional derivatives of the energy functional with respect to the orbitals $\phi_j(\mathbf{r})$. The other possibility, perhaps more clearly in contact with the spirit of the Hohenberg-Kohn theorems, is to take derivatives with respect to the density. Here, we explore both approaches, which ultimately, of course, yield the same result.

1.4.2 Taking derivatives $\frac{\delta}{\delta\phi_j^*(\mathbf{r})}$

Here, to ease the notation, we omit the spin index, which is irrelevant in the reasoning. To include the spin, the vector $\mathbf{r}$ can be substituted by the duple $(\mathbf{r},\sigma)$ and the integral symbol $\int d\mathbf{r}$ interpreted as $\sum_\sigma \int d\mathbf{r}$.

We will start this discussion considering the Hohenberg-Kohn functional in the very particular case that there is no interaction potential $\hat{V}_{ee}$. Of course, in this case the functional $F[n]$ can be identified with the kinetic energy of the non-interacting fermions in the ground state. We thus write:

$$T(n) := E^0(v(n)) - \int v(n)n(\mathbf{r})\, d^3\mathbf{r},$$

and, again, we know this is well-defined because the Hohenberg-Kohn theorem guarantees that for a given n there is a unique v, and thus a unique T.
In the non-interacting system, modelled by the free hamiltonian $\hat{\mathcal{H}}^0$, necessarily the ground state is a Slater determinant.
Because of this, we take the natural domain of T to be densities arising from a ground state given in the form of a Slater determinant. If such a Slater determinant is $\Psi = (N!)^{-1/2}\det\left(\phi_j(\mathbf{r}_k)\right)_{jk}$, with the spin-orbitals orthonormalized, then the electronic density is just $n(\mathbf{r}) = \sum_j |\phi_j(\mathbf{r})|^2$.

The kinetic energy is thus:

$$T \quad n = \sum_j |\phi_j|^2 \Big) = \frac{-\hbar^2}{2m}\sum_k \langle\phi_k|\Delta|\phi_k\rangle,$$

The energy in the non-interacting case is then written as:

$$E^0(v) = \min_n \left\{ T(n) + \int v(\mathbf{r})n(\mathbf{r})\, d\mathbf{r} \right\}$$

where, again, the set of candidates are the n's corresponding to ground states and this is further rewritten as:

$$E^0(v) = \min_{\phi_j} \left\{ \sum_k \frac{-\hbar^2}{2m}\langle\phi_k|\Delta|\phi_k\rangle + \langle\phi_k|v|\phi_k\rangle \;:\; \langle\phi_j|\phi_l\rangle = \delta_{jl} \right\}$$

We now return to the case with interactions, $\hat{V}_{ee} \neq 0$. In that case, we write the Hohenberg-Kohn functional as $F_{HK}(n) = T_s(n) + E_H(n) + E_{XC}(n)$, where E_H is the Hartree energy and E_{XC} is the exchange and correlation functional. It can thus be written:

$$E(v) = \min_{\phi_j}\{\sum_k \frac{-\hbar^2}{2m}\langle\phi_k|\Delta|\phi_k\rangle + \langle\phi_k|v|\phi_k\rangle + E_H(n) + E_{XC}(n) :\; \langle\phi_j|\phi_l\rangle = \delta_{jl}\}$$

Next we need some calculus to compute the variation of the previous expression. A key fact that we will be using is that to find the minimum of an expression such as that of above it is enough to take variations with respect to the complex conjugates $\phi_j^*(\mathbf{r})$. Also, since we are trying to put emphasis in the electronic density, n, instead of on the multi-electronic wave function, we would like to express those variations in

terms of variations with respect to the density. To achieve that, note that from $n(\mathbf{r}) = \sum_j \phi_j^*(\mathbf{r})\phi_j(\mathbf{r})$ we have $\frac{\delta n(\mathbf{r})}{\delta \phi_j^*(\mathbf{r}')} = \delta(\mathbf{r}-\mathbf{r}')\phi_j(\mathbf{r})$ and thus, since for any functional J we can write:

$$\frac{\delta J}{\delta \phi_j^*(\mathbf{r})} = \int\left(\frac{\delta J}{\delta n(\mathbf{r}')}\frac{\delta n(\mathbf{r}')}{\delta \phi_j^*(\mathbf{r})}d\mathbf{r}',\right.$$

we can finally write the important relationship:

$$\frac{\delta J}{\delta \phi_j^*(\mathbf{r})} = \frac{\delta J}{\delta n(\mathbf{r})}\phi_j(\mathbf{r}).$$

Also, recall now all the facts:

$$T(n=\sum \phi_j\phi_j^*) = \frac{-\hbar^2}{2m}\sum\langle\phi_j|\Delta|\phi_j\rangle \ : \ \text{for } (N!)^{-1/2}\det(\phi_j(\mathbf{r}_k))_{j,k} \text{ a ground state}$$

which allows us to write:

$$\frac{\delta T}{\delta \phi_j^*(\mathbf{r})} = \int\left(\frac{\delta T}{\delta n(\mathbf{r}')}\frac{\delta n(\mathbf{r}')}{\delta \phi_j^*(\mathbf{r})}d\mathbf{r}' = \frac{\delta T}{\delta n(\mathbf{r})}\phi_j(\mathbf{r}).\right.$$

We now can proceed to take variations, introducing in principle Lagrange multipliers λ_{jk} for the constraints $\langle\phi_j|\phi_k\rangle = \delta_{jk}$. Nevertheless, since the operator arising from the Euler-Lagrange equation for the critical point is hermitian, then the orthogonality is automatically guaranteed, and we only have to deal with the normalization constraints with Lagrange multipliers $\lambda_{jj} = -\epsilon_j$ for the constraints $\langle\phi_j|\phi_j\rangle = 1$. Minimizing the energy $E[n]$ with respect to the orbitals thus yield:

$$\left.\frac{-\hbar^2}{2m}\Delta + v_{\text{ext}}(\mathbf{r}) + \frac{\delta E_H[n]}{\delta n(\mathbf{r})} + \frac{\delta E_{XC}[n]}{\delta n(\mathbf{r})}\right)\left(\phi_j(\mathbf{r}) = \epsilon_j\phi_j(\mathbf{r}),\right.$$

Therefore, by comparing with the effective problem, the resulting Kohn-Sham equations are:

$$\left.\frac{-\hbar^2}{2m}\Delta + v_{\text{eff}}(\mathbf{r})\right)\left(\phi_j(\mathbf{r}) = \epsilon_j\phi_j(\mathbf{r}),\right.$$

where the effective potential is precisely the potential defined above: v_{eff} is $v_{\text{ext}} + v_H + v_{XC}$ with $v_H = \frac{\delta E_H}{\delta n}$ and $v_{XC} = \frac{\delta E_{XC}}{\delta n}$.

We can be a little bit more specif, writing the analytical form of the things we already know. The energy of the system is:

$$E(n) = \sum\langle\phi_j|\hat{t}_j|\phi_j\rangle - \frac{e^2}{4\pi\epsilon_0}\sum_\alpha\int\left(\frac{Z_\alpha}{|\mathbf{r}_\alpha-\mathbf{r}|}n(\mathbf{r})d\mathbf{r}+\right.$$
$$\left.\frac{e^2}{8\pi\epsilon_0}\int\left(\frac{n(\mathbf{r})n(\mathbf{r}')}{|\mathbf{r}-\mathbf{r}'|}d\mathbf{r}d\mathbf{r}' + E_{XC}(n)\right.\right.$$
$$\text{for } \hat{t}_j = \frac{-\hbar^2}{2m_e}\Delta_{r_j} \text{ and } n(r) = \sum_j|\phi_j|^2.$$

(Note that here we have gotten rid of the spin variables for ease of notation). And by applying the variation we have the Kohn-Sham equations:

$$\frac{-\hbar^2}{2m_e}\Delta - \frac{e^2}{4\pi\epsilon_0}\sum_j \frac{Z_j}{|\mathbf{r}-\mathbf{R}_j|} + \frac{e^2}{4\pi\epsilon_0}\int\left(\frac{n(\mathbf{r}')}{|\mathbf{r}-\mathbf{r}'|}d\mathbf{r}' + V_{XC}(n)\right)\phi_j(\mathbf{r}) = \epsilon_j\phi_j(\mathbf{r}). \quad (1.16)$$

1.4.3 Taking derivatives $\frac{\delta}{\delta n(\mathbf{r})}$

We aim to find a non-interacting system whose density reproduces that of the interacting system. That, we want to find a one-electron problem (eq. 1.14)

$$-\frac{\hbar^2}{2m}\Delta + v_{\text{eff}}(\mathbf{r})\Big)\phi_i(\mathbf{r}) = \varepsilon_i\phi_i(\mathbf{r}),$$

with a $v_{\text{eff}}(\mathbf{r})$ such that the ground state density, n, of the interacting system coincides with the density, n_s of the non-interacting system,

$$n(\mathbf{r}) = n_s(\mathbf{r}) = \sum_j f_j|\phi_j(\mathbf{r})|^2.$$

The exact energy functional of the interacting system can be splitted as:

$$E[n] = T_s[n] + E_H[n] + E_{ext}[n] + E_{xc}[n], \quad (1.17)$$

where $T_s[n]$ is the kinetic energy of the non-interacting system with density $n(\mathbf{r})$. Notice that, in terms of the orbitals,

$$T_s[n] = -\frac{\hbar^2}{2m}\sum_j f_j\int\phi_j^*(\mathbf{r})\Delta\phi_j(\mathbf{r})d\mathbf{r}. \quad (1.18)$$

Since we wish to minimize the energy with respect to n to find the Ground state, We want to take variations of the density, δn, preserving always the same number of electrons, $\int n(\mathbf{r})d\mathbf{r} = N$, so that $\int\delta n(\mathbf{r})d\mathbf{r} = 0$. Notice that, using the effective equations 1.14, the term 1.18 equals

$$T_s = \frac{\hbar^2}{2m}\sum_j f_j\int\phi_j(\mathbf{r})\Delta\phi_j(\mathbf{r})d\mathbf{r} = \sum_j f_j\int\phi_j^*(\mathbf{r})(\varepsilon_j - v_{\text{eff}}(\mathbf{r}))\phi_j(\mathbf{r})d\mathbf{r} =$$
$$\sum_j f_j\varepsilon_j - \int\left(n(\mathbf{r})v_{\text{eff}}(\mathbf{r})d\mathbf{r}.\right.$$

Therefore, $\frac{\delta T_s[n]}{\delta n}$ can be casted as

$$\frac{\delta T_s[n]}{\delta n(\mathbf{r})} = -v_{\text{eff}}(\mathbf{r}).$$

On the other hand, turning to the interacting system and minimizing its energy, it is immediate to see that $\frac{\delta E_{ext}[n]}{\delta n(\mathbf{r})} = v_{\text{ext}}(\mathbf{r})$ and $\frac{\delta E_H[n]}{\delta n(\mathbf{r})} = v_{\text{H}}(\mathbf{r})$, where $v_H(\mathbf{r}) = \int\left(\frac{n(\mathbf{r}')}{|\mathbf{r}-\mathbf{r}'|}d\mathbf{r}'\right.$ and $E_H[n] = \frac{1}{2}\int\left(\frac{n(\mathbf{r})n(\mathbf{r}')}{|\mathbf{r}-\mathbf{r}'|}d\mathbf{r}d\mathbf{r}'\right.$. Next we define in the obvious way

$v_{xc}(\mathbf{r}) := \frac{\delta E_{xc}[n]}{\delta n(\mathbf{r})}$. If we evaluate $\frac{\delta E[n]}{\delta n(\mathbf{r})}$ at the Ground state density, we have, since that is a minimum of the functional,

$$\frac{\delta E[n]}{\delta n(\mathbf{r})} = -v_{\text{eff}}(\mathbf{r}) + v_{ext}(\mathbf{r}) + \frac{E_H[n(\mathbf{r})]}{\delta n} + \frac{E_{xc}[n(\mathbf{r})]}{\delta n} = 0.$$

We thus finally get for the effective potential:

$$v_{\text{eff}}(\mathbf{r}) = v_H(\mathbf{r}) + v_{ext}(\mathbf{r}) + v_{xc}(\mathbf{r}) \tag{1.19}$$

1.5 Exchange-correlation Functionals

The most problematic terms in the splitting of the energy functional, $E[n]$, is of course the exchange and correlation functional E_{XC}, whose precise analytical form cannot be known. There are a lot of ways around this. In the Hartree-Fock approximation (see appendix A) the wave-function is approximated as a Slater determinant, Φ. For Slater determinants, the integral defining the electrostatic operator can be calculated exactly in terms of the participating orbitals, and the result is the classical electrostatic energy (referred to as the Hartree part) plus a new term called the exchange-energy.

$$E_{ee} = \langle \Phi | \hat{V}_{ee} | \Phi \rangle \approx E_{\text{hartree}} + E_x.$$

This new terms arises from the antisymmetry the non-interacting wavefunction Φ, and as such can be regarded as a modification of the the electrostatic energy due to Pauli's exclusion principle. Whatever remains is called the correlation energy, $E_{\text{corr}} = E - E_{\text{HF}}$.

For the correlation energy, LDA (Local Density Approximation) is the most basic approximation, and already very useful [31].
It is based on analyzing the Homogeneous Electron Gas, an unbounded system in which the electronic density is assumed to be constant and compensated by a background of positive charges. In this model, it is possible to estimate the energy density (*i.e*, energy per unit of volume), $\epsilon = \epsilon_{LDA}(n)$ and thus the exchange-correlation energy density, $\epsilon_{xc,LDA}(n)$. In the LDA approximation, we estimate the XC energy as

$$E_{xc,LDA}[n] := \iint\!\!\!\!\!\!\left(n(\mathbf{r}) \epsilon_{xc,LDA}(n(\mathbf{r})) d\mathbf{r}. \right. \tag{1.20}$$

The exchange in the HEG can be calculated by plugging solutions to to the free electron problem, wave planes $\phi_{\mathbf{k}}(\mathbf{r}) \approx e^{\mathbf{k}\cdot\mathbf{r}}$, into the expression for the exact exchange as seen in the second term in Hartree-Fock theory, see eq. 1.25 below, which after some computations leads to

$$\epsilon_{x,LDA}(n) = -\frac{-e^2(3\pi^2)^{4/3}}{4\pi^3} n^{1/3}. \tag{1.21}$$

As for the correlation, the limits of very low and very high density can be calculated by means of the Random Phase Approximation [32–34] and Monte-Carlo simulations [35] for intermediate values of n. Both results can be adequately interpolated to get the result in the form of an involved mixture of logarithm dependencies and power series expressions [36, 37]. However, the LDA approximation suffers from several limitations due the simplicity of the HEG model, like the infra-estimation of

the electronic gap, unbound negative ions or incorrect asymptotics for the correlation potentials, which inherits the decay behaviour of the density, contrary to the correct power laws [25]. In order to overcome these deficiencies, more sophisticated functionals have been developed; mainly, the so-called GGAs (Generalized Gradient Approximations) [38], which are based on expansions of the energy in terms of not only the density but also on powers of its derivatives, $|\nabla n(\mathbf{r})|$. The most successful ones are, for example, the BLYP functional and the PBE functional [39, 40], which correct many of the fundamental shortcomings of LDA. This functionals cannot have an arbitrary form, but actually need to satisfy some physical constraints. One of the key objects analyzed is the so called exchange-correlation hole, which measures how the joint probability of two or more electrons departs from the case of independent electrons. To wit, if we define the two-particle density, $n_2(\mathbf{r}, \mathbf{r}')$, for a system of N electrons as

$$n_2(\mathbf{r}, \mathbf{r}') = N(N-1) \int\left(|\Psi(\mathbf{r}, \mathbf{r}', \mathbf{r}_3, \cdots, \mathbf{r}_N)|^2 d\mathbf{r}_3 \cdots d\mathbf{r}_N. \tag{1.22}$$

then, for non-interacting classical systems, it will hold that $n_2(\mathbf{r}, \mathbf{r}') = n(\mathbf{r})n(\mathbf{r}')$. For noninteracting systems where we impose Pauli's exclusion principle; that is, when the wave-function can be written as $\Psi(\mathbf{r}_1, \cdots, \mathbf{r}_N) = (N!)^{-1/2} \det\left(\phi_j(\mathbf{r}_k)\right)_{jk}$, it holds that

$$n_2(\mathbf{r}, \mathbf{r}') = n(\mathbf{r})n(\mathbf{r}') - |\sum_{j=1}^{N} \phi_j^*(\mathbf{r}')\phi_j(\mathbf{r})|^2. \tag{1.23}$$

Note that even for a non-interacting system, the mere fact of imposing the antisymmetry of the wave-function introduces some degree of correlation: the exchange, which encodes Pauli's exclusion principle. For interacting systems this is no longer true, but we can write

$$n_2(\mathbf{r}, \mathbf{r}') = n(\mathbf{r})n(\mathbf{r}') + n(\mathbf{r})n_{xc}(\mathbf{r}').$$

And, since $\int n(\mathbf{r})d\mathbf{r} = N$ and $\int\int n_2(\mathbf{r}, \mathbf{r}') = N(N-1)$, it is apparent from inspection that we must impose

$$\int\left(n_{xc}(\mathbf{r})d\mathbf{r} = -1. \tag{1.24}$$

The importance of the term n_2 is obvious when we realize that, since $\hat{V}_{ee}$ is a two body operator, it holds that

$$\langle\Psi|\hat{V}_{ee}|\Psi\rangle = \frac{1}{2}\int\int\left(\frac{n_2(\mathbf{r}, \mathbf{r}')}{|\mathbf{r} - \mathbf{r}'|} d\mathbf{r}d\mathbf{r}'.$$

Thus, giving an exchange-correlation functional is equivalent to giving an exchange-correlation hole, and the sum rule in eq. 1.24 is a restriction on such functionals. For example, as a basic example, we can plug eq. 1.23 into the expression for $\langle\Psi|\hat{V}_{ee}|\Psi\rangle$ to get

$$\langle\Psi|\hat{V}_{ee}|\Psi\rangle = \frac{1}{2}\int \frac{n(\mathbf{r})n(\mathbf{r}')}{|\mathbf{r} - \mathbf{r}'|} d\mathbf{r}d\mathbf{r}' - \frac{1}{2}\int\left(\frac{\sum_{j,k}^{N} \phi_j(\mathbf{r})\phi_k(\mathbf{r})\phi_j^*(\mathbf{r}')\phi_k^*(\mathbf{r}')}{|\mathbf{r} - \mathbf{r}'|} d\mathbf{r}d\mathbf{r}', \tag{1.25}$$

which is the Hartree-Fock approximation to the Coulomb energy.

Refined exchange-correlation functionals have been designed by combining the

above mentioned GGA functionals and the exact expressions for exchange in Hartree-Fock theory. These so-called hybrid functionals are very expensive from the computational point of view, since they imply the calculation of integrals such as the one seen in the second term of eq. 1.25, but allow for a greater precision. The most typical ones are the B3LYP functional [41], which defines $E_{xc}^{B3LYP} = E_x^{LDA} + a_0(E_x^{HF} - E_x^{LDA}) + a_x(E_x^{GGA} - E_x^{LDA}) + E_c^{LDA} + a_c(E_c^{GGA} - E_c^{LDA})$, where the a's are parameters adjusted by means of some benchmark computations and the PBE0 [42], which more directly makes the mixture $E_{xc}^{PBE0} = \frac{1}{4}E_x^{HF} + \frac{3}{4}E_x^{PBE} + E_c^{PBE}$.

However, the mentioned functionals sometimes still fail to capture some features of highly correlated systems, where the many body effects cannot be entirely pick up on a one-electron approximation. Many-body methods, that try to go beyond the fundamental limits of one-electron approximations, have been developed for such cases. For example, the GW method [43], post-Hartree-Fock methods [13], the numerical renormalization group or DFT+U functionals have been developed [44]. Chapter 5 is partly devoted to such a case.

It is worth mentioning that the cited functionals (LDA, BLYP, PBE and the hybrids B3LYP or PBE0) are in principle developed for systems without spin polarization. The extension to situations where the density $n(\mathbf{r})$ is splitted between unequal contributions for spin-up and spin-down electrons, $n_\uparrow(\mathbf{r}) \neq n_\downarrow(\mathbf{r})$ is not trivial and must be derived carefully. For example, in the HEG, the exchange -which is obtained by plugging the plane waves into the exact exchange integral- can be seen to have the simple form

$$E_x^{LSDA}[n_\uparrow, n_\downarrow] = \frac{1}{2}\left(E_x^{LDA}[2n_\uparrow] + E_x^{LDA}[2n_\downarrow]\right)($$

However, the same simple superposition principle is far from true for the correlation energy. A Random Phase Approximation [32–34] calculation can be employed to approximate the result in terms of the full density $n(\mathbf{r})$ and the "normalized" magnetization $m(\mathbf{r}) = \dfrac{n_\uparrow(\mathbf{r}) - n_\downarrow(\mathbf{r})}{n(\mathbf{r})}$. An approximate density energy $\epsilon_{c,LDA}(n, m)$ is then extracted, based on interpolating the limits with zero magnetization ($m = 0$, the LDA case) and the case with total polarization ($m = 1$). Then the correlation energy is estimated again as:

$$E_{xc,LSDA}[n] := \int\left(n(\mathbf{r})\epsilon_{xc,LSDA}(n(\mathbf{r}), m(\mathbf{r}))d\mathbf{r}. \tag{1.26}$$

1.6 Alternatives to the Kohn-Sham functional

The stationary functional

So far we have defined, for every possible external potential v, a energy functional in terms of the density

$$n \to E_v[n],$$

which has the minimizer n_v (the Ground state density of Hamiltonian $\mathcal{H}_v$). It is interesting and natural, however, to define a more general functional in which we allow n and v to vary simultaneously [45]: Consider a pair $(n(\mathbf{r}), v(\mathbf{r}))$ and consider

the one-particle Schrödinger problem

$$\left(-\frac{\hbar}{2m}\Delta + v(\mathbf{r})\right)\phi_j(\mathbf{r}) = \varepsilon_j\phi_j(\mathbf{r}), \tag{1.27}$$

and call $\varepsilon_j[v]$ to the eigenvalues ε_j to emphasize the dependence on the potential v. Then we define the stationary functional as

$$E[n,v] := \sum_j f_j\varepsilon_j[v] - \int n(\mathbf{r})v(\mathbf{r})d\mathbf{r} + E_H[n] + E_{xc}[n] + E_{\text{ext}}[n]. \tag{1.28}$$

At self-consistency, this functional is stationary with respect to both variables. Indeed, notice that the variations are:

$$\begin{aligned}\frac{\delta E[n,v]}{\delta n(\mathbf{r})} &= -v(\mathbf{r}) + v_{\text{eff}}(\mathbf{r}),\\ \frac{\delta E[n,v]}{\delta v(\mathbf{r})} &= n[v](\mathbf{r}) - n(\mathbf{r}),\end{aligned} \tag{1.29}$$

where $n[v](\mathbf{r})$ is the density resulting from 1.27, that is, $n[v](\mathbf{r}) = \sum_j f_j|\phi_j(\mathbf{r})|^2$ and $v_{\text{eff}}(\mathbf{r})$ is the Kohn-Sham effective potential depending on n, $v_{\text{eff}}(\mathbf{r}) = v_{\text{ext}}(\mathbf{r}) + v_{\text{H}}(\mathbf{r}) + v_{\text{xc}}(\mathbf{r})$ The stationary property is then clear and, furthermore, it can be shown that at the stationary points the functional $E[n,v]$ is minimal with respect to n (for well-behaved densities with the appropriate mathematical conditions; see below) and maximal with respect to v. The maximality part is easy, since

$$\frac{\delta^2 E[n,v]}{\delta v(\mathbf{r})\delta v(\mathbf{r}')} = \frac{\delta n[v](\mathbf{r})}{\delta v(\mathbf{r})}$$

and the density decreases when the potential increases.

Harris functional

Self-consistency can be computational expensive in certain situations. A non-self-consistent approach to the Kohn-Sham equations has been proposed in [46, 47]. In this case, a new energy functional is defined: A starting density, $n_0(\mathbf{r})$, which is usually taken as the density of atomic fragments, i.e, $n_0(\mathbf{r}) = \sum q_j^0|\chi_j(\mathbf{r})|^2$, (where q_j^0 is the neutral charge corresponding to the j-th orbital), is plugged into 1.14 and just one iteration is solved; that is, we solve the problem:

$$\left(-\frac{\hbar^2}{2m}\Delta + v_{\text{eff}}[n_0(\mathbf{r})]\right)\phi_i(\mathbf{r}) = \varepsilon_i\phi_i(\mathbf{r}). \tag{1.30}$$

for a fixed density n_0 and we estimate the energy as:

$$E_{\text{Harris}} = \sum_{j\in\text{occupied}} \varepsilon_j - \tfrac{1}{2}\int v_{\text{H}}[n_0]n_0(\mathbf{r})\,\mathrm{d}r - \int v_{\text{xc}}[n_0]n_0(\mathbf{r})\,\mathrm{d}r + E_{\text{xc}}[n_0]. \tag{1.31}$$

The functional was originally introduced by Harris as a simplified way to study the energy of weakly interacting fragments [46] and its properties were further studied in detail in later publications[48]. This approximation, closely related to Tight-Binding methods [47], usually takes as the starting point the sum of neutral atomic

densities, which for a number of systems can be expected to be reasonably close to the ground state density of the system. For a given input potential, V_0, and an input density, n_0, giving n as output density in one iteration of the Kohn-Sham equations, the difference between the Kohn-Sham and the Harris functional can be written as

$$E[n] - E_{\text{Harris}}[n] = \int\left(V_0(\mathbf{r})(n(\mathbf{r}) - n_0(\mathbf{r})) + E_{Hxc}[n] - E_{Hxc}[n_0], \right. \tag{1.32}$$

where $E_{Hxc}[n] = E_H[n] + E_{xc}[n]$. Now, in the minimizer (the Ground state density), by expanding in powers of $\delta n(\mathbf{r}) = n(\mathbf{r}) - n_0(\mathbf{r})$, and since linear terms cancel out, we can write, following [47, 49],

$$E[n] - E_{\text{Harris}}[n] = \frac{1}{2}\int\left(K(\mathbf{r},\mathbf{r}')\delta n(\mathbf{r})\delta n(\mathbf{r}')d\mathbf{r}d\mathbf{r}', \right. \tag{1.33}$$

where

$$K(\mathbf{r},\mathbf{r}') = \frac{\delta^2 E_{Hxc}[n]}{\delta n(\mathbf{r})\delta n(\mathbf{r}')}|_{n=n_0} = \frac{1}{|\mathbf{r}-\mathbf{r}'|} + \frac{\delta^2 E_{xc}[n]}{\delta n(\mathbf{r})\delta n(\mathbf{r}')}|_{n=n_0} \tag{1.34}$$

Although the Harris functional coincides with the Kohn-Sham energy if $n_0 = n = n_{gs}$ (with n_{gs} the Ground state energy which minimizes the Kohn-Sham functional), it is worth noticing that the Harris functional itself is not variational, which is clear from eq. 1.33 .

Bringing everything together

Notice that both the Kohn-Sham and the Harris functionals can bee seen as particular cases of the stationary functional: When $n[v] = n$, then

$$E_{KS}[n] = E[n, v],$$

and when $v = v_{\text{eff}}[n]$,

$$E_{\text{Harris}}[n] = E(n, v).$$

To apply these functionals (Harris or the double stationary one) in a finite dimensional setting, we limit ourselves to sums of atomic-like densities [46] of the form

$$n(\mathbf{r}) = n_0(\mathbf{r}) + \sum_\alpha \delta q_\alpha |\chi_\alpha(\mathbf{r})|^2, \tag{1.35}$$

where $n_0(\mathbf{r})$ is the density corresponding to the neutral atoms combined, the $\{\chi_\alpha(\mathbf{r})\}$ are a basis of atomic-like localized orbitals and the $\{\delta q_\alpha\}$ are the deviations from the neutral charges (α labeling the orbitals of the system). Correspondingly, the potential can be written as

$$v(\mathbf{r}) = v_0(\mathbf{r}) + \sum_\alpha \delta v_\alpha I_\alpha(\mathbf{r}), \tag{1.36}$$

where the I_α are a set of coefficients, in principle very general. We will study one approach to these coefficients in detail in the next chapter. Now we can conveniently define the functional in terms of the $(\{q_\alpha\}, \{v_\alpha\})$ (or $(\{\delta q_\alpha\}, \{\delta v_\alpha\})$). We then have for the derivatives:

$$\begin{aligned} \frac{\partial E(\{\delta q_\alpha\}, \{\delta v_\alpha\})}{\partial \delta q_\alpha} &= \int (v_{\text{eff}}(\mathbf{r}) - v(\mathbf{r}))|\chi_\alpha(\mathbf{r})|^2 d\mathbf{r} \\ \frac{\partial E(\{\delta q_\alpha\}, \{\delta v_\alpha\})}{\partial \delta v_\alpha} &= \int\left((n[v](\mathbf{r}) - n(\mathbf{r}))I_\alpha(\mathbf{r})d\mathbf{r}, \right. \end{aligned} \tag{1.37}$$

where the first of these equations will always be 0 for the Harris functional. As for the second, it will be interesting if, with a sum of atomic-like densities such as in 1.35, we could make it also zero, thus enforcing the variational principle also to hold within a Harris formalism.

1.7 Fireball

1.7.1 The Method

Fireball is an Quantum Molecular Dynamics local-pseudoatomic-orbital DFT code of high efficiency. It has its origins in the seminal work of Sankey and Niklewski in 1989 [50], in which the Fireball orbitals were defined (see below) and the scheme of tabulation-interpolation for the integrals defining the matrix elements in the electronic structure calculation was first defined. Originally a Harris-like type of calculation, later the method was refined in a self-consistent manner [51], see the second point below for details. The method is based in two key ideas that we summarize in two different points here: the construction of the basis set and the approximation for the energy functional and the density.

1) The basis set is composed of pseudoatomic wavefunctions

$$\chi(\mathbf{r}) = f(r)Y_{l,m}(\Omega) \tag{1.38}$$

(here Ω is the angular coordinates on the sphere), where $Y_{l,m}(\Omega)$ is a real-valued spherical harmonic and $f(r)$ is a radial function whose values are tabulated up to a certain cut-off radius, R_c, while $f(R_c) = 0$ and for $r > R_c$ the wave-function is always zero, $f(r) = 0$. These orbitals, the *Fireball* orbitals, where first introduced in [50] and correspond to slightly excited pseudo-atomic orbitals (the true orbitals being recovered in the limit $R_c \to \infty$), which are appropriate to describe systems with covalent bonds. This reduces dramatically the number of interactions to be calculated. When calculating the integrals defining the energy or the potentials, the angular part is analytical and only the radial part has to be dealt with numerically. The basis sets are optimized (in terms of the shape of the orbitals, their corresponding charge, their cut-off or also the number of orbitals on each atom) to reproduce, on a given benchmark, quantities such as, in solids, the bulk modulus, the band structure, lattice constants, or, in molecules, bond lengths, relative geometries, dissociation energies, etc.

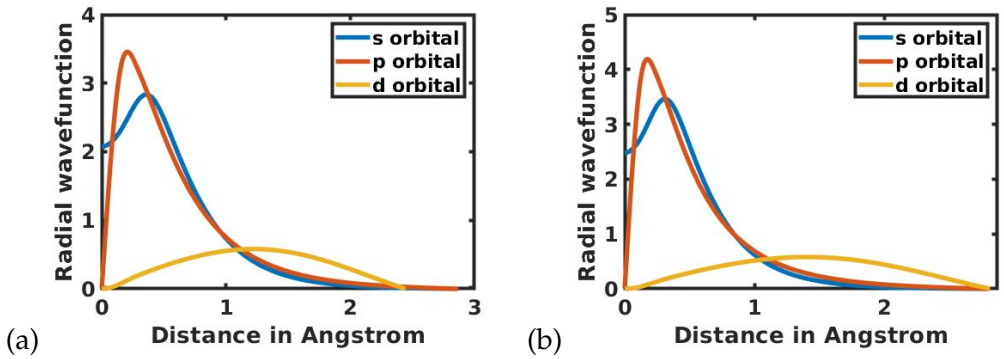

FIGURE 1.1: Radial part of some Fireball wavefunctions basis: (a) Nitrogen (b) Oxygen.

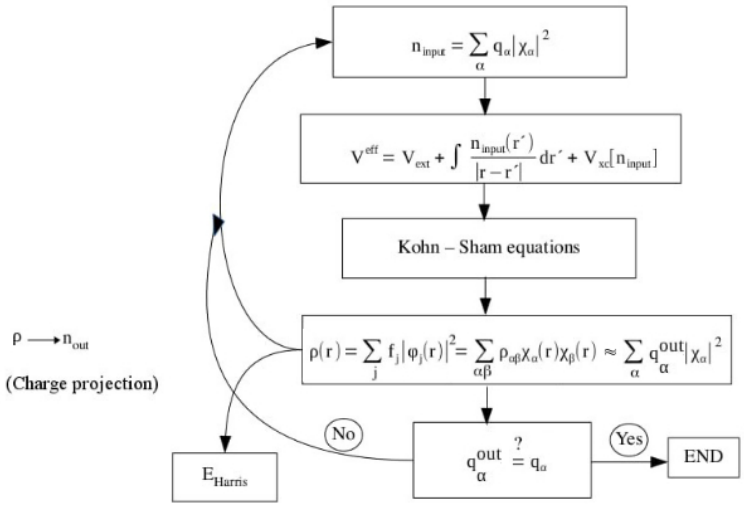

FIGURE 1.2: Scheme summarizing how the self-consistent loop works in DFT calculations and, more particularly, in Fireball: Self-consistency is defined in terms of the projected charges, q_α, and not the full spatial density $n(\mathbf{r})$.

2) The Kohn-Sham energy functional, 1.15, is substituted by a self-consistent version of the Harris-Foulkes functional discussed in the previous section [51, 52]. At each step of the iteration, the output density $n(\mathbf{r}) = \sum_j f_j |\phi_j(\mathbf{r})|^2$ resulting from one iteration of 1.14 is further approximated by a density of the form

$$n(\mathbf{r}) = \sum_j f_j |\phi_j(\mathbf{r})|^2 \approx \sum_j q_\alpha |\chi_\alpha(\mathbf{r})|^2, \tag{1.39}$$

which is key in the reduction of the computational complexity (see the section on charge projections below for details on this). That is; in Fireball the density from which the effective potential is calculated is approximated as a superposition of atomic densities. In a pure Harris approach, we would take a starting density, most typically the density corresponding to neutral atoms,

$$n_0(\mathbf{r}) = \sum_\alpha q_\alpha^0 |\chi_\alpha(\mathbf{r})|^2,$$

construct from this the Hartree potential, $v_H[n_0]$ and the exchange-correlation potential, $v_{xc}[n_0]$, to calculate the effective potential $v_{\text{eff}}[n_0]$ and solve the eigenvalue problem

$$\left(-\frac{\hbar^2}{2m}\Delta + v_{\text{eff}}[n_0(\mathbf{r})]\right)\phi_i(\mathbf{r}) = \varepsilon_i \phi_i(\mathbf{r}),$$

as shown in the previous section. In Fireball, however, the ouput density, $n(\mathbf{r}) := n_{\text{out}}(\mathbf{r}) = \sum_j f_j |\phi_j(\mathbf{r})|^2$ is approximated as seen in eq. 1.39 above, and the loop is repeated [3]: the projected density is taken as a new input density; that is $n_{\text{in}}(\mathbf{r}) =$

[3] A technical note: The construction of the input density is a bit more subtle. Let us consider a given input density $n_{\text{in}}(\mathbf{r}) = n_1(\mathbf{r}) = \sum_\alpha q_\alpha^1 |\chi_\alpha(\mathbf{r})|^2$, which is used to construct the effective potential $v_{\text{eff}}[n_1(\mathbf{r})]$. This generates from 1.14 an output density $n(\mathbf{r}) = \sum_j f_j |\phi_j(\mathbf{r})|^2$, which, as mentioned in the

$\sum_\alpha q_\alpha |\chi_\alpha(\mathbf{r})|^2$ is used as a new n_0 to define a new effective potential and the problem

$$\left(-\frac{\hbar^2}{2m}\Delta + v_{\text{eff}}[n_{\text{in}}(\mathbf{r})]\right)\phi_i(\mathbf{r}) = \varepsilon_i\phi_i(\mathbf{r}),$$

is then solved.
In this way, only integrals depending of up to three different centers ("atomic sites") are required, which implies an important increase of the efficiency. In this way, all the interactions can be calculated a priori and stored in tables, so that, during simulations, no integrals have to be computed "on the fly", and a interpolation scheme based on the values found on the tables is employed to calculate the necessary quantities.

Furthermore, in Fireball, self-consistency is defined not in terms of the spatial density $n(\mathbf{r})$, as in standard DFT, but in terms of the occupation numbers $\{q_\alpha\}_\alpha$; that is, as seen in the scheme in figure 1.2, the loop ends when the output charges q_α are (within a given tolerance) equal to the input charges. Another key step here is how the output charges $\{q_\alpha\}$ are extracted from the full density $\rho(\mathbf{r})$. The is achieved by means of the so-called charge projections -methods to prescribe how a given electronic density is splitted between the different basis orbitals. We study these methods in detail in the next section and also in chapter 2. Interestingly, self-consistency in terms of the $\{q_\alpha\}$ also presents a close relationship with the OO-DFT method described in this chapter and to be discussed further in chapter 5. Fireball, therefore, can be seen as sort of an hybrid between the standard $n(\mathbf{r})-$DFT and OO-DFT, an is an ideal framework where to test the advances on the latter.

When calculating the potential, we also make use of yet another approximation, the so-called "spherical approximation", in which the partial charges of orbitals with the same quantum number l are assumed to be equal; that is, charge is assumed to be equally distributed among all p orbitals, among all d orbitals of each atom, etc. This allows important simplification on the tables where interactions are stored. To illustrate fully the spherical approximation, let us consider a given orbital $|\chi_{a,\mu}\rangle$, where a labels the atom and μ the orbital inside atom a. Now decompose further the orbital index μ into n, l, m, where the three letters label the usual quantum numbers. Then the spherical approximation can be summarized by writing

$$q_{a,n,l,m} = q_{a,n,l,m'}. \tag{1.40}$$

Fireball, relying fundamentally in these approximations -that we can summarize, most importantly, on the Fireball orbitals in 1.38 with a cut-off radius and on the approximation 1.39 for the electronic density, and secondarily also on the spherical approximation, 1.40- achieves in this way a balance of accuracy and efficiency which is specially suitable for the calculation of properties of very large systems or for performing Quantum Molecular Dynamics (See the section about the calculation of the forces for details on this, or chapter 4 to see an important application of Fireball as Quantum Molecular Dynamics software).

text, is further approximated as $n(\mathbf{r}) \approx n_2(\mathbf{r}) = \sum_\alpha q_\alpha^2 |\chi_\alpha(\mathbf{r})|^2$. The input density at the next step of the self-consistency loop is, however, not taken to be n_2, since such an approach introduces sharp changes in the density which may spoil the convergence. Instead, the input density at the next step is defined as a mixing between n_1 and n_2, for example a linear mixing, $n_{\text{in}}(\mathbf{r}) = \beta n_1(\mathbf{r}) + (1-\beta)n_2(\mathbf{r})$. There are many mixing algorithms available. For details, see [53, 54]

1.7.2 Calculation of the matrix elements

The Kohn-Sham equations 1.14 are transformed into a system of linear equations by expanding the eigenstates in terms of the wavefunctions of our basis,

$$|\phi_j\rangle = \sum_\alpha c_{j\alpha}|\chi_\alpha\rangle. \tag{1.41}$$

. Then, by defining

$$\begin{aligned} S_{\mu\nu} &= \langle\chi_\mu|\chi_\nu\rangle \\ h_{\alpha\beta} &= \langle\chi_\mu|\hat{h}|\chi_\nu\rangle, \end{aligned} \tag{1.42}$$

where $\hat{h} = \frac{-\hbar}{2m}\Delta + v_{\text{eff}}[n_{\text{in}}(\mathbf{r})]$, the Kohn-Sham equations can expressed as:

$$\sum_\beta h_{\alpha\beta}c_{j\beta} = \epsilon_j \sum_\beta S_{\alpha\beta}c_{j\beta}. \tag{1.43}$$

The problem is then one of algebra (simultaneous diagonalization of two quadratic forms) once we are able to calculate the integrals defining the matrix elements $h_{\alpha\beta}$ and $S_{\alpha\beta}$. These integrals, however, cannot be stored for any possible geometry.

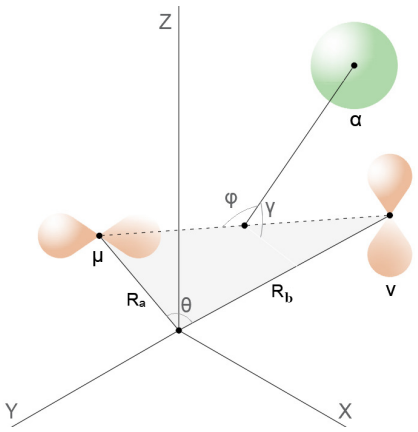

FIGURE 1.3: A generic three-center configuration. With the atoms a and b located on the z axis (with $\theta = \pi$) and $\gamma = 0$, the integrals are calculated and stored in values for different values of φ and a grid of values of the distances. Generic values of θ and γ can be recovered from the appropriate rotations, in similarity with the Slater-Koster tables [50].

Consider, for starters, the simplest case, that of the overlap, $S_{\mu\nu} = \langle\chi_\mu|\chi_\nu\rangle$. The integrals we store in the tables correspond to the case in which both atoms are over the Z axis; that is, we calculate (writing now explicitly the centers of the orbitals)

$$\int\left(\chi^*_\mu(\mathbf{r})\chi_\nu(\mathbf{r} - d\hat{\mathbf{z}})d\mathbf{r}\right.$$

for a range of values of d (up to the point where the two orbitals do not overlap anymore).

Next, turning our attention to $h_{\alpha\beta}$, we see that we should calculate separately the kinetic contribution, the Hartree elements and the exchange-correlations. The same

idea applies then for the kinetic energy matrix elements, $T_{\mu\nu} = \langle\chi_\mu|\hat{p}^2|\chi_\nu\rangle$, or, in general, for any matrix element $\langle\chi_\mu|\hat{o}|\chi_\nu\rangle$ if the operator $\hat{o}$ does not depend on other orbitals. The integrals $S_{\mu\nu}$ or $T_{\mu\nu}$ for a generic geometry are then easily obtained by using the Slater-Koster tables [55], extensively used in Tight-binding calculations to represent generic integrals in terms of combinations of the basic $ss, s\sigma, \sigma\sigma, \sigma\pi$ or $\pi\pi$ integrals (see [50] for details).

The integrals for the electrostatic interactions are already more involved, since the relative position of the three atoms depends on more variables, as seen in the figure above. In view of eq. 1.40, whenever we have an interaction in which a potential is created by an atomic-like density associated to an orbital $|\chi_\alpha\rangle$, we can make use of the radial part of the wavefunction:

$$\chi^S_{a,n,l}(\mathbf{r}) = \sqrt{\frac{1}{2l+1}\sum_m |\chi_{a,n,l,m}|^2(\mathbf{r})} = \sqrt{\frac{1}{2l+1}\sum_m f^2_{a,n,l}(r)Y^2_{l,m}(\Omega)} = \sqrt{\frac{1}{4\pi}} f_{a,n,l}(r). \tag{1.44}$$

[4] Therefore, all the electrostatic integrals of the type:

$$\int\int \chi_\mu(\mathbf{r}) \frac{|\chi_\alpha(\mathbf{r}')|^2}{|\mathbf{r}-\mathbf{r}'|} \chi_\nu(\mathbf{r}) d\mathbf{r} d\mathbf{r}'$$

are always calculated like

$$\int\int \chi_\mu(\mathbf{r}) \frac{|\chi^S_\alpha(\mathbf{r}')|^2}{|\mathbf{r}-\mathbf{r}'|} \chi_\nu(\mathbf{r}) d\mathbf{r} d\mathbf{r}'. \tag{1.45}$$

Writing again explicitly the centers of the orbitals, we could write this as:

$$\int\int \chi_\mu(\mathbf{r}-\mathbf{R}_a) \frac{|\chi^S_\alpha(\mathbf{r}'-\mathbf{R}_c)|^2}{|\mathbf{r}-\mathbf{r}'|} \chi_\nu(\mathbf{r}-\mathbf{R}_b) d\mathbf{r} d\mathbf{r}'. \tag{1.46}$$

That is, if we consider, as an example, the p-orbitals, we will not need to compute the potentials generated by each p-orbital, but just the potential generated by the corresponding spherical orbital.

As seen in the seminal work by Sankey and Niklewski, the dependency on the angles θ and γ seen on the image can be worked out analytically in a similar spirit to the Slater and Koster's tables thanks to the form of the Fireball orbitals as products of radial functions and a spherical harmonics (see again [50] for details). The tables for these three center integrals are then calculated for geometries with the vectors $\mathbf{R}_a$ and $\mathbf{R}_b$ located over the z-axis. We can calculate such integrals for different values of $|\mathbf{R}_a - \mathbf{R}_b|$ and $|\mathbf{R}_c - \frac{\mathbf{R}_a+\mathbf{R}_b}{2}|$ on a grid and for a reduced number of different values of the angle φ The result for a generic angle φ is then obtained by interpolation with Lagrange polynomials (the natural choice when angular dependency and spherical harmonics are involved).

[4] Recall we can write the basis orbitals as

$$\chi_{a,n,m,l}(\mathbf{r}) = f_{a,n,l}(r)Y_{l,m}(\Omega),$$

that is, a radial part times an spherical harmonic

While the Hartree matrix elements, of the form 1.45 above, depend on three centers, the exchange-correlation matrix elements present a great difficulty, since the non-linear dependency with the density of the potential implies many centers in the integrals. For the LDA functional, the XC energy is

$$E_{xc}[n] = \int\!\!\!\!\!\!\int n(\mathbf{r})\epsilon(n(\mathbf{r}))d\mathbf{r} \tag{1.47}$$

and thus the corresponding potential is

$$v_{xc}(\mathbf{r}) = \epsilon(n(\mathbf{r})) + n(\mathbf{r})\epsilon'(n(\mathbf{r})). \tag{1.48}$$

The exact matrix elements are in principle the integrals

$$v_{\mu\nu} = \int\!\!\!\!\!\!\int \chi^*_\mu(\mathbf{r}-\mathbf{R}_a)v_{xc}(\mathbf{r})\chi_\nu(\mathbf{r}-\mathbf{R}_b)d\mathbf{r}, \tag{1.49}$$

but, since ϵ depends non-linearly on n, it is clear that 1.49 is a many-centers integral. Appropriate approximations need therefore to be developed in order to express this matrix elements in terms of three-center integrals that can then be tabulated.

One of the first of such approximation is found on [50], the **Sankey-Niklewski approximation** where, for each matrix element $\langle\chi_\mu|v_{xc}[n]|\chi_\nu\rangle$, an expansion on the density is performed around an average density

$$\overline{n}_{\mu\nu} = \langle\chi_\mu|n|\chi_\nu\rangle / \langle\chi_\mu|\chi_\nu\rangle = n_{\mu\nu}/S_{\mu\nu},$$

where

$$\langle\chi_\mu|n|\chi_\nu\rangle = \int\!\!\!\!\!\!\int \chi^*_\mu(\mathbf{r})n(\mathbf{r})\chi_\nu(\mathbf{r})d\mathbf{r}$$

[5].

Notice that, in this case, we can approximate

$$\langle\chi_\mu|v_{xc}[n]|\chi_\nu\rangle \approx \langle\chi_\mu|v_{xc}[\overline{n}_{\mu\nu}]|\chi_\nu\rangle = v_{xc}[\overline{n}_{\mu\nu}]S_{\mu\nu},$$

and the linear term in the Taylor series around $\overline{n}_{\mu\nu}$ vanishes.

An alternative approximation, **the Horsfield approach** , considers separately the on-site case (when the two orbitals χ_α and χ_β belong to the same atom) and the off-site case (when the orbitals are located on different atoms.) In the following, let us denote by latin subscripts the atoms of the system, and let us define

$$n_a = \sum_{\mu\in a} q_\mu|\chi_\mu(\mathbf{r})|^2,$$

that is, the density on atom a. With this notation, we can discuss now the two of Horsfield's approximations:

Horsfield on-site terms

[5] Notice the slight abuse of notations. Usually, we write $\langle\chi_\mu|\hat{O}|\chi_\nu\rangle$, with $\hat{O}$ and operator, which could be in particular the density operator at a given point, $\hat{n}(\mathbf{r})$. However, here this notation means something different: For a function (Not an operator) $f(\mathbf{r})$, we define $\langle\chi_\mu|f|\chi_\nu\rangle = \int\!\!\!\!\!\!\int \chi^*_\mu(\mathbf{r})f(\mathbf{r})\chi_\nu(\mathbf{r})d\mathbf{r}$.

Let us call a to the atom on which orbitals μ and ν are located. Then we can approximate:

$$\langle\chi_\mu|v_{xc}[n]|\chi_\nu\rangle = \langle\chi_\mu|v_{xc}[n_a]|\chi_\nu\rangle + \sum_{b\neq a}\langle\chi_\mu|v_{xc}[n_a+n_b]-v_{xc}[n_a]|\chi_\nu\rangle.$$

Horsfield off-site terms

Let us call a and b to the atoms on which orbitals μ and ν are respectively located. Then we can approximate:

$$\langle\chi_\mu|v_{xc}[n]|\chi_\nu\rangle = \langle\chi_\mu|v_{xc}[n_a+n_b]|\chi_\nu\rangle + \sum_{c\neq a,b}\langle\chi_\mu|v_{xc}[n_a+n_b+n_c]-v_{xc}[n_a+n_b]|\chi_\nu\rangle.$$

McWEDA approximation

The McWEDA (Multi center Weighted Exchange-correlation Density Approximation) [56] method was developed, combining these two approaches (Sankey-Niklewski and Horsfield), to create a practical scheme which overcomes the deficiencies of the previous approximations (for example, the Sankey-Niklewski neglects the contributions of terms with zero overlap or may yield terms with opposite sign, and the Horsfield is computationally very costly and the on-site approximation often needs further numerical corrections).

McWEDA on-site terms

Let us, as before, use a to label the atom on which the orbitals and located and let us use other latin letter for the other atoms. We begin by splitting

$$\langle\chi_\mu|v_{xc}[n]|\chi_\nu\rangle = \langle\chi_\mu|v_{xc}[n_a]|\chi_\nu\rangle + \langle\chi_\mu|v_{xc}[n]-v_{xc}[n_a]|\chi_\nu\rangle. \tag{1.50}$$

The first term here, which has just one-center, will be calculated exactly, while the second term will be aproximated by a scheme very similar to the one found in Sankey-Niklewski. To avoid the problems with the zero-overlap , we expand around a symmetrically average density: The two orbitals χ_μ and χ_ν can be written, as mentioned above, as the product of a radial function times an spherical harmonic,

$$\chi_\mu(\mathbf{r}) = f_\mu(r)Y_{l_\mu m_\mu}(\theta,\varphi)$$

and

$$\chi_\nu(\mathbf{r}) = f_\nu(r)Y_{l_\nu m_\nu}(\theta,\varphi)$$

. The spherical approximation in Fireball consists in keeping just the radial part, that is, $\chi^s_\mu(\mathbf{r}) = \sqrt{\frac{1}{4\pi}}f_\mu(r)$, and analogously for the ν orbital. We then define

$$\overline{n}^s_{\mu\nu} = \frac{\langle\chi^s_\mu|n|\chi^s_\nu\rangle}{\langle\chi^s_\mu|\chi^s_\nu\rangle},$$

which contrasts with the definition of $\overline{n}_{\mu\nu}$ on the Sankey-Niklewski scheme. What we do next is to expand the second term in eq. 1.50 around $\overline{n}^s_{\mu\nu}$. By defining

$$\overline{n}^s_{a,\mu\nu} = \frac{\langle \chi^s_\mu | n_a | \chi^s_\nu \rangle}{\langle \chi^s_\mu | \chi^s_\nu \rangle},$$

we can finally write

$$\begin{aligned}\langle \chi_\mu | v_{xc}[n] | \chi_\nu \rangle \approx & \langle \chi_\mu | v_{xc}[n_a] | \chi_\nu \rangle + v_{xc}[\overline{n}^s_{\mu\nu}] S_{\mu\nu} + v'_{xc}[\overline{n}^s_{\mu\nu}] \left(\langle \chi_\mu | n | \chi_\nu \rangle - \overline{n}^s_{\mu\nu} S_{\mu\nu} \right) \Bigg(- \\ & v_{xc}[\overline{n}^s_{a,\mu\nu}] S_{\mu\nu} - v'_{xc}[\overline{n}^s_{a,\mu\nu}] \left(\langle \chi_\mu | n_a | \chi_\nu \rangle - \overline{n}^s_{a,\mu\nu} S_{\mu\nu} \right) \Bigg(\end{aligned} \tag{1.51}$$

McWEDA off-site terms

Here, as above, the orbitals μ and ν are assumed to be located respectively on atoms a and b. We can apply the same idea as in the on-site case by defining

$$\overline{n}^s_{ab,\mu\nu} = \frac{\langle \chi^s_\mu | n | \chi^s_\nu \rangle}{S_{\mu\nu}},$$

and then, splitting and expanding as above, we have

$$\begin{aligned}& \langle \chi_\mu | v_{xc}[n] | \chi_\nu \rangle = \langle \chi_\mu | v_{xc}[n_a + n_b] | \chi_\nu \rangle + \langle \chi_\mu | v_{xc}[n] - v_{xc}[n_a + n_b] | \chi_\nu \rangle \approx \\ & \langle \chi_\mu | v_{xc}[n_a + n_b] | \chi_\nu \rangle + v_{xc}[\overline{n}^s_{\mu\nu}] S_{\mu\nu} + v'_{xc}[\overline{n}^s_{\mu\nu}] \left(\langle \chi_\mu | n | \chi_\nu \rangle - \overline{n}^s_{\mu\nu} S_{\mu\nu} \right) \Bigg(- \\ & v_{xc}[\overline{n}^s_{a,\mu\nu}] S_{\mu\nu} - v'_{xc}[\overline{n}^s_{ab,\mu\nu}] \left(\langle \chi_\mu | n_a + n_b | \chi_\nu \rangle - \overline{n}^s_{ab,\mu\nu} S_{\mu\nu} \right) \Bigg(\end{aligned} \tag{1.52}$$

Lastly, we should also take into account that, in practice, as mentioned above, the effective potential should include the pseudo-potentials, which are non-local in nature. A detailed account on how to deal with these terms can be found in [50].

1.7.3 Charge projections

The solutions $|\phi_j\rangle$ to the Kohn-Sham equations yield the density of the effective non-interacting system as

$$n(\mathbf{r}) = \sum_j f_j |\phi_j(\mathbf{r})|^2, \tag{1.53}$$

where f_j are the occupation numbers for the eigenstates, defined in general in terms of the Fermi-Dirac distribution for a given temperature T. For $T = 0$, this means that $f_j = 1$ for all $j \leq N$ and 0 otherwise, with N the number of electrons in the system. The reason for equation 1.53 (let us consider first the case of zero temperature) is that the Ground State, in the effective one-particle problem, is the Slater determinant $|\Phi\rangle = \text{Alt}\left(\bigotimes_{j=1}^N |\phi_j\rangle \right)$ and for any one electron operator, $\hat{t}$, with extension $\hat{T}$ to the $N-$particle Hilbert space, it holds that the expected value over Slater determinants is just the sum of the expected values over each single-particle orbital:

$$\langle \Phi | \hat{T} | \Phi \rangle = \sum_j^N \langle \phi_j | \hat{t} | \phi_j \rangle.$$

Equation 1.53 follows then from substituting $\hat{t} = \hat{n}(\mathbf{r})$.

On the other hand, each eigenstate can be written in terms of the basis functions as:

$$|\phi_j\rangle = \sum_\alpha c_{j\alpha}|\chi_\alpha\rangle. \tag{1.54}$$

Plugging this into equation 1.53 we get

$$n(\mathbf{r}) = \sum_{\alpha,\beta} \rho_{\alpha,\beta}\chi^*_\alpha(\mathbf{r})\chi_\beta(\mathbf{r}), \tag{1.55}$$

with $\rho_{\alpha,\beta} = \sum_j f_j c^*_{j\alpha}c_{j\beta}$, (we could omit the complex conjugates whenever we are dealing with real-valued orbitals, and we need not worry about complex-valued quantities as long as we are not dealing with periodic systems.)

The expression in equation 1.55 is already useful but presents complications: since it depends on products $\chi_\alpha(\mathbf{r})^*\chi_\beta(\mathbf{r})$, and since the computation of the electrostatic energy involves integrals with $n(\mathbf{r})n(\mathbf{r}')$ in the integrand, this would imply that we need to deal with integrals with wavefunctions centered at four different atoms. As mentioned in the previous section, this is computational costly, and it is desirable to make approximations so that only integrals up to three centers are needed. This is the reason why we need to find numbers q_α such that equation 1.55 can be approximated as

$$n(\mathbf{r}) \approx \sum_\alpha q_\alpha |\chi_\alpha(\mathbf{r})|^2. \tag{1.56}$$

To be more clear in the following discussion, we will explicitly label atom numbers and orbitals numbers. The labels α and β encode both atoms and orbitals; that is, a given α specifies an atom of the system and one of its orbitals. This is convenient for a synthetic formulation, but now it will be illuminating to rewrite 1.55 as:

$$n(\mathbf{r}) = \sum_{a,b,\mu\in a,\nu\in b} \rho_{a,b,\mu,\nu}\chi^*_{a,\mu}(\mathbf{r})\chi_{b,\nu}(\mathbf{r}), \tag{1.57}$$

where $\mu \in a$ is shorthand to indicate that the index μ runs over the orbitals of atom a. All the charge methods that we study here or in next chapter are based on the existence of a basis set of local orbitals, as summarized in 1.56. However, this is not the only possibility, and, in the context of plane-waves DFT or other quantum chemistry calculations, it is interesting also to define the partial charges assigned to each atom by direct integration of the electron density $n(\mathbf{r})$ in real space. In order to achieve this, precise criterion on how to assign spatial domains to each atom are needed, and a number of works and methods are devoted to such a matter [57–70]. The Quantum Theory of Atoms-in-Molecules (AIM-QT)[58–60] method, for example, divides the electron density into non-overlapping regions of space around the different atomic positions: Each atom a is assigned a subspace C_a, and the $\{C_a\}$ form a partition of a set containing the support of n (that is, the set of points where n is non-zero), then one can simply define $q_a = \int_{C_a} n(\mathbf{r})d\mathbf{r}$. In the Hirshfeld (HIR)[57] (or stockholder) method the electron density at each point in space, $n(\mathbf{r})$, is assigned a relative probability to belong to each atom. This weight in turn is defined to be proportional to the value of the neutral atom electron density at that point.

(a) **Mulliken charges**

The first approach, dating back from long before DFT, is known as "Mulliken charges" [71] and is based on splitting the non-diagonal bond charge equally between each atom. This method has been widely used in Molecular Dynamics and

Conceptual Chemistry and has a very simple implementation that also has made it popular for charge projection in DFT and Quantum Chemistry computations. Equation 1.57 may be split as:

$$n(\mathbf{r}) = \sum_{a,\mu\in a,\nu\in a} \rho_{a,a,\mu,\nu}\chi^*_{a,\mu}(\mathbf{r})\chi_{a,\nu}(\mathbf{r}) + \sum_{a\neq b,\mu\in a,\nu\in b} \rho_{a,b,\mu,\nu}\chi^*_{a,\mu}(\mathbf{r})\chi_{b,\nu}(\mathbf{r}). \tag{1.58}$$

Defining the overlap $S_{a,b,\mu,\nu} = \int \chi^*_{a,\mu}(\mathbf{r})\chi_{b,\nu}(\mathbf{r})dr$, each partial charge $q_{a,\mu}$ is defined as:

$$q_{a,\mu} = \sum_{a,\mu} \rho_{a,a,\mu,\mu} + \sum_{b\neq a,\nu} \frac{1}{2}\left(\rho_{a,b,\mu,\nu}S_{a,b,\mu,\nu} + \rho_{b,a,\nu,\mu}S_{b,a,\nu,\mu}\right) \tag{1.59}$$

The last term above simplifies to $\sum_{b\neq a,\nu} \rho_{a,b,\mu,\nu}S_{a,b,\mu,\nu}$ in the case of real-valued basis orbitals, which is for instance the case if one is dealing with a cluster (not periodic systems) on Fireball, but we keep the expression in 1.59, valid for the general case with complex-valued quantities. Notice that on every atoms the basis functions are orthonormalized so that $S_{a,a,\mu,\nu} = \delta_{\mu,\nu}$.

(b) **Löwdin charges** Mulliken charges suffer from various limitations or ill behaviours [72, 73], and, although widely used, other methods have been explored. One of the most popular is based on Löwdin's othonormal orbitals [74]. The best way to conceptualize Löwdin's orbitals is probably through the following question: What is the orthonormal basis set of wavefunctions, $\{l_\alpha\}$, closest to the basis of pseudo-atomic orbitals $\{\chi_\alpha\}$ in quadratic average? More mathematically, but avoiding the most technical aspects (about functional spaces), we are looking for $\{l_\alpha\}$ as:

$$\underset{\{\langle l_\alpha|l_\beta\rangle=\delta_{\alpha,\beta}\}}{\arg\min} \quad \sum_\alpha \int \left((l_\alpha(\mathbf{r}) - \chi_\alpha(\mathbf{r}))^2\, dr\right). \tag{1.60}$$

In practice these orbitals are searched in the linear span of the $\{\chi_\alpha\}$, and then the problem of determining the Löwdin orbitals becomes one of simple algebra. Each Löwdin orbital can be expressed in the basis of atomic orbitals

$$|l_\alpha\rangle = \sum a_{\alpha\alpha'}|\chi_{\alpha'}\rangle.$$

We want to impose the condition $\langle l_\alpha|l_\beta\rangle = \delta_{\alpha\beta}$, which algebraically becomes

$$\sum_{\alpha'\beta'} a_{\alpha\alpha'}a_{\beta\beta'}S_{\alpha'\beta'} = \delta_{\alpha\beta}.$$

If we restrict ourselves to symmetric transformations, so that the matrix A formed by the $a_{\alpha\beta}$ is symmetric, then this equation can recasted as

$$ASA = \mathrm{Id}.$$

Since S is symmetric, its root square must exist, so that $A = S^{-1/2}$, the Löwdin transformation, gives us the explicit form of the orbitals:

$$|l_\alpha\rangle = \sum_\beta \left(S^{-1/2}\right)_{\alpha,\beta}|\chi_\beta\rangle. \tag{1.61}$$

Now let us go back to equation 1.53. In place of equation 1.54 we can write

$$|\phi_j\rangle = \sum_\alpha b_{j\alpha}|l_\alpha\rangle. \tag{1.62}$$

Notice that the matrix of $c'_{j\alpha}$s and $b'_{j\alpha}$s are related by the Löwdin transformation $S^{-1/2}$. Now we can write an equation similar to 1.58, but in this case splitting diagonal and non-diagonal terms:

$$n(\mathbf{r}) = \sum_\alpha \tilde{\rho}_{\alpha,\alpha}|l_\alpha(\mathbf{r})|^2 + \sum_{\alpha\neq\beta} \tilde{\rho}_{\alpha,\beta} l^*_\alpha(\mathbf{r}) l_\beta(\mathbf{r}), \tag{1.63}$$

with $\tilde{\rho}_{\alpha,\beta} = \sum_j f_j b^*_{j\alpha} b_{j\beta}$, Now there are two approximations: first, the non-diagonal terms are neglected on the basis that their integrals are zero (recall that $\int l_\alpha(\mathbf{r}) l^*_\beta(\mathbf{r}) dr = \delta_{\alpha,\beta}$), giving us the simplified expression $\sum_\alpha \tilde{\rho}_{\alpha,\alpha}|l_\alpha(\mathbf{r})|^2$, which means the Löwdin charges will be

$$q_\alpha = \tilde{\rho}_{\alpha,\alpha} \tag{1.64}$$

However, keeping Fireball in mind, this is still not enough for our purposes (the implementation of a three-center scheme of a self-consistent version of the Harris-Foulkes functional), since when writing the l'_αs again in terms of the χ'_αs, we would end up with a two-center "input density", thus yielding again four-center integrals in the calculation of the electrostatic energy. The next approximation is then substituting directly the Löwdin orbitals by the pseudo-atomic orbitals, which finally gives us:

$$n(\mathbf{r}) \approx \sum_\alpha \tilde{\rho}_{\alpha,\alpha}|\chi_\alpha(\mathbf{r})|^2, \tag{1.65}$$

(c) **NPA charges** The Natural Population Analysis [75] tries to correct the shortcomings of Löwdin charges by assigning weighs to the orbitals based on their occupation. Equation 1.60 can be substituted by

$$\underset{\{\langle l_\alpha|l_\beta\rangle=\delta_{\alpha,\beta}\}}{\arg\min} \quad \sum_\alpha \int \left(w_\alpha(n_\alpha) \left(l_\alpha(\mathbf{r}) - \chi_\alpha(\mathbf{r})\right)^2 dr \right), \tag{1.66}$$

where the weights $w_\alpha(n_\alpha)$ aim to give more importance to the filled orbitals; that is, the w_α are positive increasing functions. In the original NPA approach, a self-consistency is performed, in which each times some occupation numbers n_α are obtained, the orthonormal orbitals and charges are re-calculated by using again 1.66. In Fireball, when using pseudo-atomic orbitals, a simplification is available: We predefine which orbitals are occupied or empty in an atom (for example, the p-orbitals in a carbon atom are defined to be "occupied", while the d-orbitals are defined to be "unoccupied"). We assign beforehand weights w_α to each type of orbitals and just one iteration of 1.66 is performed, which already implies an important improvement in systems where the d-orbitals might be artificially overcharged.

1.8 OO-DFT

There is an alternative formulation of DFT in which the second quantization language is exploited. In Orbital-Occupancy Density Functional Theory (OO-DFT) [76–

78], DFT is combined with the Local Combination of Atomic Orbitals (LCAO) approach and the key quantity, instead of $n(r)$, is the set of occupation numbers $n_{\alpha\sigma}$. Taking $|l_{\alpha\sigma}\rangle$ as our orthonormal basis of localized orbitals (in practice these would be the Löwdin basis associated to a atomic-like basis, as described in the previous section), the occupation numbers are just $n_{\alpha,\sigma} = \sum_j f_j |\langle l_{\alpha\sigma}|\phi_j\rangle|^2$, where the $|\phi_j\rangle$ are the Kohn-Sham eigenstates. Notice that this coincides with the definition of Löwdin charges in eq. 1.64. The most general second-quantization hamiltonian can be written as:

$$\hat{H} = \sum_{\alpha\sigma} t_{\alpha\beta} \left(\hat{c}^\dagger_{\alpha\sigma}\hat{c}_{\beta\sigma} + \text{h.c}\right) + \frac{1}{2}\sum_{\alpha,\beta,\gamma,\delta,\sigma,\sigma'} \mathcal{O}^{\beta\delta\sigma'}_{\alpha\gamma\sigma}\hat{c}^\dagger_{\alpha\sigma}\hat{c}^\dagger_{\beta\sigma'}\hat{c}_{\delta\sigma'}\hat{c}_{\gamma\sigma}. \tag{1.67}$$

If the interaction term is the coulombian interaction, as before, the we ca write:

$$\mathcal{O}^{\beta\delta\sigma'}_{\alpha\gamma\sigma} = \iint l^*_{\alpha\sigma}(\mathbf{r}) l^*_{\beta\sigma'}(\mathbf{r}') \frac{1}{|\mathbf{r}-\mathbf{r}'|} l_{\gamma\sigma}(\mathbf{r}) l_{\delta\sigma'}(\mathbf{r}') d\mathbf{r} d\mathbf{r}', \tag{1.68}$$

where, in principle, each l can belong to a different atom (the index α includes atom labeling), and thus be centered at a different point in space. In OO-DFT, being after all a one-electron approximation, we want to solve the problem by considering an effective single-particle hamiltonian, $\hat{h}_1 = \sum_{\alpha\sigma} v^{\text{eff}}_\alpha \hat{n}_{\alpha\sigma} + \sum_{\alpha\sigma} t_{\alpha\beta}\left(\hat{c}^\dagger_{\alpha\sigma}\hat{c}_{\beta\sigma} + \text{h.c}\right)$, following the same ideas that we encounter in standard DFT. The Hartree-Fock part of the many body term in 1.67 is defined by the application of Wick's theorem, valid when computing expected values over Slater determinants:

$$\langle \hat{c}^\dagger_{\alpha\sigma}\hat{c}^\dagger_{\beta\sigma'}\hat{c}_{\delta\sigma'}\hat{c}_{\gamma\sigma}\rangle = \langle \hat{c}^\dagger_{\alpha\sigma}\hat{c}_{\gamma\sigma}\rangle\langle \hat{c}^\dagger_{\beta\sigma'}\hat{c}_{\delta\sigma'}\rangle - \langle \hat{c}^\dagger_{\alpha\sigma}\hat{c}_{\delta\sigma'}\rangle\langle \hat{c}^\dagger_{\beta\sigma'}\hat{c}_{\gamma\sigma}\rangle. \tag{1.69}$$

This simple factorization is of course not true for the many-body wave-function, but can be used as an approximation: the Hartree-Fock approximation. In practice, however, the mean-field approximations we use over this hamiltonian retain only diagonal contributions; that is, terms depending on the charges $n_{\alpha\sigma}$, and not on the $\langle \hat{c}^\dagger_{\alpha\sigma}\hat{c}_{\beta\sigma}\rangle$. Whatever remains is known as the *static* electron correlation[6], and finding appropriate forms for it in the context of OO-DFT will be one of the subjects of chapter 5. In such models, our hamiltonian will be described by a few parameters such as

$$U = \mathcal{O}^{\alpha\alpha\bar{\sigma}}_{\alpha\alpha\sigma} = \iint |l_{\alpha\sigma}(\mathbf{r})|^2 \frac{1}{|\mathbf{r}-\mathbf{r}'|} |l_{\alpha\bar{\sigma}}(\mathbf{r}')|^2 d\mathbf{r} d\mathbf{r}',$$

$$U' = \mathcal{O}^{\beta\beta\sigma'}_{\alpha\alpha\sigma} = \iint |l_{\alpha\sigma}(\mathbf{r})|^2 \frac{1}{|\mathbf{r}-\mathbf{r}'|} |l_{\beta\sigma'}(\mathbf{r}')|^2 d\mathbf{r} d\mathbf{r}',$$

and

$$J = \mathcal{O}^{\beta\alpha\sigma}_{\alpha\beta\sigma} = \iint l^*_{\alpha\sigma}(\mathbf{r}) l_{\beta\sigma}(\mathbf{r}) \frac{1}{|\mathbf{r}-\mathbf{r}'|} l^*_{\alpha\sigma}(\mathbf{r}') l_{\beta\sigma}(\mathbf{r}') d\mathbf{r} d\mathbf{r}'.$$

In order to implement a DFT scheme in this formalism, we need an analogue of the Hohenberg-Kohn theorem in terms of the $n_{\alpha\sigma}$. In the rest of this section, which is theoretical in nature, we drop the spin index σ to lighten the notation and reduce the number of indices. The greek indices can always be thought as encoding both orbital number and spin. We will retrieve this index in chapter 5, where we will come back to these objects.

Theorem 3. ***Hohenberg-Kohn theorem*** *The set of occupation numbers n_α determines the external potential v_α up to a constant.*

[6] The full correlation energy also has a contribution to the kinetic energy

Proof. Let us define two hamiltonians, $\hat{H}_v = \hat{H}_0 + \sum_\alpha v_\alpha \hat{n}_\alpha$ and $\hat{H}_u = \hat{H}_0 + \sum_\alpha u_\alpha \hat{n}_\alpha$. First, let us notice that, if v_α and u_α differ in more than a constant, the Ground States $|\Phi_v\rangle$ and $|\Phi_u\rangle$ cannot be equal. To prove it, assume the opposite, so that we have $\hat{H}_v|\Phi\rangle = E_v|\Phi\rangle$ and $\hat{H}_u|\Phi\rangle = E_u|\Phi\rangle$. Subtracting both equations we get:

$$\sum_\alpha (v_\alpha - u_\alpha)\hat{n}_\alpha|\Phi\rangle = (E_v - E_u)|\Phi\rangle.$$

Now let us define $|l_\alpha\rangle$ as the orthonormal set of basis wavefunctions associated to sites α and defining operators $\hat{c}^\dagger_\alpha$. Calling $N = \langle\Phi|\hat{N}|\Phi\rangle$, the total number of electrons, we define the collection of all Slater determinants formed by N of the orbitals $|l_\alpha\rangle$. Calling, for brevity, $\vec{\alpha} = (\alpha_1, \cdots, \alpha_N)$, the set of N-Slater determinants $|L_{\vec{\alpha}}\rangle := |\alpha_1, \cdots, \alpha_N\rangle := \text{Alt}\left(\bigotimes_{j=1}^N |l_{\alpha_j}\rangle\right)$ forms a basis of the space of many-body $N-$electron wavefunctions.

Taking the projection over $\langle L_{\vec{\beta}}|$ and introducing on the left the approximation of the identity $\sum_{\vec{\gamma}} |L_{\vec{\gamma}}\rangle\langle L_{\vec{\gamma}}| = 1$ now yields:

$$\sum_{\alpha,\vec{\gamma}} (v_\alpha - u_\alpha)\langle L_{\vec{\beta}}|\hat{n}_\alpha|L_{\vec{\gamma}}\rangle\langle L_{\vec{\gamma}}|\Phi\rangle = (E_v - E_u)\langle L_{\vec{\beta}}|\Phi\rangle.$$

Next use $\langle L_{\vec{\beta}}|\hat{n}_\alpha|L_{\vec{\gamma}}\rangle = \delta_{\vec{\gamma}\vec{\beta}} \sum_j \delta_{\alpha\beta_j}$ to finally get $\sum_j (v_{\beta_j} - u_{\beta_j})\langle L_{\vec{\beta}}|\Phi\rangle = (E_v - E_u)\langle L_{\vec{\beta}}|\Phi\rangle$, which implies $\sum_j (v_{\beta_j} - u_{\beta_j}) = (E_v - E_u)$ must hold for all $\vec{\beta}$. Since $E_v - E_u$ is a constant, by permuting the last identity we get that for all α and all β, it holds that $v_\alpha - u_\alpha = v_\beta - u_\beta$, which proves that indeed $|\Phi_v\rangle$ and $|\Phi_u\rangle$ cannot be equal if v_α and u_α differ in more than a constant.

Now the proof follows the same step as in the original proof by Hohenberg and Kohn: Assume the two hamiltonians $\hat{H}_v$ and $\hat{H}_u$ differing in more than a constant have the same occupation numbers $\{n_\alpha\}$. Then we can write

$$\begin{aligned} E_v =& \langle\Phi_v|\hat{H}_0 + \sum_\alpha v_\alpha \hat{n}_\alpha|\Phi_v\rangle < \langle\Phi_u|\hat{H}_0 + \sum_\alpha v_\alpha \hat{n}_\alpha|\Phi_u\rangle = \\ & E_u + \langle\Phi_u|\sum_\alpha (v_\alpha - u_\alpha)\hat{n}_\alpha|\Phi_u\rangle = E_u + \sum_\alpha (v_\alpha - u_\alpha)n_\alpha. \end{aligned}$$

We can reason in the same way but interchanging the labels u and v, thus reaching the inequality $E_u < E_v + \sum_\alpha (u_\alpha - v_\alpha)n_\alpha$. Adding both inequalities we get the contradiction $E_v + E_u < E_u + E_v$, which proves the theorem. □

Next, from the uniqueness of this inverse problem, one can use the same arguments as in the case of standard DFT to see that the energy can be defined as a function of the occupation numbers, $E = E[\{n_\alpha\}]$. In principle, as in the standard DFT, this functional is defined only on the very narrow space of ground state occupation numbers $\{n_\alpha\}$ coming from a certain potential $\{v_\alpha\}$. Split now the energy of a hamiltonian $\hat{H}_v$ as

$$E[n_\alpha] = E_0[n_\alpha] + \sum_\alpha v_\alpha n_\alpha,$$

and call $\{n^v_\alpha\}$ to the ground state occupation numbers obtained from hamiltonian $\hat{H}_v$. The variational principle thus applies as:

$$E[\{n^u_\alpha\}] \geq E[\{n^v_\alpha\}] = E_0\,, \tag{1.70}$$

where the $\{n_\alpha^u\}$ are ground state occupation numbers for a different potential $\{u_\alpha\}$. Analogously to the case of standard DFT, we can define

$$F_{LL}[\{n_\alpha\})] = \min_{|\Psi\rangle\to\{n_\alpha\}} \langle\Psi|\hat{H}_0|\Psi\rangle = \min_{|\Psi\rangle\to\{n_\alpha\}} \langle\Psi|\hat{T}_{el}+\hat{V}_{ee}|\Psi\rangle, \tag{1.71}$$

and, so, the energy functional can be extended and written, for each set of v_α, as:

$$E[\{n_\alpha\}] = F_{LL}[\{n_\alpha\}] + \sum_\alpha v_\alpha n_\alpha, \tag{1.72}$$

whose domain can be appropriately extended following the Levy-Lieb constrained search approach and general arguments presented for the case of standard DFT to the space of $N-$representable occupation numbers $\{n_\alpha\}$ (occupation numbers derived from a anti-symmetric wavefunction, which does not need to be a Ground state wavefunction of a hamiltonian of the type $\hat{H}_v$).

OO Kohn-Sham equations

Next, to develop the Kohn-Sham scheme, we split the energy for $\hat{H}$ as a function of the occupation numbers in the following way:

$$E[\{n_\alpha\}] = T_s[\{n_\alpha\}] + E_H[\{n_\alpha\}] + E_{xc}[\{n_\alpha\}] + \sum_\alpha v_\alpha n_\alpha\ , \tag{1.73}$$

where E_H and E_{xc} are the Hartree and exchange-correlation energies and T_s, which plays here the same role as the kinetic energy does in standard Kohn-Sham theory, is defined as the expected value of $\sum_{\alpha,\beta} t_{\alpha\beta}\hat{c}_\alpha^\dagger\hat{c}_\beta$ over the Slater determinant Ground State $|\Phi\rangle$ of the one-electron hamiltonian,

$$\hat{h}_1 = \sum_{\alpha,\beta} t_{\alpha\beta}\hat{c}_\alpha^\dagger\hat{c}_\beta + \sum_\alpha v_\alpha^{eff}\hat{n}_\alpha$$

where the potentials $\{v_\alpha^{eff}\}$ are chosen so that the solution of $\hat{h}_1$ yields, precisely, the occupation numbers $\{n_\alpha\}$. Then,

$$T_s[\{n_\alpha\}] = E_1[\{n_\alpha\}] - \sum_\alpha v_\alpha^{eff} n_\alpha\ , \tag{1.74}$$

where $E_1[\{n_\alpha\}]$ is the ground state energy for $\hat{h}_1$,

$$E_1 = \langle\Phi|\hat{h}_1|\Phi\rangle$$

To derive the Kohn-Sham equations in the OO formalism, following the same ideas presented in the case of standard DFT, we must take the functional derivatives of the energy functional 1.73 and also of the one-electron energy 1.74. To that end, let us call $|\phi_j\rangle$ to the one-particle eigenstates of hamiltonian $\hat{h}_1$. These eigenstates can be expanded in the basis of localized orthonormal orbitals, $|l_\alpha\rangle$ as:

$$|\phi_j\rangle = \sum_\alpha c_{j\alpha}|l_\alpha\rangle. \tag{1.75}$$

The occupation numbers can then be written as $n_\alpha = \sum_j f_j c_{j\alpha}^* c_{j\alpha}$, and, as we did for the standard DFT, we take the derivatives $\dfrac{\partial E[\{n_\gamma\}]}{\partial c_{j\alpha}^*}$. As above, we must of course

incorporate the restriction consisting on the orbitals being normalized, $\sum_\alpha c^*_{j\alpha} c_{j\alpha} = 1$, whose associated Lagrange multiplier will just be the energy of the $j-$th Kohn-Sham eigenstate, ε_j. We thus have, taking the derivative and equaling it to zero:

$$0 = \frac{\partial T_s}{\partial c_{j\alpha}} + \sum_\gamma \frac{\partial}{\partial n_\gamma} \quad E_H[\{n_\beta\}] + E_{xc}[\{n_\beta\}] + \sum_\beta v_\beta n_\beta \Bigg) \frac{\partial n_\gamma}{\partial c_{j\alpha}} + \frac{\partial}{\partial c_{j\alpha}} \sum \varepsilon_k \quad 1 - \sum_\alpha c^*_{k\alpha} c_{k\alpha} \Bigg) \Bigg(\tag{1.76}$$

which, in view of $\frac{\partial T_s}{\partial c_{j\alpha}} = \sum_\beta t_{\alpha\beta} c_{j\alpha}$, takes us to:

$$\sum_\beta t_{\alpha\beta} c_{j\beta} + \left(\frac{\partial E_H}{\partial n_\alpha} + \frac{\partial E_{xc}}{\partial n_\alpha} + v_\alpha \right) c_{j\alpha} = \varepsilon_j c_{j\alpha}. \tag{1.77}$$

Similarly as we did above for the case of standard DFT, **we can derive the Kohn-Sham equations by taking derivatives with respect to the occupation numbers** n_α. In this case, we start also by writing again the energy for $\hat{H}$ as a function of the occupation numbers in the following way:

$$E[\{n_\alpha\}] = T_s[\{n_\alpha\}] + E_H[\{n_\alpha\}] + E_{xc}[\{n_\alpha\}] + \sum_\alpha v_\alpha n_\alpha \,, \tag{1.78}$$

where E_H and E_{xc} are the Hartree and exchange-correlation energies and T_s plays here the same role as the kinetic energy does in standard Kohn-Sham theory. This is defined using a system of non-interacting electrons as an effective problem,

$$\hat{h}_1 = \sum_{\alpha,\beta} t_{\alpha\beta} \hat{c}^\dagger_\alpha \hat{c}_\beta + \sum_\alpha v^{eff}_\alpha \hat{n}_\alpha$$

where the potentials $\{v^{eff}_\alpha\}$ are chosen so that the solution of $\hat{h}_1$ yields, precisely, the occupation numbers $\{n_\alpha\}$. Algebraically, this problem becomes

$$\sum_\beta t_{\alpha\beta} c_{j\beta} + v^{eff}_\alpha c_{j\alpha} = \varepsilon_j c_{j\alpha}. \tag{1.79}$$

Then,

$$T_s[\{n_\alpha\}] = E_1[\{n_\alpha\}] - \sum_\alpha v^{eff}_\alpha n_\alpha \,,$$

where $E_1[\{n_\alpha\}]$ is the ground state energy for $\hat{h}_1$.

Taking now over the energy $E_1[\{n_\alpha\}]$ variations δn_α such that $\sum_\alpha \delta n_\alpha = 0$, we get, analogously as before:

$$\frac{\partial T_s}{\partial n_\alpha} = -v^{eff}_\alpha. \tag{1.80}$$

On the other hand, turning now our attention to eq. 1.78 for the total energy, we see that, when evaluating in the ground state occupation numbers the derivatives, we get

$$\frac{\partial E[\{n_\gamma\}]}{\partial n_\alpha} = \frac{\partial T_s[\{n_\alpha\}]}{\partial n_\alpha} + \frac{\partial E_H[\{n_\alpha\}]}{\partial n_\alpha} + \frac{\partial E_{xc}[\{n_\alpha\}]}{\partial n_\alpha} + v_\alpha = 0,$$

so that, by using eq. 1.80, we finally get

$$v^{eff}_\alpha = v^H_\alpha + v^{xc}_\alpha + v_\alpha.$$

1.9 Molecular Dynamics

1.9.1 Obtaining the Forces from a DFT calculation

Our discussion about the Born-Oppenheimer approximation and the adiabatic separation allows us to study the dynamics of the nuclei in the following manner: for every given configuration of the nuclei, $\{\mathbf{R}_a\}$ (here a is an index labeling the atoms in the system), we calculate the electronic ground state, which depends parametrically on the $\{\mathbf{R}_a\}$; that is, $E = E(\{\mathbf{R}_a\})$. If the nuclei are being treated classically, the next step is to calculate the forces, $\mathbf{F}_a = -\nabla_{\mathbf{R}_a} E(\{\mathbf{R}_b\})$, and then integrate Newton equations. We then find the new position of the nuclei after a certain δt, the time step (whose value can vary depending on the system; in out simulations, as we will see later, its value is taken as 0.5fs), find again the electronic ground state energy, and iterate the process. It is then necessary to investigate how can we calculate the derivatives $-\nabla_{\mathbf{R}_a} E(\{\mathbf{R}_b\})$ from the result extracted in a DFT calculation. In principle, the answer is immediate. The energy $E(\{\mathbf{R}_a\})$, which in DFT we calculated as a functional of the density, has a explicit dependence with the $\{\mathbf{R}_a\}$ in the potential created by the nuclei, and a implicit dependence through the dependence of $n(\mathbf{r})$ on $\{\mathbf{R}_a\}$. By the variational principle, we know that $\frac{\delta E}{\delta n(\mathbf{r})}|_{n=n_0} = 0$, with n_0 the ground state density. Thus, we have:

$$\begin{aligned}\mathbf{F}_a = -\nabla_{\mathbf{R}_a} E(\{\mathbf{R}_b\}) = -\int\left(\frac{\delta E}{\delta n(\mathbf{r})}|_{n=n_0}\nabla_{\mathbf{R}_a} n(\mathbf{r})d\mathbf{r} + \nabla_{\mathbf{R}_a} E(\{\mathbf{R}_b\})|_{\text{explicit}} = \\ \nabla_{\mathbf{R}_a} E(\{\mathbf{R}_b\})|_{\text{explicit}} = -\frac{1}{2}\int \frac{Z_a n(\mathbf{r})}{|\mathbf{r}-\mathbf{R}_\mathbf{a}|^3}(\mathbf{r}-\mathbf{R}_a)\,d\mathbf{r} - \frac{1}{2}\sum_b \frac{Z_a Z_b}{|\mathbf{R}_b-\mathbf{R}_\mathbf{a}|^3}(\mathbf{R}_b-\mathbf{R}_a).\end{aligned} \tag{1.81}$$

Alternatively, this follows from Hellmann-Feynman's theorem [79, 80] which, in general, shows that given a hamiltonian depending on a continuous parameter, λ (which in this case can be any of the components of any of the $\mathbf{R}_a$), $\hat{H}_\lambda$, an eigenvector $|\psi_\lambda\rangle$ and the corresponding eigenvalue, E_λ, it holds that

$$\frac{\partial E_\lambda}{\partial \lambda} = \langle\psi_\lambda|\frac{\partial \hat{H}_\lambda}{\partial \lambda}|\psi_\lambda\rangle, \tag{1.82}$$

which follows immediately from the product rules for derivatives by using $\frac{\partial}{\partial\lambda}\langle\psi_\lambda|\psi_\lambda\rangle = 0$, because of normalization of the eigenstates.

This prescribes a nicely simple way to compute the forces. However, in practical calculations, the application of this relation is limited, and the deficiencies of the basis set employed or, more in general, the fact that the variational principle is not fulfilled perfectly, leads to errors. Several works have been devoted to this problem, starting with Pulay's contribution, [81], in which the limitations of the basis are addressed by including in some approximate way the term $\int\left(\frac{\delta E}{\delta n(\mathbf{r})}|_{n=n_0}\nabla_{\mathbf{R}_a} n(\mathbf{r})d\mathbf{r}\right.$.

In Fireball, for example, where the use of the Harries functional implies strictly the lack of the variational principle, it is unavoidable to try to find a way to calculate the derivatives $\nabla_{\mathbf{R}_a} E[n]$ in a more involved fashion. Let us look again at the Kohn-Sham equations, either in the form 1.14 or 1.77. In the first case, let us represent the eigenstates in the local orbitals basis set as $|\phi_j\rangle = \sum_\alpha c_{j\alpha}|\chi_\alpha\rangle$a then plug this

expansion into eq. 1.14. In any case, we end up with a matrix equation looking like:

$$\sum_\beta h_{\alpha\beta} c_{j\beta} = \varepsilon_j \sum_\beta S_{\alpha\beta} c_{j\beta}.$$

Our first step is to take the derivative of $\sum_j f_j \varepsilon_j$, the sum of the occupied energies. By the product rule we have:

$$\sum_\beta \left(\nabla_{\mathbf{R}_a} h_{\alpha\beta}\right) c_{j\beta} + \sum_\beta h_{\alpha\beta} \nabla_{\mathbf{R}_a} c_{j\beta} = \sum_\beta \left(\nabla_{\mathbf{R}_a} \varepsilon_j\right) S_{\alpha\beta} c_{j\beta} + \sum_\beta \varepsilon_j \left(\nabla_{\mathbf{R}_a} S_{\alpha\beta}\right) c_{j\beta} + \sum_\beta \varepsilon_j S_{\alpha\beta} \nabla_{\mathbf{R}_a} c_{j\beta}.$$

Though this derivative seems, in principle, computationally very demanding, the work is greatly simplified by multiplying by $c_{j\alpha}$, summing on α, using $\sum_{\alpha\beta} S_{\alpha\beta} c_{j\beta} c_{j\alpha} = 1$ (which follows from expanding $\langle \phi_j | \phi_j \rangle = 1$) and using the own eigenvalue equation. We finally multiply by f_j and sum on j to find:

$$\sum_j f_j \nabla_{\mathbf{R}_a} \varepsilon_j = \sum_{j\alpha\beta} f_j c^*_{j\alpha} c_{j\beta} \nabla_{\mathbf{R}_a} h_{\alpha\beta} - \sum_j f_j \varepsilon_j c^*_{j\alpha} c_{j\beta} \nabla_{\mathbf{R}_a} S_{\alpha\beta}, \tag{1.83}$$

which gives an easy way to compute the derivatives of the sum of occupied eigenvalues $\sum_j f_j \varepsilon_j$. The derivatives of the matrix elements $h_{\alpha\beta}, S_{\alpha\beta}$ (recall that $h_{\alpha\beta} = \langle \chi_\alpha | \hat{h}_1 | \chi_\beta \rangle$, with $\hat{h}_1$ the effective one-electron hamiltonian and $S_{\alpha,\beta} = \langle \chi_\alpha | \chi_\beta \rangle$, the overlap matrix) are calculated from values stored in tables before hand. The derivatives of $S_{\alpha\beta}$ are stored without complications, but the $h_{\alpha\beta}$ depend on the $\{q_\gamma\}$. The derivatives that are actually calculated a priori are the ones corresponding to the neutral charges $\{q^0_\gamma\}$; that is, from te tables we can directly get $\nabla_{\mathbf{R}_a} \langle \chi_\alpha | \hat{h}^0_1 | \chi_\beta \rangle$, where $\hat{h}^0_1$ is the effective hamiltonian corresponding to the neutral atoms density $n_0(\mathbf{r}) = \sum_\alpha q^0_\alpha |\chi^S_\alpha(\mathbf{r})|^2$ The hamiltonian $\hat{h}_1$ depends of course on the density, $n(\mathbf{r}) = \sum_\gamma q_\gamma |\chi^S_\gamma(\mathbf{r})|^2$, and what we can do in general is expand it like

$$\hat{h}_1 = \hat{h}^0_1 + \delta \hat{h}_1, \tag{1.84}$$

or, equivalently,

$$h_{\alpha\beta} = h^0_{\alpha\beta} + \delta h_{\alpha\beta}, \tag{1.85}$$

the first term corresponding to the neutral charges and the second one to the charge transfer. For the Hartree terms, this expansion is trivial and is linked directly to the splitting of the density as

$$\sum_\alpha q_\alpha |\chi_\alpha(\mathbf{r})|^2 = \sum_\alpha q^0_\alpha |\chi_\alpha(\mathbf{r})|^2 + \sum_\alpha \delta q_\alpha |\chi_\alpha(\mathbf{r})|^2. \tag{1.86}$$

Since the linear superposition principle applies for the Hartree part, the Hartree part of $\delta h_{\alpha\beta}$, call it $\delta h^h_{\alpha\beta}$, is just

$$\delta h^h_{\alpha\beta} = \sum_\gamma \delta q_\gamma \langle \chi_\alpha | \frac{|\chi_\gamma|^2}{|\mathbf{r} - \mathbf{r}'|} | \chi_\beta \rangle, \tag{1.87}$$

and the derivative of this terms is computed by tabulating the derivatives of the monopole terms $\langle\chi_\alpha|\frac{|\chi_\gamma|^2}{|\mathbf{r}-\mathbf{r}'|}|\chi_\beta\rangle$ and neglecting $\nabla_{\mathbf{R}_a}\delta q_\gamma$. Therefore, we can write

$$\nabla_{\mathbf{R}_a} h^h_{\alpha\beta} \approx \underbrace{\nabla_{\mathbf{R}_a} h^{h,0}_{\alpha\beta}}_{\text{tabulated}} + \sum_\gamma \delta q_\gamma \underbrace{\nabla_{\mathbf{R}_a}\langle\chi_\alpha|\frac{|\chi_\gamma|^2}{|\mathbf{r}-\mathbf{r}'|}|\chi_\beta\rangle}_{\text{tabulated}}. \tag{1.88}$$

For the exchange-correlation terms, with complicated non-linear dependencies which make the simple superposition principle no longer valid, we need other approximations. In this case, we expand in power series around the neutral charges and the non-linear functions of the density are approximated by superpositions of densities of pairs of atoms (see, for example, the McWEDA method [56] or the section on exchange-correlation in chapter 2). Looking then at the expression of the energy functional, 1.15, or, in the case or Fireball, more correctly 1.31, corresponding to the Harris functional, the forces are:

$$\nabla_{\mathbf{R}_a} E[n] = \nabla_{\mathbf{R}_a}\sum_j f_j\varepsilon_j - \nabla_{\mathbf{R}_a}\frac{1}{2}\int\!\!\int\frac{n(\mathbf{r})n(\mathbf{r}')}{|\mathbf{r}-\mathbf{r}'|}d\mathbf{r}d\mathbf{r}' - \nabla_{\mathbf{R}_a}\int\!\!\int v_{xc}[n(\mathbf{r})]n(\mathbf{r})d\mathbf{r} + \nabla_{\mathbf{R}_a}E_{xc}[n], \tag{1.89}$$

where the first term is calculated according to 1.83, the second term according to 1.88 and the exchange-correlation terms (the third and fourth terms above and also the corresponding xc terms in 1.83) are calculated expanding around the neutral charges and using approximations such as the ones commented above (see [56] for details).

Neglecting the derivatives $\nabla_{\mathbf{R}_a}\delta q_\gamma$, whose calculation is extremely costly and whose contribution is typically very small may lead to a small error in the forces which makes the structures found by dynamical relaxation not exactly equal with the structures with the smallest energies. In Chapter 2, we study, on the basis of the Stationary functional, a charge projection method that makes stationary the self-consistent charges in a self-consistent Harris calculation, thus allowing us to calculate the forces with perfect accuracy without the need of calculating the $\nabla_{\mathbf{R}_a}\delta q_\gamma$.

1.9.2 Verlet Algorithm

Molecular Dynamics is a computer simulation method which tackles the problem of the integration of Newton's equations of motion, usually written as

$$m_j\frac{d^2\mathbf{r}_j}{dt^2} = -\nabla_{\mathbf{r}_j}V(\mathbf{r}_1,\cdots,\mathbf{r}_N). \tag{1.90}$$

Given such a system of Ordinary Differential Equations (ODEs), there is a number of methods available to integrate them, such as the Euler method and the family of Runge-Kutta methods. However, the Verlet integrator [82], although it might imply a certain loss of precision compared to high-order Runge-Kutta methods, has the advantage of preserving with high accuracy the energy and being symplectic, which means that the volumes in phase space are preserved under time evolution (an essential property of the micro-canonical ensemble which follows from the Liouville theorem). The Verlet algorithm we are interested in also calculates the velocities (since we need them to calculate, for example, the kinetic energy) is known as Velocity-Verlet and is summarized as follows (we omit here the particle label for

ease of notation):

$$\begin{aligned}\mathbf{r}(t+\Delta t) &= \mathbf{r}(t) + \mathbf{v}(t)\Delta t + \frac{1}{2}\mathbf{a}(t)\Delta t^2,\\ \mathbf{v}(t+\Delta t) &= \mathbf{v}(t) + \frac{\mathbf{a}(t)+\mathbf{a}(t+\Delta t)}{2}\Delta t,\end{aligned} \tag{1.91}$$

where $\mathbf{v}$ and $\mathbf{a}$ are, respectively, the velocity and the acceleration. To implement the integrator, we first calculate

$$\mathbf{r}(t+\Delta t) = \mathbf{r}(t) + \mathbf{v}(t)\,\Delta t + \frac{1}{2}\mathbf{a}(t)\Delta t^2.$$

Then we calculate $\mathbf{a}(t+\Delta t)$ from V, the potential, evaluating it at $\mathbf{r}(t+\Delta t)$ and finally we calculate

$$\mathbf{v}(t+\Delta t) = \mathbf{v}(t) + \frac{1}{2}\left(\mathbf{a}(t)+\mathbf{a}(t+\Delta t)\right)\Delta t.$$

1.9.3 Langevin thermostat

In practice, all dynamical simulations we are interested in take place at a given finite temperature; that is, in the Canonical Ensemble, and not in the Micro-canonical Ensemble, where the energy is preserved. To this end, many thermostats have been proposed which simulate the coupling of the system with a thermal bath. Here, we review briefly the Langevin thermostat [83], based on Langevin equation for the Brownian motion [84], which is implemented in every major Molecular Dynamics software package and has received further attention and generalizations, for example, to non-markovian frameworks [85, 86]. Langevin equation starts off by writing Newton's equation plus a friction term and a white noise coming from the thermal bath:

$$m_j\frac{d^2\mathbf{r}}{dt^2} = -\nabla_{\mathbf{r}}V(\mathbf{r}_1,\cdots,\mathbf{r}_N) - \gamma\frac{d\mathbf{r}}{dt} + \xi(t). \tag{1.92}$$

The idea is that the system is formed by particles (the brownian particles, which in full generality can be thought as out-of-the-equilibrium particles) coupled to a bath of much faster particles which hit the slow particles stochastically. The $\xi(t)$ is a vector random variable which follows a gaussian distribution (white noise) and whose components must satisfy the relationship

$$\langle\xi_j(t)\xi_k(t')\rangle = 2\gamma\beta^{-1}\delta_{j,k}\delta(t-t'), \tag{1.93}$$

which is actually an instant of the fluctuation-dissipation theorem (since it gives a relationship between the drag, the dissipation, quantified by the γ, and the fluctuations measured by the correlation) which can be derived by imposing that the velocities follow a Maxwell distribution.

In equilibrium, it can be seen that the expected values in the Langevin dynamics reproduce the Canonical ensemble averages. We can easily see this behaviour in a one-dimensional example, letting $\gamma/m \to \infty$ (overdamping, when there are no accelerations, or, in other words, when the inertia has a very small contribution to the overall dynamic). The Langevin equation becomes

$$-\gamma\frac{dr}{dt} - \frac{\partial V(r)}{\partial r} + \xi(t) = 0,$$

where the noise is characterized as above by the fluctuation-dissipation theorem. Now, we would like to compute the probability of the particle finding itself at position r, $P(r)$. To that end, notice that for any function ϕ it holds that

$$\gamma \frac{d\langle \phi(r(t)) \rangle}{dt} = \langle \gamma \phi'(r(t)) \frac{dr}{dt} \rangle = \langle -\phi'(r(t)) \frac{\partial V}{\partial r} + \phi'(r(t)) \xi(t) \rangle. \tag{1.94}$$

The expected value of any function $f(r)$ is $\langle f \rangle = \int P(r) f(r) dr$. As long as $r(t)$ is finite, the expected value in eq. 1.94 equals 0, because in equilibrium the expected value does not depend on the time t. Next we use the Stratonovich interpretation for stochastic integrals, which defines the stochastic integral of a stochastic process $X(t)$ with respect to a brownian process (such as the one given by $\xi(t)$) as the limit of the Riemann sum [7] taking the middle points of each interval of the partition, i.e,

$$\int X(t) d\xi(t) := \lim_{N \to \infty} \sum_{j=1}^{N} \frac{X(t_{j+1}) + X(t_j)}{2} \left(\xi(t_{j+1}) - \xi(t_j) \right) \tag{1.95}$$

. We thus get:

$$\langle -\phi'(r) \frac{\partial V}{\partial r} + \beta^{-1} \phi''(r) \rangle = 0, \tag{1.96}$$

where we make use of the probability density function $P(r)$. This is done by explicitly computing the average,

$$\int \left(\left(\phi'(r) \frac{\partial V}{\partial r} P(r) + \beta^{-1} \phi''(r) P(r) \right) d\mathbf{r} = \int \left(\left(\phi'(r) \frac{\partial V}{\partial r} P(r) - \beta^{-1} \phi'(r) P'(r) \right) dr = 0, \right. \right. \tag{1.97}$$

where the second term was integrated by parts (hence the negative sign). Since this is true for arbitrary functions ϕ, we have:

$$\frac{\partial V}{\partial r} P(r) + \beta^{-1} P'(r) = 0,$$

thus recovering the Boltzmann distribution

$$P(r) \propto \exp\left(-\beta V(r)\right).$$

[7] In ordinary Riemann sums, how we pick the points in the intervals of the partition is, of course, irrelevant by definition for all integrable functions. However, the stochastic processes present correlations among themselves for different times, and thus interpreting a stochastic integral demands specifying how the points are taken.

Chapter 2

Advances in Fireball

Goodness gracious, great balls of fire

Jerry Lee Lewis

In this chapter we detail part of the work done on the Fireball code, which includes an improvement of how the long-range Hartree matrix elements are computed, the implementation and testing of new charge projection methods and a new approximate scheme to calculate the exchange-correlation.

2.1 Approximating the Exchange-Correlation matrix elements

We have seen in the previous chapter several methods to approximately calculate the Exchange-correlation matrix elements.

Including the Exchange-Correlation (XC) energy and potential in Fireball is challenging because of the three-center approximation. The XC functionals exhibit non-linear dependencies on the density (and, in principle, also possibly on its derivatives), with powers of different exponents, which, when expressed in terms of the basis orbitals, would yield many-centers expressions. Approximations are thus needed to deal with this issue, and here we explore one combined with the McWEDA approach [56] -studied in the previous chapter- which is based on the simple idea of expanding the xc potential to linear order around neutral charges (or, equivalently, the energy to second order)

This scheme makes use of the properties of the stationary functional and, crucially, on a expansion of the form 1.36.

Introductory remarks

Let us call, in general throughout all this chapter, n to the input density, $n(\mathbf{r}) = \sum_\alpha q_\alpha |\chi_\alpha(\mathbf{r})|^2$, formed by a superposition of atomic-like densities, and ρ to the "full" output unprojected density, $\rho(\mathbf{r}) = \sum_j f_j |\phi_j(\mathbf{r})|^2 = \sum_{\alpha,\beta} \rho_{\alpha\beta}\chi_\alpha(\mathbf{r})\chi_\beta(\mathbf{r})$. It will also be useful to define q^0_α, n_0 as the charges for the configuration where all atoms are neutral, and $\delta q_\alpha = q_\alpha - q^0_\alpha, \delta n = n - n_0$ as the charge transfer.

Given any part of the effective potential, V, (which can be the Hartree, exchange or correlation contribution), its contribution U to the energy in the stationary functional, taking into account the term coming from the sum of the eigenvalues and the double-counting corrections, is:

$$U = \int \rho(\mathbf{r})V[n]d\mathbf{r} - \iint\!\!\Big(n(\mathbf{r})V[n]d\mathbf{r} + E[n]. \tag{2.1}$$

Note that the first term is just part of the sum of the eigenvalues, $\sum_j \varepsilon_j$, and could be rewritten as $\sum_j \langle \phi_j | \hat{v} | \phi_j \rangle$. The other two terms are double-counting and the corresponding functional, according to the definition of the stationary functional. Next, let us define $V_{\alpha\beta}$ as the matrix elements on the Fireball basis χ_α of the potential operator $\hat{v}$. We can then write:

$$\int \rho(\mathbf{r}) V[n(\mathbf{r})] d\mathbf{r} = \sum \rho_{\alpha,\beta} V_{\alpha,\beta} \tag{2.2}$$

and

$$\int n(\mathbf{r}) V[n(\mathbf{r})] d\mathbf{r} = \sum q_\alpha V_{\alpha,\alpha}. \tag{2.3}$$

Each $V_{\alpha,\beta} = \int \chi^*_\alpha(\mathbf{r}) V[n(\mathbf{r})] \chi_\beta(\mathbf{r}) d\mathbf{r}$ is itself a function of the density, $V_{\alpha,\beta} = V_{\alpha,\beta}[n]$ and since -as mentioned above- the dependence is non-linear, these matrix elements cannot be possibly computed in a three-center scheme.

The key idea

The central ingredient in this scheme is to expand the potential linearly around neutral charges, $V(\mathbf{r}) = V^0(\mathbf{r}) + \delta V(\mathbf{r})$, which, in terms of the matrix elements can be written as:

$$V_{\alpha,\beta} = V^0_{\alpha,\beta} + \delta V_{\alpha,\beta} \tag{2.4}$$

and

$$U = U^0 + \delta U, \tag{2.5}$$

where we have separated a neutral and charged contribution. This expansion is of course trivial in the Hartree case, but for the Exchange-correlation it is an approximation.

Indeed, notice that for the Hartree potential, $V^h[n(\mathbf{r})] = \int \frac{n(\mathbf{r}')}{|\mathbf{r} - \mathbf{r}'|} d\mathbf{r}'$, so that we can write:

$$V^h_{\alpha,\beta} = V^{0,h}_{\alpha,\beta} + \sum_\gamma I^{\gamma,h}_{\alpha\beta} \delta q_\gamma, \tag{2.6}$$

where

$$I^{\gamma,h}_{\alpha\beta} = \int \int \chi^*_\alpha(\mathbf{r}) \frac{|\chi_\gamma(\mathbf{r}')|^2}{|\mathbf{r} - \mathbf{r}'|} \chi_\beta(\mathbf{r}) d\mathbf{r} d\mathbf{r}' \tag{2.7}$$

and, thus, $V^{0,h}_{\alpha,\beta}$, the neutral charges contribution of the Hartree, is just $V^{0,h}_{\alpha,\beta} = \sum_\gamma q^0_\gamma I^{\gamma,h}_{\alpha\beta}$. Analogously, we can try to approximate the exchange correlation potential matrix elements in a similar fashion:

$$V^{xc}_{\alpha,\beta} = V^{0,xc}_{\alpha,\beta} + \sum_\gamma I^{\gamma,xc}_{\alpha\beta} \delta q_\gamma, \tag{2.8}$$

Expansion for the energy

In general, for any component of the energy (let us here denote by E either the

Hartree, the exchange or the correlation contribution), we can expand around neutral charges to second order to get an estimation. In the case of the Hartree contribution, this second-order expansion is exact, as we can check readily from:

$$E_h[n] = \int \frac{n_0(\mathbf{r})n_0(\mathbf{r}')}{|\mathbf{r}-\mathbf{r}'|}d\mathbf{r}'d\mathbf{r} + \int\left(\delta n_0(\mathbf{r})\frac{n(\mathbf{r}')}{|\mathbf{r}-\mathbf{r}'|}d\mathbf{r}'d\mathbf{r} + \frac{1}{2}\int\int\left(\frac{1}{|\mathbf{r}-\mathbf{r}'|}\delta n(\mathbf{r})\delta n(\mathbf{r}')d\mathbf{r}d\mathbf{r}', \tag{2.9}$$

The exchange-correlation energy is also expanded around neutral atomic charges to second order in a similar way:

$$E_{xc}[n] = E_{xc}[n_0] + \int \delta n(\mathbf{r})V_{xc}[n_0]d\mathbf{r} + \frac{1}{2}\int \nu_{xc}|_{n=n_0}(\mathbf{r},\mathbf{r}')\delta n(\mathbf{r})\delta n(\mathbf{r}')d\mathbf{r}d\mathbf{r}', \tag{2.10}$$

but the expression, of course, can be used in general for the Hartree component or for the whole energy adding together the Hartree and exchange-correlation potentials and ν kernels. This second order expression, which was exact for the Hartree contribution, is of course only an approximation for the exchange-correlation.

The exchange-correlation energy is written usually as an integral function in terms of an energy density, $\epsilon_{xc}(n)$, so that, for instance in LDA we have $E_{xc}[n] = \int\left(n(\mathbf{r})\epsilon_{xc}(n(\mathbf{r}))d\mathbf{r}$. If E is the Hartree part and we wanted to write it in this way, the dependency is non-local, $\epsilon_h(\mathbf{r}) = \frac{1}{2}\int\left(\frac{n(\mathbf{r}')}{|\mathbf{r}-\mathbf{r}'|}d\mathbf{r}'$ while, for the exchange-correlation energy we would take ϵ_{xc} as the exchange-correlation energy density. The kernel $\nu(\mathbf{r},\mathbf{r}')$ for the Hartree case is just

$$\nu_h(\mathbf{r},\mathbf{r}') = \frac{1}{|\mathbf{r}-\mathbf{r}'|}, \tag{2.11}$$

while for the exchange-correlation has the form

$$\nu_{xc}(\mathbf{r},\mathbf{r}') = f(n(\mathbf{r}))\delta(\mathbf{r}-\mathbf{r}'). \tag{2.12}$$

For example, in LDA, this functional expansion is equivalent to expand ϵ_{xc} as a function of $n(\mathbf{r})$ in its Taylor series around $n_0(\mathbf{r})$ for every $\mathbf{r}$, so that

$$\begin{aligned} V_{xc}(n) &= \epsilon'_{xc}(n(\mathbf{r}))n(\mathbf{r}) + \epsilon_{xc}(n(\mathbf{r})) \\ f(n(\mathbf{r})) &= \epsilon''_{xc}(n(\mathbf{r}))n(\mathbf{r}) + 2\epsilon'_{xc}(n(\mathbf{r})). \end{aligned} \tag{2.13}$$

Notice, however, that here we assume no dependency on ∇n in the exchange-correlation terms, and in practice, in Fireball, such dependencies are only included in the neutral zeroth-order term.

Form of the integral Kernels

Next, considering the global kernel $\nu(\mathbf{r},\mathbf{r}') = \nu_h(\mathbf{r},\mathbf{r}') + \nu_{xc}(\mathbf{r},\mathbf{r}')$ define the quantities

$$\begin{aligned} I^{\gamma}_{\alpha,\beta} &= \int\left(\chi_\alpha(\mathbf{r})|\chi^S_\gamma(\mathbf{r}')|^2\nu|_{n=n_0}(\mathbf{r},\mathbf{r}')\chi_\beta(\mathbf{r})d\mathbf{r}d\mathbf{r}' \\ \tilde{I}^{\gamma}_{\alpha,\beta} &= \int\left(\chi^S_\alpha(\mathbf{r})|\chi^S_\gamma(\mathbf{r}')|^2\nu|_{n=n_0}(\mathbf{r},\mathbf{r}')\chi^S_\beta(\mathbf{r})d\mathbf{r}d\mathbf{r}', \end{aligned} \tag{2.14}$$

where the superindex S stands for the spherical orbital 1.44,

$$\chi^S_\alpha(\mathbf{r}) = \sqrt{\frac{1}{2l+1}\sum_{m=-l}^{l}|\chi_{a,l,m}(\mathbf{r})|^2}.$$

With these definitions, notice next that we can write

$$\frac{1}{2}\int\int \nu|_{n=n_0}(\mathbf{r},\mathbf{r}')\delta n(\mathbf{r})\delta n(\mathbf{r}')d\mathbf{r}d\mathbf{r}' = \frac{1}{2}\sum_{\alpha,\beta}\tilde{I}^{\beta}_{\alpha,\alpha}\delta q_\alpha \delta q_\beta, \tag{2.15}$$

and, if view of the first order Taylor expansion [1] $V[n] = V[n_0] + \nu[n_0]\delta n(\mathbf{r})$, also

$$\delta V_{\alpha,\beta} = \sum_\gamma I^\gamma_{\alpha,\beta}\delta q_\gamma. \tag{2.16}$$

Also, this allows us also to write, for the charge transfer component δU of the total energy (see equations 2.1 and 2.5):

$$\delta U = \sum_{\alpha\beta}\rho_{\alpha\beta}\delta V_{\alpha\beta} - \sum_\alpha\left(q_\alpha - \frac{1}{2}\delta q_\alpha\right)\delta V_{\alpha,\alpha} \tag{2.17}$$

Approximations for the integrals

The problem of how to include the Exchange-correlation will be complete if we specify how to calculate $I^{\gamma,xc}_{\alpha\beta}$ and $\tilde{I}^{\gamma,xc}_{\alpha\beta}$. A possibility we have explored and implemented is to express the more complicated $I^{\gamma,xc}_{\alpha\beta}$ in terms of the spherical integral as:

$$I^{\gamma,xc}_{\alpha\beta} = A_{\alpha\beta}\tilde{I}^{\gamma,xc}_{\alpha\alpha} + B_{\alpha\beta}\tilde{I}^{\gamma,xc}_{\beta\beta}, \tag{2.18}$$

where $A_{\alpha\beta}$ and $B_{\alpha\beta}$ are certain coefficients defined to weigh appropriately each contribution. For instance, one can choose these weights using the Mulliken-Dipole charge projection, which is the example we have tried (see section 2.2.2). On the other hand, the integrals defining $\tilde{I}^{\beta,xc}_{\alpha\alpha}$ are calculated by the following approximation: First let us call a and b to the atoms to which α and β belong, respectively, and call $n_{a,0}$ and $n_{b,0}$ to the neutral densities of these atoms, that is, $n_{a,0}(\mathbf{r}) = \sum_\mu q^0_\mu|\chi^S_{a,\mu}(\mathbf{r})|^2$ and analogously for b. The we approximate the integrals as:

$$\begin{aligned}\tilde{I}^{\beta,xc}_{\alpha,\beta} \approx \int |\chi^S_\alpha(\mathbf{r})|^2 v_{xc}|_{n=n_{a,0}+n_{b,0}}(\mathbf{r},\mathbf{r}')|\chi^S_\beta(\mathbf{r}')|^2 d\mathbf{r}d\mathbf{r}' = \\ \int |\chi^S_\alpha(\mathbf{r})|^2 f(n_{a,0}(\mathbf{r}) + n_{b,0}(\mathbf{r}))|\chi^S_\beta(\mathbf{r})|^2 d\mathbf{r},\end{aligned} \tag{2.19}$$

which is a suitable two-center integral storable in tables, in the style described in the previous chapter.

[1] As mentioned above, for the Hartree contribution such an expansion is an exact expression.

2.2 Charge projections

As commented in detail in chapter 1, a key ingredient of the Fireball method, based on a self-consistent version of the Harris functional, is the charge projection. That is, given an output density, $n(\mathbf{r}) = \sum_j f_j |\phi_j(\mathbf{r})|$, where the $|\phi_j\rangle$ are the eigenstates obtained from solving the Kohn-Sham equations 1.14, we want to find $\{q_\alpha\}_\alpha$ such that $\sum_\alpha q_\alpha |\chi_\alpha(\mathbf{r})|^2$ approximates the density, where the $|\chi_\alpha\rangle$ are the pseudo-atomic orbitals of the basis. A charge projection method is of interest not only because of its usefulness for DFT calculations, but also for the conceptual understanding of chemical systems and for the development of models used in classical dynamics, where partial charges need to be defined (see the section on QM/MM methods in chapter 4).

2.2.1 Minimum square error approach

A very natural approach to defining the q_α is to try to minimize the quadratic error of $\sum_\alpha q_\alpha |\chi_\alpha(\mathbf{r})|^2$ and $\sum_j f_j |\phi_j(\mathbf{r})|^2$. That is, we wish the partial charges to yield a projected density closest in quadratic average to the full unprojected density. With such goal in mind, we find extremal points of the function (where the q_α's are the variables)

$$D(\{q_\alpha\}) = \frac{1}{2} \int \left(\sum_j f_j |\phi_j(\mathbf{r})|^2 - \sum_\alpha q_\alpha |\chi_\alpha(\mathbf{r})|^2 \right)^2 dr.$$

The restriction, of course, is that the total number of electrons is N, $\sum_\alpha q_\alpha = N$, so we apply then the Lagrange multipliers method by redefining:

$$D(\{q_\alpha\}) = \frac{1}{2} \int \left(\sum_j f_j |\phi_j(\mathbf{r})|^2 - \sum_\alpha q_\alpha |\chi_\alpha(\mathbf{r})|^2 \right)^2 d\mathbf{r} + L(\sum_\alpha q_\alpha - N).$$

For simplicity, we order the basis orbitals elements with just one index, as before, χ_α ($1 \leq \alpha \leq B$; and B number of elements in the basis). Let us call:

$$n(\mathbf{r}) = \sum_{j \in \text{occupied}} |\phi_j(\mathbf{r})|^2,$$

and

$$\tilde{n}(\mathbf{r}) = \sum_\alpha q_\alpha |\chi_\alpha^S(\mathbf{r})|^2.$$

We would like to find q'_αs minimizing in average the error when approximating n by $\tilde{n}$. We can write

$$|\phi_j\rangle = \sum_\alpha c_{j,\alpha} |\chi_\alpha\rangle.$$

By the theorem of the Lagrange multipliers to find critical points with restrictions, we need therefore to solve the system of equations:

$$\frac{\partial D(\{q_\alpha\})}{\partial q_\alpha} = 0, \qquad \alpha = 1, ..., B$$
$$\sum_\alpha q_\alpha = N$$

We have:

$$\frac{\partial D(\{q_\alpha\})}{\partial q_\alpha} = 2\int(\tilde{n}(\mathbf{r}) - n(\mathbf{r}))\frac{\partial \tilde{n}(\mathbf{r})}{\partial q_\alpha} + L.$$

Clearly, $\frac{\partial \tilde{n}(\mathbf{r})}{\partial q_\alpha} = |\chi^S_\alpha(\mathbf{r})|^2$ and thus, for each α, we have:

$$\begin{aligned}
&0 = L + \int((\tilde{n} - n)|\chi^S_\alpha|^2 dr = \\
&L + \int \sum_{\alpha_1} q_{\alpha_1}|\chi^S_{\alpha_1}(\mathbf{r})|^2|\chi^S_\alpha(\mathbf{r})|^2 - \sum_{\alpha_2,\alpha_3}\rho_{\alpha_2,\alpha_3}\chi_{\alpha_2}(\mathbf{r})\chi_{\alpha_3}(\mathbf{r})|\chi^S_\alpha(\mathbf{r})|^2\Big)d\mathbf{r} = \\
&L + \sum_{\alpha_1} I_{\alpha_1,\alpha_1,\alpha} q_{\alpha_1} + C_\alpha,
\end{aligned}$$

where we have renamed $\rho_{\mu\nu} = \sum_{j\in\text{occupied}} c^*_{j\mu}c_{j\nu}$ (the density matrix), $I_{\alpha,\mu,\tau} = \int \chi_\alpha(\mathbf{r})\chi_\mu(\mathbf{r})|\chi^S_\tau(\mathbf{r})|^2 d\mathbf{r}$ and $C_\alpha = -\sum_{\alpha_2,\alpha_3}\rho_{\alpha_2,\alpha_3} I_{\alpha_2,\alpha_3,\alpha}$.

Calling $J_{\alpha,\alpha'} = I_{\alpha,\alpha,\alpha'}$, we finally reach a linear system of $B+1$ equations for the unknown q_α and L :

$$\begin{aligned}
\sum_{\alpha'} J_{\alpha',\alpha} q_\alpha + L &= -C_\alpha \\
\sum_{\alpha} q_\alpha &= N
\end{aligned}$$

Defining the vector of unknown variables, x:

$$\begin{pmatrix} q_{\alpha_1} \\ . \\ . \\ q_{\alpha_B} \\ L \end{pmatrix}$$

The matrix of coefficients, A:

$$\begin{pmatrix} J_{11} & \dots & J_{B1} & 1 \\ J_{12} & \dots & J_{B2} & 1 \\ . & \dots & . & 1 \\ . & \dots & . & 1 \\ J_{1B} & \dots & J_{BB} & 1 \\ 1 & \dots & 1 & 0 \end{pmatrix}$$

And the vector of independent terms, c:

$$\begin{pmatrix} C_{\alpha_1} \\ . \\ . \\ C_{\alpha_B} \\ N \end{pmatrix}$$

We can state our problem simply as:

$$Ax = C.$$

The construction of the matrix elements involve only three-center integrals and solving the linear system gives the occupation numbers minimizing the average quadratic error. However, although this charge projection yields results very similar to Löwdin's for minimal basis, it fails for double basis of systems with many orbitals, where some of the occupation numbers may result negative and some other above the natural upper bounds.

2.2.2 Generalized Mulliken projection

The Mulliken projection presented in chapter 1 is very intuitive, but presents several problems that can be related with the fact that the splitting of non-diagonal charges into equal parts is arbitrary. The only physical concept employed in their construction is the charge. However, we will now see how the inclusion of yet another physical quantity, namely the electric dipole, undoes the arbitrarity in the splitting of the non-diagonal charges.

Given a non-diagonal contribution to the full unprojected density ρ for orbitals α and β, $\rho_{\alpha\beta}\chi^*_\alpha(\mathbf{r})\chi_\beta(\mathbf{r})$, its Mulliken contribution to the charge q_α (or q_β) is just $\frac{1}{2}\rho_{\alpha\beta}S_{\alpha\beta}$. The final charges q_α satisfy of course $\sum_\alpha q_\alpha = N$. The arbitrarity in Mulliken's splitting is solved here by imposing that the partial charges q_α and q_β reproduce the component of the electric dipole formed by orbitals $|\chi_\alpha\rangle$ and $|\chi_\beta\rangle$ along the axis connecting the two atoms. Let us be more precise:

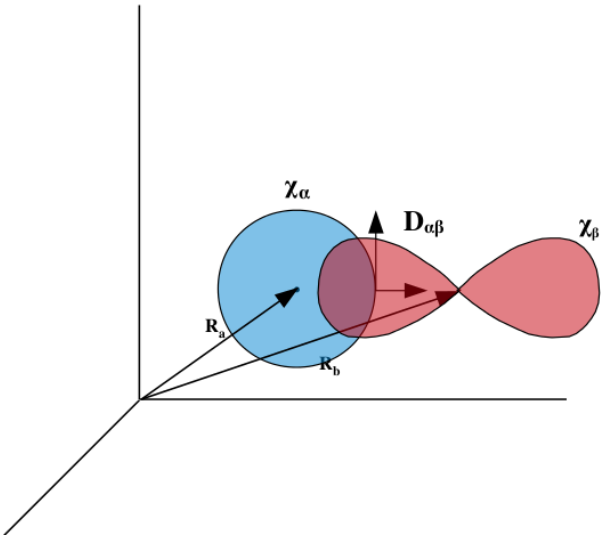

FIGURE 2.1: The dipole, $\mathbf{D}_{\alpha\beta}$, between an s and a p orbital.

Define $\mathbf{D}_{\alpha\beta}$ as the dipole between orbitals α and β centered around the center of the bond axis; that is, if $\mathbf{R}_a$ and $\mathbf{R}_b$ are the locations of the atoms on which orbitals $|\chi_\alpha\rangle$ and $|\chi_\beta\rangle$ are, respectively, then, $\mathbf{D}_{\alpha\beta}$ is defined as

$$\mathbf{D}_{\alpha\beta} = \int \left(\mathbf{r} - \frac{\mathbf{R}_a + \mathbf{R}_b}{2}\right) \chi_\alpha(\mathbf{r})\chi_\beta(\mathbf{r}) d\mathbf{r}. \tag{2.20}$$

The quantity we want to reproduce with the new projection is the component of this dipolar moment along the direction of the bond axis, that is:

$$D^{\parallel}_{\alpha\beta} = \mathbf{D}_{\alpha\beta} \cdot \frac{\mathbf{R}_a - \mathbf{R}_b}{d_{ab}},$$

where $d_{ab} = |\mathbf{R}_a - \mathbf{R}_b|$. Unfortunately, we cannot hope to reproduce the whole dipole, which is a vector, since we do not have enough degrees of freedom. The non-diagonal charge $\rho_{\alpha\beta}$ is splitted in two fractions,let us call them x and y, one to be added to the charge of atom a and the other one to be added to the charge of atom b. Having two degrees of freedom, however, allows us to take into account one more scalar besides the global charge, and it is reasonable to take this scalar to be the largest component of the dipolar moment. Each term $\rho_{\alpha\beta}\chi_\alpha(\mathbf{r})\chi_\beta(\mathbf{r})$ is approximated in the projected density as $x|\chi_\alpha(\mathbf{r})|^2 + y|\chi_\beta(\mathbf{r})|^2$. The conservation of charge imposes the conservation of the monopolar moments

$$\rho_{\alpha\beta}S_{\alpha\beta} = x + y.$$

Without an additional relation, x is arbitrary and, as mentioned above, in the Mulliken projection is taken to be $\frac{1}{2}\rho_{\alpha\beta}S_{\alpha\beta}$ Next we implement the dipole condition, imposing that $\rho_{\alpha\beta}\chi_\alpha\chi_\beta$ should give the same parallel component of the dipole as $x|\chi_\alpha|^2 + y|\chi_\beta|^2$. Notice that the dipole moment of this charge distribution, centered, as before, at $\frac{\mathbf{R}_a+\mathbf{R}_b}{2}$, is:

$$x\int |\chi_\alpha(\mathbf{r})|^2 \left(\mathbf{r} - \frac{\mathbf{R}_a+\mathbf{R}_b}{2}\right) d\mathbf{r} + y\int |\chi_\beta(\mathbf{r})|^2 \left(\mathbf{r} - \frac{\mathbf{R}_a+\mathbf{R}_b}{2}\right) d\mathbf{r} =$$
$$\underbrace{x\int |\chi_\alpha(\mathbf{r})|^2 (\mathbf{r}-\mathbf{R}_a)\, d\mathbf{r}}_{0} + x\left(\frac{\mathbf{R}_a-\mathbf{R}_b}{2}\right)\underbrace{\int |\chi_\alpha(\mathbf{r})|^2 d\mathbf{r}}_{1} +$$
$$\underbrace{y\int |\chi_\beta(\mathbf{r})|^2 (\mathbf{r}-\mathbf{R}_b)\, d\mathbf{r}}_{0} - y\left(\frac{\mathbf{R}_a-\mathbf{R}_b}{2}\right)\underbrace{\int |\chi_\beta(\mathbf{r})|^2 d\mathbf{r}}_{1} =$$
$$x\frac{\mathbf{R}_a-\mathbf{R}_b}{2} - y\frac{\mathbf{R}_a-\mathbf{R}_b}{2}.$$

Some comments are in order: the integrals on the right side on the second and third line yield 1 because the wavefunctions are of course normalized. The fact that the integrals yielding zero vanish is a bit more involved, and follows from the spherical approximation: When projecting the charges, we assume that all orbitals with the same angular momentum are equally occupied. This in turn means that we can substitute the above orbitals for their spherical averages. Given any radial function, $f(\mathbf{r})$, the integral $\int f(\mathbf{r})\mathbf{r}d\mathbf{r}$ is zero, because it is odd in all the components of $\mathbf{r}$. The integrals above are of this sort, except for the fact that the origin is shifted to the atom position; i.e., $\mathbf{R}_a$ or $\mathbf{R}_b$. By projecting over the direction given by $\mathbf{R}_a - \mathbf{R}_b$, we see that the conservation of the component of the dipolar moment along the bond axis, implies the equation:

$$\rho_{\alpha\beta}D^{\parallel}_{\alpha\beta} = \left(x\frac{\mathbf{R}_a-\mathbf{R}_b}{2} - y\frac{\mathbf{R}_a-\mathbf{R}_b}{2}\right)\left(\frac{\mathbf{R}_a-\mathbf{R}_b}{d_{ab}} =\right.$$
$$x\frac{d_{ab}}{2} - y\frac{d_{ab}}{2}.$$

Solving then the system of equations

$$\begin{aligned} x + y &= \rho_{\alpha\beta} S_{\alpha\beta} \\ x\frac{d_{ab}}{2} - y\frac{d_{ab}}{2} &= \rho_{\alpha\beta} D^{\parallel}_{\alpha\beta} \end{aligned}$$

we get:

$$\begin{aligned} x =& \rho_{\alpha\beta}\left(\frac{1}{2}S_{\alpha\beta} + \frac{D^{\parallel}_{\alpha\beta}}{d_{ab}}\right) \\ y =& \rho_{\alpha\beta}\left(\frac{1}{2}S_{\alpha\beta} - \frac{D^{\parallel}_{\alpha\beta}}{d_{ab}}\right) \end{aligned} \tag{2.21}$$

Next, introducing the notation

$$\begin{aligned} A_{\alpha\beta} &= \frac{S_{\alpha\beta}}{2} + \frac{D^{\parallel}_{\alpha\beta}}{d_{ab}}, \\ B_{\alpha\beta} &= \frac{S_{\alpha\beta}}{2} - \frac{D^{\parallel}_{\alpha\beta}}{d_{ab}}, \end{aligned} \tag{2.22}$$

we can finally write the Mulliken Dipole charges as

$$q_\alpha = \sum_\beta \rho_{\alpha\beta} A_{\alpha\beta} + \rho_{\beta\alpha} B_{\beta\alpha} \tag{2.23}$$

These charges have been implemented in Fireball and employed for different purposes. For starters, it is already interesting from the conceptual point of view that the ambiguity present in Mulliken charges is solved simply by the inclusion of another very physical notion; namely, that the most important component of the dipolar moment should be conserved.

Besides, it presents very interesting properties which we summarize in the following tables, containing data extracted from calculations performed on test molecules [73].

Conceptually speaking, probably the most important property of the Mulliken-Dipole charge projection is the sum rule that it naturally yields for the total dipole of a molecule. Given charges $q_\alpha = q_{a,\mu}$, the dipole created by the point-like charges is just $\mathbf{D}_p = \sum_{a,\mu\in a} q_{a,\mu}\mathbf{R}_a$. However, this will be (unless fitted artificially) very different from the total electronic dipole of the molecule, which can be obtained by integrating the full density:

$$\mathbf{D}_T = \int\!\!\int \rho(\mathbf{r})\mathbf{r}d\mathbf{r},$$

since the point-like charges do not collect the effects of the intra-atomic dipoles and the orthogonal component of the inter-atomic dipoles. The Mulliken-Dipole charges pick up the most important component of the inter-atomic dipoles, though, but still a potentially large part of the total dipole is missing from the charges. Indeed, the s and p orbitals of carbon, oxygen or nitrogen, for example, form dipoles which conform an important fraction of the total dipole. Calling $\mathbf{D}_{\text{intra}}$, the Mulliken-Dipole projection is the only projection (see tables) for which, approximately, the sum rule $\mathbf{D}_T = \mathbf{D}_p + \mathbf{D}_{\text{intra}}$ holds. To calculate the total dipole of a molecule, $\mathbf{\Delta}_T$, we also have to add the point charges of the nuclei, Q_a, so that we have $\mathbf{\Delta}_T = \mathbf{D}_T + \sum_a Q_a\mathbf{R}_a$.

We can bring all the point-like charges together in a term $\mathbf{\Delta}_Q$ defining $\delta_a = Q_a - \sum_{\mu \in a} q_{a,\mu}$. If we then define $\mathbf{\Delta}^0_{I,a}$ as the intra-atomic dipole of atom a, then we have

$$\mathbf{\Delta}_T = \sum_a \left(\delta_a \mathbf{R}_a + \mathbf{\Delta}^0_{I,a} \right) + \delta\mathbf{\Delta},$$

where $\delta\mathbf{\Delta}$ is the residual dipole, consisting of the orthogonal components of the inter-atomic dipoles. In the following table, we can see the values of these three quantities as calculated with the Mulliken-Dipole projection for three molecules with large intra-atomic dipoles: hydrogen fluoride, water and ammonia.

	HF	H_2O	NH_3
$\mathbf{\Delta}_T$	**1.75**	**1.77**	**1.45**
$\mathbf{\Delta}_Q$	1.29	0.90	0.55
$\mathbf{\Delta}^0_{I,m}$	0.47	0.73	0.61
$\delta\mathbf{\Delta}$	0.00	0.13	0.29

TABLE 2.1: Molecular dipoles (in Debye) for the HF, H_2O and NH_3 molecules: the total dipole, $\mathbf{\Delta}_T$; the dipole due to the M-D partial atomic charges, $\mathbf{\Delta}_Q = \sum_m \delta_a \mathbf{R}_a$; the intra-atomic dipoles $\mathbf{\Delta}^0_{I,m}$ in the F, O or N atoms; and the residual dipole $\delta\mathbf{\Delta}$. Notice that $\mathbf{\Delta}_T = \mathbf{\Delta}_Q + \mathbf{\Delta}^0_{I,m} + \delta\mathbf{\Delta}$.

Notice that, as commented above, the Mulliken-Dipole projection favors the sum rule, where the total dipole can be recovered as the sum of the point-like charges, the intra-atomic dipoles and the (usually very small) residual components of the inter-atomic dipoles (orthogonal to the component over the bond axis, which is encoded in the point-like charges). The residual dipoles can be incorporated in renormalized intra-atomic dipoles as:

$$\mathbf{\Delta}_{I,a} = \mathbf{\Delta}^0_{I,a} - \frac{1}{2} \sum_{\mu \in a, b \neq a, \nu \in b} \left(\rho_{a\mu,b\nu} \mathbf{D}^{\perp}_{a\mu,b\nu} + \rho_{b\nu,a\mu} \mathbf{D}^{\perp}_{b\nu,a\mu} \right),$$

where $\mathbf{D}^{\perp}_{a\mu,b\nu}$ is the component orthogonal to the bond axis of the inter-atomic dipoles formed by orbital μ in atom a and orbital ν in atom b. We have decided to write here the labels α in terms of both atoms and orbitals to show clearly the distinction between intra- and inter-atomic terms.

The following table shows the components of all the dipoles, as decomposed above, for the the formaldehyde molecule shown in the figure above. The second half of the table shows the renormalized intra-atomic dipoles, where the orthogonal components of the inter-atomic dipoles have been included in the $\mathbf{\Delta}_{I,a}$.

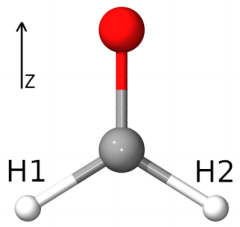

FIGURE 2.2: Formaldehyde molecule

.

	X	Y	Z
$\mathbf{\Delta}_T$	0.00	0.00	-1.80
$\mathbf{\Delta}_Q$	0.00	0.00	-3.44
$\mathbf{\Delta}^0_{I,O}$	0.00	0.00	-1.17
$\mathbf{\Delta}^0_{I,C}$	0.00	0.00	2.37
$\delta\mathbf{\Delta}$	0.00	0.00	0.44
$\mathbf{\Delta}_{I,O}$	0.00	0.00	-0.99
$\mathbf{\Delta}_{I,C}$	0.00	0.00	2.41
$\mathbf{\Delta}_{I,H1}$	0.00	0.18	0.11
$\mathbf{\Delta}_{I,H2}$	0.00	-0.18	0.11

TABLE 2.2: Cartesian X, Y, Z dipole components (in Debye) for the H_2CO (formaldehyde) molecule in the geometry shown in Figure 2.2: $\mathbf{\Delta}_T$ is the total dipole; $\mathbf{\Delta}_Q = \sum_a \delta_a \mathbf{R}_a$ is the dipole due to the M-D partial atomic charges; $\mathbf{\Delta}^0_{I,C}$ and $\mathbf{\Delta}^0_{I,O}$ are the intra-atomic dipoles, for the C and O atoms; $\delta\mathbf{\Delta}$ is the residual dipole. $\mathbf{\Delta}_{I,C}$, $\mathbf{\Delta}_{I,O}$, $\mathbf{\Delta}_{I,H1}$ and $\mathbf{\Delta}_{I,H2}$ are the renormalized intra-atomic dipoles.

2.2.3 Stationary charges

Recall that the Harris functional, which we are using in a self-consistent way in Fireball, can be written in terms of the double functional described in section 1.6 as

$$E_{\text{Harris}}[\{q_\alpha\}] = E[\{q_\alpha\}, v_{\text{eff}}[\{q_\alpha\}]].$$

Following then eqs. 1.37 and using the chain rule, we see that the derivatives of the Harris functional reduce to the second term in 1.37. If the relationship between the full output density, ρ, and the charges was such that this second term vanished, it would follow that our charges q_α would constitute a stationary point of the Harris functional.

We already know that for the output density $\rho[v]$ we have the expansion

$$\rho[v](\mathbf{r}) = \sum_{\mu\nu} \rho_{\mu\nu} \chi^*_\mu(\mathbf{r}) \chi_\nu(\mathbf{r}),$$

while, on the other hand, the density $n(\mathbf{r})$, the input density in the stationary functional, sum of atomic-like densities:

$$n(\mathbf{r}) = \sum_\alpha q_\alpha |\chi^S_\alpha(\mathbf{r})|^2.$$

It is apparent from a straight-forward calculation that the condition $\dfrac{\partial E(\{\delta q_\alpha\}, \{\delta v_\alpha\})}{\partial \delta v_\alpha} = \int (\rho[v](\mathbf{r}) - n(\mathbf{r})) I_\alpha(\mathbf{r}) d\mathbf{r} = 0$, which warrants the desired stationary property of the Harris functional, may be recasted as:

$$\sum_{\mu\nu} \rho_{\mu\nu} I^\alpha_{\mu\nu} = \sum_\beta q_\beta \tilde{I}^\alpha_{\beta\beta}, \tag{2.24}$$

Where

$$\begin{aligned} I^\gamma_{\alpha\beta} &= \int \chi_\alpha(\mathbf{r}) I_\gamma(\mathbf{r}) \chi_\beta(\mathbf{r}) d\mathbf{r}, \\ \tilde{I}^\gamma_{\beta\beta} &= \int |\chi^S_\beta(\mathbf{r})|^2 I_\gamma(\mathbf{r}) d\mathbf{r} \end{aligned} \tag{2.25}$$

are the sames I's studied in detail in section 2.1. This gives a system of linear equations which, when satisfied, will imply that the q_α are stationary. Here, of course, the $\rho[v]$ has to be the output density induced by the $\{q_\alpha\}$, which suggest a self-consistent procedure: In the context of a self-consistent Harris calculation in which self-consistency is defined in terms of the occupation numbers $\{q_\alpha\}$ (Fireball), some given atomic-like density $n(\mathbf{r})$ yields a density $\rho[v_{\text{eff}}(n)]$, and from it we define the "new" charges $\{q_\alpha\}$ by solving the system 2.24, thus defining a new input charge $n(\mathbf{r})$ for the next step. [2]

Interestingly, we encounter again condition 2.24 when studying how the charge projection can be tuned to minimize the error in the forces. To enforce the conservation of the number of electrons, $\sum_\alpha q_\alpha = N$, we just add this equation and, to have the same number of variables, a Lagrange multiplier Λ, so that the real equations we solve are:

$$\{\sum_{\mu\nu}\rho_{\mu\nu}I^{\alpha}_{\mu\nu} = \Lambda + \sum_{\beta} q_\beta \tilde{I}^{\alpha}_{\beta\beta}\}_\alpha,$$

$$N = \sum_\alpha q_\alpha$$

Minimizing the error in the forces

As mentioned in the previous chapter when discussing the calculation of the forces, neglecting $\nabla_{\mathbf{R}_a} q_\alpha$ may lead to small errors. These error is best reflected in the fact that the structures found as the equilibrium ones in a dynamical relaxation (based on the forces) is not in perfect agreement with the least energy structures. For instance, the bond-lengths for certain molecules in the dynamics can turn out to be slightly larger than what they should be. The stationary charges provide a way around this, since the variational property allows us to neglect the implicit dependence of the energy on the $\{q_\alpha\}$. The stationary charges described by eq. 2.24 are very general and depend on the how the matrix elements $I^{\gamma}_{\alpha\beta}$ are calculated. As mentioned above, the only requisite is the existence of such $I^{\gamma}_{\alpha\beta}$ for which eq. 2.8 holds.

Interestingly, two of the charge projections described above, namely, the Mulliken projection and the Mulliken-Dipole approximation, can be seen as particular cases of the stationary charges if the matrix elements are approximated in a coherent way. Indeed, coming back at eq. 2.18, it is immediate to see that the Mulliken charges correspond to the simple approximation

$$A_{\alpha,\beta} = \frac{S_{\alpha,\beta}}{2}$$

and

$$B_{\alpha,\beta} = \frac{S_{\alpha,\beta}}{2}$$

while

$$A_{\alpha,\beta} = \frac{S_{\alpha,\beta}}{2} - \frac{p_{\alpha,\beta}}{d_{BC}}$$

[2] As commented in chapter 1, the new charges are actually mixed with the ones from the previous step to so smoothen the self-consistent procedure [53, 54].

and

$$B_{\alpha,\beta} = \frac{S_{\alpha,\beta}}{2} + \frac{p_{\alpha,\beta}}{d_{BC}},$$

are linked in turn to the Mulliken-Dipole charges. Note, however, that the Mulliken or the Mulliken-Dipole charges do not demand in any way any particular approximation for the matrix elements, and they do not require even the approach in eq. 2.8 (they can be used, of course, with any of the methods for approximating the Exchange-correlation exposed in the previous chapter), but if we wanted these charges to be strictly variational with respect to the Harris functional, we would need to approximate the matrix elements in this manner. The stationary charges are, however, more general, and we have also explored the possibility of including the Hartree contributions exactly (without resorting to the unnecessary approximation 2.18) and using approximation 2.18 only for the Exchange-correlation integrals.

Let us denote by R any coordinate of any atom of the system. For U any contribution of the energy, the derivative $\frac{\partial U}{\partial R}$ can be written as

$$\frac{\partial U}{\partial R} = \frac{\partial U}{\partial R}|_{\text{explicit}} + \sum_{\gamma} \frac{\partial U}{\partial q_\gamma} \frac{\partial q_\gamma}{\partial R}. \tag{2.26}$$

Finding expressions and approximations for U such that the contribution of the second term is minimal is therefore of interest. In particular, notice that for charges $\{q^0_\gamma\}$ constituting a stationary point, it must hold $\frac{\partial E[\{q_\gamma\}]}{\partial q_\alpha}|_{q=q^0} = 0$, and thus, as discussed in the previous chapter, the calculation of the forces would only concern the calculation of the explicit derivatives.

Now, if we make the approximation 2.18:

$$I^\gamma_{\alpha,\beta} = A_{\alpha,\beta}\tilde{I}^\gamma_{\alpha,\alpha} + B_{\alpha,\beta}\tilde{I}^\gamma_{\beta,\beta}, \tag{2.27}$$

and if the charges are defined as the solution of the resulting system of equations 2.24:

$$q_\alpha = \sum_\beta \rho_{\alpha\beta}A_{\alpha\beta} + \rho_{\alpha\beta}B_{\alpha\beta},$$

then, neglecting the derivatives $\frac{\partial q_\gamma}{\partial R}$ does not affect the calculation of the forces, $\frac{\partial U}{\partial R}$.

In particular, as we illustrated above, we could choose $A_{\alpha,\beta} = \frac{S_{\alpha,\beta}}{2} - \frac{p_{\alpha,\beta}}{d_{BC}}$ and $B_{\alpha,\beta} = \frac{S_{\alpha,\beta}}{2} + \frac{p_{\alpha,\beta}}{d_{BC}}$, which would turn q_α into the Mulliken-Dipole charges.

From the discussion about charge projections and the use of the variational property in the calculation of the forces (see Chapter 1) this follows easily, since these charges correspond to a stationary point of the Harris functional and, as such, the derivatives $\frac{\partial E}{\partial q_\gamma}$ must vanish. We recall briefly here an explicit proof:

Let us to that end compute the derivative of $\sum_{\alpha,\beta}\rho_{\alpha\beta}h_{\alpha\beta}$, with $h_{\alpha\beta}$ the matrix elements of the hamiltonian in the Fireball basis. For that we use the relationship

$$\frac{\partial}{\partial R}\sum_{\alpha,\beta}\rho_{\alpha\beta}h_{\alpha\beta} = \sum_{\alpha,\beta}\rho_{\alpha\beta}\frac{\partial h_{\alpha\beta}}{\partial R} - \sum_{j\in\text{occ}}\varepsilon_j c_{\alpha j}c_{\beta j}\frac{\partial S_{\alpha\beta}}{\partial R}. \tag{2.28}$$

To derive this relation we use the fact $1 = \sum_{\alpha,\beta} c_{\alpha,j}c_{\beta,j}S_{\alpha\beta}$, which follows immediately from the orthonormalization of the eigenvectors, we derive both sides, apply the chain rule and multiply by ε_j to get:

$$\sum_{\alpha,\beta}\sum_{j\in\text{occ}}\varepsilon_j\left(\frac{\partial c_{\alpha j}}{\partial R}c_{\beta j} + c_{\alpha j}\frac{\partial c_{\beta j}}{\partial R}\right) = -\sum_{\alpha,\beta}\sum_{j\in\text{occ}}\varepsilon_j c_{\alpha j}c_{\beta j}\frac{\partial S_{\alpha\beta}}{\partial R}.$$

We finally get

$$\frac{\partial U}{\partial R} - \frac{\partial U}{\partial R}|_{\text{explicit}} = \sum_{\alpha,\beta,\gamma}\rho_{\alpha\beta}I^{\gamma}_{\alpha\beta}\frac{\partial q_\gamma}{\partial R} - \sum_{\alpha,\gamma}q_\alpha\tilde{I}^{\gamma}_{\alpha\alpha}\frac{\partial q_\gamma}{\partial R}, \tag{2.29}$$

which equals zero if the q_α are taken to be the stationary charges.

We have tested the effect of the new method in some systems and we offer here an example of the slight improvement on the relaxation of a complex system. Below, we compare the result with Mulliken-Dipole charges and the old way to account for the charge-transfer (blue curves) with the result obtained by this new method based on the splitting 2.8 and the approximation 2.18.

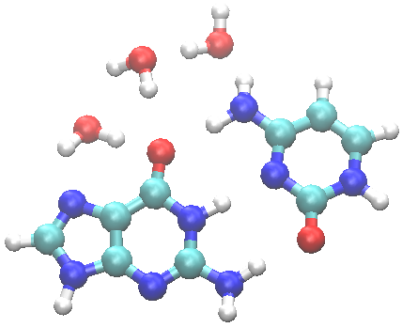

FIGURE 2.3: A guanine cytosine base-pair with three water molecules in their neighborhood.

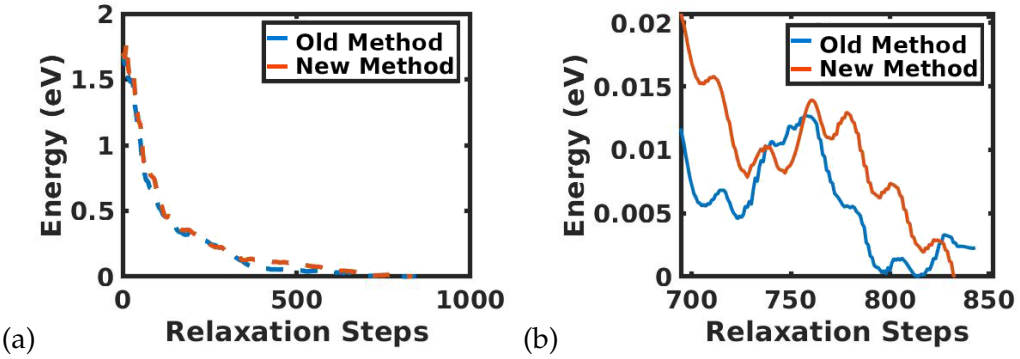

FIGURE 2.4: Relaxation of the system shown in fig. 2.3, using in one case the Mulliken-Dipole charges with the standard procedure to deal with the charge transfer terms, and in the other case using our new method and the stationary charges.

We thus see in the figures that, although superficially both methods perform almost identically, and convergence is attained almost in the same number of steps, when zooming in, the small error in the forces, which leads to the converged structure not being identical to the one with the least energy, disappears.

2.3 Long range interactions

As mentioned in the first chapter, the Fireball method is based crucially in the storage of the interactions in tables for a range of distances between the interacting atoms. Additionally, the cut-off radii of the atoms is finite, which reduces drastically the size of the tables and of the number of interactions that need to be computed. Given three atomic orbitals, χ_μ, χ_ν and χ_α, belonging respectively to atoms a, b and c (which coordinates, respectively, $\mathbf{R}_a, \mathbf{R}_b$ and $\mathbf{R}_c$), let us consider the contribution to the matrix element $h_{\mu,\nu}$ given by the monopolar potential created by the orbital χ_α. The potential will be just $q_\alpha \int \frac{|\chi_\alpha^S(\mathbf{r}'-\mathbf{R}_c)|^2}{|\mathbf{r}-\mathbf{r}'|} d\mathbf{r}'$, where q_α is the projected charge over orbital α and the superscript S indicates that we are taking the spherical approximation, in which the charges of orbitals of the same atom with the same angular momentum number will be taken to be equal. The Hartree contributions to the matrix elements, $h_{\mu\nu}$, in Fireball, look then like

$$D^\alpha_{\mu\nu} = q_\alpha \int \int \left(\chi_\mu(\mathbf{r}-\mathbf{R}_a) \frac{|\chi_\alpha^S(\mathbf{r}'-\mathbf{R}_c)|^2}{|\mathbf{r}-\mathbf{r}'|} \chi_\nu(\mathbf{r}-\mathbf{R}_b) d\mathbf{r} d\mathbf{r}' \right. \tag{2.30}$$

However, this has, in principle, one important draw-back: These elements can only be computed from the tables when the distance between the atoms is such that there is an overlap between the wave-functions.

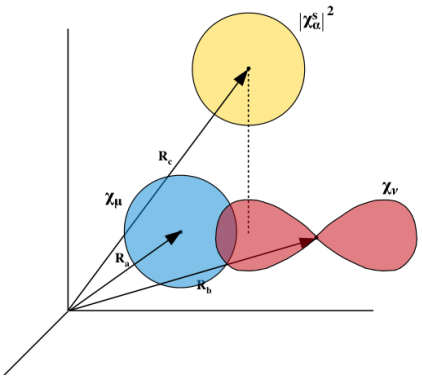

FIGURE 2.5: Scheme showing the locations of two orbitals, χ_μ, χ_ν interacting with a distant spherical charge distribution, $|\chi^S_\alpha|^2$.

To study the long range behaviour, first let us briefly recall the Legendre expansion. If $r > r'$, we can expand in spherical harmonics the term $\dfrac{1}{|\mathbf{r}-\mathbf{r}'|}$, which gives:

$$\frac{1}{|\mathbf{r}-\mathbf{r}'|} = \sum_{n=0}^{\infty} \frac{r'^n}{r^{n+1}} P_n(\cos\alpha), \tag{2.31}$$

where P_n are the Legendre polynomials and α is the angle formed by the two vectors $\mathbf{r}$ and $\mathbf{r}'$, so that $\cos\alpha = \dfrac{\mathbf{r}\cdot\mathbf{r}'}{rr'}$. We neglect terms beyond second order and thus, since $P_0(x) = 1$ and $P_1(x) = 1$, get the (dipolar) approximation:

$$\frac{1}{|\mathbf{r}-\mathbf{r}'|} \approx \frac{1}{r} + \frac{\mathbf{r}\cdot\mathbf{r}'}{r^3}. \tag{2.32}$$

The long-range approximation is valid when atom C is far away from both A and B, which, obviously, must have non-zero overlap in order for the integral in 2.30 to be non-zero. Define $\mathbf{R}_{bc} = \dfrac{\mathbf{R}_a + \mathbf{R}_b}{2}$ and $\mathbf{R} = \mathbf{R}_c - \mathbf{R}_{bc}$. The atom C being "far away" then means that R is large compared to $\mathbf{r}' - \mathbf{r} + \mathbf{R}$, for all the relevant $\mathbf{r}$ and $\mathbf{r}'$. We know make the expansion:

$$\begin{aligned} &\frac{1}{|\mathbf{r}-\mathbf{r}'|} = \frac{1}{|\mathbf{R} - (\mathbf{r}' - \mathbf{r} + \mathbf{R})\,|} \approx \\ &\frac{1}{R} + \frac{\mathbf{R}\cdot(\mathbf{r}' - \mathbf{r} + \mathbf{R})}{R^3}. \end{aligned} \tag{2.33}$$

Next, if we define

$$\mathbf{P}_{a\mu,b\nu} = \int\!\!\int \chi_\mu(\mathbf{r}-\mathbf{R}_a)\chi_\nu(\mathbf{r}-\mathbf{R}_b)\,(\mathbf{r}-\mathbf{R}_{bc})\,d\mathbf{r}, \tag{2.34}$$

and if we notice that, due to the spherical symmetry, $\int\!\!\int |\chi^S_\alpha(\mathbf{r}')|^2\,(\mathbf{r}'-\mathbf{R}_c)\,d\mathbf{r}' = 0$, then, the matrix element in 2.30 can be approximated in the long range as:

$$D^\alpha_{\mu\nu} = q_\alpha \left(\frac{S_{a\mu,b\nu}}{R} + \frac{\mathbf{P}_{a\mu,b\nu}\cdot\mathbf{R}}{R^3} \right). \tag{2.35}$$

We cannot, however, store in tables exactly the quantities $\mathbf{P}_{a\mu,b\nu}$ for every possible position in space of the atoms. We can only store in tables this integrals when the atoms A and B have a particular geometry; we decide, following the convention in Fireball tables, to store them when both atoms are located over the z-axis. During a simulation, we have then to perform a rotation to recover the desired rotation. It should be noted that this procedure involves, however, two simultaneous rotations: we must rotate the vector itself, but also, as with any other interaction in Fireball, the spherical harmonics corresponding to the orbitals χ_μ and χ_ν. We then define a "molecular" system of coordinates, whose coordinates and vectors we will refer to with $\mathbf{x}, \mathbf{X}$,..., by imposing that $\mathbf{X}_{bc} = 0$, both atoms A and B are located over the z axis and atom C is located on the $x-z$ plane. This defines an affine transformation, ϵ, rotating and translating the axis so that $\mathbf{r} = \epsilon(\mathbf{x})$. Calling $\sigma_{a\mu,b\nu}$ and $\mathbf{\Pi}_{a\mu,b\nu}$ correspondingly to the overlap and the dipole in the molecular system of coordinates, we can define

$$K^\alpha_{\mu\nu} = q_\alpha \left(\frac{\sigma_{a\mu,b\nu}}{X} + \frac{\mathbf{\Pi}_{a\mu,b\nu} \cdot \mathbf{X}}{X^3} \right), \tag{2.36}$$

where now $\mathbf{X} = \mathbf{X}_c$. The numbers $K^\alpha_{\mu\nu}$ can now be easily extracted from the tables for the overlap and the dipole, which are calculated beforehand.

The spherical harmonics in the molecular system of coordinates are not the same as in the crystalline system of coordinates of the simulation, but any rotated spherical harmonic can be expressed as a linear combination of spherical harmonics of the same angular momentum. We will write, for simplicity,

$$\chi_\mu(\mathbf{r}) = \sum_{\mu' \in a} A_{\mu\mu'} \chi^m_{\mu'}(\mathbf{r}),$$

where the superscript m refers to the molecular system of coordinates, a is the atom to which the orbital belongs and $A_{\mu\mu'}$ are the coefficients of the transformation. These coefficients depend on the angular momentum number of the orbital and in Fireball they are implemented for p and d orbitals.

When computing the forces, we will need to take derivatives of the $\mathbf{P}_{a\mu,b\nu}$, and, for that, we need to write this vector as

$$\epsilon \left(\mathbf{\Pi}_{a\mu,b\nu} \right) \left(\right.$$

and apply the chain rule.

In the crystalline system of coordinates, the derivatives must be taking with respect to the positions of atoms A,B and C to compute the corresponding contributions to the forces. On the one hand, for atom A we have (we drop here the atomic subindices a and b for ease of notation):

$$\begin{aligned} \nabla_{\mathbf{R}_a} D^\alpha_{\mu\nu} = q_\alpha \quad & \frac{\nabla_{\mathbf{R}_a} S_{\mu,\nu}}{R} + \frac{S_{\mu\nu}\mathbf{R}}{R^3} + \frac{\left(\nabla_{\mathbf{R}_a} \mathbf{P}_{\mu\nu}\right)}{R^3} \left(\mathbf{R} \right. \\ & - \frac{1}{2}\frac{\mathbf{P}_{\mu\nu}}{R^3} + \frac{3}{2}\frac{\left(\mathbf{P}_{\mu\nu} \cdot \mathbf{R}\right)\mathbf{R}}{R^5} \Bigg), \Bigg(\end{aligned} \tag{2.37}$$

and similarly for atom B. For atom C, on the other hand, we have:

$$\nabla_{\mathbf{R}_c} D^{\alpha}_{\mu\nu} = q_\alpha \quad -\frac{S_{\mu\nu}\mathbf{R}}{R^3} + \frac{\mathbf{P}_{\mu\nu}}{R^3} - 3\frac{\left(\mathbf{P}_{\mu\nu}\cdot\mathbf{R}\right)\mathbf{R}}{R^5}\Bigg)\cdot\Bigg(\tag{2.38}$$

All terms are here direct except for $\nabla_{\mathbf{R}_a}\mathbf{P}_{\mu\nu}$, which must be computed from $\nabla_{\mathbf{X}_a}\mathbf{\Pi}_{\mu\nu}$, extracted from the tables, and the derivatives of the coefficients $A_{\mu\mu'}$.

Chapter 3

Free Energy Methods

We haven't got the money, so we'll have to think

Ernest Rutherford

3.1 Introduction

Suppose we would like to study a certain transformation (e.g, a chemical reaction, a conformational change) taking place in a system with coordinates $\{q_j\}$ defined by hamiltonian $\mathcal{H} = T + U$, with T the kinetic energy and U the potential energy, and assume this transformation can be described by the transition of a certain function of the coordinates, $\xi(q_1, \ldots, q_M)$, from one value ξ_0 to another ξ_1. This function will be referred to as the "reaction coordinate". This transformation could be a bond length, the rotation of an angle, etc. The function $\xi(q_1, \ldots, q_M)$ could be a vector; that is, there could be several of these reaction coordinates having importance for the description of the transformation. To describe the relative probabilities of the system finding itself at different values of the reaction coordinate, and thus be able to know the probability of the transformation taking place, estimate the expected life-times of the different conformations, etc, we would like to compute the probability density for a range of possible values of ξ, $P(z)$. [1] The probability profile is related to the so-called *Free Energy profile* by

$$\exp\left(-\beta F(z)\right) = P(z), \tag{3.1}$$

where $\beta = \dfrac{1}{kT}$ (with T the temperature and k the Boltzmann's constant)

and the probability density to find the system with $\xi(q_1, \ldots, q_N) = z$ can be written just as

$$P(z) = \langle \delta(\xi - z) \rangle. \tag{3.2}$$

The Free Energy is a concept familiar from standard thermodynamics, where is defined (for example, for systems at constant temperature and constant volume) as

$$F = U - TS, \tag{3.3}$$

where U is the internal energy of the system, S is the entropy and T is the temperature. [2] Thus, the Free Energy is the amount of work that the system can do in an

[1] Let us ξ to denote the function encoding the reaction coordinate and z for the different values ξ can take.

[2] Strictly speaking this is the Helmholtz Free Energy, while the Gibbs Free Energy, defined for systems at constant pressure, P, is defined in terms of the enthalpy: $G = H - TS$, with $H = U + PV$.

adiabatic trajectory, i.e, in a reversible process. In that sense, F can be understood as that part of the total internal energy which is not "doomed" to keep the temperature of the system (the entropic component) and can thus be, ideally, employed to exert work. The link between the thermodynamical concept and the statistical one is provided by the equation

$$F = -\beta^{-1} \log Z \tag{3.4}$$

with Z the partition function

$$Z = \int \int \Big(e^{-\beta \mathcal{H}(q',p')} dq' dp'. \tag{3.5}$$

Ergodicity

Theoretically, finding $F(z)$ is immediate: Before going on, some comments are in order: The average $\langle \delta(\xi - z) \rangle$ is taken over the statistical ensemble our system is thought to be in. In this context, we always consider our system to be at equilibrium in a Canonical Ensemble. That amounts to say that the probability of a structure with positions $q = \{q_j\}$ and momenta $p = \{p_j\}$ is just

$$P(q, p) = Z^{-1} e^{-\beta \mathcal{H}(q,p)}. \tag{3.6}$$

As we know, the average of any classical observable A in the canonical ensemble is just

$$Z^{-1} \int \int \Big(A(q, p) e^{-\beta \mathcal{H}(q,p)} dq dp.$$

The kinetic terms always cancel out as long as we are not interested in quantities depending explicitly on the momenta, so we can simplify it all by defining

$$Q = \int \Big(e^{-\beta U(q)} dq$$

as the "configurational partition function" (which we will call just partition function by abusing notation) and by ignoring all the dependencies on p. These integrals are impossible to compute except for very specific simple systems. Even numerically, for large systems with thousands of atoms with tons of different interactions, computers cannot solve them. One strategy to compute these integrals is to use the so-called Ergodic Property. In simple terms, ergodicity means that "ensemble average can be substituted by temporal averages for large enough times". Mathematically, this means that if we leave the system evolve along a trajectory, then:

$$\langle A \rangle := \frac{\int \int \Big(A(q, p) e^{-\beta \mathcal{H}(q,p)} dq dp}{\int \Big(\int \Big(e^{-\beta \mathcal{H}(q',p')} dq' dp'} = \lim_{T \to \infty} \frac{1}{T} \int_0^T \Big(A(q(t), p(t)) dt$$

For instance, if the dynamics is hamiltonian, so that the system evolves according to the hamiltonian flow with hamiltonian $\mathcal{H}$, then ergodicity is known to hold. It is actually an easy consequence of a deep and beautiful theorem, Poincare's recurrence theorem, which states that in the microcanonical ensemble a system always re-visits in finite time arbitrarily small neighbourhoods of any initial state.

Quasi-non ergodicity

With this said, our problem would look easy: $\langle \delta(\xi - z) \rangle$ could be computed from

a trajectory to give a good estimate of $P(z)$. In the identity above, however, we have a limit when the time goes to infinity, and of course we cannot perform an infinite simulation. It turns out that in most problems of interest the time needed for ergodicity to (approximately) hold is far larger than the achievable simulation time with modern computers. We refer to this phenomenon as "quasi-non-ergodicity", since ergodicity really holds in the system, but in the time scale we have access to it seems to be violated. The reason ergodicity is hindered is that our system typically presents several "valleys" and barriers in its energetic landscape of such a magnitude that the expected time spent on those valleys or the expected time needed to surpass those barriers is always far greater than the time scales accessible in the simulations. Thus, in our short simulations, we cannot obtain a good sampling of the configuration space, which seems to kill our hopes of computing averages by using the ergodic identity. However, if we could in some way "help" the system to sample more quickly the configuration space, then we could effectively use the ergodic identity.

Enhanced Sampling

This help could be accomplished by introducing an external fictional potential V depending on the reaction coordinates ξ alone (since we only need to enhance and accelerate the sampling over the possible values of the reaction coordinates), which flattens the energetic landscape and allows ξ to take a wide range of values in much shorter simulation times. Some care must be taken, since, of course, the averages in the new system $U+V$ differ from the averages in the real system of interest. However, there is a simple way to relate the probability densities in both systems. Call $P_U(\xi)$ to the real probability density of interest, and call $P_{U+V}(\xi)$ the probability obtained in the fake system. We have:

$$\begin{aligned} P_{U+V}(z) = \langle \delta(\xi - z) \rangle_{U+V} = e^{\beta F_{U+V}} \iint \left(e^{-\beta(U(q)+V(q))} \delta(\xi(q_1, \ldots, q_M) - z) dq = \right. \\ e^{-\beta V(z)} e^{\beta F_{U+V}} \int e^{-\beta U(q)} \delta(\xi - z) dq = e^{-\beta V(z)} e^{\beta F_{U+V}} \frac{e^{-\beta F_U}}{e^{-\beta F_U}} \iint \left(e^{-\beta U(q)} \delta(\xi - z) dq = \right. \\ e^{-\beta(V(z)+F_U-F_{U+V})} P_U(z). \end{aligned} \tag{3.7}$$

Therefore, we have:

$$P_U(z) = \exp\left(\beta \left[V(z) + F_U - F_{U+V}\right]\right) P_{U+V}(z),$$

which could in principle be used to estimate P_U from the knowledge of P_{U+V}. The idea would be to choose the fictional potential V so that in the biased system we have the ergodic property for the typical time scale of our simulations, which would in turn mean that we could make the approximation $P_{U+V}(z) = n_{U+V}^{-1} N(z)$, where n_{U+V} is the total number of snapshots taken in the simulation with the bias potential and $N(z)$ is the number of snapshots with $\xi(q) = z$.

However, if we want to get a good estimation of $P_U(z)$ from $P_{U+V}(z)$, we would need the sampling in the system $U+V$ to be extensive in the reaction-coordinate-space and nearly uniform. This could only be done if we knew before-hand the energetic landscape, which of course we do not!

It would be interesting to have a similar identity in the case we allow for different temperatures, that is, different β's. Let us know write explicitly the potential energies and temperatures of each P. In this case, we need to make a more explicit use of ergodicity:

$$\begin{aligned} P_{U,\beta}(z) &= Q_{U,\beta}^{-1} \int\!\!\int \delta\left(\xi(q)-z\right) \exp\left(-\beta U(q)\right) dq = \\ & Q_{U,\beta}^{-1} Q_{U+V,\beta'} Q_{U+V,\beta'}^{-1} \int\!\!\int \delta\left(\xi(q)-z\right) \exp\left(-(\beta-\beta')U(q)\right) \exp\left(-\beta' V(q)\right) \exp\left(-\beta'(U(q)+V(q))\right) = \\ & Q_{U,\beta}^{-1} Q_{U+V,\beta'} \exp\left(\beta' V(z)\right) \left\langle \exp\left(-(\beta-\beta')U(\cdot)\right) \delta(\xi(\cdot)-z) \right\rangle_{U+V}, \end{aligned} \tag{3.8}$$

where the $\langle\ \rangle_{U+V}$ denotes the average taking in the system described by potential $U+V$. **Umbrella Sampling** In practice, almost always several potentials V are used and the different estimations for $P_U(z)$ are combined in some way. These potentials are most typically taken to be harmonic potentials centered around some value of interest:

$$V(q) = \frac{k}{2}\left(\xi(q)-z_0\right)^2, \tag{3.9}$$

where z_0, the center of the harmonic potential, is taken as a value around which we would like to explore, and the "elastic" constant k is taken large enough so that the reaction coordinate $\xi(q)$ will only exhibit adequately small oscillations around z_0. These potentials, due to their shape, are referred to as Umbrella Potentials, and the sampling resulting from them as Umbrella Sampling [87].

If we had a huge computational power, far beyond what the most powerful supercomputers in existence are capable of providing, we would not need to go through all this trouble: just integrating Newton (or Schrödinger) equations would be enough. Since this is not the case, we need to come up with solutions and approximations, and, of course, many approaches are available. We could thus say, echoing Rutherford's words, that we haven't got the ~~money~~ limitless computational power, so we'll have to think.

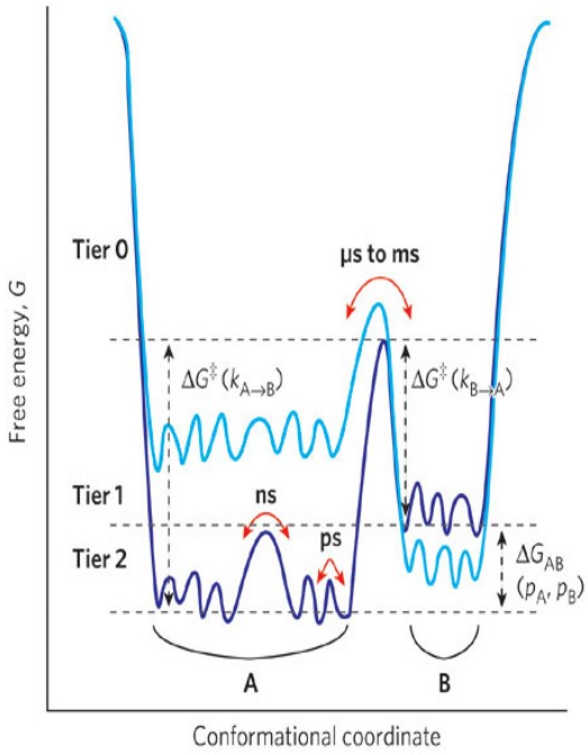

FIGURE 3.1: Schematic representation of time-scales and free energy barriers. Reaction time increases exponentially with the height of the barrier, and relatively small changes in Free energy can lead to dramatic changes in expected life-time of certain conformations.

3.2 Umbrella Integration Scheme

In the section we will study how the information of different Umbrella Sampling simulations can be combined to extract a global estimate of the Free Energy.

We present here two ideas: The first one is how to Umbrella Sampling and Thermodynamic Integration [?¿] are combined to yield another Free Energy method, the so-called Umbrella Integration [88]. The second point, which combined with the first yields a novel Umbrella Integration method, is our own proposal for a Free Energy method, which is based on approximating the Dirac delta by smooth functions.

1) **Umbrella Sampling and Umbrella Integration**

Since it is difficult to know beforehand which is the appropriate bias V to enhance ergodicity, usually we take several bias harmonic potentials $V_1, \dots, V_M$, each of those give us a different estimation $P_j(z)$ for $P_U(z)$, and what we do to is to combine them all in an appropriate fashion. To simplify notations, let us write the average of a quantity A in the following fashion:

$$\overline{A^j} = \langle A \rangle_{U+V_j}.$$

We can then write eq. 3.8 as:

$$P_j(z) = Q_{U,\beta}^{-1} Q_{U+V_j,\beta_j} \exp\left(\beta_j V_j(z)\right) \overline{\exp\left(-(\beta-\beta_j)U(\cdot)\right)\delta(\xi(\cdot)-z)^j}. \tag{3.10}$$

In Umbrella Integration [88], in practice always for all $\beta_j = \beta$, the probability densities $P_j(z)$ in the biased systems are substituted by gaussians with the observed means and typical deviation. Therefore, for the $j-$th window we have a mean μ_j and a standard deviation σ_j. Equation 3.10 then becomes

$$P_j(z) = Q_{U,\beta}^{-1} Q_{U+V_j,\beta} \exp\left(\beta V_j(z)\right) \left(\frac{1}{\sqrt{2\pi\sigma^2}} \exp \quad -\frac{(z-\mu_j)^2}{2\sigma_j^2}\right)\left(\tag{3.11}$$

Here we take logarithms to reach:

$$-\beta^{-1} \log P_j(z) = -V_j(z) + \beta^{-1} \frac{(z-\mu_j)^2}{2\sigma_j^2} + C, \tag{3.12}$$

where C is an unimportant constant which vanishes when we take derivatives. If we did not take derivatives, however, the value of this constant, which relates the partition functions of the unbiased and the biased systems, would be an important obstacle. Next, from each of these estimates for $P_j(z)$, we construct an estimate for the Free Energy:

$$F_j(z) = -\beta^{-1} \log P_j(z) \tag{3.13}$$

And thus write, for the derivative of the Free Energy:

$$\frac{dF_j(z)}{dz} = -\beta^{-1} \frac{d}{dz} \log P_j(z) = -V_j'(z) + \beta^{-1} \sigma_j^{-2} (z - \mu_j). \tag{3.14}$$

and we combine all these estimations in a weighted manner:

$$\frac{dF(z)}{dz} = \sum_j c_j(z) \frac{dF_j(z)}{dz}, \tag{3.15}$$

with weights taken as normalized weights in terms of the same probability distributions:

$$c_j(z) = \frac{G_j(z)}{\sum_j G_j(z)}, \tag{3.16}$$

where the $G_j(z)$ are the gaussian functions representing the density probability in the corresponding biased system:

$$G_j(z) = \frac{1}{\sqrt{2\pi\sigma^2}} \exp \quad -\frac{(z-\mu_j)^2}{2\sigma_j^2}\Bigg)\Bigg($$

. Putting all together we finally have:

$$\frac{dF(z)}{dz} = \sum_j c_j(z) \left(-V_j'(z) + \beta^{-1} \sigma_j^{-2} (z - \mu_j)\right), \tag{3.17}$$

and by constructing these estimates for a grid of z values we can construct the derivative of the Free Energy and proceed to integrated it to finally get the Free Energy profile $F(z)$.

2) **Approximations of the convolution identity**

It is well known that given any mass-concentrating, normalized, almost everywhere positive and integrable ϕ, the succession $n\phi(nx)$ converges to the δ function in the distributional sense as $n \to \infty$. Let us pick any smooth function with this characteristic and pick a large n. What we do now is to make the substitution $\delta(\xi(q) - z) \to n\phi(n(\xi(q) - z))$ in definition 3.2:

$$P(z) = Q^{-1} \int\!\!\int e^{-\beta U(q)} \delta(\xi(q) - z) dq$$

. The only free parameter here is the n. In principle, the larger n is the better, but as n increases the number of potentials that we need to use also increases, since we need to be able to cover a continuous interval of values of the reaction coordinate xi. The number of potentials used must be consistent with the size of the grid. Here, something similar happens with the choice of n. When taking derivatives with respect to z, we have $\frac{\partial}{\partial z}[n\phi(n(\xi(q) - z))] = -n^2\phi'(n(\xi(q) - z))$. A straight-forward computation leads us to:

$$\frac{\partial}{\partial z} \log\ P_j(z) = \beta_j V'(z) - n \frac{\overline{\phi'(n(\xi(\cdot) - z)) \exp\left(-(\beta - \beta_j)U(\cdot)\right)^j}}{\overline{\phi(n(\xi(\cdot) - z)) \exp\left(-(\beta - \beta_j)U(\cdot)\right)^j}}. \tag{3.18}$$

The case of equal temperatures has the form:

$$\frac{\partial}{\partial z} \log\ P_j(z) = \beta V'(z) - n \frac{\overline{\phi'(n(\xi(\cdot) - z))^j}}{\overline{\phi(n(\xi(\cdot) - z))^j}}. \tag{3.19}$$

And we plug these estimations again into eq. 3.15 to get an estimation of $\frac{\partial F(z)}{\partial z}$ which, upon integration, yields $F(z)$. It is also interesting to consider how this method can be applied to the estimation of the second derivative, $H(z)$, which is the hessian in the case we are dealing with multi-dimensional reaction coordinates. Notice that we can always assume to be working with radial functions, so that basically the identity above also holds in general, with the exception that the sequence of functions approximating the δ is now:

$$n^d \phi(nx),$$

where d is the number of reaction coordinates. Taking again derivatives with respect to z, we find:

$$\frac{\partial^2}{\partial z^2} \log P_j(z) = \beta V''(z) + n^2 \frac{\overline{\phi''\left(n(\xi(\cdot) - z)\right)^j}}{\overline{\phi\left(n(\xi(\cdot) - z)\right)^j}} - n^2 \left(\frac{\overline{\phi'\left(n(\xi(\cdot) - z)\right)^j}}{\overline{\phi\left(n(\xi(\cdot) - z)\right)^j}} \right)^2. \tag{3.20}$$

This seems to be a clear improvement over Umbrella Integration, where the estimation given by each bias potential for the Hessian is a constant.

The function ϕ can be chosen with great generality; a natural choice would be, for example, to take as ϕ a normalized Gaussian, $\phi(x) = \frac{1}{\sqrt{\pi}} e^{-x^2}$.

3.3 WHAM equations

The idea behind WHAM (Weighted Histogram Analysis Method) is to perform several simulations with different bias potentials, $V_j(z)$, get for each one of those a different estimation of $P_0(z)$, which we will call $P_j(z)$, and to combine the information of all those estimations in the form of a linear combination:

$$P_0(z) \approx \sum_{j=1}^{R} c_j(z) P_j(z), \tag{3.21}$$

where $P_j(z)$ is estimated as

$$P_j(z) = n_j^{-1} \exp\left[\beta \left(V_j(z) + F_0 - F_j\right)\right] N_j(z),$$

where now n_j is the total number of data points in the simulation with potential V_j, $N_j(z)$ is the total number of points in that simulation with $\xi(q) = z$, and F_0 and F_j denote respectively the free energies of the unbiased system and that of the system with bias potential V_j. The coefficients $c_j(z)$ are subjected to the condition $\sum_j c_j(z) = 1$.

In practice, of course, this definition of $N_j(z)$ is absurd, since one has a finite amount of data. The practical definition -an approximation to the δ, so to speak- is

$$N_j(z) = \sum_{s=1}^{n_j} \epsilon^{-1} \chi_{I_z}(z_{j,s}),$$

where $z_{j,s}$ is the value of teh reaction coordinate xi at the $s-$th snapshot of the $j-$th simulation, $I_z = [z - \epsilon/2, z + \epsilon/2]$ for an appropriate width ϵ (which must be conveniently chosen depending on how many simulations we make and how peaked the potentials are) and $\chi_{I_z}(x)$ is the so-called characteristic function of the interval I_z, which is defined as 1 whenever $x \in I_z$ and 0 otherwise. From now on, we will call it just χ_z for brevity. ϵ is a parameter of our choice. The only important detail is that this function is divided by ϵ, so that $\lim_{\epsilon \to 0^+} \epsilon^{-1} \chi_z(x) = \delta(x)$

The main problem is thus how to choose these coefficients $c_j(z)$, and the answer is the core of the WHAM strategy. In the combination $\sum_{j=1}^{R} c_j(z) P_j(z)$, with $P_j(z) = n_j^{-1} e^{\beta(V_j(z) + F_0 - F_j)} N_j(z)$, each $N_j(z)$ is a random variable. In WHAM, **the coefficients $c_j(z)$ are determined by finding the minimum of the statistical error (the variance) $\sigma^2 \left[\sum_{j=1}^{R} c_j(z) P_j(z)\right]$** under the condition $\sum_j c_j(z) = 1$.

Derivation of the WHAM equations The $N_j(z)$ are pairwise uncorrelated in the $j-$th index (but, beware, not in z!), so we have:

$$\sigma^2 \left[\sum_j c_j(z) P_j(z)\right] = \sum_j c_j^2(z) \sigma^2(P_j),$$

which equals:

$$\sum_j c_j^2(z) n_j^{-2} \exp\left[2\beta \left(V_j(z) + F_0 - F_j\right)\right] \sigma^2(N_j(z)).$$

Applying the method of Lagrange multipliers method to the problem of minimizing this quantity above under the normalization condition $\sum_j c_j(z) = 1$, we have that,

for a certain constant $\tilde{C}$, it holds:

$$2c_j(z)\sigma^2(P_j) = \tilde{C},$$

so:

$$c_j(z) = \frac{C}{\sigma^2(P_j(z))}.$$

The normalization condition then implies:

$$c_j(z) = \frac{[\sigma^2(P_j(z))]^{-1}}{\sum_k [\sigma^2(P_k(z))]^{-1}}.$$

As noted before, $\sigma^2(P_j(z)) = n_j^{-2} \exp\left[2\beta\left(V_j(z) + F_0 - F_j\right)\right] \sigma^2(N_j(z))$, so the key is to compute the variances $\sigma^2(N_j(z))$, and it is in this computation that the technicalities of the WHAM derivation appear.

Let us forget for a moment about the j index and focus on an arbitrary simulation, in which we estimate the probability density precisely as $n^{-1}N(z) = n^{-1}\sum_{s=1}^{n} \epsilon^{-1}\chi_{I_z(z_s)}$, with z_s the $s-$th snapshot of the simulation and $I_z = [z - \epsilon/2, z + \epsilon/2]$, with ϵ a certain tolerance of our choice. We remind also that $\chi_I(x)$ is the characteristic function of the interval I, meaning that $\chi_I(x)$ is 1 if $x \in I$ and 0 otherwise.

The expectation is linear, so $\langle N(z)\rangle = \sum_{s=1}^{n} \epsilon^{-1}\langle\chi_z(z_s)\rangle$, and these expectations are:

$$\langle\chi_z(z_s)\rangle = p \times 1 + (1-p) \times 0,$$

with p the probability of "falling" in the interval I_z. It is a fact of life that ergodicity is equivalent with subsets of the configurational/phase space being visited a certain constant times the volume of that subset in the configurational/phase space. Thus, assuming ergodicity (it doesn't hold in general, but it can be assumed to hold for the observable we are interested in), p must be a constant times ϵ. For a fixed z, we then finally get

$$p = \epsilon n^{-1}\langle N(z)\rangle.$$

Next we compute the variance, $\sigma^2\left(\sum_{s=1}^{n} \epsilon^{-1}\chi_z(z_s)\right) = \epsilon^{-2}\langle(\sum_{s=1}^{n}\chi_z(z_s) - \langle\chi_z\rangle)^2\rangle$. This is splitted into two parts: an uncorrelated one, $\langle\sum_{s=1}^{n}\left(\chi_{I_z(z_s)} - \langle\chi_z\rangle\right)^2\rangle$, and a part containing the correlations, $2\sum_{s=1}^{n}\sum_{s'=s+1}^{n}\langle\chi_z(z_s)\chi_z(z_{s'})\rangle - \langle\chi_z\rangle^2$. Let us call z_0 to the value of the reaction coordinate $\xi(q)$ at the beginning of the simulation, an in general, as before, we will call z_s to the value of ξ at the $s-$th snapshot. We write the first uncorrelated part as $n\left(\langle\chi_z^2\rangle - \langle\chi_z\rangle^2\right)$ and the second uncorrelated part, following [89] is approximated as:

$$2n\sum_{s=1}^{n}\left(1 - \frac{s}{n}\right)\left(\langle\chi_z(z_0)\chi_z(z_s)\rangle - \langle\chi_z\rangle^2\right)$$

Defining $\Delta\chi_z^s$ as $\chi_z(z_s) - \langle\chi_z(z_s)\rangle$, and extracting a common factor $\langle\chi_z^2\rangle - \langle\chi_z\rangle^2$, we have:

$$\langle\left(\sum_{s=1}^{n}\chi_z(z_s) - \langle\chi_z\rangle\right)^2\rangle = n\left(1 + 2\sum_{s=1}^{n}(1 - \frac{s}{n})\frac{\langle\Delta\chi_z^0\Delta\chi_z^s\rangle}{\langle\Delta\chi_z\rangle}\right)\left(\langle\chi_z^2\rangle - \langle\chi_z\rangle^2\right)$$

Therefore, defining

$$\tau(z) = \sum_{s=1}^{n}(1 - \frac{s}{n})\frac{\langle \Delta\chi_z^0 \Delta\chi_z^s \rangle}{\langle \Delta\chi_z \rangle}$$

as the correlation time of the simulation and

$$g(z) = (1 + 2\tau(z))n$$

we have reached the important equation:

$$\sigma^2(N(z)) = \sigma^2 \left(\sum_{s=1}^{n} \epsilon^{-1}\chi_z(z_s) \right) = \epsilon^{-2} g(z) \left(\langle \chi_z^2 \rangle - \langle \chi_z \rangle^2 \right) =$$
$$\epsilon^{-2} g(z)(p - p^2) \approx \epsilon^{-2} g(z) p = \epsilon^{-2} g(z) \langle N(z) \rangle \epsilon = \epsilon^{-1} g(z) \langle N(z) \rangle$$

This identity is key in the derivation of the WHAM equations. Each variance $\sigma^2(N_j(z))$ is thus approximated as $\epsilon^{-1} g_j(z) \langle N_j(z) \rangle$, with $g_j(z)$ defined as above for the particular $j-$th simulation. Furthermore, $\langle N_j(z) \rangle$ is approximated as:

$$\langle N_j(z) \rangle \approx N_j(z) = n_j \exp\left[-\beta \left(V_j(z) + F_0 - F_j \right)\right] P_j(z) \approx$$
$$n_j \exp\left[-\beta \left(V_j(z) + F_0 - F_j \right)\right] P_0(z),$$

with $P_0(z)$ the true probability density we are looking for. This approximation is very natural: the first step is the most evident for the average, since we only have one $j-$th simulation, so as to speak. The second one is just the inversion we derived previously relating probability densities between two different systems. And the last step is just a refinement: we substitute the estimated $P_j(z)$ from the $j-$th simulation with the correct probability density $P_0(z)$.

Next, plugging all this information in our equation $P_0(z) = \sum_j c_j(z) P_j(z)$, we have that:

$$P_0(z) = \sum_j c_j(z) P_j(z) = \sum_{j=1}^{R} \frac{\exp\left[-\beta(V_j(z) - F_j)\right] n_j g_j(z)^{-1} P_j(z)}{\sum_{k=1}^{R} \exp\left[-\beta(V_k(z) - F_k)\right] n_k g_k(z)^{-1}} =$$
$$\sum_{j=1}^{R} \frac{\exp\left[-\beta(V_j(z) - F_j)\right] n_j g_j(z)^{-1} n_j^{-1} N_j(z) \exp\left[\beta(V_j(z) - F_j)\right] \exp(\beta F_0)}{\sum_{k=1}^{R} \exp\left[-\beta(V_k(z) - F_k)\right] n_k g_k(z)^{-1}} =$$
$$e^{\beta F_0} \sum_{j=1}^{R} \frac{g_j(z)^{-1} N_j(z)}{\sum_{k=1}^{R} \exp\left[-\beta(V_k(z) - F_k)\right] n_k g_k(z)^{-1}}$$

This depends on the F_j, which of course are not known. Ideally, $P_0(z) = e^{\beta F_0} \int e^{-\beta U} \delta(\xi - z) dq$, and, calling $\tilde{P}_j(z)$ to the probability density of the system with the potential V_j, (Beware! Do not confuse this with $P_j(z)$, which is the estimation of the probability density in the Unbiased system gotten from the simulation with potential V_j) we have:

$$\frac{N_j(z)}{n_j} \approx \tilde{P}_j(z) = e^{\beta F_j} \iint e^{-\beta U} e^{-\beta V_j(\xi)} \delta(\xi - z) dq.$$

We then have:

$$P_0(z) e^{-\beta V_j(z)} = e^{\beta F_0} e^{\beta F_j} e^{-\beta F_j} \iint e^{-\beta U} e^{-\beta V_j(\xi)} \delta(\xi - z) dq = e^{\beta F_0} e^{-\beta F_j} \tilde{P}_j(z).$$

Integrating both sides of this equation we have:

$$e^{-\beta F_j} = e^{-\beta F_0} \int\!\!\!\int P_0(z) e^{-\beta V_j(z)} dz.$$

Finally, we can write:

$$\begin{aligned}
e^{-\beta F_j} &= e^{-\beta F_0} \int\!\!\!\int P_0(z) e^{-\beta V_j(z)} dz = \\
&\int\!\!\!\int \sum_{k=1}^{R} \frac{g_k(z)^{-1} N_k(z) e^{-\beta V_j(z)}}{\sum_{l=1}^{R} n_l^{-1} g_l(z)^{-1} e^{-\beta(V_l(z)-F_l)}} dz = \\
&\int\!\!\!\int \sum_{k=1}^{R} \frac{g_k(z)^{-1} e^{-\beta V_j(z)} \sum_{s=1}^{n_k} \epsilon^{-1} \chi_z(z_{k,s})}{\sum_{l=1}^{R} n_l^{-1} g_l(z)^{-1} e^{-\beta(V_l(z)-F_l)}} dz = \\
&\epsilon^{-1} \sum_{k=1}^{R} \sum_{s=1}^{n_k} \int\!\!\!\int \frac{g_k(z)^{-1} e^{-\beta V_j(z)} \chi_z(z_{k,s})}{\sum_{l=1}^{R} n_l^{-1} g_l(z)^{-1} e^{-\beta(V_l(z)-F_l)}} dz,
\end{aligned}$$

where $z_{k,s}$ is the value of ξ at the $s-$th snapshot of the $k-$th simulation. Calling $V_j^{k,s}$ to the value of the $j-$th potential at the $s-$th snapshot of the $k-$th simulation, we can compute each of the previous integrals as:

$$\int\!\!\!\int \frac{g_k(z)^{-1} e^{-\beta V_j(z)} \chi_z(z_{k,s})}{\sum_{l=1}^{R} n_l^{-1} g_l(z)^{-1} e^{-\beta(V_l(z)-F_l)}} dz \approx \epsilon \frac{g_k^{-1} e^{-\beta V_j^{k,s}}}{\sum_{l=1}^{R} n_l^{-1} g_l^{-1} e^{-\beta(V_l^{k,s}-F_l)}},$$

which, when plugged into the equation above gives **the final self-consistent WHAM equations**:

$$e^{-\beta F_j} = \sum_{k=1}^{R} \sum_{s=1}^{n_k} \frac{g_k^{-1} e^{-\beta V_j^{k,s}}}{\sum_{l=1}^{R} n_l^{-1} g_l^{-1} e^{-\beta(V_l^{k,s}-F_l)}}. \tag{3.22}$$

In practical implementations, one solves this equations within a self-consistent iterative approach: we pick an initial Ansatz, in which all the F_j are zero, plug that into the right-hand side of the equation, extract new F_k, introduce these into the right-hand side, and so on until the inputs and the outputs differ in no more than a certain tolerance (whose value is chosen by the user). Once the F_j have been determined self-consistently, we employ eqs. 3.21 and 3.1 to get the desired estimation for the probability density and, thus, the Free Energy profile, $F(z)$.

In Grossfield's implementation [90], the $g_k(z)$ are assumed to be equal for different k, so that they cancel out of the WHAM equations. However, sometimes, the strong correlations observed near barriers/transition states, particularly in chemical reactions, suggest that it might be interesting to take those factors g_k into account.

3.4 Steered Molecular Dynamics

An alternative approach to Umbrella Sampling is to add to the system a potential varying in time. Most typically, this is also an harmonic potential, but whose center is "dragged" along a certain direction:

$$V(\xi(\{q_j\}), t) = \frac{k}{2} \left(\xi(q) - f(t)\right)^2, \tag{3.23}$$

where $\xi(q)$ is the reaction coordinate as a function of all the $\{q_j\}$ and $f(t)$ is the function encoding the value of the center of the harmonic potential. With this type of potential, for instance, by letting $\xi(\{q_j\})$ be a bond distance or an angle, we can force a chemical reaction to happen and study how the rest of the system reacts (other bonds, partial charges, electronic levels, and so on, see chapter 4). Here, we study how Steered Molecular Dynamics can be employed to actually calculate Free energy differences and profiles.

3.4.1 Thermodynamic Integration

Suppose we want to find the difference of free energies between a system with hamiltonian H_0 and another one with hamiltonian H_1.

The partition function of each of this intermediate systems is just $Z_\lambda = \int \exp\left(-\beta H_\lambda\right) dqdp$, and the free energy by definition is just $F_\lambda = -\beta^{-1} \log Z_\lambda$. Formally:

$$F_1 - F_0 = \int_0^1 \frac{dF_\lambda}{d\lambda} d\lambda,$$

but we have:

$$\frac{dF_\lambda}{d\lambda} = -\beta^{-1} \frac{d(Z_\lambda)/d\lambda}{Z_\lambda} = Z_\lambda^{-1} \int \frac{dH_\lambda}{d\lambda} \exp(-\beta H_\lambda) d\lambda = \langle \frac{dH_\lambda}{d\lambda} \rangle_\lambda,$$

where the brackets with the subindex λ indicate average in the ensemble defined by H_λ.

In conclusion, we have:

$$F_1 - F_0 = \int_0^1 \langle \frac{dH_\lambda}{d\lambda} \rangle_\lambda d\lambda. \tag{3.24}$$

To use this in practice we perform a simulation in which we change slowly the value of λ from 0 to 1. A particular case of extreme relevance would be steering an Umbrella potential as described above.

If this looks suspicious, that's because it is: The whole idea is based on the assumption that as we switch the value of λ, our system remains in equilibrium, so that the probability density in phase space is given at each step by the canonical one, $P(q,p) = Z_\lambda^{-1} e^{-\beta H_\lambda(q,p)}$. Although this assumption can be justified if the switching is performed slowly enough, in practice, no matter how well thermalized our initial system is, when changing λ the probability density will lag behind the equilibrium distribution and would need some time to converge to the canonical probability density. This is thus an *adiabatic approximation*, in which changes are assumed to be so slow that the system can be thought to reach thermodynamic equilibrium infinitely quickly. The adiabatic process are reversible, i.e, without variation of the entropy, and from standard thermodynamics we know that in them it holds that the work performed to go from one state S_0 to another S_1 equal the free energy difference between S_1 and S_2, $F_1 - F_0 = W$. Thermodynamic integration is thus nothing but a formalization of this concept, where the parameter λ is employed to artificially "move" the system from one state to other. In particular, we can use as $\lambda-$dependent part of the hamiltonian H_λ a temporal-dependent Umbrella potential such as in eq. 3.23, and use eq. 3.24 and the average work at each step to compute a Free Energy profile. However, in generic processes in which adiabaticity is too strong an assumption, the identity $F_1 - F_0 = W$ is no longer valid, and we strictly have an inequality, $F_1 - F_0 < W$, stating that some work has been "dissipated", not usefully

employed for the transformation [3]. Below, we discuss the Jarzynski identity, which, as a theoretical generalization of this method, in principle overcomes this difficulty.

3.4.2 The Jarzynski identity

Thermodynamic Integration, in which the work along a single trajectory is employed to calculate the Free Energy assuming adiabaticity, can be regarded as a limit case of a much more general method, in which the properties of out-of-equilibrium processes are exploited. In the following, I will follow closely Jarzynski's original works [91–93] and stick to the assumption that our systems evolve along a Langevin dynamics. Imagine we have two systems given, one with hamiltonian H_1 and another one with hamiltonian H_2, and imagine we want to compute the free energy difference between these two systems. We can connect the two systems with a continuous path of hamiltonians H_λ, as is done in the technique of thermodynamic integration. If we let the system evolve as we change λ (fast or slow), the trajectories thus obtained joining the first system and the second will be in general of course out of the equilibrium. We can think of our original system as one thermalized, where the probability density is the canonical one, $P(q,p) = Z_1^{-1}\exp\left(-\beta H_1(q,p)\right)$. The evolution of this probability density is assumed to be markovian and is thus governed by a deterministic equation of the form:

$$\frac{dP_\lambda(q,p)}{dt} = \int \hat{R}_\lambda P_\lambda(q,p) := \int R_\lambda(q,p;q',p')P_\lambda(q,p)dq'dp',$$

(we are closely following Jarzynski's original notation here) where $R_\lambda(q,p;q',p')$ is the derivative of the transition probability function and the time dependence is assumed to be contained exclusively in the parameter λ. The operator $\hat{R}_\lambda$ can be explicitly described in the context of Langevin dynamics, and arises directly from the Fokker-Planck equation associated to the Langevin equation:

$$\hat{R}_\lambda P_\lambda(q,p) = \{H_\lambda, P_\lambda\} + \gamma\frac{\partial(pP_\lambda)}{\partial p} + \frac{D}{2}\frac{\partial^2 P_\lambda}{\partial p^2},$$

with γ and D related by $\gamma = \frac{\beta D}{2}$ (the fluctuation-dissipation theorem).

Along a particular trajectory, the work W exerted on the system to make the transformation from the system H_1 to the system H_2 is defined as:

$$W = \int_0^{t_s} \dot{\lambda}\frac{\partial H_\lambda}{\partial \lambda}dt.$$

In general, the work along a trajectory is greater than the free energy difference, and only in adiabatic paths, in which equilibrium can be assumed at each step, is the work equal to the free energy difference, which serves as a different validation of the thermodynamic integration technique. Indeed, $\Delta F = \int_0^1 \langle\frac{\partial H_\lambda}{\partial \lambda}\rangle_\lambda d\lambda$ is just a particular case of $W = \int \dot{\lambda}\frac{\partial H_\lambda}{\partial \lambda}dt$ combined with the fact $W = \Delta F$ in adiabatic trajectories.

Summing up, we only have a equality relating the work along a trajectory to free energy in equilibrium, and out of the equilibrium it seems we can only formulate inequalities, such as the Second Principle of Thermodynamics mentioned in the previous section (which is nothing but the statistical fact $W \geq \Delta F$). Taking this into

[3] This is just a formulation of the Second Principle of Thermodynamics

account, it is certainly amazing that there is an identity relating work performed in out-of-equilibrium simulations with equilibrium free energy differences. This identity, called Jarzynski's identity, states that:

$$\exp\left(-\beta\Delta F\right) = \overline{\exp\left(-\beta W\right)}, \tag{3.25}$$

where the over-line indicates that we are taking averages over all the possible trajectories joining the system H_1 with the system H_2. This is a bit tricky, since a lot of technicalities have to be consider in order for this "path integral" to make any sense at all.
[4]

There are several proofs of the Jarzynski equation. Jarzynski's original idea was to introduce a modified density whose evolution equation admits an easy solution with the form of a canonical density. He defined $Q(z,t)$ as the average of $\exp\left(-\beta W\right)$ for all trajectories up to time t passing by z at time t. Next, Jarzynski defined the function

$$g(z,t) = P_\lambda(z)Q(z,t)$$

and computed its evolution equation, which turns out to be:

$$\frac{\partial g}{\partial t} = \left(\hat{R}_\lambda - \beta\dot{\lambda}\frac{\partial H_\lambda}{\partial \lambda}\right) g.$$

To prove this equation we need to understand how the path integral involved in the definition of $\overline{\exp\left(-\beta W\right)}$ is understood. Again, we follow Jarzynski's notation. For dm a measure in the space of all trajectories connecting system H_1 to system H_2, and for $\mathcal{P}(z(t))$ the probability density of choosing the particular path $z(t)$, we have:

$$\overline{\exp\left(-\beta W\right)} := \int\!\!\!\int\!\!\!\left(\mathcal{P}(z(t))\exp\left(-\beta W\right) dm.\right.$$

To make sense of this, we need to discretize the path. Let $t_0 = 0, t_1 = \delta t, \ldots, t_n = n\delta t, \ldots, t_N = N\delta t = t_s$, be a partition of the time interval of the simulation ($\delta = t_s/N$). Let us call $z_n = z(t_n)$. We think of λ evolving in discrete steps $\delta\lambda = 1/N$, happening at times $t_1, t_2, \ldots$. We pick an euclidean measure in the space of all path, so that in the discrete approximation to the path integral we just have:

$$\int dm = \int dz_0 \int\!\!\!\int\!\!\!\left(dz_1 \ldots \int\!\!\!\int\!\!\!\left(dz_N.\right.\right.$$

On the other hand, the probability density of each path, $\mathcal{P}(z(t))$ can be written, in the discretization, as a product of the corresponding transition probabilities. Indeed, let us define $P^{\delta t}_{\lambda_j}(z_{j-1}|z_j)$ as the probability of transitioning from z_{j-1} to z_j in a time δt when the underlying hamiltonian is H_λ and let $p_0(z)$ denote the canonical probability density with underlying hamiltonian H_0. Then in the discretized case we have:

$$\mathcal{P}(z(t)) = p_0(z_0)\prod_{j=1}^{N} P^{\delta t}_{\lambda_j}(z_{j-1}|z_j).$$

[4] In what follows, we call $z = (q,p)$, as Jarzynski does, for brevity

On the other hand, the work along the discretized trajectory can be expressed as:

$$W(z(t)) = \sum_{n=1}^{N} H_{\lambda_n}(z_{n-1}) - H_{\lambda_{n-1}}(z_{n-1}) := \sum_{n=1}^{N} \delta H_n(z_{n-1}),$$

having defined $\delta H_n(z) = H_{\lambda_n}(z) - H_{\lambda_{n-1}}(z)$.

These are all the ingredients needed to define the path integral. What we need now is to define the equivalent of the function $g(z,t)$ defined above in the discretized setting. Taking an intermediate M between 0 and N, we can define:

$$g(z,t_M) := g_M(z) := \int\left(p_0(z_0)\prod_{j=1}^{M-1}\left(P_{\lambda_j}^{\delta t}(z_{j-1}|z_j)\right)\left(\exp\quad -\beta\sum_{n=1}^{M}\delta H_n(z_{n-1})\right)P_{\lambda_M}^{\delta t}(z_{M-1}|z)dz_0dz_1\ldots dz_{M-1}.\right.$$

In particular, notice that for $M = N$ we have the trivial relationship $\overline{\exp\left(-\beta W\right)} = \int\left(g_N(z)dz.\right.$

Now, notice that by definition, there is an immediate recursive relation between the g_M:

$$g_{M+1}(z) = \int\left(g_M(z_M)e^{-\beta\delta H_{M+1}(z_M)}P_{\lambda_{M+1}}^{\delta t}(z_M|z)dz_M.\right.$$

The idea now is to expand in power series of δt the two terms $e^{-\beta\delta H_{M+1}(z_M)}$ and $P_{\lambda_{M+1}}^{\delta t}(z_M|z)dz_M$. Since δt is assumed to be small (and actually we are about to take the limit $\delta t \to 0$), we make the first-order / linear approximations:

$$\begin{aligned} e^{-\beta\delta H_{M+1}(z_M)} =& 1 - \beta\delta H_{z_{M+1}}(z_M) \\ P_{\lambda_{M+1}}^{\delta t}(z_M|z)dz_M =& \delta(z_M - z) + R_{\lambda_{M+1}}(z_M,z)\delta t, \end{aligned}$$

where $R_\lambda(z,z')$ is, we remind, the time derivative of the probability transition function.

Plugging these two Taylor expansions into the recursion relation above:

$$\frac{g_{M+1}(z) - g_M(z)}{\delta t} = -\beta g_M(z)\frac{\delta H_{M+1}(z)}{\delta t} + \int\left(g_M(z_M)R_{\lambda_{M+1}}(z_M,z)dz_M.\right.$$

Passing to the limit $\delta t \to 0, N \to \infty$, and recalling that $\lambda(t) = t/t_s$, we finally have, as stated above:

$$\frac{\partial g}{\partial t} = \left(\hat{R}_\lambda - \beta\dot{\lambda}\frac{\partial H_\lambda}{\partial\lambda}\right)g(z,t).$$

The next step, simpler but smart, is to realize that $g(z,t) = Z_0^-1\exp\left[-\beta H_\lambda(z)\right]$, and this is basically the final idea of the derivation, since the rest is now trivial:

$$\begin{aligned} &\overline{\exp\left[-\beta W\right]} = \int\left(g(z,t_s)dz = \right. \\ &Z_0^{-1}\int\left(\exp\left[-\beta H_1(z)\right]dz = \frac{Z_1}{Z_0} = \right. \\ &\exp\left(-\beta\Delta F\right). \end{aligned}$$

In practice, the way the Jarzynski identity is employed to compute the free energy profiles along a distance defining a chemical reaction is as follows: First of all,

steered molecular simulations are performed, in which we drag our reaction coordinate of interest along a certain path. We accomplish so by defining a harmonic potential of variable center: $V_\lambda = K(\xi - \lambda(t))^2$. Our typical problem is that we have a chemical reaction "defined" by the transition of ξ from value z_0 to value z_1. We then perform several of this trajectories starting from independent conformations corresponding to system H_1 and calculate the work on each of them. Each single trajectory yields an approximation to the Free Energy profile via Thermodynamic Integration, and, although taking the average formally does not give anything useful, taking the exponential averages as in eq. 3.25 yields the desired equilibrium Free Energy profile.

3.5 Some Applications

All the free energy methods studied in previous sections have been applied to obtain free energy profiles and maps in a number of systems.

3.5.1 Proton transfer in DNA

The problem we studied with the greatest detail was that of proton transfer reaction in guanine-cytosine base-pairs (see chapter 4), where we tested all the different methods available. In such setting, all the method were essentially equivalent, and even Thermodynamic Integration (which can be thought as an extremal case of Jarzynski's identity with just one trajectory) yields an accurate result. As an example, we show here a comparison between two applications of Jarzynski's identity over sets of six trajectories, one of them slow (7 ps each trajectory) and other fast (1 ps each trajectory), and WHAM and UI (which yield practically the same result, except for WHAM being slightly more noisy)

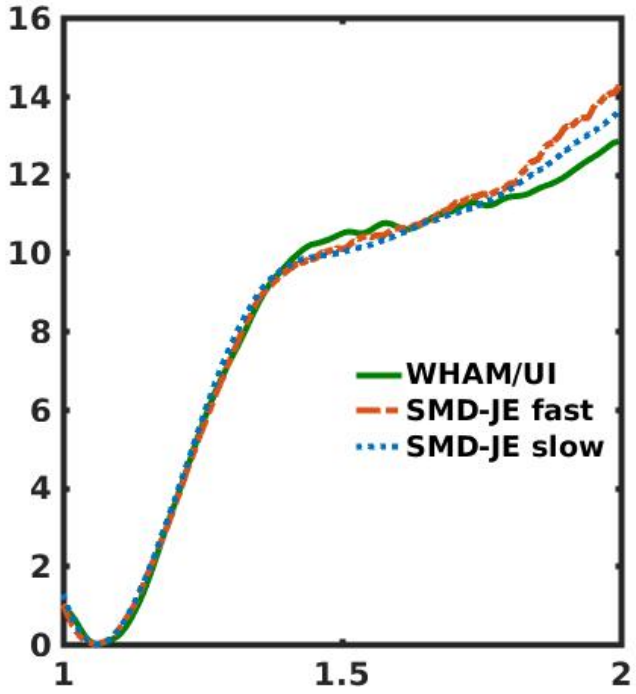

FIGURE 3.2: Free Energy in kcal/mol in terms of a distance d, in Armstrong, between an hydrogen and a nitrogen atom (see fig 4.1). $d \approx 1.1$, where the minimum is located, corresponds to the usual configuration in DNA base-pairs. Configurations with $d > 1.5$ correspond to rare tautomeric forms which are mutagenic because they alter the canonical complementarity of base-pairs (see chapter 4).

This comparison shows that Jarzynski's is to be trusted in this particular problem (for details, see chapter 4). Since Jarzynski is much more efficient that Umbrella Sampling, where many more configurations need to be sampled, this makes it the method of choice for most problems. However, as we will later explain, in this case the proton transfer is a quasi-adiabatic process, meaning that Thermodynamic Integration alone is already quite useful, while the true interest of Jarzynski's identity lies in its potential application for processes out of equilibrium, where he identity still holds true. However, in practice, such processes (for example, the movement of proton H4 in the guanine-cytosine base-pair, see again chapter 4) require a tremendous number of trajectories for the application of Jarzynski's identity to converge, which makes it very costly or even unfeasible, and suggest that Jarzynski's approach is precisely most useful when it is trivial; that is, when just one trajectory yields a good accurate result.

3.5.2 Si adatoms oscillating on a surface

Another problem, in which we applied WHAM, was the calculation of a Free Energy map for different configurations of the heights of four Si adatoms on the surface K/Si(111):B, with one potassium atom per $\sqrt{3} \times \sqrt{3}$ unit cell.

This system has received much attention in research because at room temperature its observed non-metallic $\sqrt{3} \times \sqrt{3}$ has been regarded as a Mott phase.

However, DFT calculations yield as the Ground State a CDW (Charge Density Wave) $2\sqrt{3} \times \sqrt{3}$ structure, both at room temperatures and at lower temperature. To resolve the apparent contradiction, long molecular dynamics are performed where the system is seen to present quick fluctuations at room temperature between degenerate CDW $2\sqrt{3} \times \sqrt{3}$, which explains the observed non-metallic $\sqrt{3} \times \sqrt{3}$ structure as a dynamical average. Furthermore, the simulations show that the free diffusive regime of the K atoms promote the oscillation of the Si adatoms.Therefore, it was of interest to compute the two-dimensional Free Energy map for the transition between two different CDW states using WHAM. Finally, using these results it is possible to estimate a $2\sqrt{3} \times \sqrt{3} \leftrightarrow \sqrt{3} \times \sqrt{3}$ transition temperature lower than 90 K.

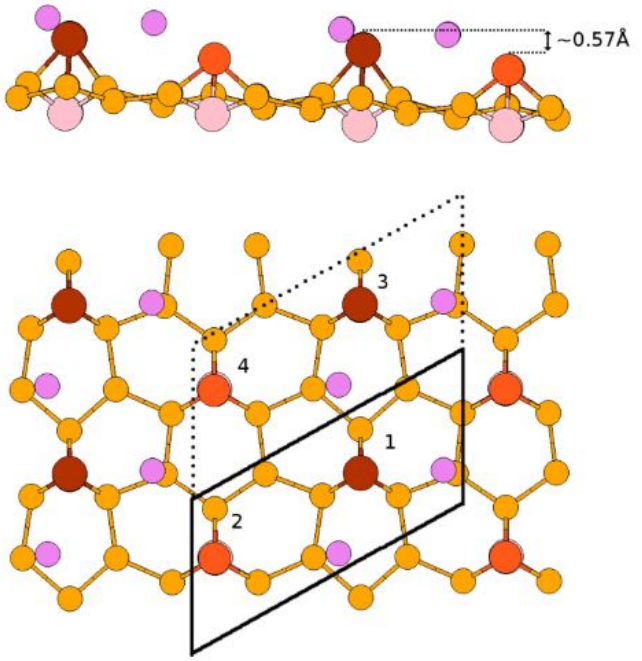

FIGURE 3.3: Figure extracted from [94] representing the system. In brown and orange, the Si adatoms, and in purple the K atoms diffusing over the surface

We define reaction coordinates in terms of the height of two Si atoms of the unit cell with respect to the surface, while the other two Si adatoms are restrained with umbrella potentials, in such a way that one remains above and the other below the surface.

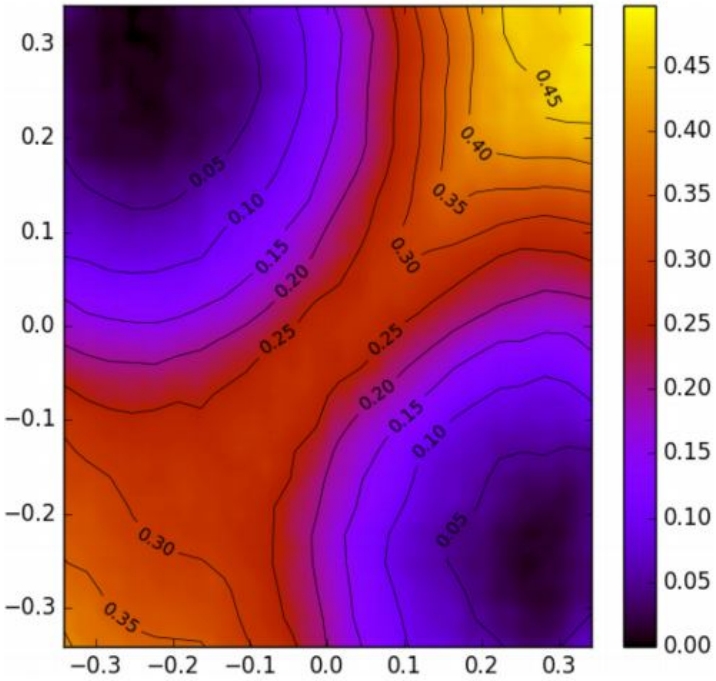

FIGURE 3.4: Free energy map in terms of the heights of two of the Si adatoms at T = 450 K.

The map integrates the information of around 1.3×10^6 configurations which, as commented above, is post-processed with WHAM. In particular, a 36×36 grid of umbrella windows and 1000 configurations on each window were employed, where on each window the constant used for the umbrella potentials was $k = 600 kcal/mol^{-2}$. The free energy barrier between the two minima is 0.29 eV, 0.06 eV lower than the static barrier (total energy difference between the configurations).

The Free Energy results can then be used to estimate the transition temperature, T_c, at which the system transits from the CDW $2\sqrt{3} \times \sqrt{3}$ configuration to the fluctuating non-metallic $\sqrt{3} \times \sqrt{3}$ configuration which is experimentally observed at large temperatures. For that, the free energy barriers can be plugged into an Arrhenius equation,

$$\tau = C \exp(\beta \Delta G)$$

, with $\Delta G = 0.29 eV$ and C a constant determined from the jumps observed in the long free dynamics performed on the system. Assuming that this transition is defined by taking $\tau \approx 10^2 - 10^4 s$, the critical temperature for the transition is $T_c = 90 \pm 7 K$.

3.5.3 An example concerning the catalitic activity of a protein

As a last example, we show a result obtained for the Free Energy profile of an enzymatic reaction catalyzed by the papain, a cysteine-protease, and its corresponding change when a mutation is introduced in an important aminoacid of the active center of the protein. The sulphur atom S shown in yellow in fig. 3.5, which belongs to a cysteine residue, approaches the carbon atom, C, thus breaking its peptide bond with N2.

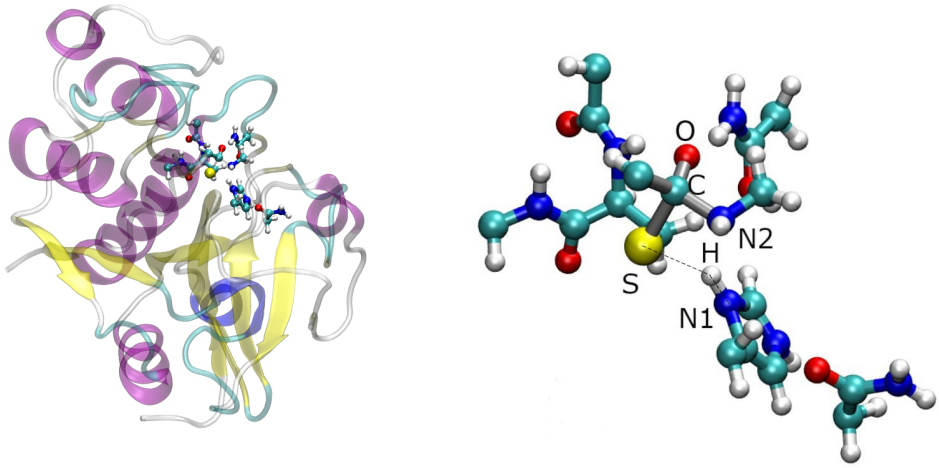

FIGURE 3.5: On the left, a snapshot of the system, with the QM region (atoms treated quantum mechanically) highlighted. On the right, snapshot of the QM region, part of the active site of the protein, in the transition state. The reaction coordinate in this case is dist(S,C)-dist(C,N2), where dist(A,B) is the distance between atoms A and B.

The low pKa of the cysteine plays a key role in the reaction, since the hydrogen H jumps over to the nitrogen N1 and this change in electrostatics is key for the cysteine to approach the peptide bond. Indeed, a well-known mutation of the papaine, the so-called C25S mutation, disrupts the catalysis by substituting the cysteine by a serine, an similar aminoacid which has an oxygen in place of the sulphur. The oxygen, having a larger pKa, tends to retain the hydrogen H, and thus prevents the nucleophilic attack on the C, making the reaction less favorable.

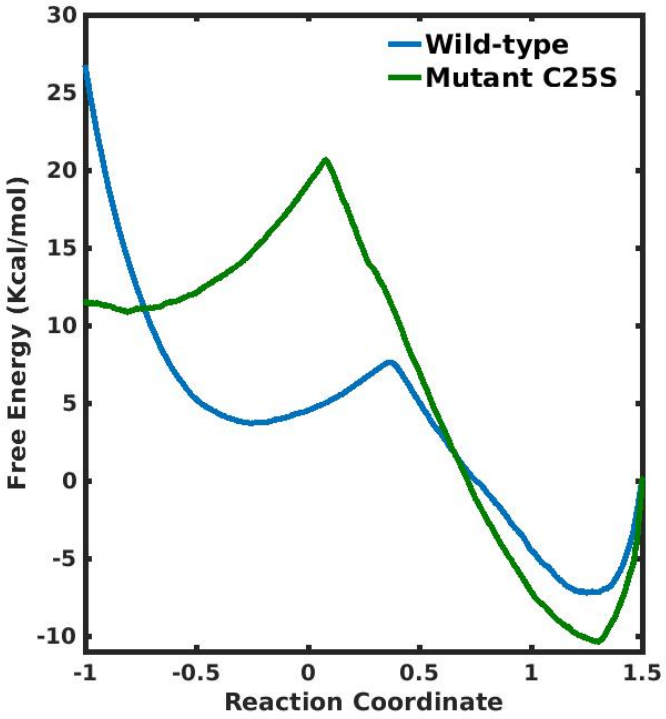

FIGURE 3.6: The increase in the Free Energies barriers means that the reaction, on the mutant, is exponentially slower.

The profiles were obtained by applying Jarzynski's identity over sets of six trajectories. The trajectories, furthermore, were selected to have different orientation, so some of them started with a value of the reaction coordinate equal to -1 (products) and some others equal to 1.5 (reactants).

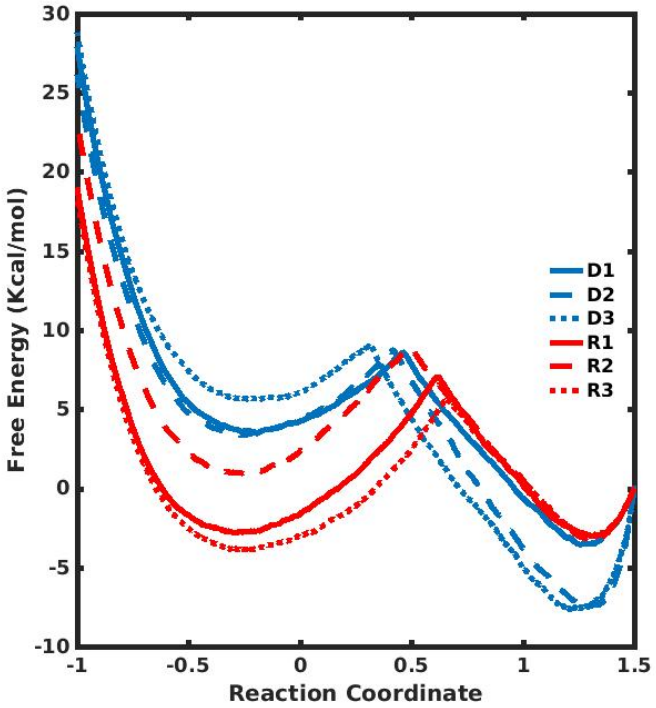

FIGURE 3.7: Results for six trajectories, three of them "direct" (starting from the reactants) and three of them "reverse" (starting from the product). Thermodynamic Integration is employed to extract the profile on each case.

The interest of this result lies in its explanatory power: A mutation known to disrupt the catalytic activity of a protein is, in the simulations, seen to increase the Free Energy barrier. This is turn, from Eyring's equations, means that the expected time to cross the barrier increases exponentially, thus possibly explaining, for instance, the molecular etiology of a pathology based on the studied mutation.

Chapter 4

Proton Transfer in DNA

Nature isn't classical, dammit, and if you want to make a simulation of nature, you'd better make it quantum mechanical, and by golly it's a wonderful problem, because it doesn't look so easy

Richard Feynman

4.1 Introduction

Proton-transfer reactions are ubiquitous throughout biochemical reactions and have therefore arisen much interest both in experimental and theoretical studies [95–98]. In many enzymatic processes [99, 100], proton transfer plays an important role. It is also relevant in water clusters [101, 102] and in many other problems where molecules interact weakly via hydrogens bridges. In particular, the significance of proton-transfer reactions in DNA was already highlighted by Watson and Crick in 1953 [103], as they noted that "spontaneous mutations may be due to a base occasionally occurring in one of its less likely tautomeric forms." Indeed, tautomerization of a nucleotide alters the canonical adenine-thymine/guanine-cytosine (A-T/G-C) correspondence, since a mismatch in the hydrogen bridges structure is introduced. The rare tautomers of the DNA bases differ from their canonical forms by the position of the H atoms, see Figure 4.1.

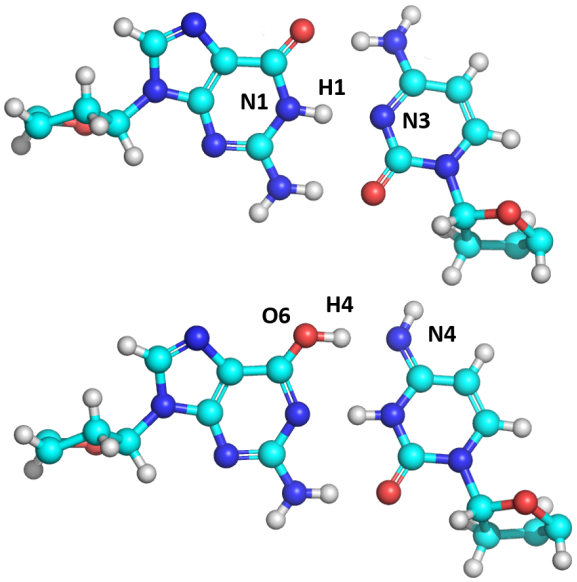

FIGURE 4.1: Proton transfer and rare tautomers: The canonical (GC, top) and rare (G*C*, bottom) tautomers; in the GC ↔ G*C* DPT reaction the H atoms H1 and H4 jump along the N1-H1-N3 and O6-H4-N4 hydrogen bonds.

For example, the rare tautomer G^* does not pair up with cytosine, C, but instead with thymine, T [104], as shown in the next figure, where the effects of the alteration in the hydrogen bridge structure on the correspondence can be easily appreciated.

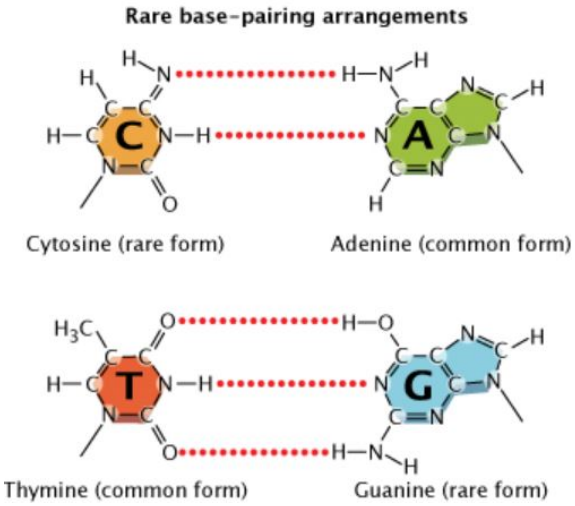

FIGURE 4.2: As seen in the figure, a cytosine or a guanine in their rare tautomeric configuration pair up not with their usual partner (respectively, a guanine and a cytosine), but with an adenine and a thymine, which implies the introduction of a substitution mutation in the genetic code. A look at the hydrogen bonds structure clarifies why the tautomerization implies alteration of the canonical complementarity.

Therefore, if at the time of DNA replication the polymerase runs over the rare tautomeric form of guanine, G^*, a substitution mutation will appear in the DNA sequence. It is then clear why it would be of interest to know the probability of these tautomerizations to take place by proton transfer, the mean life of the rare tautomeric forms and the reaction mechanisms of these processes.

To understand these processes, how they (might) take place, their likelihood, pathways, etc, it is important to be able to study them in the most realistic setting possible. DNA is a very large macromolecule, with a complex atomic structure. At the conditions found in the cells, it generally presents the double helix B-DNA form that is stabilized by the interactions with the aqueous solvent; also, at these conditions DNA is a dynamic system that displays significant atomic motions. Thus, the DNA environment, *i.e.* solvent, DNA backbone, double helix interactions and atomic dynamics at room temperature (RT), must have an important impact on the properties of the DNA bases [105], and in particular in the H transfer reactions taking place on them. In order to properly assess these effects, we make use of a QM/MM method detailed in section 4.3.

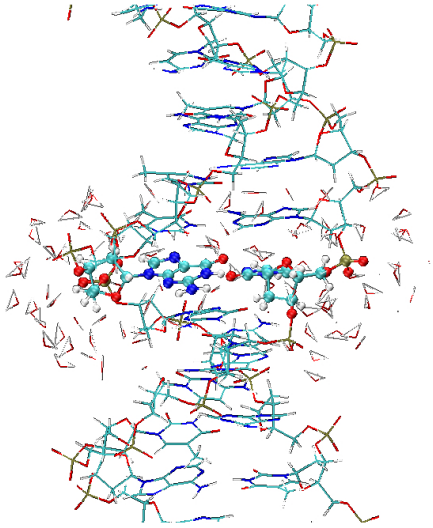

FIGURE 4.3: A snapshot of our system.

4.2 State of the Art

Proton Transfer in DNA has been studied along many years with different approaches and techniques [104, 106–122], including post-Hartree-Fock methods and different DFT's, but the relationship between proton transfer reactions and spontaneous point mutations is still under debate. The main reason behind this is the difficulty to properly assess the influence of the complex biomolecular environment on these reactions. The proton transfers accounting for tautomerization take place in the femtosecond scale, and, although experimental studies of the system exist on the gas phase, the same investigations *in vivo* have so far never performed. That is one of the reasons why computational studies accounting (at least to some degree) for the complexity of the biomolecular environment where these reactions really take place is of the utmost interest.

In the gas phase (that is, considering only the interaction between the two DNA bases), different studies for the potential energy or free energy landscapes indicate that there is no local minimum corresponding to a A*T* rare tautomer [106, 110, 113] (or there is only a very shallow minimum [114, 116]). Thus, DPT do not contribute to the presence of A* or T* rare tautomers. In the case of GC, however, the rare tautomer G*C* shown in figure 4.1 is metastable in vacuo, with values for the direct

and reverse energy barriers between the canonical and rare tautomers that could yield the formation of spontaneous point mutations [106, 110, 116].

Using Fireball or Quantum Espresso, the potential energy landscape *in vacuo* is easily reproducible and is shown in fig. 4.4.

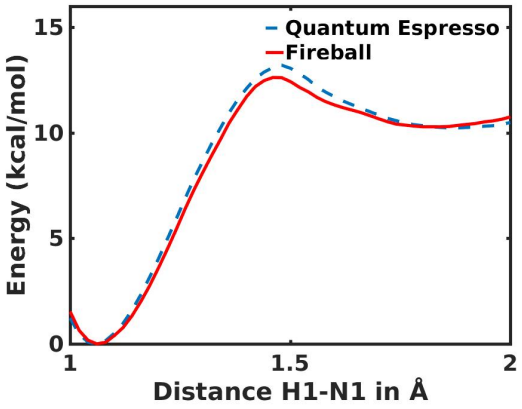

FIGURE 4.4: Potential energy (in kcal/mol) for the GC $\leftrightarrow$ G*C* reaction as a function of the reaction coordinate $d_1 = |\vec{r}_{H1} - \vec{r}_{N1}|$ (in Å), calculated using the QUANTUM ESPRESSO and FIREBALL DFT codes, see text.

This shows how the rare tautomer is a meta-stable state and, therefore, potentially responsible for mutations, as commented above. To give a very rough idea of the relevant orders of magnitude, we can employ Eyring's equation [123] from Transition State Theory to form an idea about the involved time-scales. Eyring's equation states that given a Free-Energy barrier from a reactant to the transition state, $\Delta F^{\ddagger}$, the reaction rate, k, is

$$k = \frac{1}{h\beta} e^{-\beta \Delta F^{\ddagger}}. \tag{4.1}$$

In our case, this k enters the differential equation for the chemical kinetics as

$$\frac{d[GC]}{dt} = -k[GC] + k^{*}[GC^{*}],$$

Neglecting the second term, which will usually be much smaller, this gives a half-life time $t_{1/2} = \dfrac{\log(2)}{k}$, which, compared with the characteristic times in DNA, gives us an idea of the importance of these processes. For instance, assuming a perfect "cascade" effect from the Transition State to the products (a correction of this assumption is sometimes included by means of a κ which enters as a prefactor in eq. 4.1 and accounts for recrossings of the Transition State), we can quickly see the following equivalencies between free energy barriers and half-life times:

$$\begin{aligned}
\Delta F^{\ddagger} &= 1\text{kcal/mol} \rightarrow t_{1/2} = 0.6\text{ps} \\
\Delta F^{\ddagger} &= 5\text{kcal/mol} \rightarrow t_{1/2} = 0.5n\text{s} \\
\Delta F^{\ddagger} &= 10\text{kcal/mol} \rightarrow t_{1/2} = 2\mu\text{s} \\
\Delta F^{\ddagger} &= 15\text{kcal/mol} \rightarrow t_{1/2} = 9\text{ms}.
\end{aligned}$$

The influence of the solvent, DNA backbone and base stacking on these reactions has been analyzed in a number of works [107, 110, 113, 118, 119, 121, 122, 124], but in this models either the environment is dramatically simplified or no dynamics were performed. In particular, the effect of the aqueous environment has been investigated using implicit models for the solvent or including a few water molecules around the DNA bases (microhydration) explicitly in the calculation [110, 113, 121, 122]. These studies indicate that the water molecules around the DNA bases have an important effect changing the relative stability of rare and canonical tautomers; also, the water molecules can participate in proton transfer reactions, interchanging protons with the DNA bases in a Grotthuss-like fashion. [113, 119]

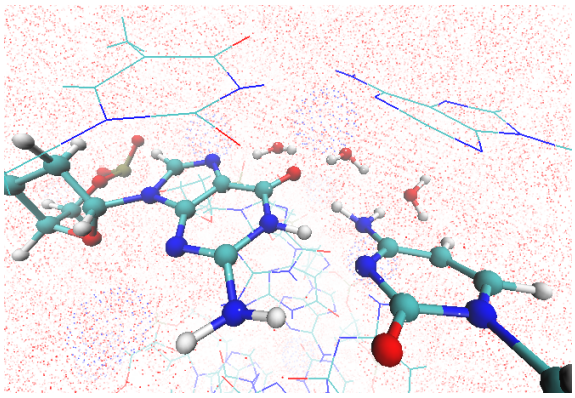

FIGURE 4.5: Snapshot showing the water molecules next to the base-pair included in the QM region, while the rest of the solvent is just shown as a dotted background.

It is also interesting to mention that in the original idea proposed by Löwdin of a Double Proton Transfer (DPT) in DNA [104], the transitions between canonical and rare tautomers are due to quantum tunneling of the protons along the hydrogen bonds. There are some recent studies [125–127] on quantum nuclear effects using path integral molecular dynamics (PIMD) [128] that estimate the minor effects that such correction might have at room temperature. A recent study [129] using an open quantum systems approach indicates that quantum tunneling does not play any role in DPT reactions in DNA, so that the jump of the protons should be entirely due to thermal activation. The combination of having a large system and a high temperature makes the quantum nuclear effects negligible.

A different situation arises when one considers proton-transfer in excited states or in ionized base-pairs. Several studies show how the barrier in this case drops dramatically and the inter-base tautomerization can become spontaneous [130–134]. These results suggest that proton-transfer could be a deactivation pathway for excited base-pairs [130, 135], which would subsequently go back to the canonical tautomer after decaying to the ground state. Thus, the tautomerization by proton-transfer could be considered, more than a source of spontaneous mutations, a defensive mechanism against radiation damage. [105, 136].

The effects of van der Waals interactions have also been considered and have been including in Fireball following Grimme [137, 138] semi-empirical approach. The effects are small but most important in the transition complex and can be appreciated in a calculation of the potential energy profile.

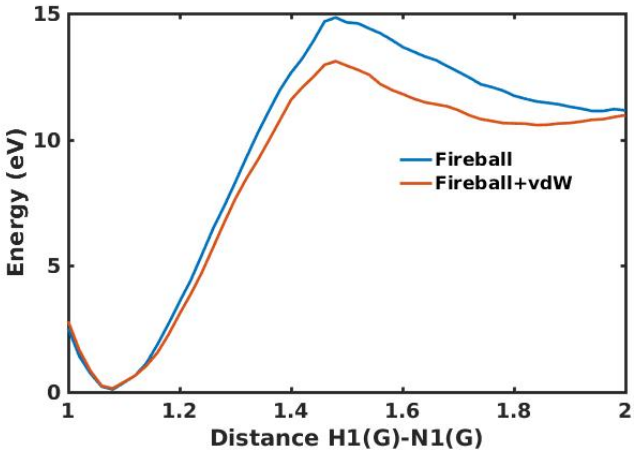

FIGURE 4.6: Potential energy without including any sort of Van der Waals corrections (blue) and including Grimme's semi-empirical corrections (red). This last curve is the one successfully compared to more accurate calculations.

4.3 QM/MM simulations

The application of DFT to very large systems is limited due to reasons of computational cost. However, in many cases, the chemical reactions of interest take place in a small subsystem and, while the rest of the atoms and molecules play a role, it might be enough to treat them at the classical level, which is dramatically more efficient from the computational point of view. In quantitative terms, classical calculations involve an algorithmic complexity of $O(N^2)$ due to the electrostatic interaction, and the exponent can be slightly lowered thanks to methods such as the Particle-Mesh Ewald Summation [139]. However, Quantum calculations involve always a complexity $O(N^{2+\epsilon})$, and typically $O(N^3)$. This suggest that a large system could be splitted into a "Quantum part", to be treated at the quantum level, usually with DFT, and a "Classical part". This is the idea behind the so-called QM/MM methods [140, 141], whose development deserved the 2013 Nobel Prize in Chemistry. The method has been specially used in bio-systems, to study, for instance, the active site on enzymes, where the role of the environment is crucial [142, 143]. For this scheme to work, an interface defining how the two subsystem interact is needed, basically specifying how the electrostatic interaction between the MM and the QM part is implemented [144]. The energy of the whole system is in practice calculated, once the embedding is defined, as

$$E = E(QM) + E(MM) + E(QM/MM). \tag{4.2}$$

The dynamics of the MM part, besides being affected by the QM part, is governed by a classical force field, which must be given a priori, either based in semi-empiric or ab initio calculations [145, 146]. The energy of the interaction term is calculated by using the density extracted from the electronic structure calculation for the QM part and the parameters of the classical force-field, so that, globally, we have to account not only for Coulomb-like interaction terms, but also van der Waals, angular potentials and dihedral potentials.

$$E(QM/MM) = \sum_{j\in MM} \int\left(\frac{q_j n(\mathbf{r})}{|\mathbf{R}_j - \mathbf{r}|}d\mathbf{r} + \sum_{k\in QM}\frac{q_k q_j}{|\mathbf{R}_j - \mathbf{R}_k|}\right) + \sum_{j\in MM, k\in QM}\left(\frac{A_{jk}}{R_{jk}^{12}} - \frac{B_{jk}}{R_{jk}^{6}}\right)\left(+\sum_{\text{bonds}} k_r(R_{jk} - r_0)^2 + \sum_{\text{angles}} k_\theta(\theta - \theta_0)^2 + \sum_{\text{torsions}}\sum_n k_{\phi,n}[\cos(n\phi + \delta_n) + 1],\right. \tag{4.3}$$

where it is understood that j is an index always labeling classical atoms, k labels always quantum atoms, and in the angular and dihedral-torsion terms always at least one of the atoms belongs to the QM region.

The design of force-field has been a key aspect of the development of molecular simulations [145] and, in particular, we have used the so-called ff14SB [146] force field, which is included in the AMBER package [147] for Molecular Dynamics. Recently, a QM/MM method which uses AMBER combined with Fireball has been developed [148] and used in a number of systems [24, 149, 150]. Furthermore, QM/MM is a hot topic of research and many different methods and applications have been explored [151–156]. The AMBER/Fireball method implements an electrostatic embedding [144] and makes use of the Link atom approach [144] to deal with the boundary of the QM region. In this approach, fictional hydrogen atoms are added covalently to the extremal QM atoms to saturate their valency. For this scheme to work, it is crucial to select carefully the ending points of the QM region, preferably in non-polar bonds, such as C-C bonds. Even so, the selection of the QM region is a delicate problem which requires careful examination [157, 158].

4.4 Results

The QM/MM method Fireball/AMBER described above has been employed in combination with all the Free Energy techniques discussed in Chapter 3 to investigate the nature of proton transfer reactions in guanine-cytosine in environment.

The most important finding can be summarized by a simple statement; namely, that **the biomolecular environment** makes the rare tautomer more unstable with respect to the transition state and thus **protects DNA from spontaneous mutations**. These results are summarized in the free energy profiles and maps that we have calculated by means of all the methods discussed in 3, performing to that end Umbrella Sampling Simulations and Steered Molecular Dynamics.

The DNA double helix is simulated by means of two DNA strands that contain 12 base pairs (sequence: TTAGGGTTAGGG) and the QM region consists of the guanine and cytosine nucleobases and their corresponding deoxyriboses, making up a total of 51 atoms, which are all located in the middle of the DNA double helix. In several calculations we have also included three water molecules in the QM region in order to decouple the effects of the micro-hydration and the effects of the rest of the environment. The rest of the DNA, water molecules and counter-ions (Na^+) are included in the MM region, that contains $\sim 1.1 \times 10^4$ atoms. The overall charge of the system is neutral. We employed the ff14SB force field [159] incorporated in the AMBER package, TIP3P water molecules [160] and the Langevin thermostat [85] for the

simulation of the Canonical Ensemble. The initial positions of the water molecules and Na^+ counter-ions are set by the *tleap* software included in AMBER [161], and the system is then thermalized at T = 300 K, first with a long MM simulation (20 ns) followed by a 100 ps QM/MM simulation from which we extract different conformations as seeds for our production runs.

4.4.1 The Ground State guanine-cytosine basepair

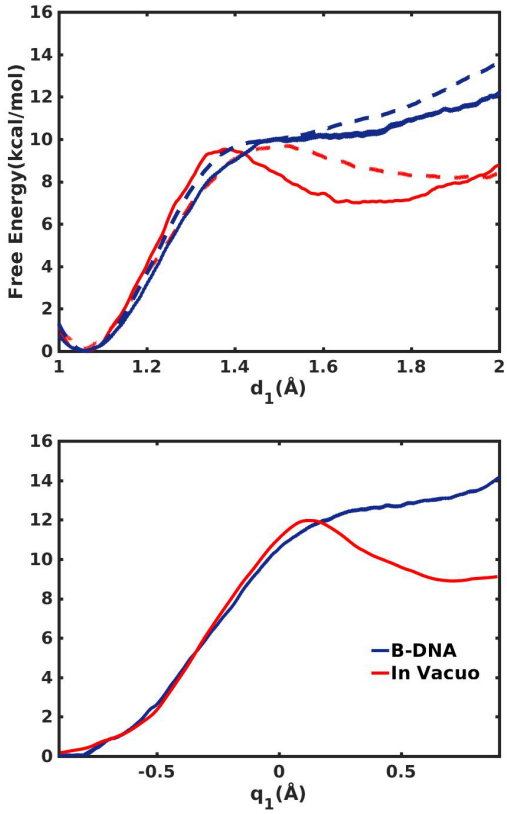

FIGURE 4.7: (A) Free energy profiles in the gas-phase (red lines) and in the DNA environment (blue lines), as a function of the reaction coordinate d_1 The dashed lines correspond to the case in which the three water molecules closer to the O6-H4-N4 hydrogen bond are included in the QM region, see text. (B) Free Energy in terms of reaction coordinate d_1.

In these results (see Fig 4.7) the "controlled" hydrogen is H1; that is, the one steered or under the influence of an Umbrella potential. The reason for this is that this proton is the most reactive one, while H4 -due mainly to the stabilizing effects of the micro-hydration- does not naturally bond to the Guanine and remains -when H1 has jumped over to the cytosine- in a state of more free oscillation. To study this, we have calculated free energy profiles in terms of the position of H4 and also we have investigated the response of each proton when one is forced, which reveals that, while the bonding of H4 to O6 (in the guanine) implies that of H1 to N3 (in the cytosine; see figure 4.1), the reverse is not true (except in vacuo).

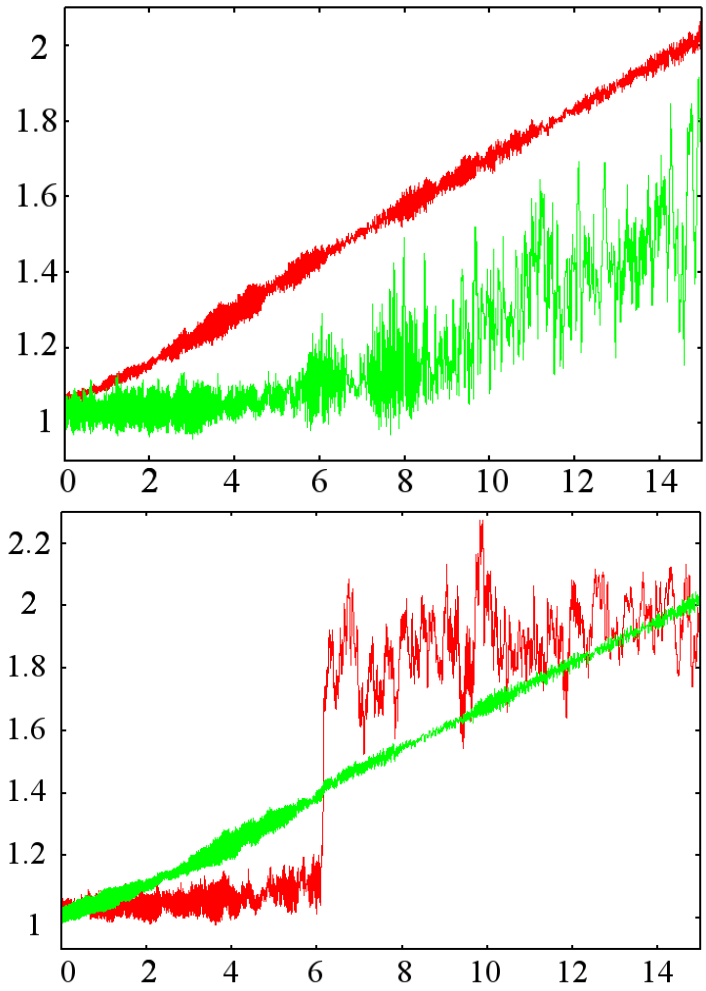

FIGURE 4.8: Example, in two different Steered Molecular Dynamics of 15000 steps of 0.5 fs each, of how the protons respond to each other when one is being steered and the other one if left unconstrained. In red: distance d(H1,N1); in green: distance(N4,H4). Above: H1 is steered. Below: H4 is steered

The H1 proton is thus seen to have a very abrupt response and remains in the cytosine once the H4 is bonded to the guanine. The H4, however, has a smoother response to the movement of H1 and does not completely bond to the guanine, which is due to the water molecules forming weak bonds with the three atoms of that hydrogen bond, O6 (in the guanine), H4 and N4 (in the cytosine) (see figure 4.1).

Yet another interesting difference is observed in SMD simulations for H1 and H4: While the trajectories when H1 are quasi-adiabatic, making thermodynamic integration a perfect method to calculate free energy profiles (a single trajectory of few picoseconds reproduces accurately the profiles obtained with Jarzynski or WHAM), the same does not apply to the trajectories in which H4 is steered. In such case, there is a strong hysteresis observed in the behaviour of H1, which can be readily appreciated when we compare "direct trajectories" (we start with H4 in the cytosine and drag it to the guanine) and "reverse trajectories" (we start with H4 in the guanine and drag it to the cytosine).

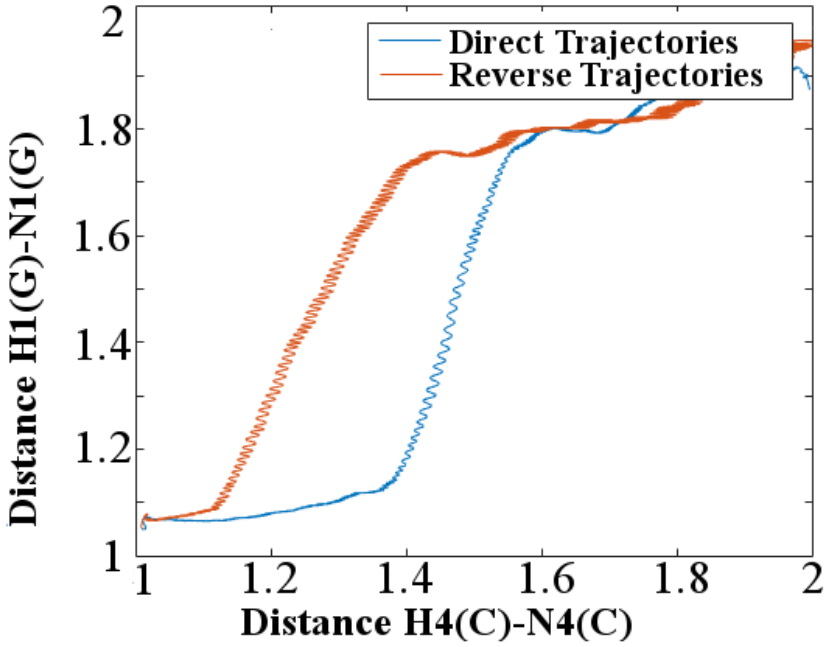

FIGURE 4.9: Hysteresis for the H4 SMD simulations observed in the behaviour of H1

Similarly, we have studied the evolution of the partial charges for the two hydrogens, H1 and H4, and for the guanine and cytosine (excluding those hydrogens), in all types of trajectories (steering H1 or steering H4) and both in vacuo and in vivo. These profiles reveal a slight charge polarization at intermediate steps of the process. The stabilization of these states with a larger charge separation by the surrounding waters and the rest of the environment is probably the reason behind the loss of relative stability of the rare tautomer. However, as seen in our free energy profiles, not only the waters, but also the rest of the environment, is key in explaining these phenomenon.

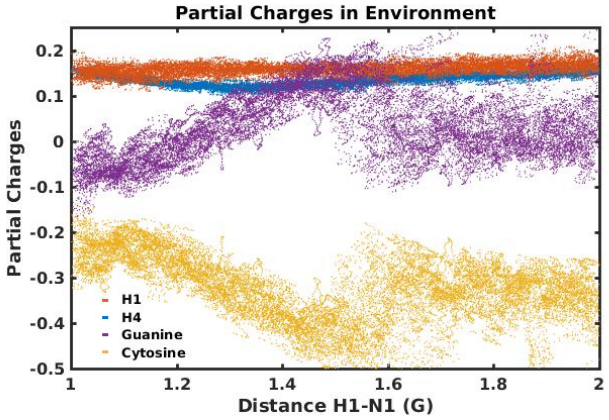

FIGURE 4.10: Evolution of the partial charges of the hydrogens H1 and H4, and of the guanine and cytosine molecules (without including on them the "travelling" H1 and H4 hydrogens) with respect to the distance d(H1,N1) in a Steered Molecular Dynamics simulation. We see an "opening", leading to a polarized situation which, although very unstable in vacuo, can be stabilized by the environment (in particular, the water molecules).

Despite the changes in the charges on the molecules, fig. 4.10, the profile shows that the charge on the reactive protons remains mostly unchanged, a finding that we can confirm by calculating charge maps (see fig. 4.11). For that, we performed a total of 900 US simulations, leaving the systems thermalize on each configuration, and we performed an average of the charge obtained for several snapshots.

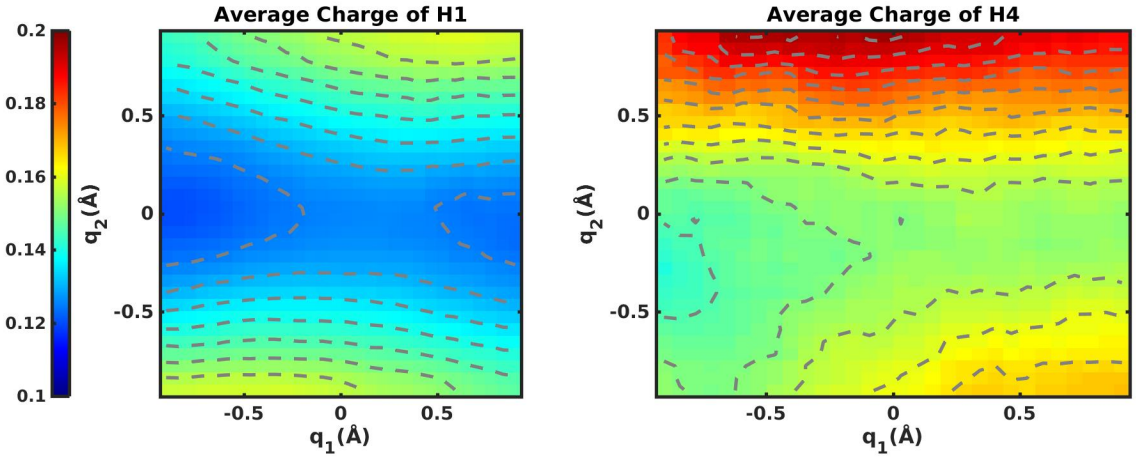

FIGURE 4.11: Map of the average charge on the H1 and H4 atoms (sum of the proton charge ($+e$) and the electron charge) as a function of the reaction coordinates q_1 and q_2. The average charge is calculated as the mean value of the charges in each of the 30×30 US windows employed in the calculation of the free energy map of Figure 4. Note the size of the scale. Units: $+e$.

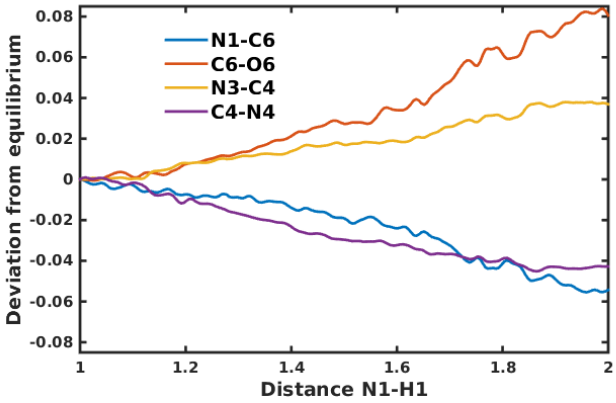

FIGURE 4.12: Deviations from the equilibrium positions in the canonical tautomer averaged over twelve SMD simulations of 1ps each. See figure 4.1 to see atom labels.

Apart from the different profiles for each case and method (The Jarzynski method for H4 profiles was not very useful, for the hysteresis and the non-adiabaticity, which translated in a wider variety of "trajectory styles", implies that probably a great number of trajectories would be needed to obtain a reliable result, and UI and WHAM were employed instead), we calculated a Free Energy Map with WHAM, and the conceptual conclusions are the ones summarized above: We see that all the mutagenic configurations are extremely unstable, and the return to the canonical tautomer must be extremely quickly (below the femtosecond scale, according to Eyring equation).

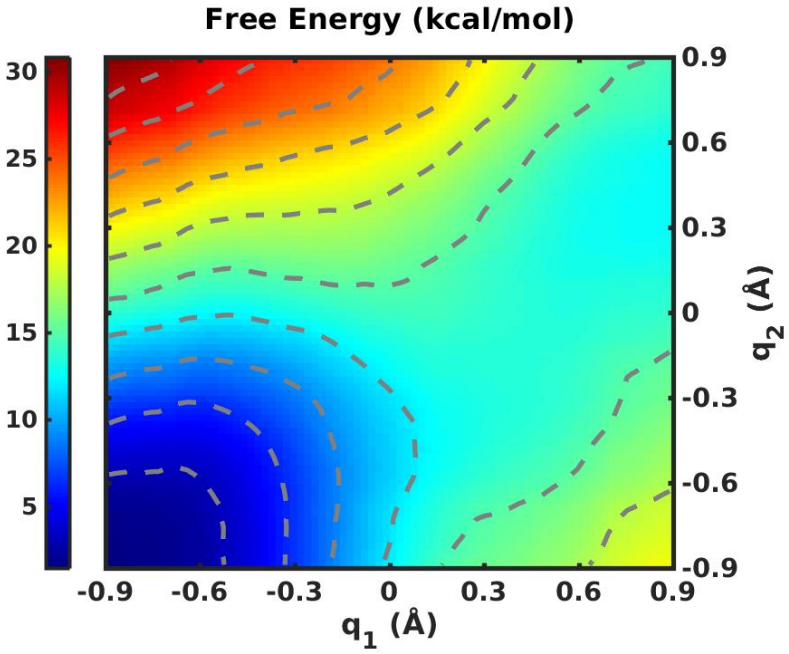

FIGURE 4.13: Free Energy Map in environment computed with the WHAM method [162] with the help of Grossfield code [90].

To corroborate this finding, we have also performed a total of fifty free dynamics starting from independent configurations corresponding to the rare tautomer (we thermalized the system in the rare tautomer configuration by means of Umbrella potentials and then performed long runs from which we extracted independent seeds, as done with our preparatory simulations). In all of them, we observe a ultra-fast return to the canonical tautomer in few femtoseconds. This offers a strong contrast with the case in vacuo, where the mutagenic configurations in free dynamics are observed to live several picoseconds, in rough agreement with the expected values from the reverse barriers and the half-life time given by Eyring equation.

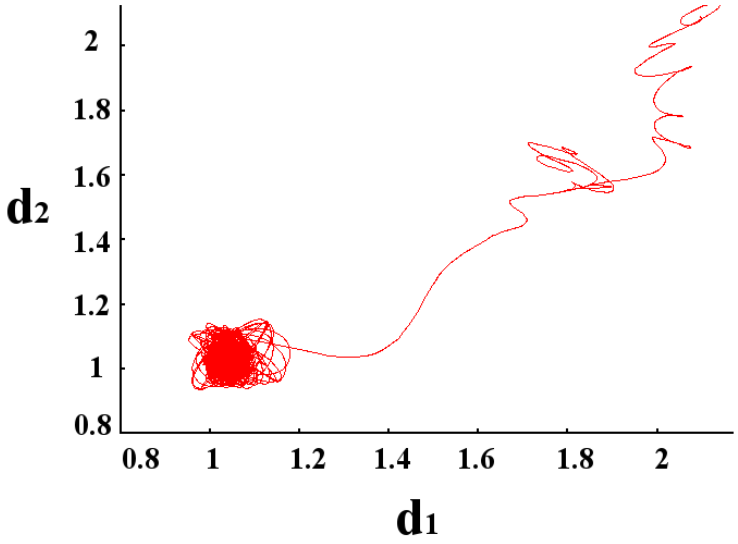

FIGURE 4.14: Evolution of the distances $d_1 = d(H1, N1)$ and $d_2 = d(H4, N4)$ in a very long (100 ps) Free Dynamics starting from the rare tautomer. The configuration space is barely visited outside the canonical tautomer.

To further elucidate the nature of the rare tautomer, we have studied the behaviour of the protons in their respective bridges. Figure 4.15 shows the probability distribution functions (PDFs) for the distances H4-O6 and H4-N4 in the rare tautomer configuration, *i.e.* adding a flat-bottom bias potential that restrains the distance H1-N1 to be $\sim$ 1.7–2.1 Å. To construct the PDFs we perform long US simulations of 50 ps and use the Kernel Density Estimator[163] over the time series of the distances. In this approach, the Density of a Random Variable is constructed by accumulating gaussians centered at each point sampled; that is, if we have results $x_1, x_2, \ldots, x_N$, all extracted from independent copies of a same Random Variable, X, the density, f, of X can be estimated as:

$$f(x) = \frac{1}{N} \sum_{j=1}^{N} \frac{1}{\sigma} G\left(\frac{x - x_j}{\sigma}\right)$$

where G is the standard normalized gaussian, $G(x) = (2\pi)^{-1/2} e^{-x^2/2}$. In the gas phase the rare tautomer is fully formed, with a H4-O6 distance $\sim$ 1.1 Å and a H4-N4

distance oscillating around $\sim$ 1.8 Å. In the DNA environment, however, there is a drastic change in the PDFs. The H4-N4 and H4-O6 PDFs are now both spread between $\sim$ 1.0-1.8 Å, and each of them is a superposition of two broad peaks centered at $\sim$ 1.15 Å and $\sim$ 1.5 Å. This situation is an indication of a low-barrier hydrogen bond (LBHB) in which the H atom can easily move between the O and N atoms; these short and strong hydrogen bonds typically enhance the stability of certain transition states in enzymatic reactions and help the catalytic activity of the protein [95, 164, 165]. Thus, when the covalent bond H1-N3 is formed in the biomolecular environment, instead of forming the corresponding O6-H4 covalent bond (see Fig. 1), the GC system prefers to form a O6-H4-N4 LBHB. This is due, in part, to the interaction with the surrounding water molecules, but also to the influence of the rest of the environment (*e.g.* see Fig. 3(a)). We remark that if the restraining bias potential is removed, the GC system reverts in an ultra-fast process to the canonical tautomer; thus, the LBHB discussed here is completely unstable (existing only in the virtual scenario of H1 being bonded to N3). On the other hand, if we restrain the distance H4-N4 to be $\sim$ 1.7–2.1 Å (instead of the distance H1-N1), the rare tautomer is fully formed for both the gas phase and the DNA environment cases.

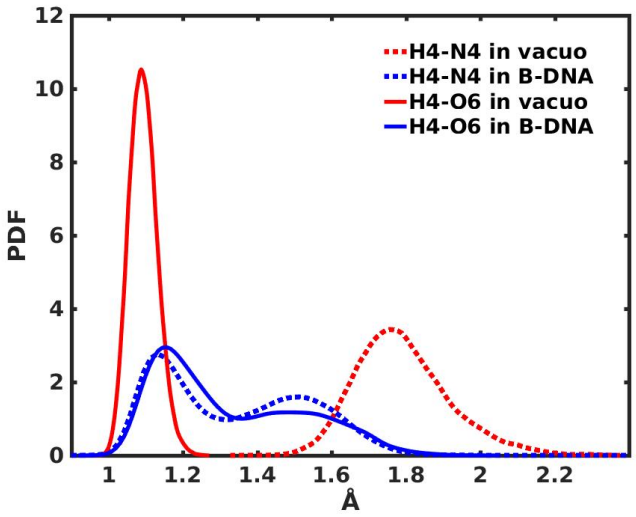

FIGURE 4.15: Probability Density Functions, calculated with the Kernel Density Estimator (see text), from Umbrella Sampling Simulation. Here, we see the probability density for the distances between the atoms indicated in the legend (see figure 4.1).

Also the Density of States projected over different atoms were calculated to assess the different impact on covalent structure of different configurations.

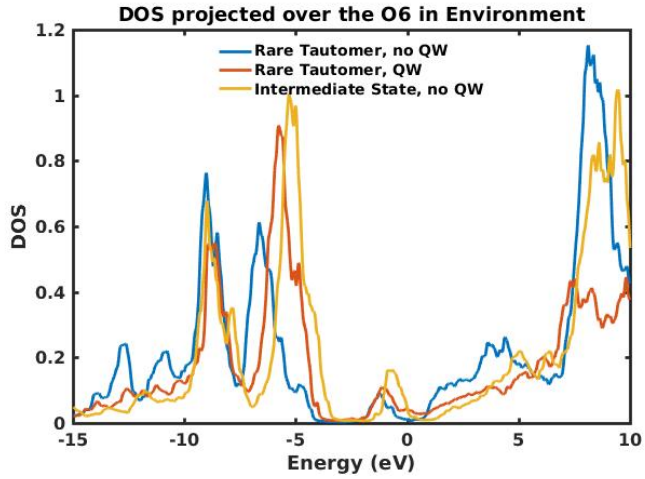

FIGURE 4.16: Local Density of States (projected on the orbitals of the oxygen atom O6 of the guanine, see figure 4.1). It is seen that, when the surrounding water molecules are present, the rare tautomer state (defined here as $d(N1, H1) > 1.8$ Å) resembles more closely the intermediate /activated complex state (defined as 1.4 Å$< d(N1, N1) < 1.6$ Å)

We have performed a detailed correlation analysis between the distance H1-N1, other bond lengths, different partial charges and the electronic gap, with the idea of trying to find to which degree are the different variables intertwined. To that purpose, we have computed the linear Pearson correlation coefficient, the Spearman rank coefficient and the Distance Correlation [166–168] between different pairs of variables (see below).
For random variables x and y (x and y could be any variable in the system, like bond lengths, partial charges, electronic gap, etc) with correspondent samples x_j and y_j, the Pearson coefficient is defined as

$$r_{xy} = \frac{\overline{(x-\overline{x})(\overline{y-\overline{y}})}}{\sigma_x \sigma_y} = \frac{\sum_j (x_j - \overline{x})(y_j - \overline{y})}{\sqrt{\sum_j (x_j - \overline{x})^2 \sum_j (y_j - \overline{y})^2}}, \tag{4.4}$$

where $\overline{x}$ denotes the mean of x and σ_x the standard deviation. The Pearson coefficient yields then a number between -1 and 1 whose absolute value indicates the degree of mutual dependence between the two variables. By its definition, however, it captures only linear dependencies between pairs of variables, but will yield small values -even 0- for variables with non-linear relationships. That is why in situations where a complete linear relationship cannot be assumed, it is interesting to calculate non-linear correlations, such as the ones named above. One possibility is found in the Spearman coefficient, defined by calculating the Pearson coefficient of the rank variables (each point x_j is assigned a value rk_j, where rk_j is the rank of x_j in all the set of values $\{x_j\}$):

$$Sr_{xy} = \frac{\overline{(rk(x) - \overline{rk(x)})(\overline{rk(y) - \overline{rk(y)}})}}{\sigma_{rk(x)} \sigma_{rk(y)}}. \tag{4.5}$$

The more involved Distance Correlation, on the other hand, is defined by considering, from a variable x with sample x_j, the set of distances between every possible pair in the sample:

$$|x_j - x_k|,$$

and by constructing a centered version of such variable:

$$dx_{jk} = |x_j - x_k| - \frac{1}{n}\sum_{k'}|x_j - x_{k'}| - \frac{1}{n}\sum_{j'}|x_{j'} - x_k| + \frac{1}{n^2}\sum_{j',k'}|x_{j'} - x_{k'}|.$$

Then we can construct the Pearson correlation coefficient for the variables dx and dy:

$$dr_{xy} = \frac{\overline{dx \cdot dy}}{\overline{dx \cdot dx} \cdot \overline{dy \cdot dy}}. \tag{4.6}$$

This quantity is zero if and only if x and y are independent random variables and the comparison with Pearson linear coefficient can be used to extract the degree of non-linear correlation between two variables.

Both in environment and in vacuo, the no-linear Distance Correlations is observed to be slightly larger that the linear correlation, which indicates a degree of non-linear dependence. Besides, the correlation is slightly greater in environment, where the Pearson coefficient is observed to be ~ 0.45 for the correlation with the charges in the hydrogens and in the guanine and around 0.35 in vacuo.

	H1,H4	MP,[d4,d5,d6,d7]	MP,[H1,H4,G,C]	MP,gap
In Vacuo H1	0.89 0.90	0.65,0.77,0.63,0.68 0.66,0.80,0.65,0.70	0.44,0.50,0.42,0.21 0.52,0.65,0.43,0.21	0.13 0.15
Environment H1	0.88 0.90	0.59,0.79,0.58,0.70 0.60,0.80,0.58,0.70	0.45,0.44,0.42,0.25 0.58,0.40,0.51,0.40	0.14 0.35
In Vacuo H4 (Direct and Reverse)	0.88 0.88	0.59,0.75,0.61,0.65 0.63,0.80,0.66,0.74	0.23,0.74,0.42,0.20 0.23,0.77,0.55,0.40	0.22 0.30
In Environment H4 (Direct and Reverse	0.91 0.89	0.57,0.81,0.67,0.72 0.67,0.83,0.68,0.74	0.26,0.71,0.13,0.06 0.30,0.72,0.55,0.58	0.22 0.29

TABLE 4.1: In this table we present the values of the Pearson correlation coefficient (first row on each entrance) and the non-linear distance correlation coefficient (second row on each entrance) in Steered Molecular Dynamics. We calculate the correlation of the Moving Hydrogen (H1 or H4) with other variables, such as the other transferring hydrogen, the distance of the heavy atoms which rearrange during the process (second column), the partial charges (third column) and the HOMO-LUMO gap.

4.4.2 Excited States

As mentioned above, a different relevant problem is proton transfer in excited states. Radiation is major source of damage for the genetic code, and its interaction with proton transfer has been the topic of many recent research works. [130–136]. We have limited our study here to singlet excited states with no degeneracy, so we have not made a full study of the problem, since we have not elucidated which is the

most relevant excited state (which one is more accessible in terms of quantum yield for typical dynamical configurations of the base pair). Although this has yet to be clarified, our results in this case show, at least at the conceptual level, the same conclusions extracted from previous works; namely, that **proton transfer becomes thermodynamically spontaneous on the excited state.**

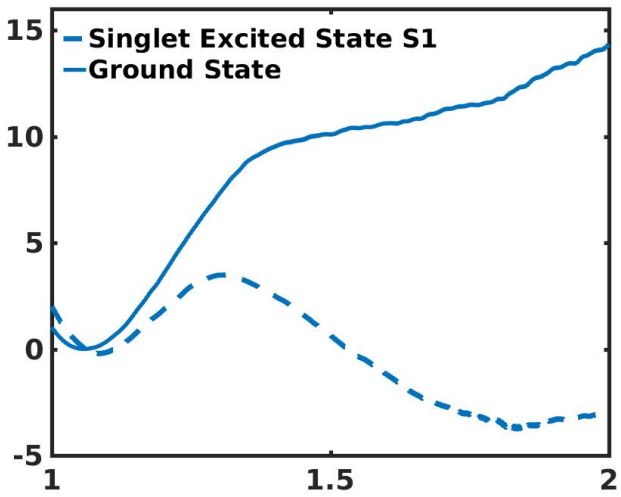

FIGURE 4.17: Free Energy of the proton transfer reaction in the Ground state (as studied above) and in the singlet excited state. The reaction coordinate in both cases, as before, is the distance $d(H_1, N_1)$ and the Free Energy has units of kcal/mol. Interestingly, we see how, in the excited base-pair, the proton transfer becomes spontaneous; i.e, the rare tautomer is thermodynamically more stable.

Furthermore, in the Excited State, being a state with charge separation, the "chemical common sense" does not apply and we cannot expect the hydrogen H4 to react to the jump of H1. Indeed, when dragging H1 we obtain from Jarzynski equality -used in the same way it was in the ground state case- the profile shown in fig. 4.17, and for all of these reactions the hydrogen atom H2 remains linked to the cytosine and does not start oscillating freely in a low-barrier-hydrogen-bond type of landscape, as was the case in the Ground State.

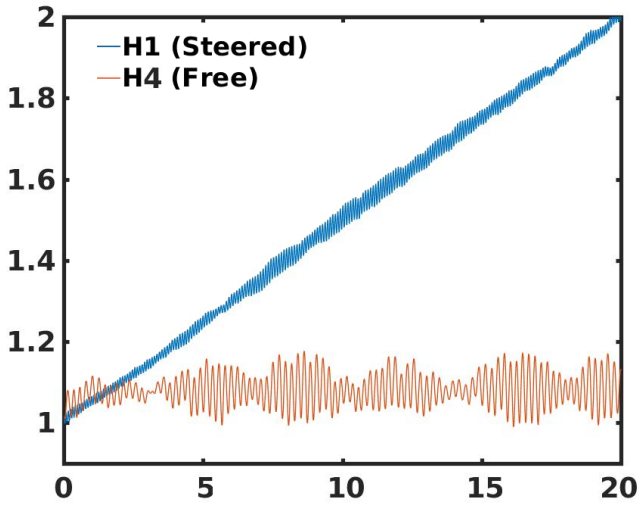

FIGURE 4.18: Example of a SMD simulation of 2000 steps (1 ps) in the excited state considered, where the steering potential affects only the distance d(H1,N1) . Blue: distance d(H1,N1). Red: Distance d(H4,N4) (see figure 4.1).

More than a mutagenic risk, this is actually seen as a potential defense mechanism against radiation damage, for the system may find it easier to decay to the Ground State when proton transfer has taken place. After decaying to the Ground State, the return to the canonical tautomer is, as we have seen, ultra-fast, so this would constitute indeed a route out of the excited state. Whether this decay takes place by conical intersection or other relaxation means is not clear, but our calculations of the electronic levels in Steered Molecular Dynamics simulations suggest that the conical intersection could be present somewhere between the transition complex and the final product.

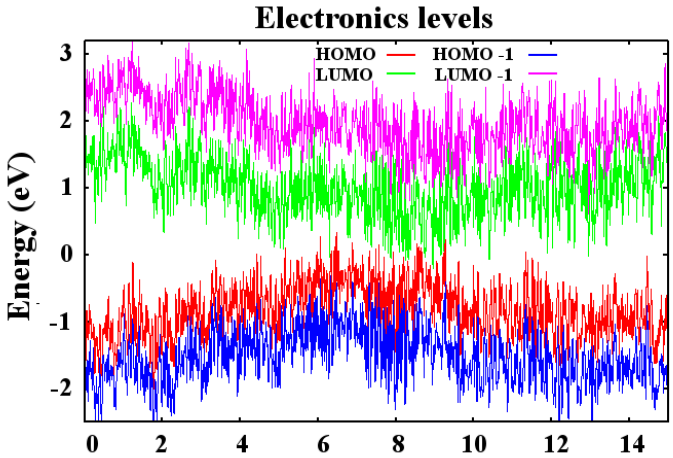

FIGURE 4.19: SMD simulation of 7.5 ps where the distance d(H1,N1) is dragged. We plot here the levels HOMO-1(blue), HOMO(red), LUMO(green) and LUMO+1(pink).

The distribution of the electronic levels over the molecule also changes dramatically in terms of the positions of the protons. While the HOMO level in the canonical

tautomer is delocalized over the guanine and cytosine, in the rare tautomer, interestingly, both the HOMO and the LUMO are strongly localized, respectively, over the guanine and the cytosine.

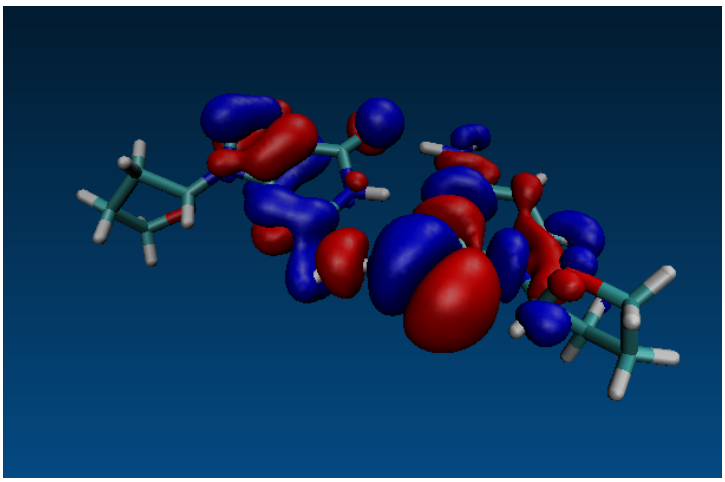

FIGURE 4.20: HOMO orbital in the canonical tautomer

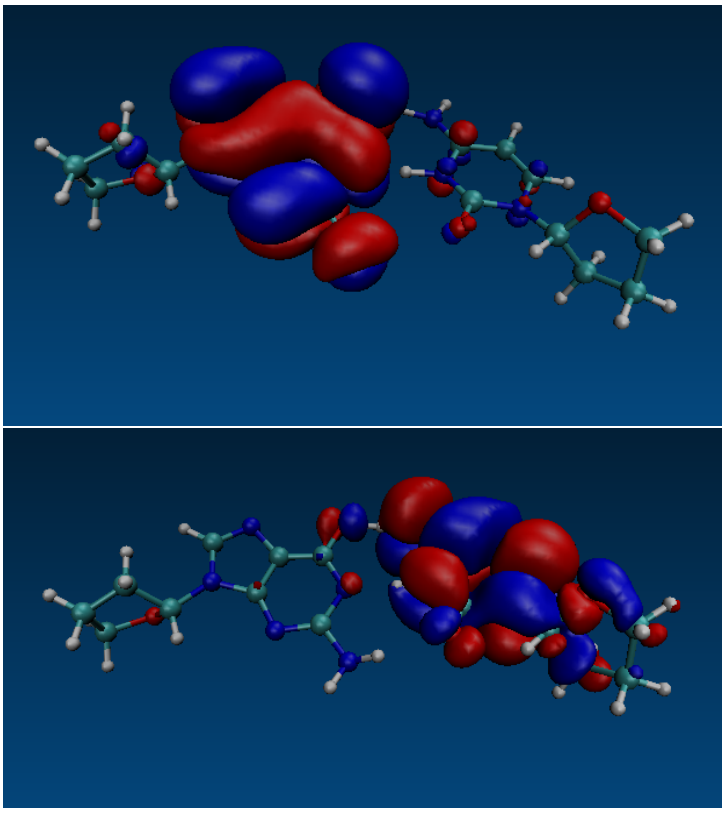

FIGURE 4.21: HOMO (above) and LUMO (below) orbitals in the rare tautomer

This suggests that, in the excited state, the rare tautomer and close configurations can be states with a strong charge separation (ionized forms) between the two bases, since the molecular orbitals where the electrons are "jumping" from or to are seen to be strongly localized on different basis. This motivates also the question of how is the Free Energy profile for the proton transfer reaction in a charged system, a

question that has been studied in some works and which, apart from its own interest, could shed some light about the nature of the reaction in the excited state, whose electronic structure seems to bear some resemblance to that of the charged system. Our result shows that for the base-pair in environment with a positive charge of +1, the proton transfer becomes, thermodynamically speaking, much easier and the rare tautomer more stable with respect to the activated complex. Grosso modo, the barrier for the cation implies that canonical tautomer will take around $1ns$ before jumping, while the barrier for the Ground State gives an expected time of several μs.

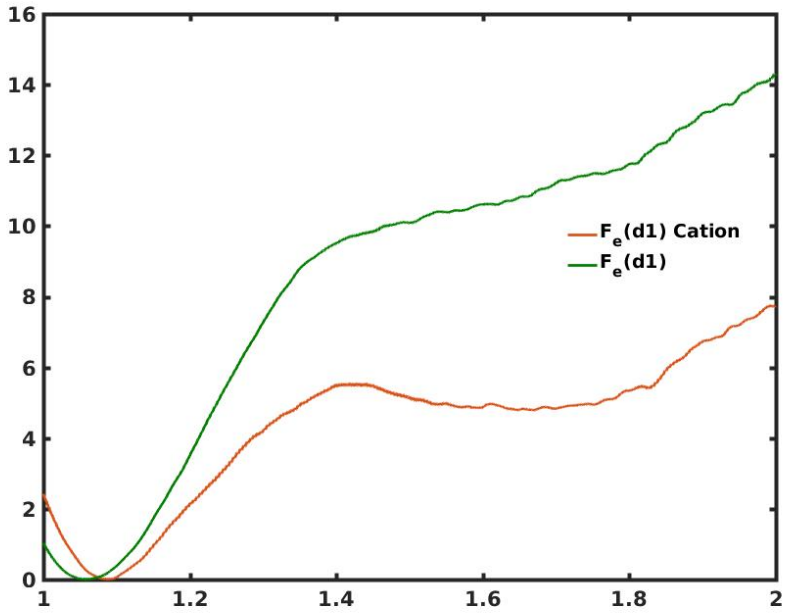

FIGURE 4.22: Free Energy in kcal/mol in terms of the distance d_1: Comparison between the cation (red) and the neutral system (green), using the reaction coordinate d(H1,N1) (see figure 4.1).

4.4.3 Intra-molecular proton transfer in guanine

As mentioned before, another (potentially) important process is intra-molecular proton transfer, which could of course also yield rare tautomers. These type of processes have been studied extensively in vacuo, and here we also provide Free Energy profiles in guanine in the environment, both in single helix and double helix. The distinction is of interest because, during DNA replication, the single helix configuration is closer to reality, and the differences in free energy are thus relevant. In vacuo, the free energy differences of the two tautomeric forms were already known to be very small, but the barriers were too high for this process to be very relevant in a short time-scale. Indeed, the barrier that we here reproduce yields a expected lifetime of ... more than twenty years!

Here, we study the transfer of $H1$ from the nitrogen $N1$ to the oxygen $O6$, and we calculate the Free energy of such a reaction in vacuo, in single helix and in a double helix (as before, adding as well the solvent and stabilizing ions).

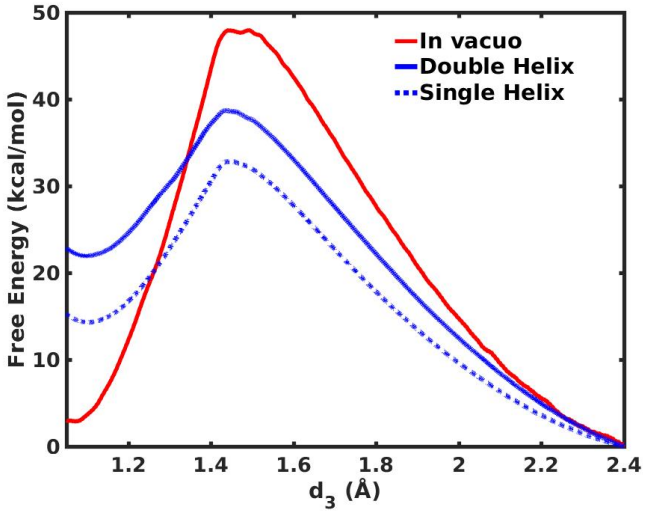

FIGURE 4.23: Intra-molecular proton transfer in the guanine: Free energy in kcal/mol in terms of the distance d_3 between H1 and O6 (see fig. 4.1).

4.4.4 Conclusions

In summary, we have analyzed H transfer reactions in guanine-cytosine base-pairs embedded in a realistic DNA biomolecular environment by means of free energy calculations based on extensive QM/MM MD simulations. We find that, although G*C* is metastable in the gas phase, this rare tautomer is not an accessible state in the DNA environment, *i.e.* the inter-base GC $\rightarrow$ G*C* DPT reaction does not take place. We have also analyzed the intra-base H transfer in Guanine for DNA in single helix or double helix configurations. Our calculations indicate that the DNA environment changes dramatically the relative stability between the canonical and rare tautomers. The QM/MM free energy calculations presented here for both inter-base and intra-base H transfer reactions demonstrate the important role of the DNA environment enhancing the stability of the genetic code against spontaneous mutations.

Chapter 5

Hubbard-Hund Hamiltonians

" [...] está en la propia esencia del trabajo teórico el que a menudo se muestra del todo alejado de lo espectacular. No se ven todas las tentativas que han ido a parar al cesto de los papeles. En el mejor de los casos, todo el trabajo, a veces de meses, queda reducido a unos resultados condensados en unas pocas cuartillas. Y cuando éstos no se alcanzan, ni aun esto queda. Parece entonces claro que uno nada hizo. Afortunadamente, no ha sido éste el caso en la presente ocasión"

Letter from Ramón Ortiz Fornaguera to José María Otero Navascués, May 6th 1953

5.1 The problem and the model

As mentioned in chapter 1, the exchange-correlation functionals of DFT are insufficient to explore the properties of systems with very high electronic correlation, like the valence d-electrons of transition metals, which present strongly localized states. In this chapter, we explore a model system from the point of view of OO-DFT (introduced in chapter 1), compute the correlation energy and potential numerically by exact diagonalization, formulate a DFT+U [44, 169] approach to account for many body correlation effects beyond the scope of typical DFT, study a brief application to the problem of spontaneous magnetization, and explore an scheme to calculate approximately the many-body Density of States beyond perturbative calculations. DFT+U is widely used method [170–173] to explore highly correlated systems, such as -to mention just a few recent application- the effect of copper ions on NiFe layers [170], the effect of doping on the magnetic properties of ZnO [171], the nature of the Mott phase and the para/ferro-magnetic phases in a number of metallic oxides [173], or also properties of biological systems such as the hemo complex [174, 175], where the high correlation effects on the d-electrons of the magnetic core iron atom, with an open-shell configuration, may be of interest to understand electronic transfer processes. While it is based in principle in the Hubbard models, recent methodological advances try to formulate schemes where also a exchange interaction is present in the DFT+U functionals [176–178]. While other many body methods have been developed, like the celebrated GW method [43] or approaches based on the numerical renormalization group, DFT+U offers an excellent balance between precision and

computational cost and simplicity.

The advantage of the OO-DFT formalism in this case is obvious, since the localized orbitals whose occupation numbers are used to define the Hohenberg-Kohn theorems and the Kohn-Sham approach (see chapter 1) are the same localized orbitals used in the model for which the DFT+U functionals are defined. Thus, in this framework, DFT+U can be formalized and the models explored can be regarded as analogies of jellium (the HEG): A model in which we can compute exactly (or with great accuracy) the exchange-correlation energy, and which is used later as the starting point to calculate the correlation of more complex systems that locally resemble the studied model.

We start by writing down the Kanamori-like Hamiltonian [179] for the $i\sigma$-states of a magnetic atom with $2M$-levels:

$$\begin{aligned}\hat{H}^A = &\sum_{i\sigma}\epsilon_{i\sigma}\hat{n}_{i\sigma} + U\sum_{i}\hat{n}_{i\uparrow}\hat{n}_{i\downarrow} + \frac{U'}{2}\sum_{i\neq j}\hat{n}_{i\sigma}\hat{n}_{j\bar{\sigma}} + \\ &\frac{U'-J}{2}\sum_{i\neq j}\hat{n}_{i\sigma}\hat{n}_{j\sigma} - \frac{J}{2}\sum_{i\neq j}\hat{c}^{\dagger}_{j\sigma}\hat{c}_{j\bar{\sigma}}\hat{c}^{\dagger}_{i\bar{\sigma}}\hat{c}_{i\sigma}\end{aligned} \tag{5.1}$$

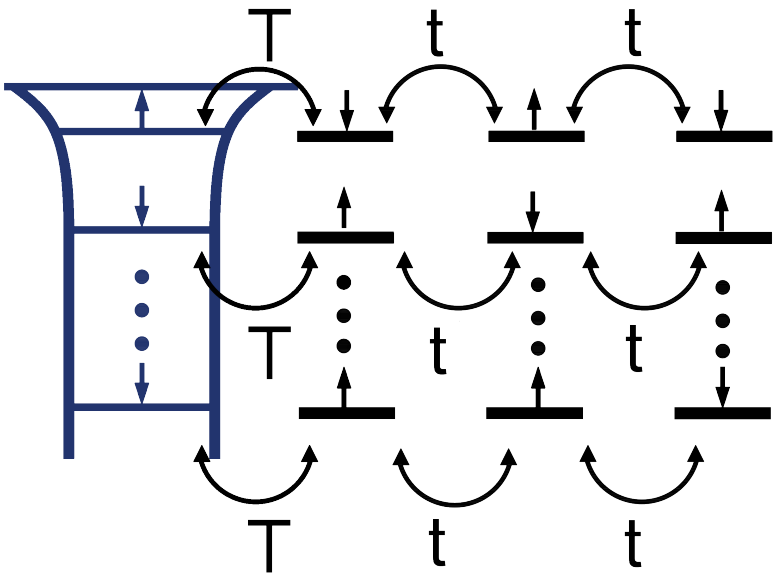

FIGURE 5.1: Schematic representation of our model system. An atomic shell of $2M$ $i\sigma$-orbitals (left), described by the atomic Hamiltonian $\hat{H}^{at}$, eq. 5.1, is connected to different channels (right), that simulate the effect of the environment, by means of a one-electron Hamiltonian $\hat{H}^{OE}$, eq. 5.2. Each channel is simulated by a chain of three sites; in each super-chain (the atomic level plus the chain) we assume to have always four electrons

.

In Equation 5.1, $\hat{c}^{\dagger}_{i\sigma}$, $\hat{c}_{i\sigma}$ and $\hat{n}_{i\sigma}$ are the usual creation, annihilation and number operators, respectively, associated with the orbital (M) and spin (2) states ($i\sigma$). U (U') is the Coulomb-interaction between the $i\uparrow, i\downarrow$ ($i\uparrow, j\downarrow$) orbitals, while $U'-J$ is the interaction between $i\sigma$ and $j\sigma$. J represents the exchange interaction between

orbitals with the same spin. The last term of the Hamiltonian represents a typical spin flip term for the $i\sigma$ and $j\sigma$ states, and its contribution is needed in order for the Hamiltonian to be rotationally invariant if $U = U' + J$ [180]. In our model, we assume each atomic orbital to interact with the environment through a channel that we simulate by three degenerate orbitals (see Figure 5.1), using the following one-electron Hamiltonian:

$$\hat{H}^{\mathrm{OE}} = \sum_{j\alpha\sigma} \epsilon_{j\alpha\sigma}\hat{n}_{j\alpha\sigma} + \sum_{j,\alpha\neq\beta,\sigma}^{n.n.} t\left(\hat{c}^{\dagger}_{j\alpha\sigma}\hat{c}_{j\beta\sigma} + \hat{c}^{\dagger}_{j\beta\sigma}\hat{c}_{j\alpha\sigma}\right) + \sum_{j\sigma} T\left(\hat{c}^{\dagger}_{j\sigma}\hat{c}_{j\alpha_1\sigma} + \hat{c}^{\dagger}_{j\alpha_1\sigma}\hat{c}_{j\sigma}\right) \quad (5.2)$$

where greek indexes (α, β) refer to states of one chain and j refers to the super-chain $\{ j, j\alpha_1, \ldots \}$.

The ground state of $\hat{H}^t = \hat{H}^A + \hat{H}^{OE}$ is calculated numerically, using a space of electronic configurations defined by the restrictions of having zero total spin and 4 electrons in each super-chain. Notice that due to the spin flip term in $\hat{H}^A$, the spin in each super-chain for a given configuration can be different from zero.

The value of t has been changed in a range from 0 to T, for $M = 2$, and we have found it to have a minor effect on the atomic correlation energy (see details below). Accordingly, we have analyzed the cases $M = 3$ or $M = 5$ taking $t = 0$, *i.e.* reducing each chain to only one atom, since for $t \neq 0$ these calculations are numerically very demanding.

In the Hubbard case, $J = 0$, the atomic hamiltonian $\hat{H}_{\mathrm{at}} = \frac{U}{2}\sum_{\alpha,\sigma\neq\beta,\sigma'} \hat{n}_{\alpha\sigma}\hat{n}_{\beta\sigma'}$ can be recasted as:

$$\hat{H}_{\mathrm{at}} = \frac{U}{2}\hat{N}\left(\hat{N} - 1\right)$$

This is interesting because it makes evident the rotational symmetry. Algebraically speaking, a hamiltonian is rotationally symmetric when it commutes with the rotation operator. The infinitesimal generator of the rotations is the angular momentum operator, $\hat{L}$, and so the rotation operators are of the form $R_{\alpha,\hat{e}} = e^{-i\alpha\hat{L}\cdot\hat{e}}$, where $\hat{e}$ is the rotation axis and α is the angle.

In the Hubbard-Hund case ($J > 0$), rotational symmetry is more involved, and, as commented above, depends on the particular relation between the many-body parameters. In this case, it is important to include also the spin operator, Spin $\hat{S} = \sum_{\alpha,\sigma,\sigma'} \hat{c}^{\dagger}_{\alpha\sigma}\vec{S}_{\sigma\sigma'}\hat{c}_{\alpha\sigma'}$, where the $\vec{S}_{\sigma\sigma'}$ are Pauli's matrices.

For any number of orbitals, imposing the relationship $U = U' + J$ makes possible to recast our hamiltonian 5.1 as :

$$\left(U - \frac{3J}{2}\right)\frac{\hat{N}\left(\hat{N} - 1\right)}{2} - J\hat{S}^2, \quad (5.3)$$

which makes explicit the rotational symmetry since $[\hat{\vec{L}}_i, \hat{S}^2] = 0$ and $[\hat{\vec{L}}_i, \hat{N}] = 0$ for any component (i) of the angular momentum operator.

For systems with three orbitals, if we add the double-hopping term to the atomic hamiltonian, $\frac{J}{2}\sum_{i\neq j,\sigma} \hat{c}^{\dagger}_{i\sigma}\hat{c}^{\dagger}_{i\overline{\sigma}}\hat{c}_{j\overline{\sigma}}\hat{c}_{j\sigma}$, the most natural relationship, $U = U' + 2J$, which arises in a natural way when considering rotations of the $p-$orbitals, also takes us to a rotationally symmetric hamiltonian,

$$\hat{H}^A = (U - 3J)\frac{\hat{N}\left(\hat{N} - 1\right)}{2} - 2J\hat{S}^2 - \frac{J}{2}\hat{L}^2 + \frac{5}{2}J\hat{N}, \quad (5.4)$$

which in this case includes an explicit dependence on the total angular momentum. When looking at the energy or the potential, the distinction between the cases $U = U' + J$ (without double-hopping) or $U = U' + 2J$ (with double-hopping) is not important: The change is associated with the modification of the energy gap, $[E(M+1) - E(M)]$, that in the new Hamiltonian is $U + (M-1)J = U' + (M+1)J$, while in the case $U = U' + J$ takes the value $U + (M-1)J = U' + MJ$. This suggests that both Hamiltonians yield the same $V^A_{eff,i\sigma}$ if we use parameters $\tilde{U}, \tilde{U}', \tilde{J}$ for the new case such that $\tilde{U}' - \tilde{J} = U' - J$ and $\tilde{U}' + (M+1)\tilde{J} = U' + MJ$, an equivalency that we have checked numerically. However, when studying the many-body Green function and DOS, the pole structure of hamiltonian 5.4 is much more complicated, and thus we have limited ourselves to the study of the $U = U' + J$ case.

5.2 Exchange-Correlation

As discussed in chapter 1, we can generalize Hohenberg-Kohn theorem and write the total energy, E^t, associated with Hamiltonian, $\hat{H}^t = \hat{H}^A + \hat{H}^{OE}$, as a function of the occupation numbers $n_{i\sigma} = \langle \hat{n}_{i\sigma} \rangle$, in such a way that $E^t = E^{\mathrm{OE}} + E^A = E^{\mathrm{OE}} + \sum_{i\sigma} \epsilon_{i\sigma} n_{i\sigma} + E^A_{Hx}[n_{i\sigma}] + E^A_{corr}[n_{i\sigma}]$, with $E^{\mathrm{OE}} = \langle \hat{H}^{\mathrm{OE}} \rangle$, $E^A_{Hx}[n_{i\sigma}]$ and $E^A_{corr}[n_{i\sigma}]$ being respectively the Hartree-exchange and correlation energies of $\hat{H}^A$ (in this model $\langle \hat{c}^\dagger_{i\sigma} \hat{c}_{j\sigma'} \rangle = 0$ and there is no intra-atomic hopping).

These quantities, E^{OE}, E^A_H and E^A_{corr}, can be calculated using the Kohn-Sham approach and the exact solution of the effective Hamiltonian:

$$\hat{H}^{eff} = \hat{H}^{\mathrm{OE}} + \sum_{i\sigma} \epsilon_{i\sigma} \hat{n}_{i\sigma} + \sum_{i\sigma} \left(V^A_{Hx,i\sigma} + V^A_{corr,i\sigma} \right) \hat{n}_{i\sigma} \tag{5.5}$$

where $V^A_{Hx,i\sigma} = \partial E^A_{Hx} / \partial n_{i\sigma}$ and $V^A_{corr,i\sigma} = \partial E^A_{corr} / \partial n_{i\sigma}$. The Hartree-Fock energy, E^A_{Hx}, neglecting non-diagonal charges, is given by:

$$\begin{aligned} E^A_{Hx}(n_{i\sigma}) =& U \sum_i n_{i\uparrow} n_{i\downarrow} + \frac{U'}{2} \sum_{i \neq j, \sigma} n_{i\sigma} n_{j\bar{\sigma}} + \frac{U' - J}{2} \sum_{i \neq j, \sigma} n_{i\sigma} n_{j\sigma} \\ =& \frac{U' - J}{2} \mathcal{N}(\mathcal{N} - 1) + \frac{U' - J}{2} \sum_{i\sigma} n_{i\sigma}(1 - n_{i\sigma}) + J \mathcal{N}_\uparrow \mathcal{N}_\downarrow + \\ & J \sum_i n_{i\uparrow} n_{i\downarrow}, \end{aligned} \tag{5.6}$$

where $\mathcal{N}_\sigma = \sum_i n_{i\sigma}$ and $\mathcal{N} = \mathcal{N}_\uparrow + \mathcal{N}_\downarrow$.

To derive this expression, we just apply in our hamiltonian 5.1 the identity that holds for expected values over Slater determinants, 1.69, which, when applied to a many-body hamiltonian, is nothing but the Hartree-Fock approximation in second quantization language.

On the other hand, we can calculate E^A in the limit $U/T \to \infty$ [181], taking into account the first Hund-rule:

$$E^A = \sum_{i\sigma} \epsilon_{i\sigma} n_{i\sigma} + \frac{U' - J}{2} N \left(2\mathcal{N} - N - 1 \right) + J(M+1)(\mathcal{N} - M)\Theta(\mathcal{N} - M), \tag{5.7}$$

where N, an integer number, is defined as: $N < \mathcal{N} < N + 1$, and Θ is the step function; remember that M is the number of i-orbitals. To understand this result,

consider first the following compact way to write the total energy for integer values in the atomic limit and Hund regime [1]:

$$E^A(N) = \left(U' - J\right)\frac{N(N-1)}{2} + J(M+1)(N-M)\Theta(N+1-M) \tag{5.8}$$

When the average charge is $\mathcal{N}$,the system will oscillate thus between the eigenstates with $N = \lfloor \mathcal{N} \rfloor$ and $N = \lfloor \mathcal{N} \rfloor + 1$ electrons. Each of this states has a weight, respectively, α and β which must satisfy $\alpha + \beta = 1$, but also $N\alpha + (N+1)\beta = \mathcal{N}$. From these two relations we have the weights: $\alpha = N - \mathcal{N} + 1$ and $\beta = \mathcal{N} - N$, and then we can calculate

$$\begin{aligned}(N - \mathcal{N} + 1)\, E^A(N) + (\mathcal{N} - N)\, E^A(N+1) = \\ \frac{U' - J}{2} N\,(2\mathcal{N} - N - 1) + J(M+1)(\mathcal{N} - M)\Theta(\mathcal{N} - M),\end{aligned}$$

Combining Equations (5.6) and (5.7) leads to:

$$\begin{aligned}E^A_{corr}(n_{i\sigma}) =& E^A - E^A_{Hx}(n_{i\sigma}) - \sum_{i\sigma}\epsilon_i n_{i\sigma} = \frac{U' - J}{2}\delta\mathcal{N}(1 - \delta\mathcal{N}) - \frac{U' - J}{2}\sum_{i\sigma} n_{i\sigma}(1 - n_{i\sigma}) \\ &+ J(M+1)(\mathcal{N} - M)\Theta(\mathcal{N} - M) - J\mathcal{N}_\uparrow\mathcal{N}_\downarrow - J\sum_i n_{i\uparrow}n_{i\downarrow},\end{aligned} \tag{5.9}$$

for $U/T \to \infty$, where $\delta\mathcal{N} = \mathcal{N} - N$ takes values between 0 and 1, $0 < \delta\mathcal{N} < 1$. For U'/T finite, we can solve numerically the many-body problem and calculate the correlation energy by means of the one-electron problem for the effective hamiltonian with the appropriate $V^A_{eff,i\sigma} = V^A_{Hx,i\sigma} + V^A_{corr,i\sigma}$. This yields $n_{i\sigma}$, E^A, and the correlation energy, E^A_{corr}. In general, when tackling the problem with the atom connected to the chains, we will need not only the Hartree-Fock energy, but also the non-interacting Kinetic energy of the system. The expressions can then be derived with respect to each $n_{i\sigma}$ to get the potentials.

[1] Let us omit the irrelevant one-electron term $\sum_{i\sigma}\epsilon_i n_{i\sigma}$ in this argument. We can reincorporate it to the global term later.

5.2.1 The Hubbard case

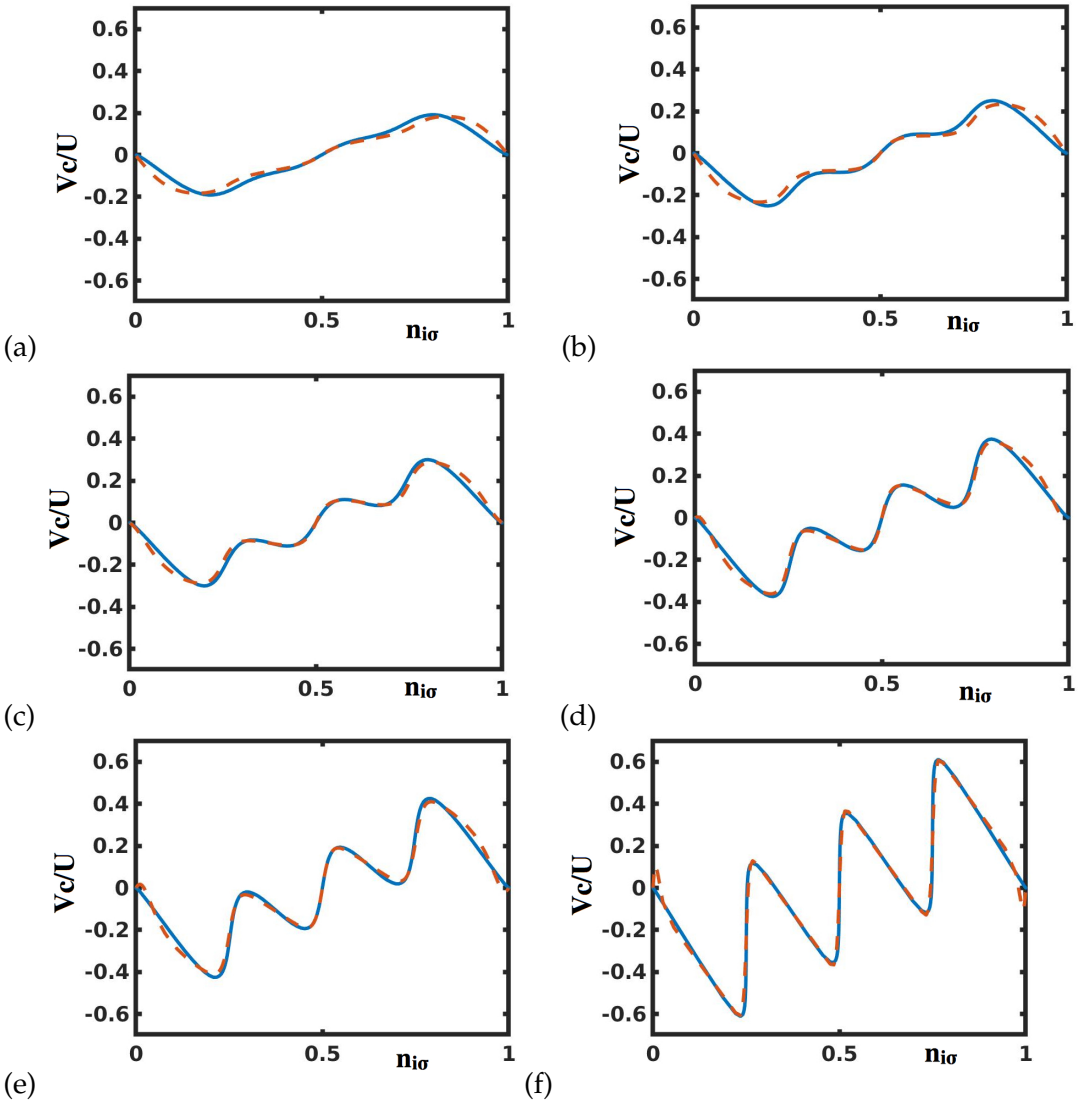

FIGURE 5.2: Correlation potential as a function of $n_{i\sigma}$ in units of U for the Hubbard case for $U/T = 4$ (a), 6 (b), 8 (c), 12 (d), 16 (e), 64 (f). Blue solid line: exact (numerical) correlation potential. Dashed orange line: fit using eqs. 5.11 and 5.12

We present our results discussing first the case $\epsilon_{i\sigma} = 0$, $n_{i\sigma} = \mathcal{N}/2M$ and $M = 2$, in the Hubbard limit: J=0 and $U = U'$. Figure 5.2 shows V^A_{corr} for $U/T = 4, 6, 8, 12, 16, 64$ as a function of $n_{i\sigma}$. For $U/T = 64$, the result is close to the atomic limit:

$$V^A_{corr,i\sigma}(n_{i\sigma}) = -U\left(\frac{1}{2} - n_{i\sigma}\right) + U\left(\frac{1}{2} - \delta\mathcal{N}\right) \quad (J = 0); \tag{5.10}$$

notice that $U\left(\frac{1}{2} - \delta\mathcal{N}\right)$ is a periodic function in the intervals $N < \mathcal{N} < N + 1$, with a saw-tooth behaviour, [181] and that $V^A_{corr,i\sigma} = U(-\delta\mathcal{N} + n_{i\sigma})$. This shows that $V^A_{eff,i\sigma} = V^A_{H,i\sigma} + V^A_{corr,i\sigma} = UN$, indicating that in this limit $V^A_{eff,i\sigma}$ is discontinuous, with the atomic level jumping by U when $\mathcal{N}$ crosses an integer number. Equation (5.10) suggests to fit the calculated values of $V^A_{corr,i\sigma}$ for different U/T (see Figure 5.2)

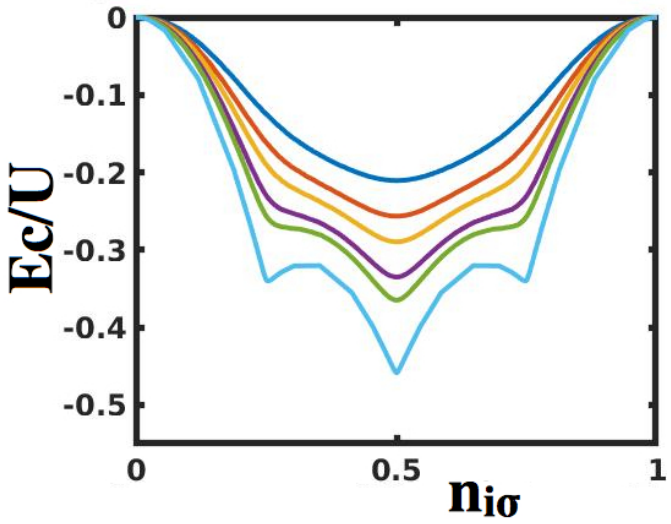

FIGURE 5.3: $E^A_{corr}(n_{i,\sigma})$ in units of U for the Hubbard case, $J = 0$, $M = 2$ and $m = 3$, and different values of $U/T = 4, 6, 8, 12, 16, 64$ (top to bottom).

by means of the equation:

$$V^A_{corr,i\sigma} = -F_1 U\left(\frac{1}{2} - n_{i\sigma}\right) + F_2 U\left(\frac{1}{2} - \delta\mathcal{N}\right), \qquad (J = 0); \tag{5.11}$$

where

$$F_k(x) = f_k \tanh(\alpha_k x(1-x)) \tag{5.12}$$

$(k = 1, 2)$, $x = n_{i\sigma}$ or $\delta\mathcal{N}$, and α_k is a constant.

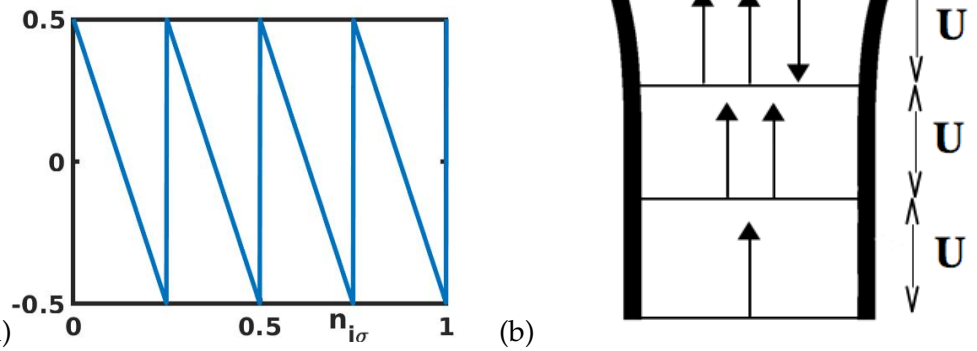

(a) (b)

FIGURE 5.4: (a) Saw-tooth behaviour of the periodic part of the correlation potential, $U\left(\frac{1}{2} - \delta N\right)$, in units of U for $M = 2$; $\mathcal{N} = \sum_{i\sigma} n_{i\sigma}$. The jump between the minima and the maxima is exactly U. (b) Atomic levels $E^A(N) - E^A(N-1) = 0, U, 2U, 3U$, for different atomic charges, $N = 1, 2, 3, 4$. Notice that the jump in the atomic levels corresponds to the jump in $U\left(\frac{1}{2} - \delta N\right)$.

U/T	4	6	8	12	16	32	64
f_1	(0.60) 0.58	(0.67) 0.62	(0.78) 0.68	(0.86) 0.71	(0.89) 0.71	(0.94) 0.80	(0.96) 0.89
f_2	(0.09) 0.15	(0.20) 0.24	(0.30) 0.31	(0.42) 0.49	(0.52) 0.60	(0.71) 0.82	(0.85) 0.92
f_3	0.15	0.24	0.35	0.51	0.65	0.79	1.0
α_1	(8.6) 9.1	(9.1) 10.2	(9.8) 12.2	(12.4) 19.6	(14.3) 20.1	(36.3) 51.1	(50.0) 52.3
α_2	(0.01) 0.08	(0.4) 0.8	(5.6) 6.2	(8.0) 8.2	(9.3) 14.1	(20.3) 17.5	(32.6) 32.1
α_3	25.2	41.2	48.7	63.4	78.5	87.3	165.5
α_4	17.0	20.8	31.0	33.1	38.0	51.4	196.1

TABLE 5.1: Values of f_i and α_i for the Hubbard (in parenthesis) and Hubbard-Hund cases.

In these Equations $F_1(n_{i\sigma}) \approx f_1$ (constant) and $F_2(\delta N) \approx f_2$ (constant, too) except for $n_{i\sigma}$ or $\delta\mathcal{N}$, respectively, close to 0 and 1, since α_1 and α_2 in eq. (5.12) are typically much larger than 1 (see Table 5.1). For $U/T << 4$, our fitting yields $f_1 \approx f_2 \approx 0$, while for $U/T >> 64$, we find the atomic limit with $f_1 \approx f_2 \approx 1$. Table 5.1 shows f_1, f_2, α_1 and α_2 as a function of U/T.

Figure 5.5 shows $V^A_{eff,i\sigma}$ for different values of U/T.

$$V^A_{eff,i\sigma} \approx (1-F_1)U\left(\frac{1}{2}-n_{i\sigma}\right)+U\left(\mathcal{N}-\frac{1}{2}\right)+F_2U\left(\frac{1}{2}-\delta\mathcal{N}\right)\Bigg(\qquad (J=0). \tag{5.13}$$

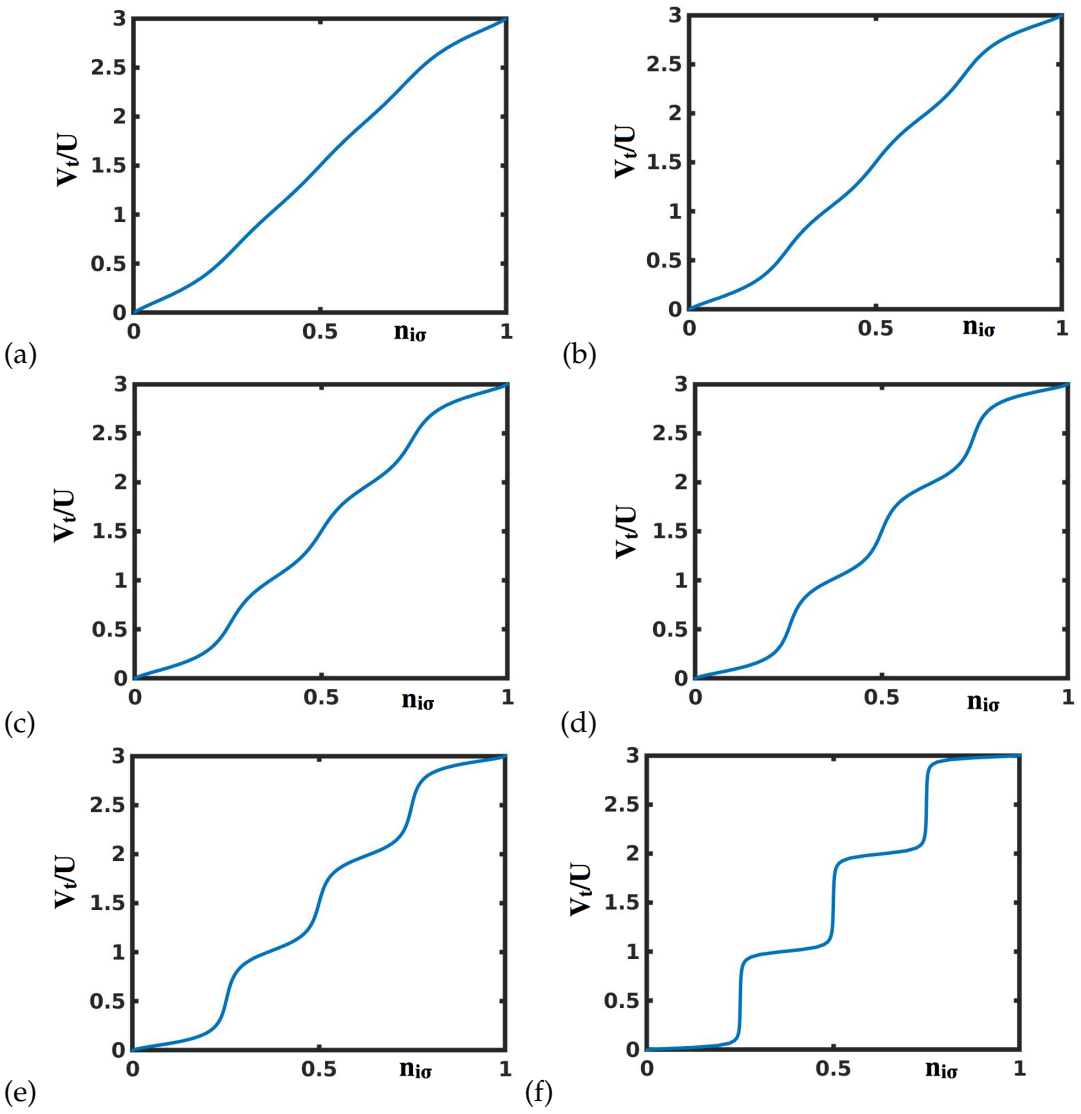

FIGURE 5.5: Effective potential as a function of $n_{i\sigma}$ in units of U, $V^A_{eff,i\sigma} = V^A_{H,i\sigma} + V^A_{corr,i\sigma}$, in the Hubbard case for U/T=4, 6, 8, 12, 16, 64, ordered from left to right and from top to bottom.

For $U/T = 64$, f_1 and f_2 approach 1, so that $V^A_{eff,i\sigma}$ is close to the atomic limit ($f_1 \approx f_2 \approx 1$) with a staircase behavior. For $U/T = 4$, $V^A_{eff,i\sigma}$ is close to a straight line, indicating that we can neglect the fluctuating term $F_2 U\left(\frac{1}{2} - \delta\mathcal{N}\right)$, and approximate Equation (5.13) by $(1 - F_1)U\left(\frac{1}{2} - n_{i\sigma}\right) + U\left(\mathcal{N} - \frac{1}{2}\right)$, and $V^A_{corr,i\sigma}$ by $(1 - F_1)U\left(\frac{1}{2} - n_{i\sigma}\right)$.

Notice that equation (5.13) is valid in the limit $U/T \to 0$, $F_1 \approx F_2 \approx 0$, for any values of $n_{i\sigma}$ even if $n_{i\sigma} \neq n_{j\sigma'}$. Moreover, it should be also realized that the atomic limit, $U/T \to \infty$, of E^A in eq. (5.7) for $J = 0$, $\frac{1}{2}UN(2\mathcal{N} - N - 1)$, only depends on the energy of the states with N and $(N + 1)$ electrons, a value that is independent from the particular occupation of the $i\sigma$ states. This indicates that the atomic limit of eq. (5.13) is also valid for $n_{i\sigma} \neq n_{j\sigma'}$. Those two limits suggest that eq. (5.13) is an appropriate interpolation of $V^A_{eff,i\sigma}$ for $n_{i\sigma} \neq n_{j\sigma'}$ with F_1 and F_2 close to the values given in Table I. This has been checked calculating the case $n_{1\uparrow} = n_{1\downarrow} \neq$

$n_{2\uparrow} = n_{2\downarrow}$. Figure 5.6 shows $V^{A}_{corr,i\sigma}$ along the lines $n_{1\sigma} - n_{2\sigma} = 0.1$; $n_{1\sigma} + n_{2\sigma} = 1$ and $n_{1\sigma} + n_{2\sigma} = 0.9$ for $U/T = 12$, compared with eq. (5.13).

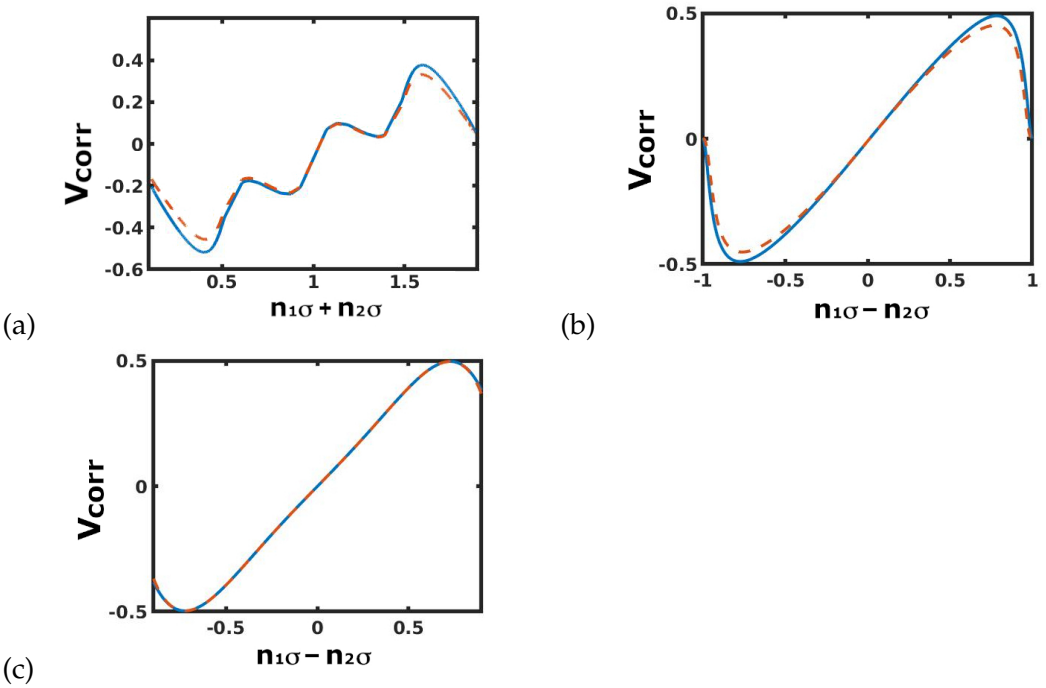

FIGURE 5.6: Correlation potential in units of U, in the Hubbard case for U/T = 12 along different relevant directions: (a) $n_{1\uparrow} - n_{2\uparrow} = 0.1$; (b) $n_{1\uparrow} + n_{2\uparrow} = 1$; (c) Curve $n_{1\uparrow} + n_{2\uparrow} = 0.9$. The potentials are calculated as derivatives of the correlation energy along the direction of the corresponding lines $n_1 \pm n_2 = \text{const}$; these potentials are plotted against $n_1 \mp n_2$. The solid blue line is the exact result, while the dashed line represents our fit using eqs. 5.11 and 5.12

We have also computed maps for the correlation energy for different numbers of levels, where we have also tested our fitting, also with $J > 0$.

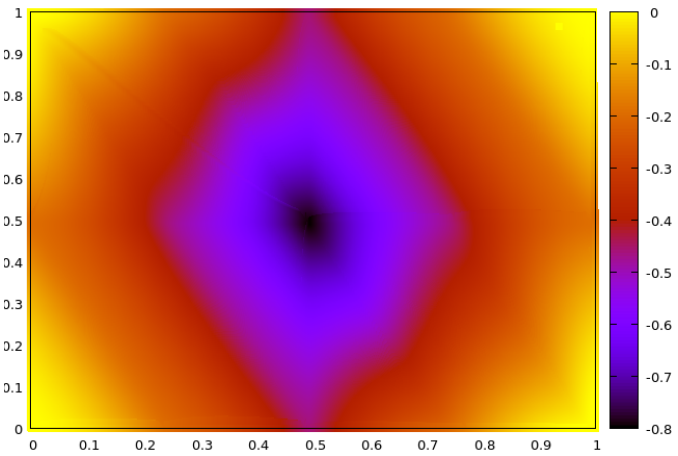

FIGURE 5.7: One Example: Correlation energy for M = 3, m = 1, U/T = 32 in the Hubbard-Hund case (J=0.1U). The horizontal axis indicates the occupation number of two orbitals, and the vertical axis is the occupation number of the third orbital.

Another possible test is to look at exact correlation energies in terms of the magnetization: For example, for the symmetric case ($n_{i\uparrow} + n_{i\downarrow} = 0.5$) we can calculate the correlation potentials in terms of the magnetization m, $m = n_{i\uparrow} - n_{i\downarrow}$ by plugging different magnetic fields and checking how the system responds in the exact numerical solution, and check that our fittings 5.11,5.12 also hold.

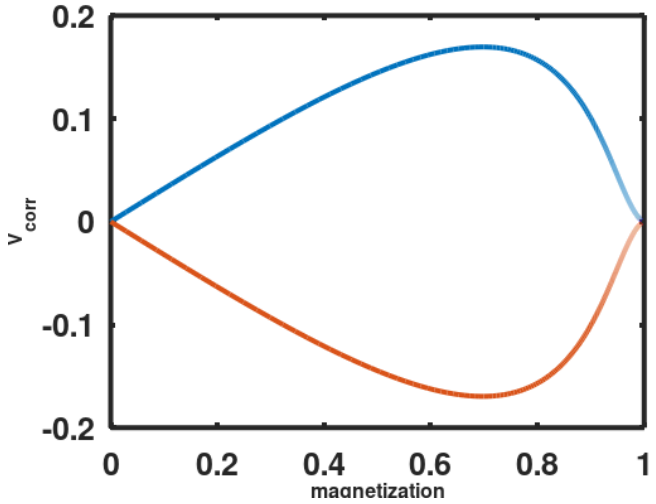

FIGURE 5.8: An example: Correlation potentials for the symmetric case ($n_{i\uparrow} + n_{i\downarrow} = 0.5$) in the Hubbard-Hund case for $U/T = 6$. In blue, positive, the correlation potential for the spin up levels; in orange, negative, the correlation potential for the spin down levels.

5.2.2 The Hubbard-Hund case.

Figure 5.9 shows our numerical results for $V^A_{corr,i\sigma}$ taking $J = 0.1U$ and $U = U' + J$. In the atomic limit, $U/T \to \infty$, $V^A_{corr,i\sigma}$ is given by:

$$V^A_{corr,i\sigma} = -(U' - J)\left(\frac{1}{2} - n_{i\sigma}\right) + (U' - J)\left(\frac{1}{2} - \delta\mathcal{N}\right) - J\left(\mathcal{N}_{\bar{\sigma}} + n_{i\bar{\sigma}}\right) + (M+1)J\Theta(\mathcal{N} - M) \tag{5.14}$$

Notice that the first two terms of this equation are the ones found in Equation (5.10) changing U by $(U' - J)$; the last two terms are new contributions associated with J. Equation (5.14) suggests to fit our calculations for $V^A_{corr,i\sigma}$ (see fig. 5.9) by the following potential:

$$V^A_{corr,i\sigma} = -F_1\left(U' - J\right)\left(\frac{1}{2} - n_{i\sigma}\right) + F_2\left(U' - J\right)\left(\frac{1}{2} - \delta\mathcal{N}\right) - F_3 J\left(\mathcal{N}_{\bar{\sigma}} + n_{i\bar{\sigma}}\right) + F_4 J(M+1) \tag{5.15}$$

where F_1 and F_2 have the same functional form as in equation (5.12), and:

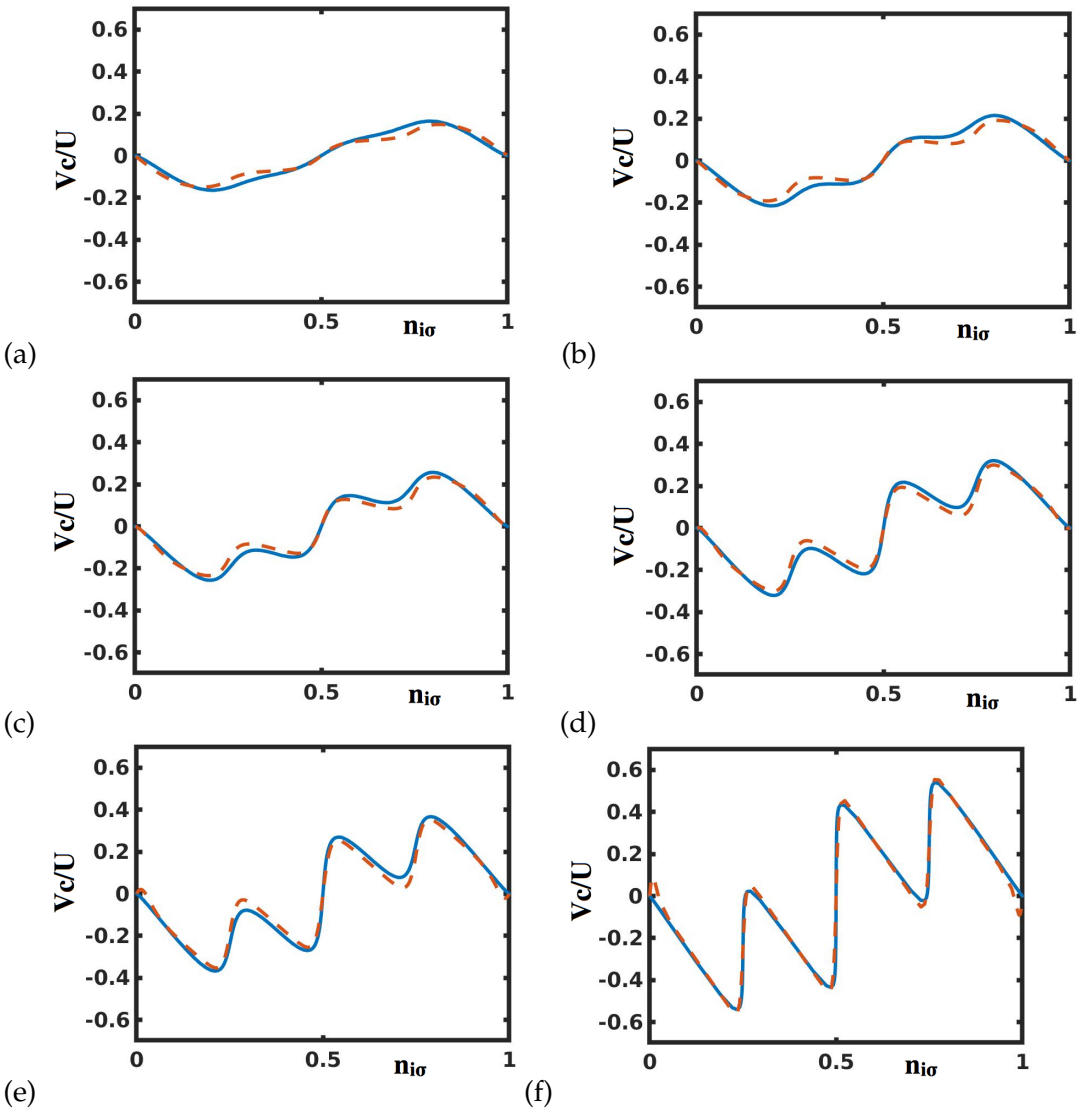

FIGURE 5.9: Correlation potential as a function of $n_{i\sigma}$ in units of U in the Hubbard-Hund case for U/T=4, 6, 8, 12, 16, 64. Blue solid line: exact (numerical) correlation potential. Dashed orange line: fit using eqs. 5.15 and 5.12

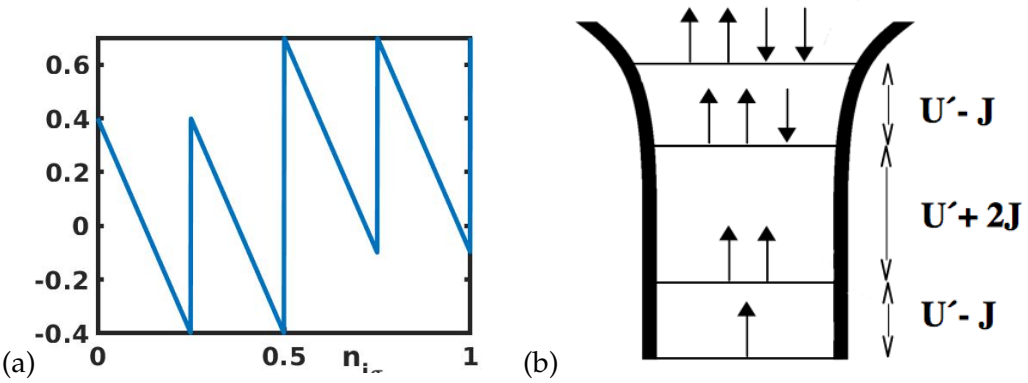

FIGURE 5.10: (a) Sawtooth behaviour of $(U' - J)\left(\frac{1}{2} - \delta N\right) + J(M + 1)\Theta(N - M)$, see equations (5.14) and (5.15), in units of U for $M = 2$; (b) Atomic levels, $E^A(N) - E^A(N-1) = 0, U' - J, 2U' + J, 3U'$, for different atomic charges, $N = 1, 2, 3, 4$. Compare with fig. 5.4; the jump between the levels for three and two electrons, $U' + 2J$ is reflected in the jump in (a) for $n_{i\sigma} = 0.5$.

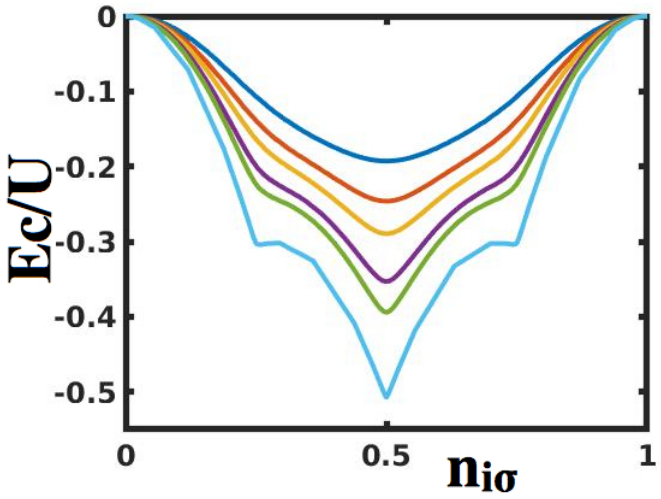

FIGURE 5.11: As Fig. 5.3 for the Hubbard-Hund case, $J = 0.1$ $M = 2$ and $m = 3$, and different values of $U/T = 4, 6, 8, 12, 16, 64$ (top to bottom).

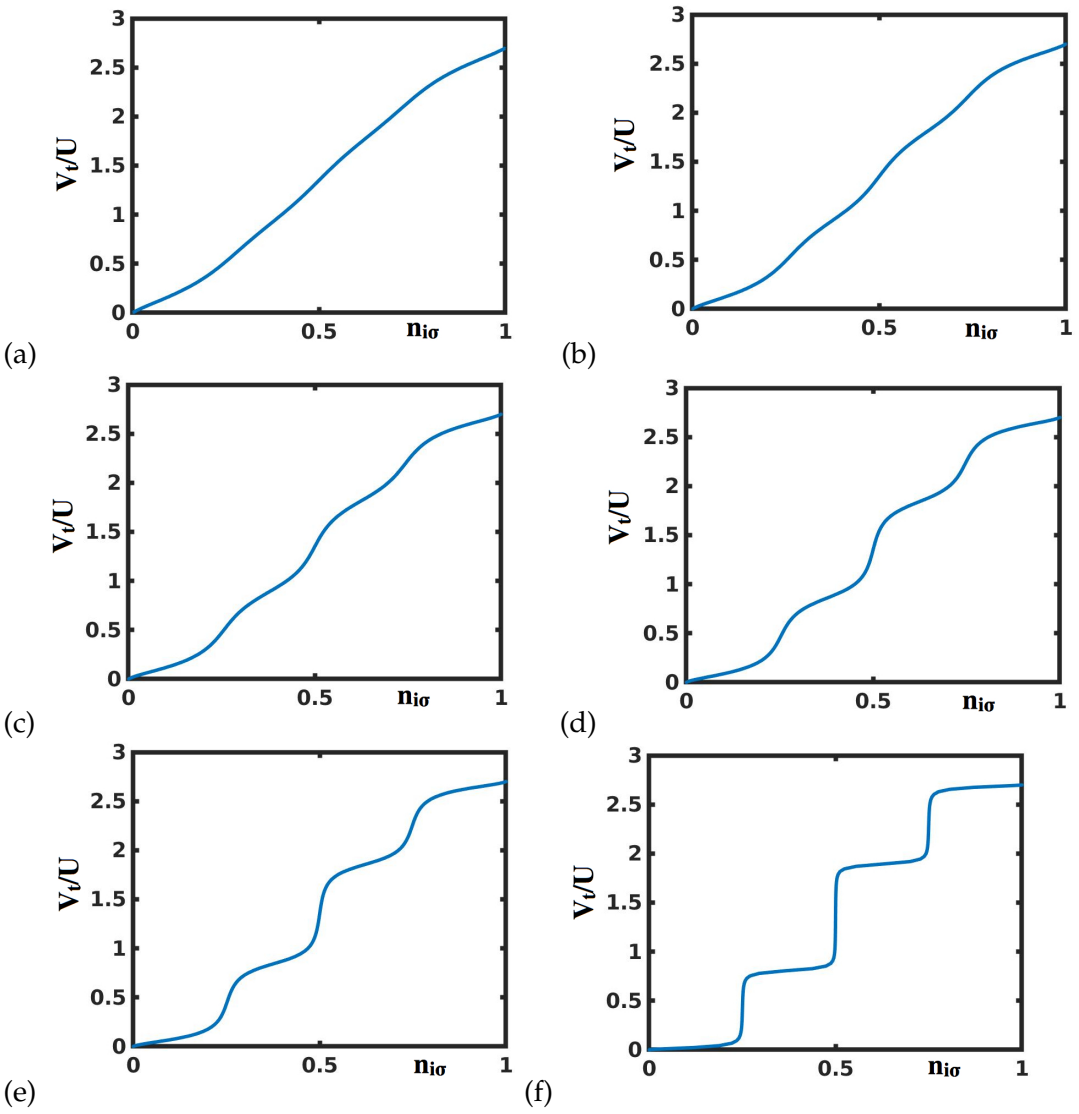

FIGURE 5.12: Effective potential as a function of $n_{i\sigma}$ in units of U, $V^A_{eff,i\sigma} = V^A_{H,i\sigma} + V^A_{corr,i\sigma}$, in the Hubbard-Hund case for U/T=4, 6, 8, 12, 16, 64.

$$\begin{aligned} F_3 &= f_3 \tanh\left(\alpha_3 x(M+1-x)\right); \qquad (x = \mathcal{N}_{\overline{\sigma}} + n_{i\overline{\sigma}}) \\ F_4 &= f_3 / \left[1 + \exp\left(-\alpha_4(\mathcal{N} - M)\right)\right] \end{aligned} \tag{5.16}$$

As in the Hubbard case, we can write $F_1 \approx f_1$, $F_2 \approx f_2$ and $F_3 \approx f_3$ if the corresponding variables are not close to their edge limits: 0 or 1 for $n_{i\sigma}$ and $\delta\mathcal{N}$, 0 or $M+1$ for $x = \mathcal{N}_{\overline{\sigma}} + n_{i\overline{\sigma}}$, and M for $\mathcal{N}$. On the other hand, for small values of U/T ($U/T << 4$), $f_i \to 0$, and $V^A_{eff,i\sigma} = V^A_{Hx,i\sigma}$ is given by:

$$V^A_{eff,i\sigma} = (U' - J)\left(\frac{1}{2} - n_{i\sigma}\right) + (U' - J)\left(\mathcal{N} - \frac{1}{2}\right) + J\left(\mathcal{N}_{\overline{\sigma}} + n_{i\overline{\sigma}}\right), \tag{5.17}$$

while for U/T large ($U/T >> 64$) $f_i \to 1$ and

$$V^A_{eff,i\sigma} = (U' - J)\left(\mathcal{N} - \frac{1}{2}\right) + (U' - J)\left(\frac{1}{2} - \delta\mathcal{N}\right) + J\,(M+1)\,\Theta(\mathcal{N} - M). \quad (5.18)$$

The last two terms in this equation are associated with the jump in the energy levels of the isolated atom. While $(U' - J)\left(\frac{1}{2} - \delta\mathcal{N}\right)$ yields the see-saw behaviour with $E(N+1) - E(N) = U' - J$, for $N \neq M$, $J\,(M+1)\,\Theta(\mathcal{N} - M)$ is associated with the energy difference $E(M+1) - E(M) = U' + MJ$ between the M and $M+1$ levels.

In general, from our fit for $V^A_{corr,i\sigma}$, we see that $V^A_{eff,i\sigma}$ can be well-fitted by:

$$\begin{aligned} V^A_{eff,i\sigma} = {} & (1 - F_1)\,(U' - J)\left(\frac{1}{2} - n_{i\sigma}\right) + (U' - J)\left(\mathcal{N} - \frac{1}{2}\right) + F_2\,(U' - J)\left(\frac{1}{2} - \delta\mathcal{N}\right) \\ & + (1 - F_3)\,J\,(\mathcal{N}_{\bar{\sigma}} + n_{i\bar{\sigma}}) + F_4 J(M+1). \end{aligned} \quad (5.19)$$

We show in Table 5.1 the values of f_1, f_2, f_3, α_1, α_2, α_3, α_4 as calculated in our fitting. In general, f_1 and f_2 are similar to the values given for the Hubbard case, although f_1 is a little smaller (and f_2 a little larger): this is due to the effective U of this case that is smaller, $U' - J = U - 2J = 0.8U$. While in the Hubbard case f_1 varies monotonically, in the Hubbard-Hund case it is observed to have a plateau for values of U/T between 8 and 16. This seems to be due to the transition to the Hubbard-Hund regime: indeed, defining the Hund subspace as those configurations satisfying the first Hund rule, we have calculated that the projection of the ground state over the Hund subspace is 66 %, 83%, and 95% for $U/T = 4$, 8 and 12, respectively. It is also interesting to realize that for $U/T \leq 6$, f_2 and f_3 are small so that $V^A_{eff,i\sigma}$ can be approximated by

$$V^A_{eff,i\sigma} = (1 - F_1)\,(U' - J)\left(\frac{1}{2} - n_{i\sigma}\right) + (U' - J)\left(\mathcal{N} - \frac{1}{2}\right) + J\,(\mathcal{N}_{\bar{\sigma}} + n_{i\bar{\sigma}})\,. \quad (5.20)$$

In this case, only the term $(U' - J)\left(\frac{1}{2} - n_{i\sigma}\right)$ is screened to $(1 - F_1)\,(U' - J)\left(\frac{1}{2} - n_{i\sigma}\right)$ by correlation effects while the exchange contribution $J\,(\mathcal{N}_{\bar{\sigma}} + n_{i\bar{\sigma}})$ remains almost unchanged.

5.2.3 M=3 and M=5.

Up to now, we have considered M=2 with 3 levels (m=3) in each of the two channels introduced in our model, see Figure 5.1. Analyzing a similar case with M= 3 or 5 is not an easy task because the exact solution of the corresponding many-body problem is numerically very demanding. Exact diagonalization is no longer possible, and thus we have taken, for M = 3 or 5, channels with only one level (m = 1). This simplification yields a good approximation to the more complete case with m = 3 as we have checked comparing, when, M = 2, the case $m = 1$ with the case $m = 3$ for a range of values of the hopping in the metallic chain, t (see eq. 5.2) . Thus, Figure 5.13 shows $V^A_{corr,i\sigma}$ for the Hubbard-Hund case, M = 2 and m = 1 or 3; the values taken for U/T are the same as in the other figures. The comparison of both cases shows that $V^A_{corr,i\sigma}$ is only slightly changed between m = 1 or 3 and that the deviation from the case $m = 1$ is monotonously increasing on t. Similarly, figure 5.14 shows the same comparison in terms of the correlation energy.

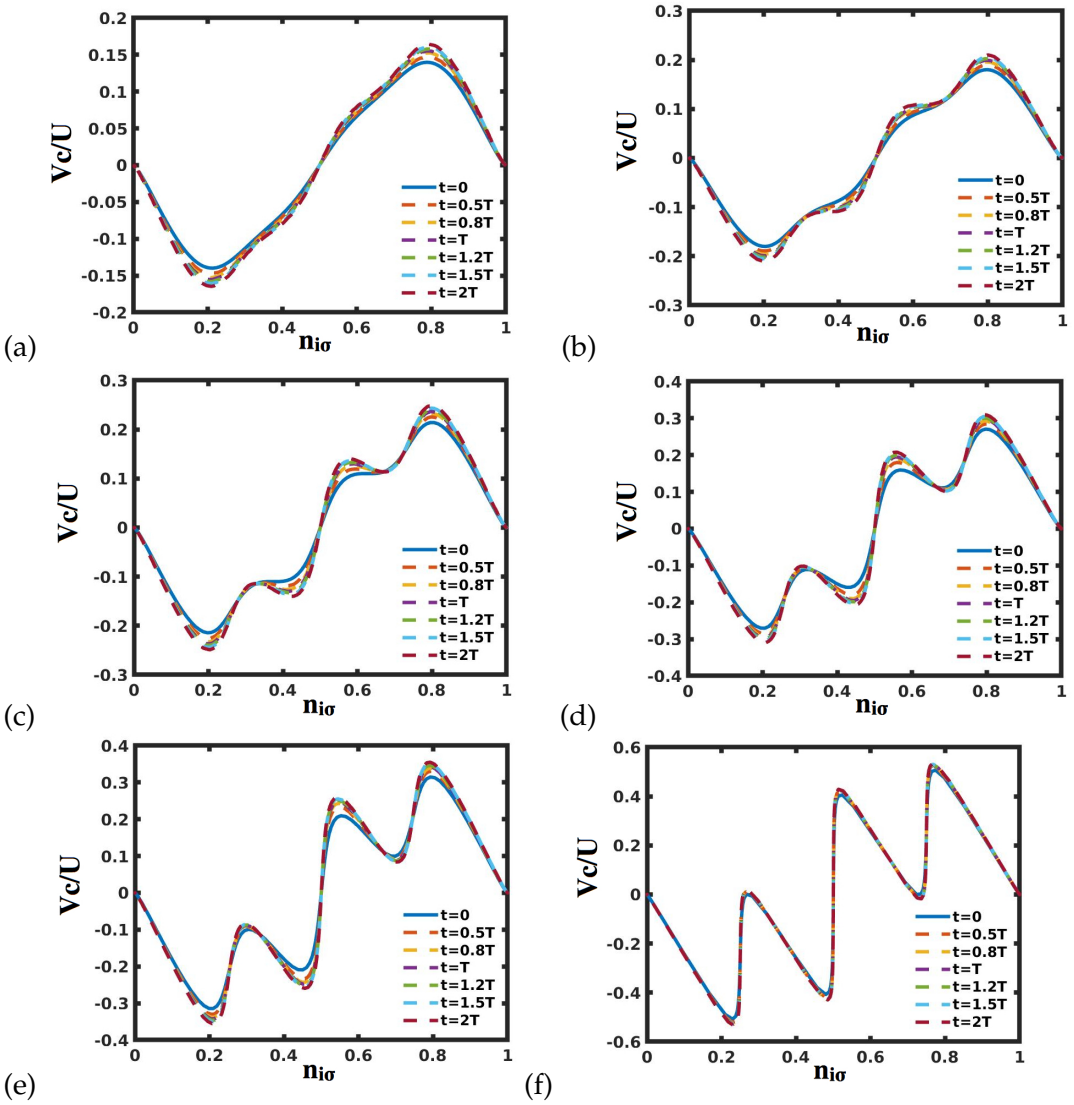

FIGURE 5.13: Correlation potential as a function of $n_{i\sigma}$ in units of U in the Hubbard-Hund case for $M = 2$, $m = 3$ (dashed lines) and $M = 2, m = 1$ (solid blue line, case $t = 0$.) for U/T = 4, 6, 8, 12, 16, 64, ordered from left to right and from top to bottom.

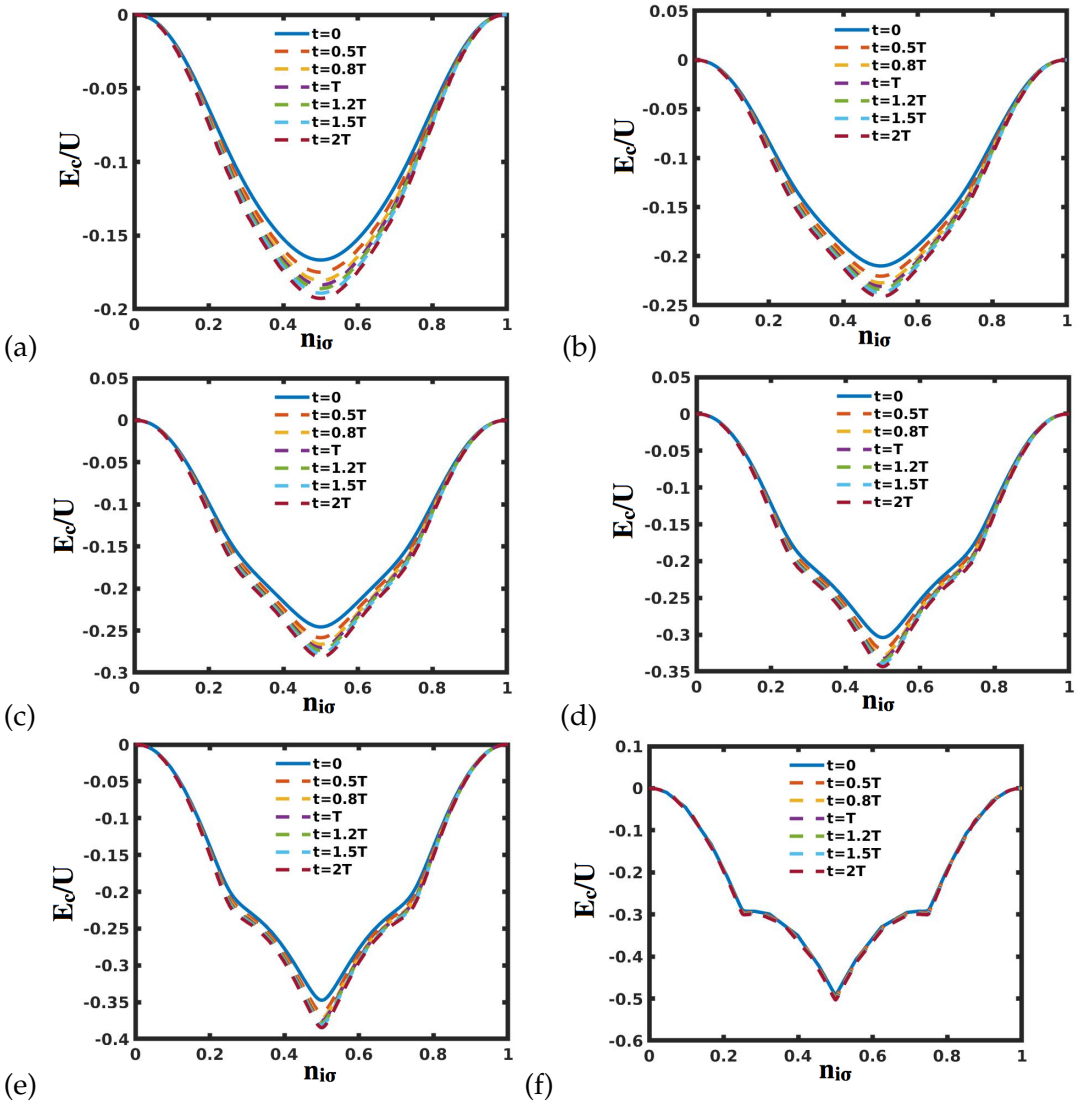

FIGURE 5.14: Correlation energy as a function of $n_{i\sigma}$ in units of U in the Hubbard-Hund case for $M = 2$, $m = 3$ (dashed lines) and $M = 2, m = 1$ (solid blue line, case $t = 0$.) for $U/T = 4, 6, 8, 12, 16, 64$.

Figure 5.15 shows $V^A_{corr,i\sigma}$ for $M = 3$ and $m = 1$, while Figure 5.18 shows the result for $M = 5$ and $m = 1$, in both cases for the Hubbard-Hund case. Tables 5.2 and 5.3 give the values of $f_1, f_2, f_3, \alpha_1, \alpha_2, \alpha_3$ and α_4 for $M = 3$ or 5, and $m = 1$, as calculated in our best fitting to $V^A_{corr,i\sigma}$, as given by equation (5.15).

As in the case $M = 2$, for $U/T \leq 6$, $V^A_{eff,i\sigma}$ can also be approximated by eq. 5.13, with the term $(U' - J)(1/2 - n_{i\sigma})$ screened to $(1 - F_1)(U' - J)(1/2 - n_{i\sigma})$ and the exchange contribution, $J\,(\mathcal{N}_{\bar{\sigma}} + n_{i\bar{\sigma}})$ unchanged

It is interesting to mention that in the more general Kanamori Hamiltonian, where the double hopping term, $\frac{J}{2}\sum_{i\neq j}\hat{c}^\dagger_{i\sigma}\hat{c}^\dagger_{i\bar{\sigma}}\hat{c}_{j\bar{\sigma}}\hat{c}_{j\sigma}$, is included, and U is taken as $U' + 2J$ in order to keep the rotational symmetry for $M = 3$, one can repeat the previous arguments and show that $V^A_{eff,i\sigma}$ in equation (5.19) is still valid, changing only the last two terms by $(1 - F_3)J\,(\mathcal{N}_{\bar{\sigma}} + 2n_{i\bar{\sigma}}) + F_4 J(M + 2)$. The point to realize is that this change is associated with the modification of the energy gap, $[E(M + 1) - E(M)]$, that in the new Hamiltonian is $U + (M - 1)J = U' + (M + 1)J$, while in the case $U = U' + J$ takes the value $U + (M - 1)J = U' + MJ$. This suggests that both

Hamiltonians yield the same $V^A_{eff,i\sigma}$ if we use parameters $\tilde{U}, \tilde{U}', \tilde{J}$ for the new case such that $\tilde{U}' - \tilde{J} = U' - J$ and $\tilde{U}' + (M+1)\tilde{J} = U' + MJ$, an equivalency that we have checked numerically. We conclude that eq. (5.19) is quite general, adjusting appropriately the last two terms to the value of $[E(M+1) - E(M)]$ as given by the corresponding model Hamiltonian.

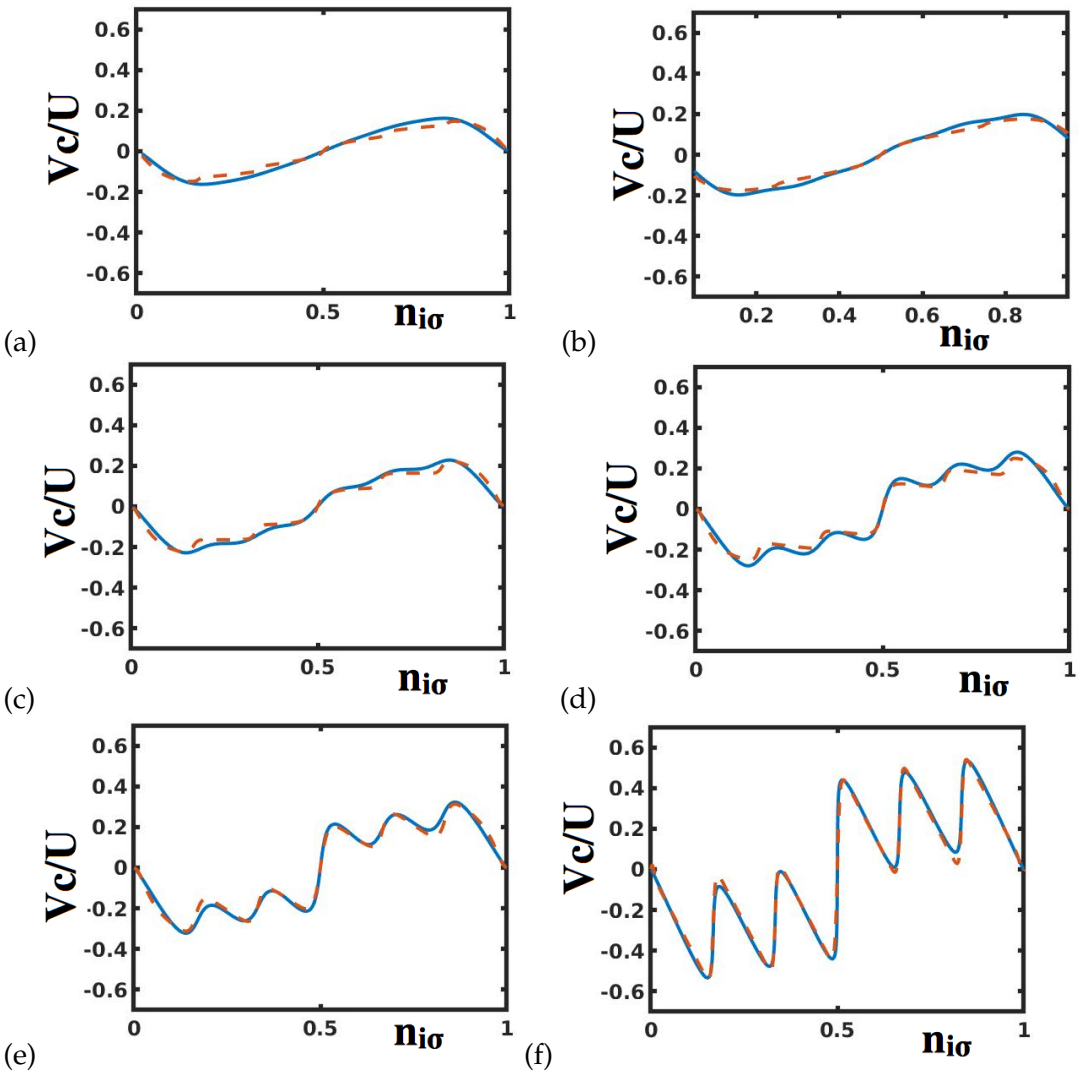

FIGURE 5.15: Same as fig. 5.9 for $M = 3$, $m = 1$.

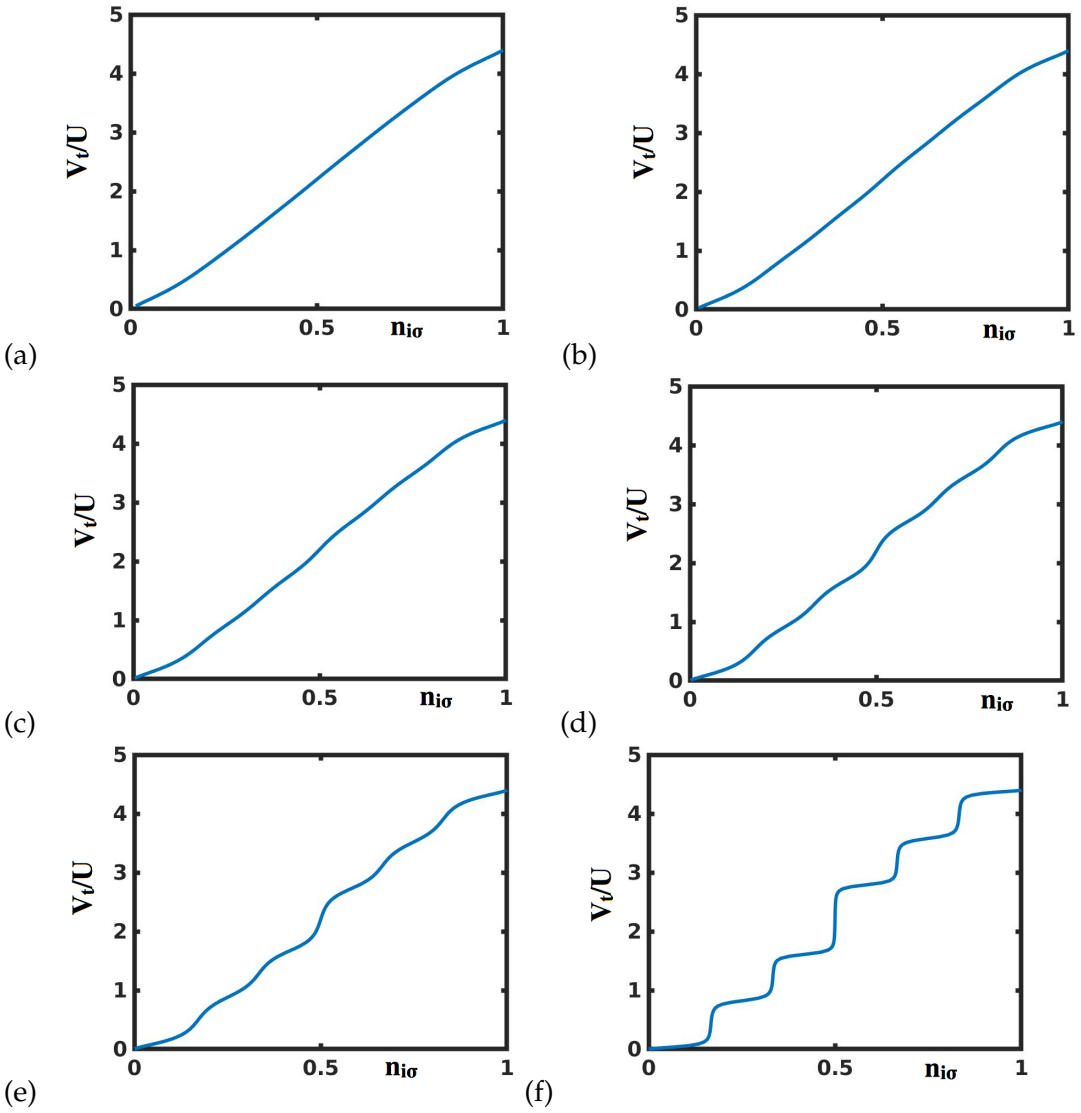

FIGURE 5.16: Effective potential, $V^A_{eff,i\sigma}$, in units of U for the Hubbard-Hund case ($J = 0.1U$), for $M = 3$, $m = 1$ and $U/T = 4, 6, 8, 12, 16, 64$.

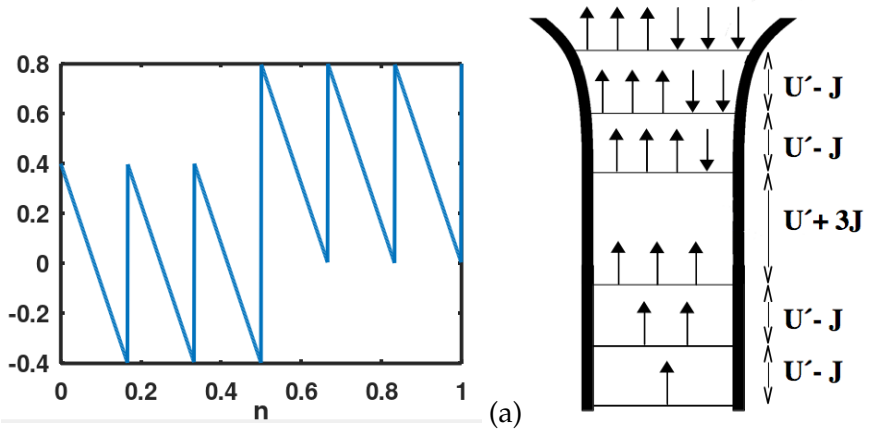

FIGURE 5.17: (a) Sawtooth behaviour of $(U'-J)\left(\frac{1}{2}-\delta N\right)+J(M+1)\Theta(N-M)$, see equation 5.14, in units of U for $M=3$; (b) Atomic levels, $E^A(N)-E^A(N-1)=0, U'-J, 2(U'-J), 3U'+J, 4U', 5U'-J$ for different atomic charges, $N=1,2,3,4,5,6$. The jump between the levels for four and three electrons, $U'+3J$ is reflected in the jump in (a) for $n_{i\sigma}=0.5$.

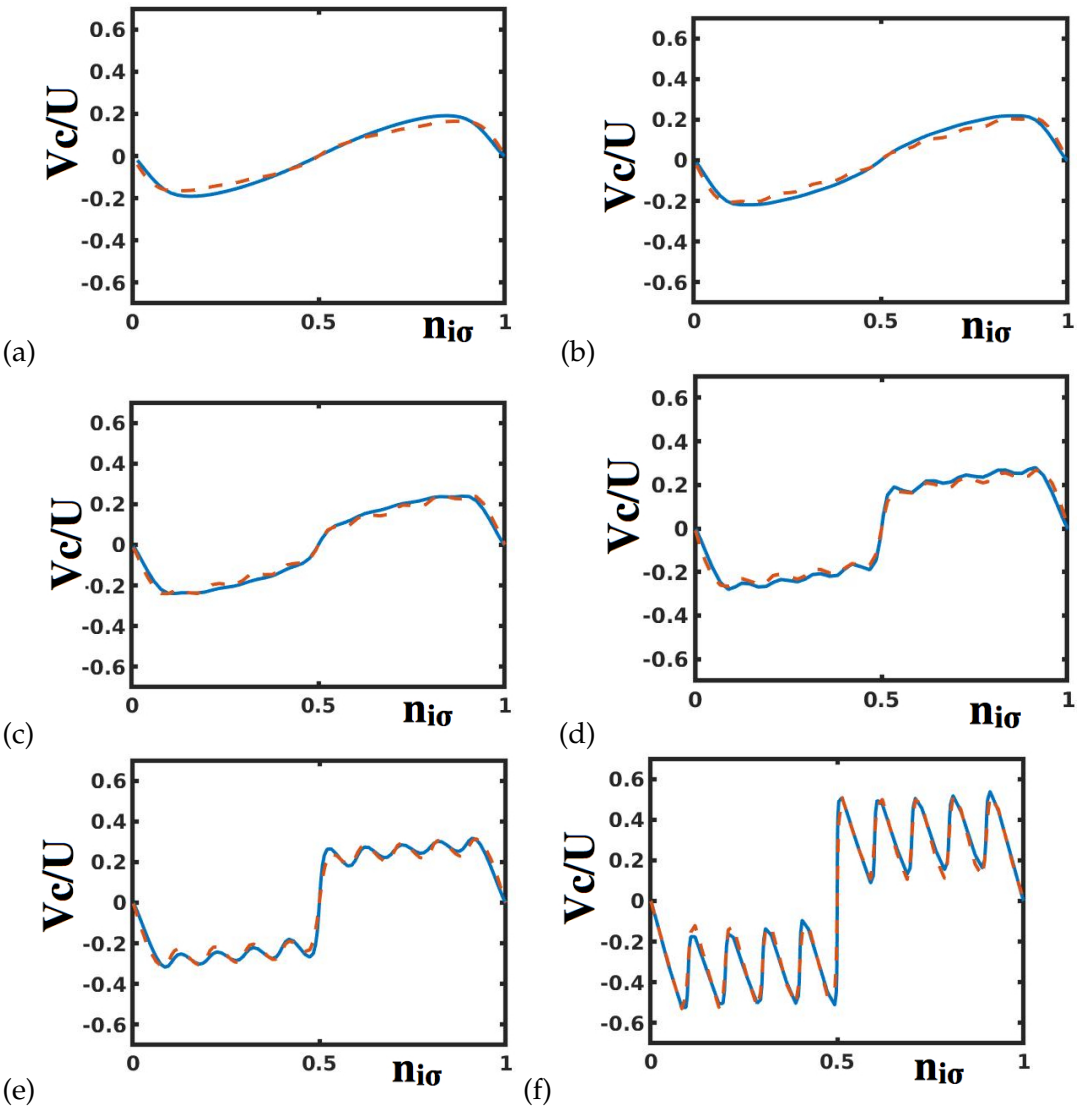

FIGURE 5.18: Same as fig. 5.9 for $M=5$, $m=1$.

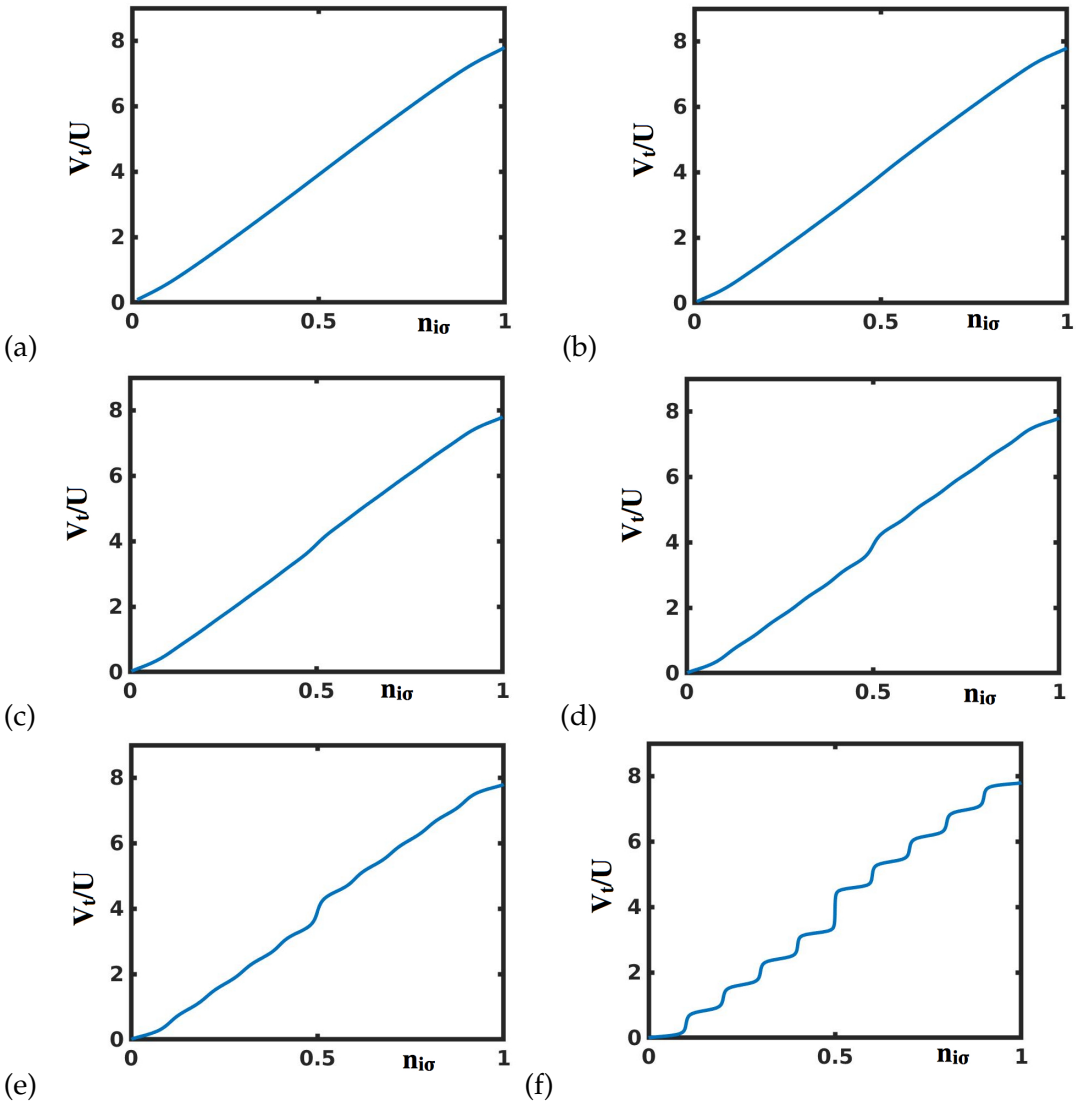

FIGURE 5.19: Effective potential, $V^A_{eff,i\sigma}$ in units of U, for the Hubbard-Hund case ($J = 0.1U$) for $M = 5$, $m = 1$ and U/T=4, 6, 8, 12, 16, 64.

It is interesting to realize that $V^A_{eff,i\sigma}$ is practically a straight line for $U/T \leq 6$ for $M = 3$ or 5 except for a small bending $n_{i,\sigma}$ near 0 or 1; even for $U/T = 8$ we find only small kinks around $n_{i,\sigma} \approx 0.5$. This shows how $V^A_{eff,i\sigma}$ can be well approximated by by neglecting the dependency on $\delta\mathcal{N}$ on eq. 5.10 for $U/T \leq 6$.

U/T	4	6	8	12	16	32	64
f_1	(0.65) 0.55	(0.70) 0.68	(0.80) 0.71	(0.83) 0.69	(0.92) 0.71	(0.88) 0.76	(0.94) 0.82
f_2	(0.00) 0.00	(0.05) 0.03	(0.10) 0.09	(0.14) 0.17	(0.31) 0.33	(0.55) 0.61	(0.76) 0.80
f_3	0.15	0.20	0.24	0.37	0.67	0.91	1.0
α_1	(10.3) 10.1	(10.5) 11.2	(11.8) 12.3	(15.4) 17.9	(16.7) 22.4	(27.8) 45.3	(62.0) 71.7
α_2	(0.01) 0.08	(0.3) 0.4	(2.6) 4.7	(5.7) 8.2	(9.7) 13.5	(22.6) 25.1	(40.9) 36.6
α_3	25.2	41.2	48.7	63.4	78.5	87.3	165.5
α_4	17.5	24.2	36.6	39.3	44.2	55.7	167.2

TABLE 5.2: Same as Table I for $M = 3$, $m = 1$.

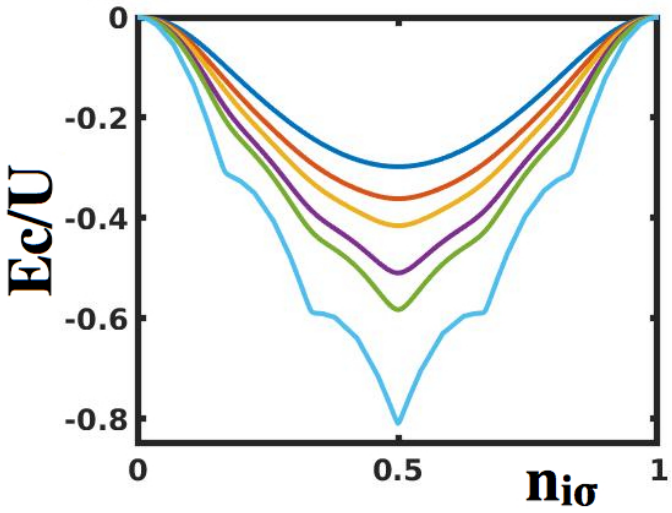

FIGURE 5.20: $E^A_{corr}(n_{i,\sigma})$ in units of U for the Hubbard-Hund case, $J = 0.1U$, $M = 3$ and $m = 1$, and different values of $U/T = 4, 6, 8, 12, 16, 64$ (top to bottom).

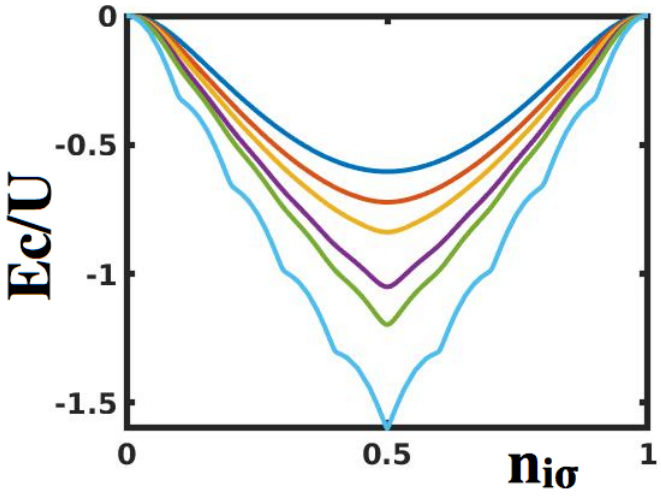

FIGURE 5.21: $E^A_{corr}(n_{i,\sigma})$ in units of U for the Hubbard-Hund case, $J = 0.1U$, $M = 5$ and $m = 1$, and different values of $U/T = 4, 6, 8, 12, 16, 64$ (top to bottom).

U/T	4	6	8	12	16	32	64
f_1	(0.66) 0.57	(0.73) 0.70	(0.82) 0.73	(0.86) 0.70	(0.88) 0.72	(0.94) 0.79	(0.96) 0.82
f_2	(0.02) 0.01	(0.09) 0.09	(0.19) 0.17	(0.30) 0.32	(0.44) 0.51	(0.62) 0.66	(0.84) 0.93
f_3	0.15	0.21	0.33	0.54	0.74	0.99	1.0
α_1	(11.7) 12.1	(13.7) 22.1	(14.4) 27.2	(19.1) 34.2	(26.4) 41.8	(38.3) 87.6	(63.7) 78.6
α_2	(0.01) 0.08	(0.3) 0.3	(4.6) 5.1	(9.2) 7.5	(10.5) 19.7	(25.4) 27.5	(35.3) 38.4
α_3	25.2	41.2	48.7	63.4	78.5	87.3	165.5
α_4	11.3	14.0	31.5	47.3	48.6	154.8	291.6

TABLE 5.3: Same as Table I for $M = 5$, $m = 1$.

5.3 DFT+U

The previous analysis can be used to derive a DFT+U potential appropriate for a magnetic atom within an environment as described by the model system shown in figure 5.1. For this purpose we introduce the effective potential associated with the double counting energy, E^{dc}_{DFT} , which is already included in the DFT-calculation. Different double counting contributions have been proposed in the literature [182], however here for the sake of simplicity we follow Lichtenstein *et al.* [183] and define:

$$E^{dc}_{DFT} = \frac{1}{2}U'\mathcal{N}(\mathcal{N}-1) - \frac{1}{2}J\mathcal{N}_\uparrow(\mathcal{N}_\uparrow - 1) - \frac{1}{2}J\mathcal{N}_\downarrow(\mathcal{N}_\downarrow - 1), \tag{5.21}$$

where the Coulomb interaction between electrons is approximated by $\frac{1}{2}U'\mathcal{N}(\mathcal{N}-1)$, and the exchange interaction is given by $\frac{1}{2}J\mathcal{N}_\uparrow(\mathcal{N}_\uparrow - 1) + \frac{1}{2}J\mathcal{N}_\downarrow(\mathcal{N}_\downarrow - 1)$. Then, the double counting energy associated with a spin-independent DFT calculation is obtained by taking $\mathcal{N}_\uparrow = \mathcal{N}_\downarrow = \mathcal{N}/2$, so that:

$$E^{dc}_{DFT} = \frac{1}{2}U'\mathcal{N}(\mathcal{N}-1) - \frac{1}{4}J\mathcal{N}(\mathcal{N}-2). \tag{5.22}$$

Combining eq. 5.19 with $V^{dc}_{DFT} = (U'-J)(\mathcal{N} - \frac{1}{2}) + \frac{1}{2}J\mathcal{N}$, leads to the following DFT+U potential:

$$\begin{aligned} V_{DFT+U,i\sigma} =& (1-F_1)(U'-J)\left(\frac{1}{2} - n_{i\sigma}\right) + F_2(U'-J)\left(\frac{1}{2} - \delta\mathcal{N}\right) + \\ & (1-F_3)J\left(\mathcal{N}_{\bar{\sigma}} + n_{i\bar{\sigma}}\right) - \frac{1}{2}J\mathcal{N} + F_4 J(M+1). \end{aligned} \tag{5.23}$$

The first term, $(1-F_1)(U'-J)(1/2 - n_{i\sigma})$, represents the conventional DFT+U potential with $(U'-J)$ instead of U, *screened by* $(1-F_1)$, while the term $F_2(U'-J)\left(\frac{1}{2} - \delta\mathcal{N}\right)$ is associated with the jump $(U'-J)$ in the atomic levels. The following exchange terms proportional to J, are dominated by $(1-F_3)J(\mathcal{N}_{\bar{\sigma}} + n_{i\bar{\sigma}})$; it represents the exchange potential interaction screened by $(1-F_3)$, that tends to favor magnetic solutions of the atom because for $\delta n_{i\sigma} = -\delta n_{i\bar{\sigma}} > 0$, $\delta V_{i\sigma} < 0$, this shift increasing the atomic magnetization.

It should be mentioned that in the limit $U/T \to 0$, with $F_1 \simeq F_2 \simeq F_3 \simeq F_4 \to 0$, with no correlation effect,the resulting DFT+U potential has already been described in the seminal work of Anisimov *el al.* [44, 184], using a mean field approximation for

the Hubbard Hamiltonian. Our work shows how those contributions are modified by going beyond that mean field solution.

Let us now apply previous arguments to two cases that have been abundantly discussed in the literature: 3*d*-transition metal oxides, MnO, FeO,CoO and NiO, and metal Fe. For the 3*d*-metal oxides Anisimov *et al* [184] have calculated, using a constrained LDA-approach, values of U' around 7.5 eV and J around 0.9 eV; the Density of States (DOS) for these materials [44, 185] yield bandwidths, Δ, in the order of 4.5 eV. From this value, we can calculate the effective hopping, T, for the channels of Figure 5.1, using the equation $T = \Delta/\sqrt{12}$ given by Desjonqueres and Spanjaard [186]. These values lead to the following quantity: $U'/T = 5.8$; for $M = 5$, we find that $F_1 \simeq 0.7$, $F_2 \simeq 0.1$ and $F_3 \simeq 0.2$. Then equation (5.23) indicates that $(U' - J) = 6.6$ eV is screened to 2.0 eV, while J is slightly changed to 0.7 eV. These results are in good agreement with GGA+U calculations [185] that have suggested that in that approach $(U' - J)$ should be reduced to an effective value of around 3 eV in order to obtain a good density of states for these 3*d*-metal oxides. Metal Fe represents a similar case, because constrained LDA calculations [44] lead to $U' = 6$ eV; in metal Fe, Δ is around 4 eV, a value that leads to U'/T around 5.5. As in the previous case, this quantity indicates that $(U' - J)$ is screened to 1.8 eV, in good agreement with the effective value of U, around 2.2 eV, calculated by Cococcioni and Gironcoli [182] using a 'linear response' approach.

These two examples show that in the DFT+U calculations of the 3*d*-transition metal crystals, $(U' - J)(1/2 - n_{i\sigma})$, in equation (5.23), is much more strongly screened than the Hubbard-Hund term, $J\,(\mathcal{N}_{\overline{\sigma}} + n_{i\overline{\sigma}})$. This result suggests that this Hubbard-Hund term might be the dominant contribution in the formation of the atomic magnetism [187].

5.4 Stoner parameter and magnetism

An interesting application of the fitting found above for the correlation potential is the study of how a system such as the one described by fig. 5.1 and eq. 5.1 can become magnetic for certain values of U/T. By adding a magnetic to hamiltonian 5.1 we can see how the charges split in spin-up and spin-down component. Furthermore, this information is useful to compute the Stoner parameter, I, and thus investigate when the system might favour magnetic solutions. Here we first show explicitly how, in the two level system, with a magnetic field which is 1% of U, magnetization appears for different values of U/T as we explore different values of the metallic band (E_F). However, this model, based on a very short metallic chain, is not convenient to explore the magnetic properties of a real system, which is highly dependent of the true shape of the density of states.

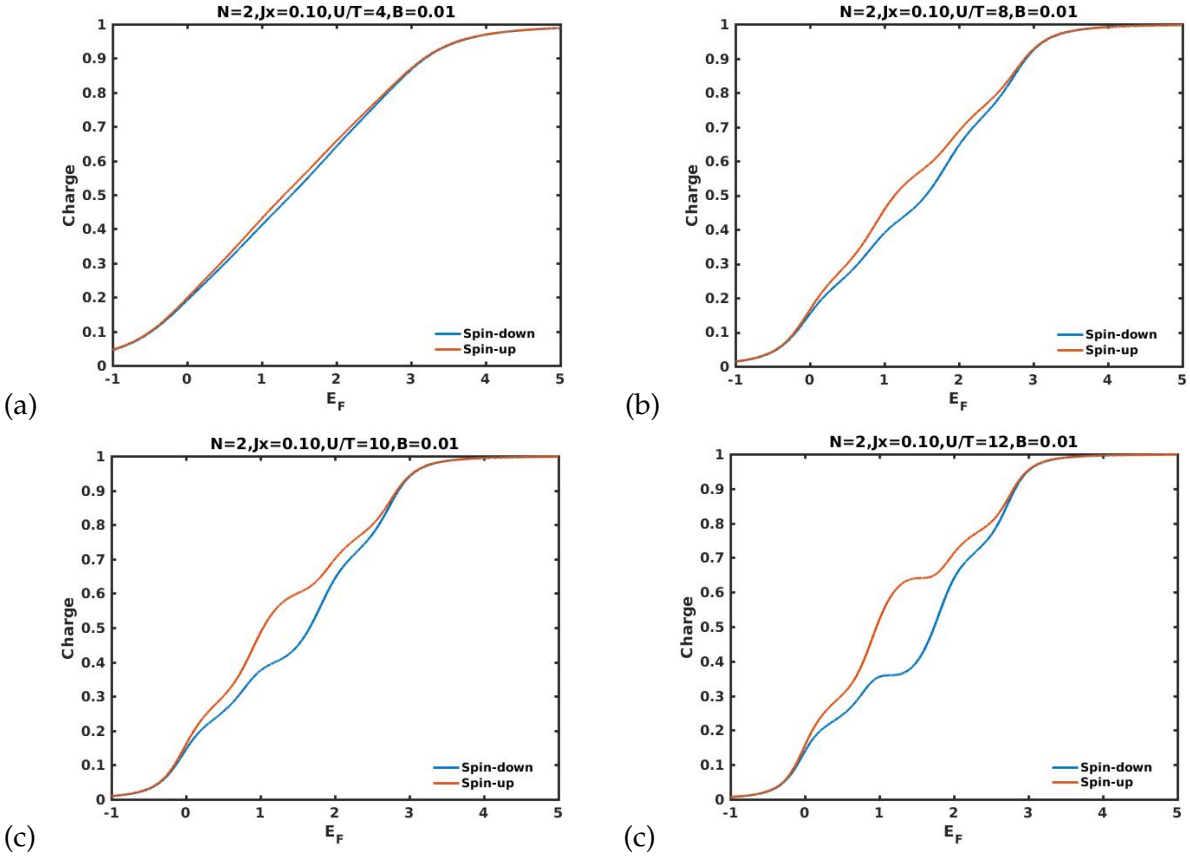

FIGURE 5.22: Magnetization for different values of U/T in our Kanamori model as we increase the energy of the metallic level (and thus occupation in the atom)

Therefore, some more realistic estimations for the DOS need to be extracted, for example for a semi-infinite chain, which, in the symmetric case, $n = 0.5$ yields at the Fermi level a density given by eq. B.19, $\rho_0(E_f) = \frac{D}{\pi T^2}$, where D is the bandwidth of the semi-infinite chain. Reasonable estimations for D, T, U and J can be obtained from accurate plane wave calculations for the band structure of solids [188]. Using our fit for the effective potential and a DOS such the one from the semi-infinite chain (see the appendix for a complete derivation), we can use a self-consistency scheme to find solutions with a LD approach for more complex model. Given initial charge and magnetization, n and m, we compute the effective potential, V^{eff}, which in turn yields new charges and magnetization.

In the Stoner Model, the effective potential is written in terms of the spin-less density and the magnetization and then is expanded to linear order in the magnetization (an approximation which should be valid when m is small compared to n):

$$V_{eff}^{\text{stoner}}{}_{\alpha\sigma} = V^0_{eff\alpha\sigma} \pm \frac{1}{2} IM,$$

where $V^0_{eff\alpha\sigma}$ is the effective potential for zero magnetization and M is the total magnetization, $M = \sum_\alpha n_{\alpha\uparrow} - n_{\alpha\downarrow}$. In practical calculations, thus, I can be calculated by introducing effective potentials reproducing a given atomic $\mathcal{N}$ and a given small

magnetization M and computing:

$$I = 2\frac{v^{eff}_{\alpha\sigma}(\mathcal{N}, M) - v^{eff}_{\alpha\sigma}(\mathcal{N}, 0)}{M}. \tag{5.24}$$

The Stoner criterion states that the Ground State will have $M > 0$ whenever

$$I \cdot \mathrm{DOS}(E_F) > 1. \tag{5.25}$$

We can use eq. 5.15 to understand the Stoner parameter in our fit. First, let us introduce some definitions:

$$\begin{aligned} n_\alpha &= n_{\alpha\uparrow} + n_{\alpha\downarrow} \\ m_\alpha &= n_{\alpha\uparrow} - n_{\alpha\downarrow} \end{aligned} \tag{5.26}$$

and let us rewrite all the dependencies in the correlation potential, which were in terms of $n_{\alpha\sigma}$, now in terms of n_α, m_α.

We can take eq. 5.15, substitute the dependencies on $n_{i\sigma}$ by dependencies on n_i and m_i, derive with respect to m_i and make all $m_j = 0$ to get here the XC contribution to the Stoner parameter in our fit:

$$\begin{aligned} \frac{\partial V^A_{corr,i\uparrow}}{\partial m_i}|_{m=0} = \frac{f_1}{2}(U'-J)\tanh\left(\frac{\alpha_1}{4}n_i(2-n_i)\right) + f_3 J \tanh\left(\frac{\alpha_3}{4}(N+n_i)(2L+2-N-n_i)\right) \\ - f_1\alpha_1\left(\frac{(1-n_i)}{2}\right)^2(U'-J)\,\mathrm{sech}^2\left(\frac{\alpha_1}{4}n_i(2-n_i)\right) \\ - \frac{1}{2}f_3\alpha_3(N+n_i-L-1)(N+n_i)J\mathrm{sech}^2\left(\frac{\alpha_3}{4}(N+n_i)(2L+2-N-n_i)\right) \end{aligned} \tag{5.27}$$

However, studying the central cases, $0 << n << 1$, it is possible to neglect the derivatives of the hyperbolic tangents and make them equal to 1, so that in the simplest case we would get just:

$$\frac{\partial V^A_{corr,i\uparrow}}{\partial m_i}|_{m=0} \approx \frac{f_1}{2}(U'-J) + f_3 J. \tag{5.28}$$

Our calculation for the Stoner parameter in our model, using our fitting 5.10 and the atomic DOS induced by the semi-elliptic metallic DOS, see eq. B.17, yields, for the case of three atomic levels, as a result an increasing curve for $I \cdot \mathrm{DOS}(E_F)$ which surpasses 1 around $U/T \approx 3.8$.

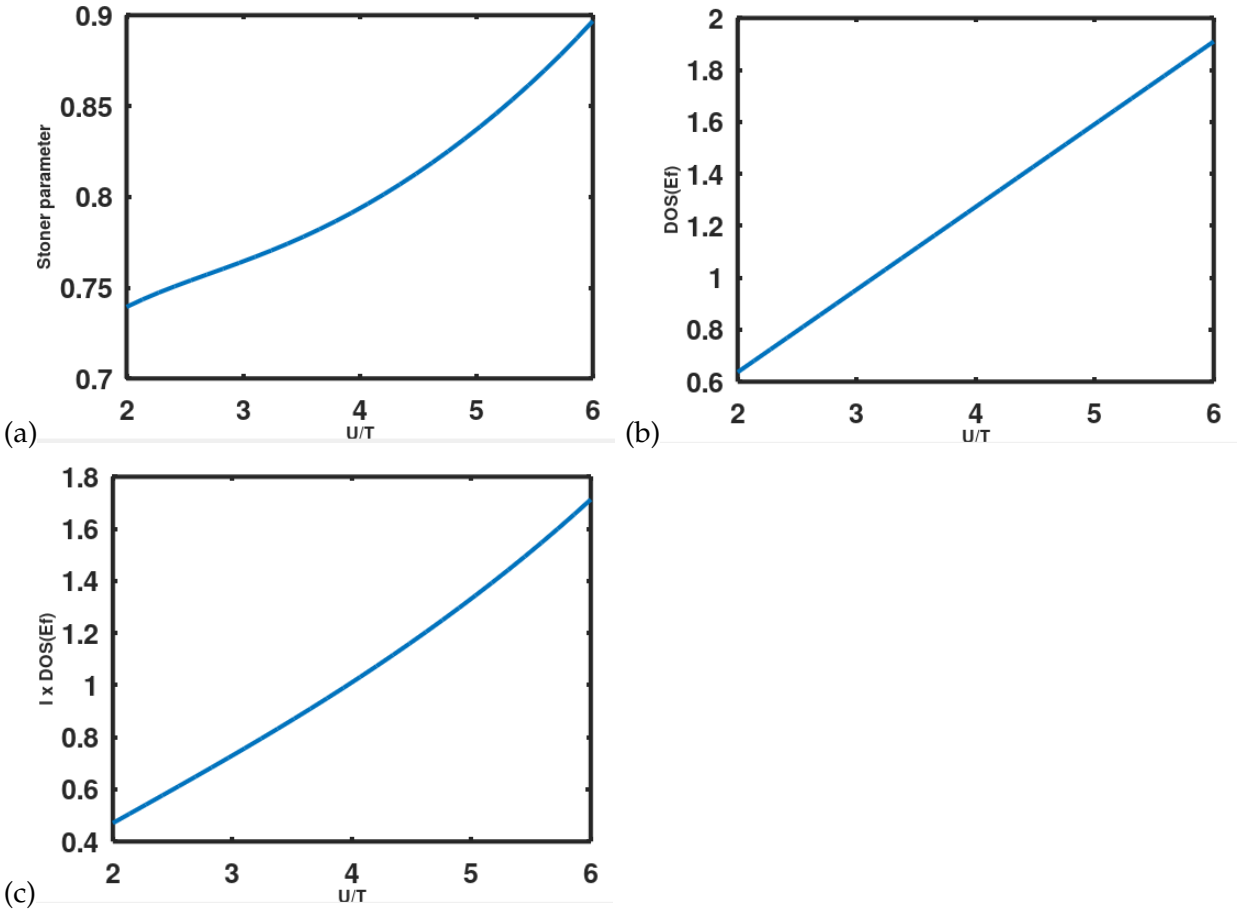

FIGURE 5.23: Evolution of the Stoner parameter to predict magnetic instabilities in the symmetric case $n_{i\uparrow} + n_{i\downarrow} = 1$

This is in good agreement with what we observe directly when looking at the magnetization in an atom connected to a metallic band:

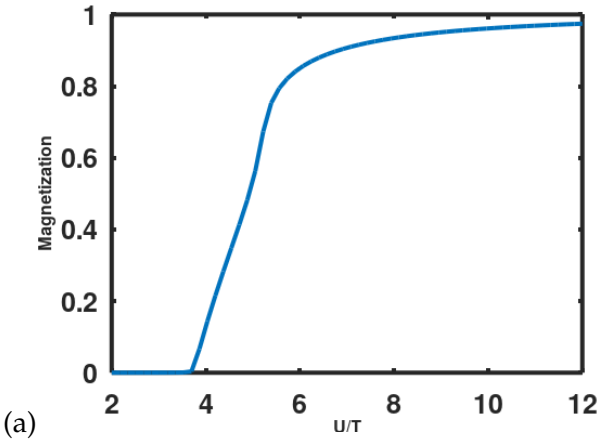

FIGURE 5.24: Magnetization, $n_{i\uparrow} - n_{i\downarrow}$, in terms of U/T for the symmetric case, $n_{i\uparrow} + n_{i\downarrow} = 1$ with all atomic levels degenerated. The transition happens at around $U/T \approx 3.8$ and for the values of interest the system has become fully magnetic. The value of m is achieved by a self-consistent procedure (see text), and a non-zero value indicates that the system favors magnetic configurations.

To calculate this, we perform a self-consistent calculation: for a given initial magnetization, m, we calculate the effective potential (using our fitting 5.13) and plug in into the eq. B.17 of the appendix B to get the density of states per spin:

$$\rho_\sigma(\omega) = \frac{T^2\rho_m(\omega)}{(\omega - V_\sigma(n,m) - T^2R(g_{\text{at}})(\omega))^2 + \pi^2T^4\rho_m^2(\omega)}, \tag{5.29}$$

where ρ_m is the DOS on the metallic level connected to the atom, g_{at} is the Green function induced on the atom, and $R(g_{\text{at}})$ denotes the real part of g_{at}.

From this we calculate the new magnetization,

$$m_{\text{out}} = \int_{-\infty}^{E_f} \rho_\uparrow(\omega) - \rho_\downarrow(\omega)d\omega$$

and iterate until self-consistency is attained.

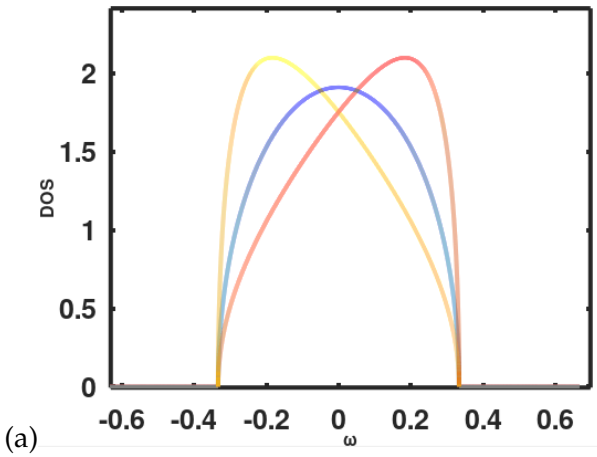

(a)

FIGURE 5.25: Density of states for the symmetric case, $n_{i\uparrow} + n_{i\downarrow} = 1$. In blue, the semi-elliptic DOS of the metallic chain. The two shifted curves are the DOS for spin up and spin down when a slight magnetization is present.

5.5 An Interpolation scheme for the self-energy

The Green function of a system is a Holy Grail which, if known, allows us to extract from it every possible information: Expected value of operators, response functions, relaxation times of excitations, density of states, etc. In general, given creation/annihilation operators $\{\hat{c}_\mu, \hat{c}_\mu^\dagger\}$ (these are usually taken as the position operators $\{\hat{\psi}(\mathbf{r}), \hat{\psi}^\dagger(\mathbf{r})\}$, but here we think of μ as a set of localized orbitals, such as the ones used in Kanamori-like models or the ones used to formulate OO-DFT in Chapter 1) we define the Green function as a matrix of elements:

$$G(\mu,\nu,t) = \frac{-i}{\hbar}\langle T[\hat{c}_\mu^\dagger(t)\hat{c}_\nu(0)]\rangle, \tag{5.30}$$

where the expected value is taken over the Ground State of the system [2], the T denotes the time-ordering operator, $T[a(t)b(t')] = \Theta(t-t')a(t)b(t') - \Theta(t'-t)b(t')a(t)$

[2] Or, if the system is described by a density matrix $\hat{\rho}$, $G(\mu,\nu,t) = \frac{-i}{\hbar}\text{Tr}\left(T\hat{\rho}[\hat{c}_\mu(t)\hat{c}_\nu^\dagger(0)]\right)$ At a finite temperature, $T > 0$ and thermodynamic equilibrium, $\hat{\rho} = e^{-\beta\hat{H}} = \sum_j e^{-\beta E_j}|\Psi_j\rangle\langle\Psi_j|$, with Ψ_0

[3] and the time dependency of the operators is to be understood in the Heisenberg picture: An operator $\hat{\mathcal{O}}$ in the Schrödinger picture evolves in the Heisenberg picture as $\hat{\mathcal{O}}(t) = e^{i\hat{H}t/\hbar}\hat{\mathcal{O}}e^{-i\hat{H}t/\hbar}$. Alternatively, we define the *retarded* Green function as

$$G^R(\mu,\nu,t) = \frac{-i}{\hbar}\Theta(t)\langle[\hat{c}_\mu(t),\hat{c}_\nu^\dagger(0)]_+\rangle, \tag{5.31}$$

where the brackets $[]_+$ denote the fermionic commutator, $[a,b]_+ = ab + ba$. One of the key quantities to be extracted from the retarded Green function is the Density of States - conceptually defined as the function mapping each possible energy to the proportion of states available at that energy, and which, mathematically, in terms of the Green function, has the form

$$DOS(\omega) = \frac{-1}{\pi}\sum_\mu \mathrm{Im}\left(G^R(\mu,\mu,\omega)\right) \tag{5.32}$$

where $G(\mu,\mu,\omega)$ is the Fourier transform of the corresponding quantities in eq. 5.30.

By defining G_0 as the non-interacting Green function, it is possible to define the so-called Self-energy, which is a measure of the potential felt by an electron due to the interactions of the surrounding medium with it. Here we define it in terms of Dyson's equation:

$$G = G_0 + G_0\Sigma G. \tag{5.33}$$

In the temporal representation of the Green function, the products of this schematic equation should be regarded as integrals convolutions, but on frequency space it indeed becomes the algebraic matrix product [189].

An accurate calculation of the Green function is a challenging problem which has triggered many important development in the last seventy years. Perturbation theory and the diagrammatic technique, first introduced by Feynman in the context of relativistic quantum field theory [190], was quickly adapted to statistical physics and non-relativistic settings [191]. Diagrammatic calculations of the response function are the foundations of the Random Phase Approximation [32–34], which has been crucial to derive exchange-correlations functionals [31, 39, 40], which in turn makes the usefulness of the technique obvious after having studied Density Functional Theory.

Here we are interested in calculating the many-body Density of States of Kanamori-Anderson hamiltonians such as in our model described by fig. 5.1 and eq. 5.1. More realistically, we could consider the atomic hamiltonian to be coupled to semi-infinite metallic chains or, in general, other systems with more complicated DOS.

Although we have managed to solve numerically the model 5.1, the calculation of the DOS, even for the simplest models, is much more demanding: the creation/annihilation operators applied at different times over the Ground State shows that is not enough to construct now the Hamiltonian matrix for a given number of electrons in the whole system: we need to construct a many-body basis (and the corresponding hamiltonian matrix elements) for all possible configurations with one more or one less electron (and, in general, for every possible orbital in the system!).

---

the Ground State and all the successive Ψ_j the excited states and E_j their corresponding energies, $G_(\mu,\nu,t) = \frac{-i}{\hbar}\sum_j e^{-\beta E_j}\langle\Psi_j|T\hat{\rho}[\hat{c}_\mu(t)\hat{c}_\nu^\dagger(0)]|\Psi_j\rangle$.

[3] Here and later in the text $\Theta(t)$ denotes the Heaviside step function.

Moreover, for the case of the atom connected to an infinite metallic chain, in principle we are clueless as to how to proceed. Here, we study the Interpolation technique for the self-energy, which was first introduced in [192] to study an Anderson model with one atomic level with applications to the problem of hydrogen chemisorption [193]. The idea consists in calculating the Self-energy in two limits and then interpolate between the two: On one hand, we calculate, with the aid of the perturbative diagrams, the interacting Self-energy to second order, treating all the many-body terms in the hamiltonian as the perturbation. On the other hand, we calculate the Green function for an isolated atom (the atomic limit, also seen in our calculations for the correlation energy and potential). Using these two results, and following the ideas found in previous works on the matter [187, 192, 194], we can proceed to combine the two results to get an interpolated interactive Self-energy which, thanks to Dyson equation, yields the Green function and thus the Density of States.

5.5.1 Second-order result

Given a one-electron hamiltonian, $\hat{h}$, by analogy with the theory of constant-coefficients linear PDE's [30], we want the Green function to be the resolvent of the hamiltonian, $\hat{g}(\omega) = (\omega \mathrm{Id} - \hat{h})^{-1}$.

To avoid the divergence problems on when ω takes the value of any of the eigenvalues, the causal Green function is the operator defined as

$$\hat{g}(\omega) = (\omega \mathrm{Id} - \hat{h} + i\eta\hat{\Theta})^{-1},$$

where $\hat{\Theta}$ is an operator that we define by setting its action over the eigenstates of the hamiltonian h:

$$\hat{\Theta}|\phi_j\rangle = |\phi_j\rangle,$$

if $|\phi_j\rangle$ is an occupied state (it appears in the Ground-state Slater determinant) and

$$\hat{\Theta}|\phi_j\rangle = -|\phi_j\rangle,$$

if $|\phi_j\rangle$ is an empty state. η is a very small number and implicitly we are always taking $\eta \to 0$ at the end of every calculation. We are calling here $\{\phi_j\}$ to the eigenfunctions of the one-electron hamiltonian, $\hat{h}$, and ϵ_j to the eigenvalues. The index j is splitted between occupied and unoccupied states, $\{o\}$ and $\{u\}$. Call $l_{\mu,\sigma}$ to the orthonormal one-particle basis functions. We have the expansion:

$$|\phi_j\rangle = \sum_{\mu,j} c_j(\mu\sigma)|l_{\mu\sigma}\rangle.$$

We want to compute $g(\mu,\nu,\sigma,\omega) = \langle\chi_{\mu\sigma}|\hat{g}(\omega)|\chi_{\nu\sigma}\rangle$. We insert twice the resolution of the identity $\sum_j |\phi_j\rangle\langle\phi_j| = 1$, (where the ϕ are eigenstates of $\hat{h}$) and employ the spectral theorem, which asserts that given a function f and an operator A, the operator $f(A)$ shares the eigenvectors of A and the eigenvalues are just the image under f of the eigenvalues of A.

$$g(\mu,\nu,\sigma,\omega) = \sum_j \frac{c_j(\nu,\sigma)c_j^*(\mu\sigma)}{\hbar\omega - \epsilon_j \pm i\eta} \tag{5.34}$$

In our problem, we only care about diagonal elements. Also, split the sum into the occupied and the unoccupied part:

$$g(\mu,\sigma,\omega) = \sum_o \frac{|c_o(\mu,\sigma)|^2}{\hbar\omega - \epsilon_o + i\eta} + \sum_u \frac{|c_u(\mu,\sigma)|^2}{\hbar\omega - \epsilon_u - i\eta}. \tag{5.35}$$

The $G_0(\omega)$ of the previous section in Dyson equation 5.56 can be taken to be precisely this simple non-interacting Green function.

This can be seen to equal the Fourier transform of [189]

$$g(\mu,\nu,t) = \frac{-i}{\hbar}\langle T[\hat{c}_\mu(t)\hat{c}^\dagger_\nu(0)]\rangle, \tag{5.36}$$

which, in the general interacting case, is taken as the definition of the Green function, as discussed in eq. 5.30: That is, we destroy an electron in state μ and then at time t we create an electron in state ν. The operator T is the time-ordering defined above.

The occupation numbers $n_{\mu\sigma}$ are

$$\langle\Phi_0|\hat{n}_{\mu\sigma}|\Phi_0\rangle = \sum_o |c_o(\mu\sigma)|^2.$$

Here $|\Phi_0\rangle$ is a Slater determinant that is the Ground State of the one-electron hamiltonian, $\hat{h}$.

If we now introduce a perturbative many-body term to the hamiltonian:

$$\hat{h} \to \hat{h} + \sum_{\mu\alpha\beta\delta\sigma\sigma'} O^{\beta\delta\sigma'}_{\mu\alpha\sigma}\hat{c}^\dagger_{\mu\sigma}\hat{c}^\dagger_{\beta\sigma'}\hat{c}_{\delta\sigma'}\hat{c}_{\alpha\sigma}$$

[4] then, the second order self-energy is computed by

$$\Sigma_{2,\mu\sigma\nu\sigma}(\omega) = \sum_{\alpha,\beta,\gamma,\tau,\lambda,\delta,\sigma'} \mathcal{O}^{\beta\delta\sigma'}_{\mu\alpha\sigma}\mathcal{O}^{\tau\lambda\sigma'}_{\gamma\nu\sigma} \quad \int_{-\infty}^{E_f}\int_{-\infty}^{E_f}\int_{E_f}^{\infty} \frac{\rho_{\alpha\sigma,\gamma\sigma}(x)\rho_{\delta\sigma',\tau\sigma'}(y)\rho_{\lambda\sigma',\beta\sigma'}(z)}{\omega - x - y + z + i\eta} dzdydx +$$
$$\int_{E_f}^{\infty}\int_{E_f}^{\infty}\int_{-\infty}^{E_f} \frac{\rho_{\alpha\sigma,\gamma\sigma}(x)\rho_{\delta\sigma',\tau\sigma'}(y)\rho_{\lambda\sigma',\beta\sigma'}(z)}{\omega - x - y + z + i\eta} dzdydx\Bigg). \tag{5.37}$$

The details on this formula and the details of the computations can be found in Appendix C. In our problem, in particular, we have to apply this perturbative result with:

$$\begin{aligned} \mathcal{O}^{\mu\mu\bar{\sigma}}_{\mu\mu\sigma} &= U \\ \mathcal{O}^{\nu\nu\sigma}_{\mu\mu\sigma} &= U' \\ \mathcal{O}^{\nu\nu\bar{\sigma}}_{\mu\mu\sigma} &= J \\ \mathcal{O}^{\nu\mu\bar{\sigma}}_{\mu\nu\sigma} &= J, \end{aligned} \tag{5.38}$$

with all other coefficients equal to zero. The result in the limit $T \to 0$ is easily seen to be

$$\Sigma_2(\omega) = C\frac{n(1-n)}{\omega - E^{\text{eff}}}, \tag{5.39}$$

[4] All interactions are independent of σ and σ' as long as there are no magnetic fields involved

where the constant C is

$$C = (2M-1)U'^2 + (2M-1)J^2 - 2(M-2)U'J. \tag{5.40}$$

(see appendix C).

5.5.2 Atomic Green Function

Let us first introduce some notation. We will use the index λ to label the basis of all the possible many-body states of the atom (here we are not dealing with the metallic chain, which is assumed to be disconnected in this limit). The Ground State wavefunction can be represented then as a superposition of the Slater determinants $\{\lambda\}$ as $|\Psi\rangle = \sum_\lambda c_\lambda |\lambda\rangle$. We will calculate only the diagonal Green functions in the Hund approximation. If all atomic levels are degenerated, all the diagonal Green functions are the same and the computation reduces to the computation of a single one. We will make our reasoning over the Green function of the first atomic level with spin up:

$$G^R(t) = \frac{-i}{\hbar}\langle\Theta(t)[\hat{c}_{1\uparrow}(t)\hat{c}^\dagger_{1\uparrow}(0)]_+\rangle.$$

To understand how to calculate this Green function, let us look first generically at the so-called Lehman decomposition. It will enough to examine, for example, the term

$$\Theta(t)\langle\hat{c}_{1\uparrow}(t)\hat{c}^\dagger_{1\uparrow}(0),\rangle$$

since the remaining one follows from an identical reasoning. Let us call $|\Psi_0\rangle$ to the Ground state and $|\Psi_n\rangle$ to the $n-$th excited state (some of them with more or less electrons that $|\Psi_0\rangle$). We can introduce the approximation of the identity $\sum_n |\Psi_n\rangle\langle\Psi_n| = 1$ to get:

$$\begin{aligned}
&\Theta(t)\langle\Psi_0|\hat{c}_{1\uparrow}(t)\hat{c}^\dagger_{1\uparrow}(0)|\Psi_0\rangle = \\
&\Theta(t)\sum_n\langle\Psi_0|\hat{c}_{1\uparrow}(t)|\Psi_n\rangle\langle\Psi_n|\hat{c}^\dagger_{1\uparrow}(0)|\Psi_0\rangle = \\
&\Theta(t)\sum_n\langle\Psi_0|e^{i\hat{H}t/\hbar}\hat{c}_{1\uparrow}e^{-i\hat{H}t/\hbar}|\Psi_n\rangle\langle\Psi_n|\hat{c}^\dagger_{1\uparrow}(0)|\Psi_0\rangle = \\
&\Theta(t)\sum_n e^{i(E_0-E_n)t/\hbar}\langle\Psi_0|\hat{c}_{1\uparrow}|\Psi_n\rangle\langle\Psi_n|\hat{c}^\dagger_{1\uparrow}(0)|\Psi_0\rangle = \\
&\Theta(t)\sum_n e^{i(E_0-E_n)t/\hbar}|\langle\Psi_0|\hat{c}_{1\uparrow}|\Psi_n\rangle|^2 = \\
&\Theta(t)\sum_n e^{i(E_0-E_n)t/\hbar}|c_n|^2.
\end{aligned} \tag{5.41}$$

Notice that here only excited states $|\Psi_n\rangle$ with one less electron than the ground state are relevant. Next, we take the Fourier transform of this quantity, for which we need to calculate:

$$\Theta(t)\langle\Psi_0|\hat{c}_{1\uparrow}(t)\hat{c}^\dagger_{1\uparrow}(0)|\Psi_0\rangle \to \iint\Theta(t)e^{i(E_0-E_n)t/\hbar}e^{i\omega t}dt.$$

Since this integral does not converge, we add an imaginary η to ω (the limit $\eta \to 0$ in the final results will be implied) to get

$$\iint\Theta(t)e^{i(E_0-E_n)t/\hbar}e^{i\omega t-\eta t}dt = \frac{i}{\hbar\omega + E_0 - E_n + i\eta}.$$

Therefore, we have the result

$$\Theta(t)\langle\Psi_0|\hat{c}_{1\uparrow}(t)\hat{c}^{\dagger}_{1\uparrow}(0)|\Psi_0\rangle \rightarrow \sum_n \frac{|c_n|^2}{\hbar\omega + E_0 - E_n + i\eta},$$

with

$$c_n = \langle\Psi_0|\hat{c}^{\dagger}_{1\uparrow}|\Psi_n\rangle.$$

Analogously, we have

$$\Theta(t)\langle\Psi_0|\hat{c}^{\dagger}_{1\uparrow}(0)\hat{c}_{1\uparrow}(t)|\Psi_0\rangle \rightarrow \sum_m \frac{|d_m|^2}{\hbar\omega + E_m - E_0 + i\eta},$$

with

$$d_m = \langle\Psi_0|\hat{c}_{1\uparrow}|\Psi_n\rangle.$$

The Green function in frequency space, then, (omitting for simplicity in this argument the $i\eta$ factors) has the abstract form

$$\sum_\lambda \frac{B_\lambda}{\omega - \epsilon_\lambda}.$$

The coefficients B_λ are simple the weights $|c_\lambda|^2$ and the ϵ_λ the associated poles (difference between levels) that arise from Lehman's representation. Notice that we will need to differentiate between the electrons (terms with d_m, where one electron is created) and the holes (terms with c_n).

Dyson equation, which can be rewritten as $G = (G_0^{-1} - \Sigma)^{-1}$ by multiplying eq. 5.33 by G_0^{-1} on the left and by G^{-1} on the right, implies that

$$\sum_\lambda \frac{B_\lambda}{\omega - \epsilon_\lambda} = \frac{1}{\omega - \tilde{E} - \Sigma},$$

with $\tilde{E}$ the effective potential in the atomic levels (to reproduce the desired charge in the non-interacting case) and Σ the self-energy. We can expand in powers of $1/\omega$ the left-hand side to reach:

$$\frac{1}{\omega}\left(\sum_\lambda B_\lambda - \frac{\sum_\lambda B_\lambda \epsilon_\lambda}{\omega} + \frac{\sum_\lambda B_\lambda \epsilon_\lambda^2}{\omega^2} + \dots\right)\left($$

and the same expansion for the right-hand side gives:

$$\frac{1}{\omega}\left(1 - \frac{\tilde{E} + \Sigma}{\omega} + \frac{\tilde{E}^2 + \Sigma^2 + 2\tilde{E}\Sigma}{\omega^2} + \dots\right)\left($$

Now, since both terms need to be equal for every ω, we can match term by term the coefficients sharing the same exponent in ω in both series expansions. Each of the resulting equations is a **sum rule**, which binds the weights B_λ together in some particular way.

The first sum rule, for example, is just

$$\sum_\lambda B_\lambda = 1,$$

which is no more that the obvious fact that the Ground state wave-function must be normalized. The second sum rule also has a physical content:

$$\sum B_\lambda \epsilon_\lambda = \tilde{E},$$

that is, the effective level has to bee to expected value of the pole energy ϵ_λ. This, as we will see in explicit calculations, can be recasted as the expression for the expected value of the charge.

Using now that, as $U \to 0$, $\Sigma \sim \sigma/\omega$ for some coefficient independent of ω and identifying the terms in $1/\omega^3$, we get that necessarily:

$$\sigma = \sum_\lambda B_\lambda \epsilon_\lambda^2 - \tilde{E}^2,$$

which is the so-called third sum rule.

To calculate the Green function in the atomic limit, let us denote here by $|\phi_k\rangle$ the many-body basis of Slater determinants specifying the configuration of electrons in the atom. Among this, we distinguish the states $|\phi_k^{\text{Hund}}\rangle$, which are those atomic configurations which satisfy Hund's first rule. We use the Lehman decomposition and, in the case $U' > 0$, we employ the Hund approximation, consisting in setting $\langle \phi_k | \Psi_0 \rangle = 0$ whenever $|\phi_k\rangle$ is not a Hund state:

$$\begin{aligned}
&\langle \Psi_0 | \hat{c}^\dagger(t)_{\mu\sigma} \hat{c}_{\mu\sigma} | \Psi_0 \rangle \approx \sum_k |\langle \phi_k^{\text{Hund}} | \Psi_0 \rangle|^2 \langle \phi_k^{\text{Hund}} | \hat{c}^\dagger(t)_{\mu\sigma} \hat{c}_{\mu\sigma} | \phi_k^{\text{Hund}} \rangle = \\
&\sum_{k,k'} |\langle \phi_k^{\text{Hund}} | \Psi_0 \rangle|^2 \langle \phi_k^{\text{Hund}} | \hat{c}^\dagger(t)_{\mu\sigma} | \phi_{k'}^{\text{Hund}} \rangle \langle \phi_{k'}^{\text{Hund}} | \hat{c}_{\mu\sigma} | \phi_k^{\text{Hund}} \rangle + \\
&\sum_{k,k'} |\langle \phi_k^{\text{Hund}} | \Psi_0 \rangle|^2 \langle \phi_k^{\text{Hund}} | \hat{c}^\dagger(t)_{\mu\sigma} | \phi_{k'}^{\text{No-Hund}} \rangle \langle \phi_{k'}^{\text{Hund}} | \hat{c}_{\mu\sigma} | \phi_k^{\text{No-Hund}} \rangle.
\end{aligned} \tag{5.42}$$

As we can see, we have splitted this part of the Green function into two parts: the one capturing exclusively transitions between Hund states, and another one taking into account transitions between a Hund state and a non-Hund state (which also contributes to the weight of different terms of the Green function in the Hund regime).

Atomic Green Function for a two level system

Let us now calculate explicitly the Green function for the case of an isolated atom with two levels, assuming all levels to be degenerate:

We are in the atomic limit, so there is no hopping with external levels. Let us call $|\Psi_0\rangle$ to the Ground State wave function. Let us call $A_0 = \langle \begin{smallmatrix} \cdot\cdot \\ \cdot\cdot \end{smallmatrix} | \Psi_0 \rangle$, $A_1 = \langle \begin{smallmatrix} \uparrow\cdot \\ \cdot\cdot \end{smallmatrix} | \Psi_0 \rangle$, $A_2 = \left\langle \begin{smallmatrix} \uparrow\cdot \\ \uparrow\cdot \end{smallmatrix} \Psi_0 \right\rangle$ ($A_3 = \left\langle \begin{smallmatrix} \uparrow\downarrow \\ \cdot\cdot \end{smallmatrix} \Psi_0 \right\rangle$ ($A_4 = \left\langle \begin{smallmatrix} \uparrow\downarrow \\ \uparrow\downarrow \end{smallmatrix} \Psi_0 \right\rangle$ (Since we assume all the level to be degenerated, clearly $A_1 = \langle \begin{smallmatrix} \cdot\cdot \\ \uparrow\cdot \end{smallmatrix} | \Psi_0 \rangle = \begin{smallmatrix} \uparrow\cdot \\ \cdot\cdot \end{smallmatrix} \Psi_0 = A_1 = \begin{smallmatrix} \downarrow\cdot \\ \cdot\cdot \end{smallmatrix} \Psi_0$ and also $A_2 = \left\langle \begin{smallmatrix} \downarrow\cdot \\ \downarrow\cdot \end{smallmatrix} \Psi_0 \right\rangle$ ($= \left\langle \frac{1}{\sqrt{2}} \left(\begin{smallmatrix} \downarrow\cdot \\ \uparrow\cdot \end{smallmatrix} + \begin{smallmatrix} \uparrow\cdot \\ \downarrow\cdot \end{smallmatrix} \right) \Psi_0 \right\rangle$. The no-Hund states have other coefficient, which we will call

A_2', and which equals $A_2' = \underset{\cdot\cdot}{\uparrow\downarrow}\,\Psi_0 = \langle \underset{\cdot\cdot}{\uparrow\downarrow}|\Psi_0\rangle = \left\langle \frac{1}{\sqrt{2}}\left(\underset{\uparrow\cdot}{\downarrow\cdot} - \underset{\downarrow\cdot}{\uparrow\cdot}\right)\middle|\Psi_0\right\rangle$.

The energies of the states over which we are projecting the wave-function are: 0 for the case of 0 electrons, 0 for the case of 1 electrons, $U' - J$ for the case of 2 electrons with spin 1, $U' + J$ for any of the cases of 2 electrons with spin 0, $3U'$ for the case of 3 electrons and $6U'$ for the case of 4 electrons. The energy differences are then: $U' - J$ for the transition to a state of a Hund state (2 electrons, spin 1) from a state with 1 electrons, $U' + J$ for the transition to a state with 2 electrons and spin 1 from the state with 1 electrons, $2U' + J$ for the transition from a Hund state (2 electrons, spin 1) to the state with 3 electrons, $2U' - J$ for the same transition but from the no-hund states (2 electrons, spin 0) and $3U'$ for the transition from the state with 3 electrons to the state with 4 electrons. The Lehmann representation then yields:

$$
\begin{aligned}
G(\omega) =& \frac{A_0}{\omega + i\eta} + \frac{A_1}{\omega - (U' + J) + i\eta} + \frac{A_1}{\omega - (U' - J) + i\eta} + \\
& \frac{\frac{1}{2}A_1}{\omega - (U' - J) + i\eta} + \frac{\frac{1}{2}A_1}{\omega - (U' + J) + i\eta} + \frac{A_2}{\omega - (2U' + J) + i\eta} + \\
& \frac{\frac{1}{2}A_2}{\omega - (2U' + J) + i\eta} + \frac{A_3}{\omega + 3U' + i\eta} + \frac{A_1}{\omega - i\eta} + \\
& \frac{A_2}{\omega - (U' - J) - i\eta} + \frac{\frac{1}{2}A_2}{\omega - (U' - J) - i\eta} + \frac{A_3}{\omega - (2U' - J) - i\eta} + \\
& \frac{\frac{1}{2}A_3}{\omega - (2U' + J) - i\eta} + \frac{\frac{1}{2}A_3}{\omega + (2U' - J) - i\eta} + \frac{A_3}{\omega - (2U' + J) - i\eta} + \\
& \frac{A_4}{\omega - 3U' - i\eta}.
\end{aligned}
\tag{5.43}
$$

Where we have highlighted in blue all the terms arising from Hund-No-Hund transitions!

If we do not want to make the Hund approximation, we would need to add:

$$
\frac{A_2'}{\omega - (2U' - J) + i\eta} + \frac{\frac{1}{2}A_2'}{\omega - (2U' - J) + i\eta} + \frac{A_2'}{\omega - (U' + J) - i\eta} + \frac{\frac{1}{2}A_2'}{\omega - (U' + J) - i\eta},
$$

and, in the Hubbard case, when $J = 0$, we would have $A_2' = A_2$.

Let us now count the number of states: There is just 1 state with 0 electrons, 4 states with 1 electron, 3 Hund states with 2 electrons and 3 no-Hund states with 2 electrons, 4 states with 3 electrons and 1 state with 4 electrons. Therefore, the first sum rule is trivially satisfied, and in this notation is written as:

$$
A_0 + 4A_1 + 3A_2 + 4A_3 + A_4 = 1.
$$

If we don't want to make an explicit use of the fact that Ψ_0 is Hund in this limit, we can write:

$$
A_0 + 4A_1 + 3A_2 + 3A_2' + 4A_3 + A_4 = 1,
$$

but in the atomic limit and with a $J \neq 0$, $A_2' = 0$, while, in the Hubbard case, with $J = 0$, we would have;

$$
A_0 + 4A_1 + 6A_2 + 4A_3 + A_4 = 1,
$$

The second sum rule, which encodes the charge per orbital, is simply:

$$4A_1 + 6A_2 + 6A_2' + 12A_3 + 4A_4 = 4n,$$

where n is the charge per orbital.

This is equivalent to

$$\sum_\lambda B_\lambda \epsilon_\lambda = \tilde{E},$$

where $\tilde{E}$ is the hartree-fock potential. This can be seen explicitly in the 2-level case from the form of the poles and the identity above relating the coefficients with the density, n, if we just notice that, in this particular case, $\tilde{E} = 3U'n$.

Finally, the third sum rule can be written explicitly in terms of two-particles correlation

$$\begin{aligned}\sum_\lambda A_\lambda \epsilon_\lambda^2 =& 3\left(n - \langle \hat{n_{1\uparrow}} \hat{n_{2\downarrow}} \rangle + \frac{3}{2}\langle \hat{n}_{1\uparrow}\hat{n}_{2\uparrow}\rangle + \frac{3}{2}\langle \hat{n_{1\uparrow}} \hat{n_{1\downarrow}} \rangle\right) J^2 + \\ & 3\left(n - \langle \hat{n_{1\uparrow}} \hat{n}_{2\downarrow}\rangle\right) J_x^2 + \\ & 3\left(\langle \hat{n}_{1\uparrow}\hat{n}_{1\uparrow}\rangle - \langle \hat{n}_{1\uparrow}\hat{n}_{1\downarrow}\rangle\right) J_x.\end{aligned}$$

From this expression is easy to see that in the limit $J \to 0$ we recover the following Hund approximation [5]:

$$\begin{aligned}\sum_\lambda A_\lambda \epsilon_\lambda^2 =& 3\left(n + \langle \hat{n}_{1\uparrow}\hat{n}_{2\uparrow}\rangle\right) J^2 + \\ & 3\left(n - \frac{1}{2}\langle \hat{n}_{1\uparrow}\hat{n}_{2\uparrow}\rangle\right) J_x^2 + \\ & 3\left(\langle \hat{n}_{1\uparrow}\hat{n}_{2\uparrow}\rangle\right) J_x.\end{aligned}$$

We thus see that here, in the Hund regime, there's only one independent two-body correlation function.

So far, we have several variables (all the $\{A_j\}$) and only three equations. Worse yet, we also need to be able to determine n and $\langle \hat{n}_{1\uparrow}\hat{n}_{2\uparrow}\rangle$ independently from these coefficients. What we do is, besides the already mentioned Hund approximation, consider as non-zero only three of the A_j. To wit, if we are exploring the system with two electrons in the atom, A_0 and A_4 will be neglected, and (always in the Hund approximation) we will retain just A_1, A_2 and A_3 [6].

To summarize the results, let us write the three sum rules in the Hund approximation. Notice that the third sum rule can be simplified extremely, since the correlation function $\langle \hat{n}_{1\uparrow}\hat{n}_{2\uparrow}\rangle$ equals $A_2 + 2A_3 + A_4$.

[5] Notice that, in the Hund regime for atoms half-filled or less (and for atoms more than half-filled the same arguments works for holes instead of electrons) we have $\langle \hat{n}_{1\uparrow}\hat{n}_{1\downarrow}\rangle = 0$ and $\langle \hat{n}_{1\uparrow}\hat{n}_{2\downarrow}\rangle = \frac{1}{2}\langle \hat{n}_{1\uparrow}\hat{n}_{2\uparrow}\rangle = 0$

[6] if we wanted to make a full calculation, we would run into two problems: There would be another variable, A_2', but still only three equations, and there would be more independent two-body correlation functions.

$$\begin{aligned} A_0 + 4A_1 + \quad & 3A_2 + 4A_3 + A_4 = 1 \\ 4A_1 + \quad & 6A_2 + 12A_3 + 4A_4 = 4n \\ & A_2 + 2A_3 + A_4 = \langle \hat{n}_{1\uparrow}\hat{n}_{2\uparrow} \rangle \end{aligned} \tag{5.44}$$

Finally, we express n and $\langle \hat{n}_{1\uparrow}\hat{n}_{2\uparrow} \rangle$ in terms of the Green function, which is attained by:

$$\begin{aligned} n &= \frac{-1}{\pi} \int_{-\infty}^{E_f} \mathrm{Im} G(\omega) d\omega \\ \langle \hat{n}_{1\uparrow}\hat{n}_{2\uparrow} \rangle &= n^2 - \frac{-1}{\pi C} \int_{-\infty}^{E_f} \mathrm{Im}\left(G(\omega)\Sigma(\omega)\right) d\omega \end{aligned} \tag{5.45}$$

Atomic Green Function for a three level system

By an analogous reasoning, we calculate the Green function for the case of an isolated atom with three levels, which in the Hund regime is:

$$\begin{aligned} G(\omega) = & \\ & \frac{A_0}{\omega + i\eta} + \frac{3A_1}{\omega - (U' - J) + i\eta} + \frac{2A_1}{\omega - (U' + J) + i\eta} + \\ & \frac{2A_2}{\omega - 2(U' - J) + i\eta} + \frac{4A_2}{\omega - (2U' + J) + i\eta} + \frac{2A_3}{\omega - (3U' + J) + i\eta} + \\ & \frac{3A_4}{\omega - 4U' + i\eta} + \frac{A_5}{\omega - (5U' - J) + i\eta} + \frac{A_1}{\omega - i\eta} + \frac{3A_2}{\omega - (U' - J) - i\eta} + \\ & \frac{2A_3}{\omega - 2(U' - J) - i\eta} + \frac{2A_4}{\omega - (3U' + J) - i\eta} + \frac{4A_4}{\omega - (3U' - 2J) - i\eta} + \\ & \frac{3A_5}{\omega - 4U' - i\eta} + \frac{2A_5}{\omega - (4U' - 2J) - i\eta} + \frac{A_6}{\omega - (5U' - J) - i\eta} \end{aligned} \tag{5.46}$$

Here, again, the terms associated to Hund/No-Hund transitions are highlighted in blue. The part not included in the Hund approximation is:

$$\begin{aligned} & \frac{2A_2'}{\omega - (U' + J)} + \frac{4A_2'}{\omega - (2U' - J)} + \frac{4A_3'}{\omega - (2U' + J)} + \frac{4A_3'}{\omega - 3U'} + \frac{4A_3'}{\omega - (2U' - J)} + \\ & \frac{4A_3'}{\omega - (3U' - 2J)} \frac{2A_4'}{\omega - (4U' - 2J)} + \frac{4A_4'}{\omega - 3U'}, \end{aligned} \tag{5.47}$$

and, as before, we would get the Hubbard case by setting $J = 0$, $A_2' = A_2$, $A_3' = A_3$ and $A_4' = A_4$.

From the normalization condition for the wave-function, as before for the case of two levels, it follows of course that the sum of the coefficient in the Hund case has to be 1:

$$A_0 + 6A_1 + 9A_2 + 4A_3 + 9A_4 + 6A_5 + A_6 = 1.$$

To check the second sum rule, we first notice, by the same argument as in the case of two levels for the expected value of the charge in terms of the A'_js, that in the Hund regime we have the identity:

$$6A_1 + 18A_2 + 12A_3 + 36A_4 + 30A_5 + 6A_6 = n,$$

where n is the charge per orbital. In general, the second sum rule, if we do not wish to make the Hund approximation, is:

$$6A_1 + 18A_2 + 12A'_2 + 12A_3 + 48A'_3 + 36A_4 + 24A'_4 + 30A_5 + 6A_6 = n.$$

On the other hand, by taking the mean-field approximation in the hamiltonian we see that the Hartree-Fock potential in the 3-levels case is:

$$V_{hx}(n) = (5U' - J)n.$$

And using the above-written Green Function, we see that indeed:

$$\sum B_\lambda \epsilon_\lambda = (5U' - J)n$$

Analogously as the case of two atomic levels, in the Hund regime we can write:

$$\begin{aligned} A_0 + 6A_1 + \quad & 9A_2 + 4A_3 + 9A_4 + 6A_5 + A_6 = 1 \\ 6A_1 + \quad & 18A_2 + 12A_3 + 36A_4 + 30A_5 + 6A_6 = 4n \\ & A_2 + \frac{4}{3}A_3 + 6A_4 + 3A_5 + A_6 = \langle \hat{n}_{1\uparrow}\hat{n}_{2\uparrow} \rangle \end{aligned} \tag{5.48}$$

Asymptotics as $U \to 0$

In any case, using the sum rules above and the factorization $\langle \hat{n}_{\mu\sigma}\hat{n}_{\nu\bar{\sigma}} \rangle \approx n_{\mu\sigma}n_{\nu\bar{\sigma}}$, valid for the non-interacting case, $U \to 0$, we can see that the atomic Green function in the non-interacting limit has the asymptotic behaviour:

$$C\frac{n(1-n)}{\omega - E},$$

where C is the same constant obtained in the second order calculation.

5.5.3 Interpolation and Results

Notice that, as shown in Appendix C, the second order self-energy in the limit $U/T \to \infty$ is

$$\Sigma_2(\omega) = C\frac{n(1-n)}{\omega - E^{\text{eff}}}, \tag{5.49}$$

with

$$C = (2M-1)U'^2 + (2M-1)J^2 - 2(M-2)U'J. \tag{5.50}$$

On the other hand, the atomic self-energy in the limit $U/T \to 0$, thanks to the sum rules studied above, is seen to behave as:

$$\Sigma_{\text{at}}(\omega) = C\frac{n(1-n)}{\omega - E}, \tag{5.51}$$

for the same constant C.

This "coincidence" is what allows us to define an adequate self-energy interpolating all the range of values between the two limits and respecting the correct asymptotic behaviours:

Indeed, if we define the interpolating Self-energy as:

$$\Sigma(\omega) := \Sigma_{\text{at}}\left(\left(E^{\text{eff}} + C\frac{n(1-n)}{\Sigma_2(\omega)}\right)\right), \tag{5.52}$$

we can readily check that, thanks to eqs. 5.49 and 5.51, the two limits calculated in the previous sections are preserved:

$$\lim_{U/T\to 0}\Sigma(\omega) = C\frac{n(1-n)}{E^{\text{eff}} + C\dfrac{n(1-n)}{\Sigma_2(\omega)} - E} = \Sigma_2(\omega), \tag{5.53}$$

and

$$\lim_{U/T\to\infty}\Sigma(\omega) = \Sigma_{\text{at}}\left(\left(E^{\text{eff}} + C\frac{n(1-n)}{C\dfrac{n(1-n)}{\omega - E^{\text{eff}}}}\right)\right) = \Sigma_{\text{at}}(\omega). \tag{5.54}$$

If the asymptotic behaviour of the atomic self-energy, $\Sigma_{\text{at}}(\omega)$, had a different constant than the limit of $\Sigma_2(\omega)$, the mismatch between the coefficients would make impossible to preserve both limits with the interpolating self-energy. In other words, the key to show that this interpolation scheme actually works is to show that, indeed, the two limits are interchangeable. Mathematically, decoupling U and T, we can write this condition as:

$$\lim_{T\to 0}\lim_{U\to 0}\Sigma(\omega) = \lim_{U\to 0}\lim_{T\to 0}\Sigma(\omega), \tag{5.55}$$

and the asymptotics in 5.53 and 5.54 show that this holds.

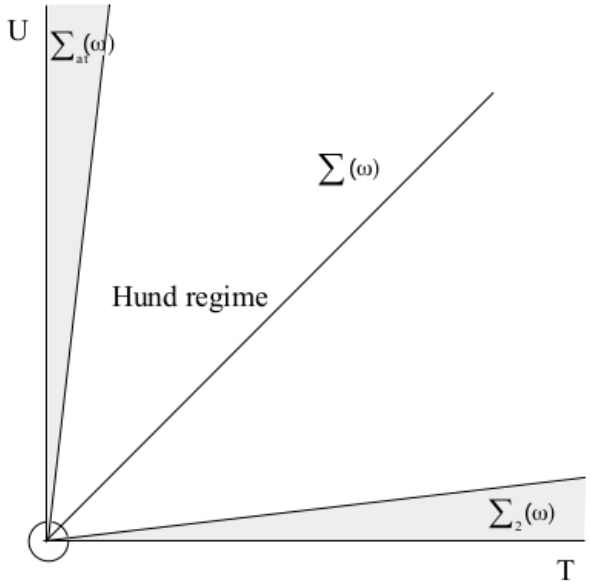

FIGURE 5.26: Graphic summary of the interpolation: The shadowed areas represent the regions where we are able to calculate the self-energy accurately: Σ_2 and Σ_{at}. The circle at the bottom left corner represents the small region where both self-energies must coincide, which is what we show by the "coincidence" in eqs. 5.49 and 5.51. The straight-line going though the middle separates (schematically) the region where the Hund regime (neglecting the A') is valid (upper half) from the region where it does not (lower half). If $J = 0$, the interpolation works of course for every U and T.

We can now use Dyson equation,

$$\Sigma(\omega) = G_0^{-1}(\omega) - G^{-1}(\omega), \tag{5.56}$$

to get the interpolated many-body Green function and from 5.32 we get the density of states, which we show here in several figures for some particular cases.

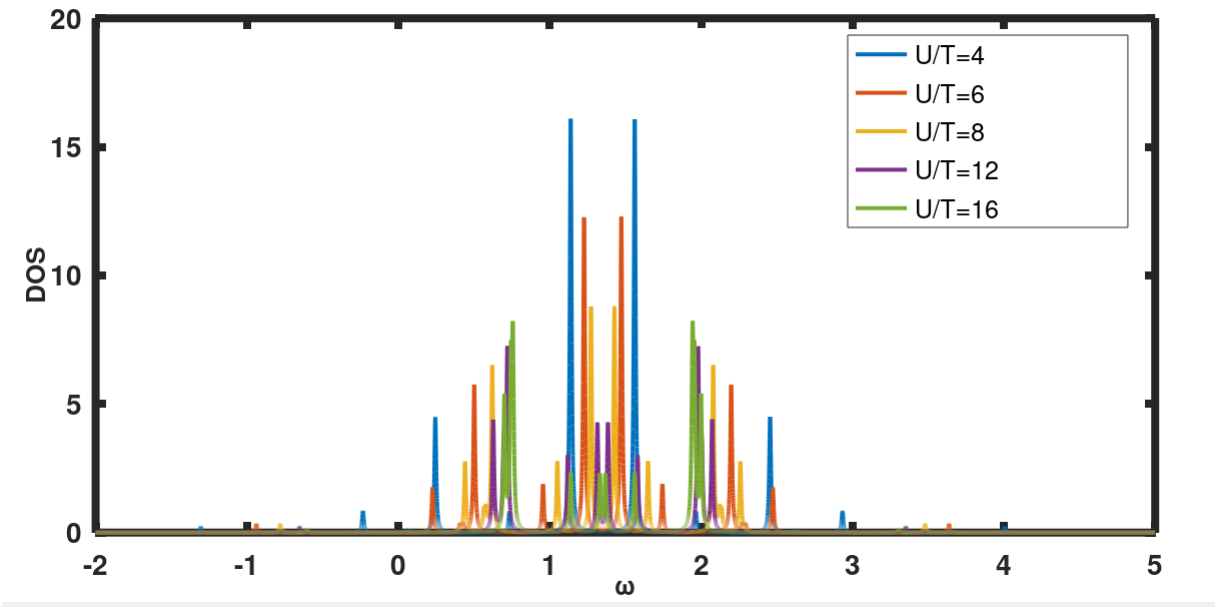

FIGURE 5.27: Density of States obtained in the symmetric case ($n = 0.5$) for two atomic levels.

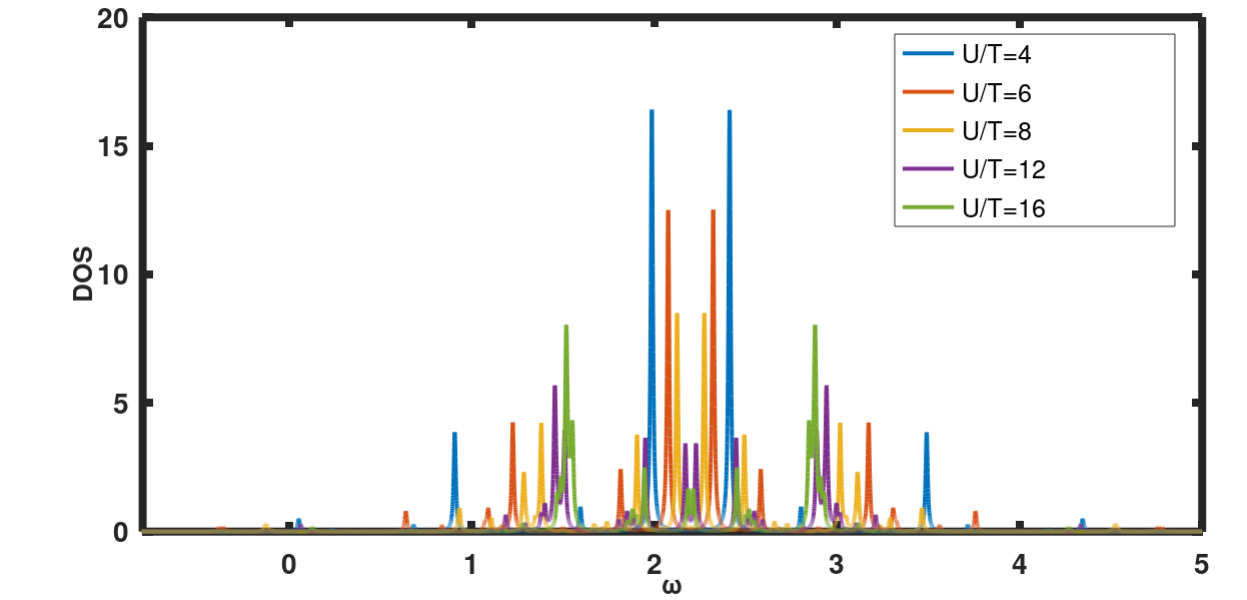

FIGURE 5.28: Density of States obtained in the symmetric case ($n = 0.5$) for three atomic levels.

We have applied here the interpolation scheme to the Hubbard-Hund case assuming all atomic levels are degenerated. In principle, we just need to apply equation 5.52, using the second order result, eq. C.3, and the atomic result in terms of the coefficients A_j, for which we need to employ the sum rules. However, the sum rules 5.44,5.48 demand the knowledge of $n_{1\uparrow}$ and $\langle \hat{n}_{1\uparrow}\hat{n}_{2\uparrow}\rangle$, and so this becomes a self-consistency problem, where these values will determine some coefficients A_j's which, in turn, will return, through the interpolated Green function and eqs. 5.45, new values for $n_{1\uparrow}$ and $\langle \hat{n}_{1\uparrow}\hat{n}_{2\uparrow}\rangle$. In full generality, the scheme would be as follows:

1) Initial values for E^{eff}, n and $\langle \hat{n}_{1\uparrow}\hat{n}_{2\uparrow}\rangle$ are proposed. Given E^{eff}, we can find the charge n_0 in the non-interacting system.

2) With n and $\langle \hat{n}_{1\uparrow}\hat{n}_{2\uparrow}\rangle$ we calculate the A_j and, thus, calculate an interpolated self-energy, $\Sigma_{\text{int}}(\omega)$, with eq. 5.52.

3) Dyson equation 5.56 can be used to calculate the Green function $G(\omega)$ from Σ_{int}, and from it we get the DOS, n and $\langle \hat{n}_{1\uparrow}\hat{n}_{2\uparrow}\rangle$.

4) We iterate the self-consistent procedure. Convergence is attained when finally $n_0 = n$.

Chapter 6

Tight-Binding models

A simple model can shed more light on Nature's workings than a series of ab initio calculations of individual cases, which, even if correct, are so detailed that they hide reality instead of revealing it. A perfect computation simply reproduces Nature, it does not explain it.

Philip W. Anderson

6.1 Tight-Binding Model from DFT

Tight-binding models are widely employed to understand, with very simple feature and at small computational cost, complex properties of materials. The tight-biding hamiltonians are one-electron hamiltonians in which certain sites $\{i\}$ are defined together with the pairwise hopping interaction between those sites:

$$\hat{H} = \sum_j \varepsilon_j \hat{n}_j + \sum_{i<j} t_{i,j} \hat{c}_j^\dagger \hat{c}_i + \text{h.c} \tag{6.1}$$

. The parameters defining a Tight-Binding hamiltonian can be adjusted to reproduce certain particular features, like band-gap, spectra, topological properties, etc, and then be used to explore further the system at hand. That is the case if we are trying to construct a toy model, but, when our model corresponds to a realistic system, most parameters of the TB model can be calculated from DFT or other quantum chemistry methods. For example, from Fireball (see Chapters 1 and 2), it is easy to construct a Tight-Binding hamiltonian by taking the hamiltonian in the Löwdin basis. We recall here that, if $|\chi_\alpha\rangle$ are the pseudo-atomic fireball orbitals, in terms of which the tables of integrals are defined, $|l_\alpha\rangle$ denote the Löwdin orbitals, which form an orthonormal basis closest to the $|\chi_\alpha\rangle$ in the sense of mean quadratic error.

Typical Tight-Binding models, like the one we are going to study in the next section, deal with the valence π-orbitals of the system, corresponding to the double or triple bonds. To extract our Tight-Binding Hamiltonian, since we were working (as we will shortly show) with a planar molecule, we positioned the molecule in the XY plane and extracted the submatrix associated to the indices linked to p_z orbitals from the Hamiltonian matrix in the Löwdin basis. The use of the Löwdin basis is crucial because the basis of wave-functions in terms of which a collection of

creation/annihilation is defined must be orthonormal in order for the second quantization language to be valid. [1]

6.2 Edge States and NQE's

The studied system is a self-assembled chain of quinoid molecules known as DABQDI (see picture below), formed by small units bonded together by hydrogen bond. Each of these units is a cyclic aliphatic molecule with a system of 12 $\pi-$conjugated electrons. Ignoring spin, and focusing on these π-orbitals, we study a system with 6 $pi-$electrons distributed among 10 possible sites

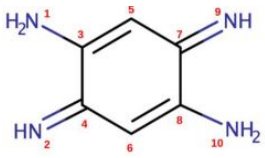

FIGURE 6.1: Elementary building unit of the chains with the employed labels in the Tight Binding calculation.

Units like the one in fig. 6.1 are linked together by hydrogen bonds of sites 1,2 and 9,10 (respectively) of contiguous units, forming long chains. These chains have been studied experimentally at very low temperatures (4 K) and in ultra-high vacuum conditions. In such conditions, the Nuclear nature of the nuclei, which is usually neglected, becomes increasingly important, most of all in the hydrogen atoms, which are light enough for the impact of the so-called Nuclear Quantum Effects (NQEs) to be drastic in the mechanical and electronic properties of the molecule [16]. STM images show the existence of edge states in long chains and manipulation experiments pulling the chain from one of its extremes show a remarkably mechanical stability which appears to hint to an enhanced hydrogen bond of an almost covalent strength.

FIGURE 6.2: (Extracted from [18]) STM image of one of the molecular chains (25 units) over a gold surface.

The molecule is subjected to a double proton transfer, precisely on those hydrogen bond linking contiguous units through sites 1,2 and 9,10, as commented above, so that it can exist in two different tautomeric forms. Furthermore, Path Integral Molecular Dynamics [17] with Fireball and the I-PI package [16] show that, at low temperatures, the hydrogens experience a dramatically lower Free Energy barrier to jump from molecule to molecule than was in predicted by standard DFT. This phenomenon that has been reported in other problems involving proton transfer at very low temperatures [14, 15]. In such an scenario, the protons undergo delocalization and are found in a deep tunneling regime in which their oscillation time is much lower than what can be predicted by means of classical DFT (without adding the NQEs) [18].

[1] Strictly speaking, by taking the resolution of the identity to be $\sum_{\alpha,\beta} S_{\alpha\beta}|\chi_\alpha\rangle\langle\chi_\beta| = 1$ it is possible to formulate the second-quantization without the assumption of orthonormality.

Our Tight-Binding model starts by calculating with Fireball the hamiltonian, h, in eV of one unit in the Löwdin basis, as detailed in the previous section. What we do next is to retain only the submatrix of the pz orbitals to get:

$$h = \begin{pmatrix} 6.02 & 0 & 3.21 & 0 & 0 & 0 & 0 & 0 & 0 & 0 \\ 0 & 3.48 & 0 & 3.65 & 0 & 0 & 0 & 0 & 0 & 0 \\ 3.21 & 0 & 2.77 & 2.75 & 3.47 & 0 & 0 & 0 & 0 & 0 \\ 0 & 3.65 & 2.75 & 2.28 & 0 & 3.06 & 0 & 0 & 0 & 0 \\ 0 & 0 & 3.47 & 0 & 2.32 & 0 & 3.06 & 0 & 0 & 0 \\ 0 & 0 & 0 & 3.06 & 0 & 2.33 & 0 & 3.47 & 0 & 0 \\ 0 & 0 & 0 & 0 & 3.06 & 0 & 2.28 & 2.75 & 3.65 & 0 \\ 0 & 0 & 0 & 0 & 0 & 3.47 & 2.75 & 2.77 & 0 & 3.21 \\ 0 & 0 & 0 & 0 & 0 & 0 & 3.65 & 0 & 3.46 & 0 \\ 0 & 0 & 0 & 0 & 0 & 0 & 0 & 3.21 & 0 & 6.02 \end{pmatrix}.$$

In this matrix, the element h_{ij} is exactly the connection t_{ij} between sites i and j of the molecule 6.1.

Now we connect a number N of units to each other. This means constructing a matrix H_N with blocks made up by copies of h and adding connections τ_{bond} between the blocks modelling the hydrogen bonds. We also add a hopping τ_{edge} between the nitrogens on sites 1 and 2 on the left end-unit of the chain and between sites 9 and 10 of the end-unit on the right: That is, defining

$$T = \begin{pmatrix} 0 & 0 & 0 & 0 & 0 & 0 & 0 & 0 & 0 & 0 \\ 0 & 0 & 0 & 0 & 0 & 0 & 0 & 0 & 0 & 0 \\ 0 & 0 & 0 & 0 & 0 & 0 & 0 & 0 & 0 & 0 \\ 0 & 0 & 0 & 0 & 0 & 0 & 0 & 0 & 0 & 0 \\ 0 & 0 & 0 & 0 & 0 & 0 & 0 & 0 & 0 & 0 \\ 0 & 0 & 0 & 0 & 0 & 0 & 0 & 0 & 0 & 0 \\ 0 & 0 & 0 & 0 & 0 & 0 & 0 & 0 & 0 & 0 \\ 0 & 0 & 0 & 0 & 0 & 0 & 0 & 0 & 0 & 0 \\ \tau_{\text{bond}} & 0 & 0 & 0 & 0 & 0 & 0 & 0 & 0 & 0 \\ 0 & \tau_{\text{bond}} & 0 & 0 & 0 & 0 & 0 & 0 & 0 & 0 \end{pmatrix}.$$

and the pair of hamiltonians for the edge units:

$$h_{\text{left}} = \begin{pmatrix} 6.02 & \tau_{\text{edge}} & 3.21 & 0 & 0 & 0 & 0 & 0 & 0 & 0 \\ \tau_{\text{edge}} & 3.48 & 0 & 3.65 & 0 & 0 & 0 & 0 & 0 & 0 \\ 3.21 & 0 & 2.77 & 2.75 & 3.47 & 0 & 0 & 0 & 0 & 0 \\ 0 & 3.65 & 2.75 & 2.28 & 0 & 3.06 & 0 & 0 & 0 & 0 \\ 0 & 0 & 3.47 & 0 & 2.32 & 0 & 3.06 & 0 & 0 & 0 \\ 0 & 0 & 0 & 3.06 & 0 & 2.33 & 0 & 3.47 & 0 & 0 \\ 0 & 0 & 0 & 0 & 3.06 & 0 & 2.28 & 2.75 & 3.65 & 0 \\ 0 & 0 & 0 & 0 & 0 & 3.47 & 2.75 & 2.77 & 0 & 3.21 \\ 0 & 0 & 0 & 0 & 0 & 0 & 3.65 & 0 & 3.46 & 0 \\ 0 & 0 & 0 & 0 & 0 & 0 & 0 & 3.21 & 0 & 6.02 \end{pmatrix}$$

and

$$h_{\text{right}} = \begin{pmatrix} 6.02 & 0 & 3.21 & 0 & 0 & 0 & 0 & 0 & 0 & 0 \\ 0 & 3.48 & 0 & 3.65 & 0 & 0 & 0 & 0 & 0 & 0 \\ 3.21 & 0 & 2.77 & 2.75 & 3.47 & 0 & 0 & 0 & 0 & 0 \\ 0 & 3.65 & 2.75 & 2.28 & 0 & 3.06 & 0 & 0 & 0 & 0 \\ 0 & 0 & 3.47 & 0 & 2.32 & 0 & 3.06 & 0 & 0 & 0 \\ 0 & 0 & 0 & 3.06 & 0 & 2.33 & 0 & 3.47 & 0 & 0 \\ 0 & 0 & 0 & 0 & 3.06 & 0 & 2.28 & 2.75 & 3.65 & 0 \\ 0 & 0 & 0 & 0 & 0 & 3.47 & 2.75 & 2.77 & 0 & 3.21 \\ 0 & 0 & 0 & 0 & 0 & 0 & 3.65 & 0 & 3.46 & \tau_{\text{edge}} \\ 0 & 0 & 0 & 0 & 0 & 0 & 0 & 3.21 & \tau_{\text{edge}} & 6.02 \end{pmatrix}$$

and calling $\mathbf{0}$ to the 10x10 matrix with all of its entries zeroes, we can finally construct

$$H_N = \begin{pmatrix} h_{\text{left}} & T & \mathbf{0} & \mathbf{0} & \cdots & \mathbf{0} & \mathbf{0} & \mathbf{0} \\ T^t & h & T & \mathbf{0} & \cdots & \mathbf{0} & \mathbf{0} & \mathbf{0} \\ \mathbf{0} & T^t & h & T & \cdots & \mathbf{0} & \mathbf{0} & \mathbf{0} \\ \vdots & \vdots & \vdots & \vdots & \vdots & \vdots & \vdots & \vdots \\ \mathbf{0} & \mathbf{0} & \mathbf{0} & \mathbf{0} & \cdots & h & T & \mathbf{0} \\ \mathbf{0} & \mathbf{0} & \mathbf{0} & \mathbf{0} & \cdots & T^t & h & T \\ \mathbf{0} & \mathbf{0} & \mathbf{0} & \mathbf{0} & \cdots & \mathbf{0} & T^t & h_{\text{right}} \end{pmatrix}$$

After constructing this block matrix (N denoting the number of h on it), we proceed to study the electronic structure of the a molecular chain for different values of the length (N) and for different values of the couple $\tau_{\text{bond}}, \tau_{\text{edge}}$. The exploration of these parameters makes sense because these hoppings are the ones that will be most affected by the NQEs and cannot be estimated in the DFT calculations. The high mechanical stability and the deep tunneling regime hint towards a larger hopping than usual, which for hydrogen bonds is around 0.25 eV, and it is for such larger hoppings that we find edge states on the chains, in concordance with the experiments, but not found in the simulations.

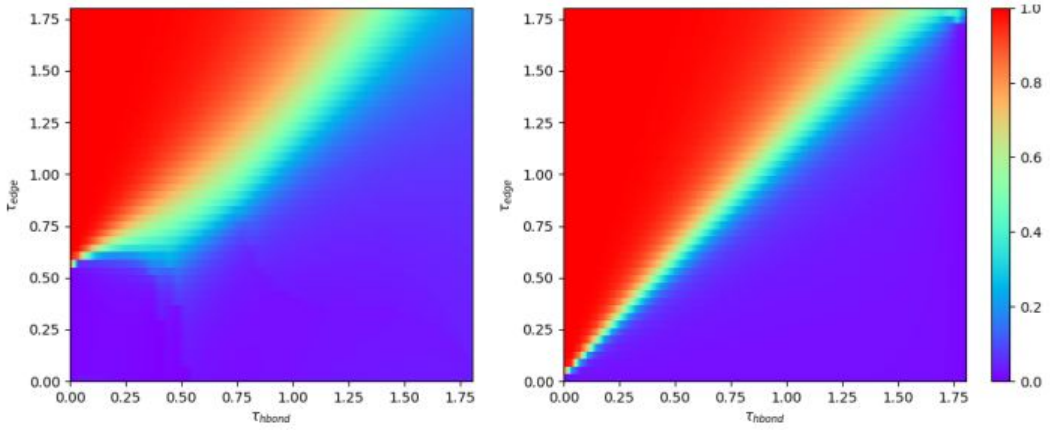

FIGURE 6.3: This shows the projection over the sites of the edges (the twenty sites corresponding to the leftmost unit and the rightmost unit) for both the HOMO and the LUMO orbitals in a chain composed by thirty units ($N = 30$; larger values do not affect the results), in terms of both $\tau_{\text{bond}}, \tau_{\text{edge}}$. If $\{|j\rangle\}$ is the basis of sites, ordered unit after unit in the molecular chain and from left to right, and every unit is labeled according to fig. 6.1, then, calling $|\text{HOMO}\rangle$ and $|\text{LUMO}\rangle$ to the eigenstates of H_N corresponding to the HOMO and LUMO orbitals, respectively, the quantities encoded by the color scale are just, on the left, $\sum_{j=1}^{10} |\langle j|\text{HOMO}\rangle|^2 + \sum_{j=10N+1}^{10N+10} |\langle j|\text{HOMO}\rangle|^2$ and on the right, $\sum_{j=1}^{10} |\langle j|\text{LUMO}\rangle|^2 + \sum_{j=10N+1}^{10N+10} |\langle j|\text{LUMO}\rangle|^2$

Conclusions

Allwissend bin ich nicht; doch viel ist mir bewußt

Faust, Goethe

As commented in the introduction, the present thesis has a dual nature, for its deals simultaneously, in an intertwined fashion, with the development of method and the applications to simulations of particular systems, and in this final section I would like to make some final comments about the most important achievements (without attempting to give a exhaustive list of everything that has been done) and what yet remains to be done.

Focusing first on the methods developed and implemented, we see (in chapters 1 and 2) that, during the doctoral thesis, a number of improvements and new approximations have been implemented in the software Fireball. We have provided a new scheme to calculate approximately the exchange-correlation matrix elements, we have corrected the long-range Hartree terms, introduced small improvements to make the code more efficient and implemented and tested some new charge projection methods. An important consequence, for instance, as discussed in detail in chapter 2, is the possibility of calculating without error the forces in the context of a self-consistent Harris DFT calculation. Further work in this line will imply, to name a few, the application of the latest improvements to develop better basis sets, the incorporation of intra-atomic dipolar terms to the potential in Fireball, the exploration of new approximation for the exchange-correlation and possibly many more.

On the other hand, turning our attention now to the applications, we have performed for the first time a detailed study of the dynamics of proton transfer in guanine-cytosine base-pairs taking into account explicitly the biomolecular environment and temperature at which these processes (might) take place. This is achieved by using a QM/MM method which offers an excellent balance between efficiency and accuracy, as detailed in Chapter 4. On this system, it is clear that there are many possible ideas and problems to be explored in the near future. Probably, one of the most enticing ones is the more thorough study of the reaction in excited states, perhaps exploring non-singlet excited states, conical intersection, etc. Many other problems can be considered. For instance, a complete study in a QM/MM setting of the Nuclear Quantum Effects would still be desirable, and probable of interest when considering the system at lower temperatures. Also, having in mind problems of biological interest, we could think of studying the same problem with slightly (or much) more complex environment, such as considering methylation (an important epigenetic factor which might affect the nature of the reaction) or the proteins present in the medium.

Turning now to the Hubbard-Hund hamiltonians in chapter 5, we have seen in practice the OO-DFT formalism, calculations for the exchange-correlation energy

and potential in a model, corresponding fittings and an interesting application to define a LDA+U scheme. Obvious extension of this work would be to consider longer chains or, in general, larger systems, where exact diagonalization is no longer possible, but other methods could also provide inside on the exchange-correlation. In these systems, we have shown briefly an scheme to calculate approximately the many-body Density of States which, in the context of a Hubbard-Hund hamiltonian, is novel. The applications of this scheme have not yet been explored and it is to be expected that they will be an active field of research in the near future.

In conclusions, it is clear that, although much remains to be done, a great deal has been learnt during the realization of the doctoral thesis.

Versión en español

Como se comentó en la introducción, la presente tesis tiene una doble naturaleza, pues se ocupa de manera simultánea del desarrollo de métodos y de sus aplicaciones a simulaciones de sistemas particulares. En esta última sección, me gustaría hacer algunos comentarios sobre los logros más importantes (sin pretender dar una lista exhaustiva de todo lo que se ha hecho) y sobre lo que queda por hacer.

Centrándonos primero en los métodos desarrollados e implementados, vemos (en los capítulos 1 y 2) que, durante la tesis doctoral, se han implementado una serie de mejoras y nuevas aproximaciones en el software Fireball. Hemos proporcionado un nuevo esquema para calcular aproximadamente los elementos de matriz de canje-correlación, hemos corregido los términos Hartree de largo alcance, introducido pequeñas mejoras para hacer el código más eficiente, e implementado y probado algunos nuevos métodos de proyección de carga. Una consecuencia importante, por ejemplo, como se analiza en detalle en el capítulo 2, es la posibilidad de calcular sin error las fuerzas en el contexto de un cálculo de Harris DFT autoconsistente. El trabajo futuro en esta línea implicará, por nombrar algunas cosas, la aplicación de las últimas mejoras para desarrollar mejores conjuntos de bases, la incorporación de términos dipolares intraatómicos al potencial en Fireball, o la exploración de nuevas aproximaciones para el canje-correlación.

Por otro lado, volviendo ahora nuestra atención a las aplicaciones, hemos realizado por primera vez un estudio detallado de la dinámica de la transferencia de protones en pares de bases guanina-citosina teniendo en cuenta explícitamente el entorno biomolecular y la temperatura a la que estos procesos ocurren (en caso de que en efecto ocurriesen). Esto se logra usando un método QM / MM que ofrece un excelente equilibrio entre eficiencia y precisión, como se detalla en el Capítulo 4. En este sistema, está claro que hay muchas ideas y problemas posibles que se explorarán en un futuro próximo. Probablemente, uno de los más atractivos es el estudio más completo de la reacción en estados excitados, quizás explorando estados excitados no singlete, intersección cónica, etc. Se pueden considerar, sin embargo, muchos otros problemas. Por ejemplo, un estudio completo en un entorno QM/MM de los efectos cuánticos nucleares aún sería deseable y probablemente de interés cuando se considera el sistema a temperaturas muy bajas. Además, teniendo en cuenta problemas de interés biológico, podríamos pensar en estudiar el mismo problema con un entorno ligeramente (o mucho) más complejo, como considerar la metilación (un factor epigenético importante que puede afectar la naturaleza de la reacción) o las

proteínas presentes en el medio.

Sobre los hamiltonianos de Hubbard-Hund en el capítulo 5, hemos visto en la práctica el formalismo OO-DFT, cálculos para la energía y el potencial de correlación de intercambio en un modelo, los ajustes correspondientes y una aplicación interesante para definir un método tipo LDA+U. Una extensión obvia de este trabajo sería considerar cadenas más largas o, en general, sistemas más grandes, donde la diagonalización exacta ya no es posible, pero donde otros métodos también podrían proporcionar información sobre el canje-correlación. En estos sistemas, hemos mostrado brevemente un esquema para calcular aproximadamente la Densidad de Estados de muchos cuerpos que, en el contexto de un hamiltoniano de Hubbard-Hund, es novedoso. Las aplicaciones de este esquema aún no se han explorado y es de esperar que sean un campo activo de investigación en un futuro próximo.

Appendix A

The Hartree-Fock approximation

Imagine we have a complete set of spin-orbitals $\{\phi_k(x)\}_k$, which can symbolically be written as $\sum_k \phi_k(x)\phi_k^*(x') = \delta(x - x')$. Given a certain choice of a *configuration interaction*, that is, a certain set of N concrete spin-orbitals $L = \{l_1, l_2, \ldots, l_N\}$, we can form the Slater determinant $\Psi_L = (N!)^{-1/2} \det\left(\phi_{l_j}(x_k)\right)$ (Then, any multielectronic molecular wave function can be expressed as:

$$\Psi(x_1, \ldots, x_N) = \sum_L C_L \Psi_L(x_1, \ldots, x_N),$$

for suitable coefficients C_L. Indeed, it can be checked that the collection of Slater determinants span the fermionic Fock space of total antisymmetric wavefunctions.

Hartree-Fock method revolves around making the Ansatz that the molecular wavefunction is a single Slater determinant, which is only an approximation to the real ground state of the system. The underlying philosophy to the Hartree-Fock method is thus that we retain the full complexity of the hamiltonian and aim to find only approximate solutions which, at least structurally speaking, resemble to those of a non-interacting system. That's the reason why the Hartree-Fock method is also beheld as a Mean-Field approximation.

Throughout this appendix, we assume that we find ourselves in the first step of the Born-Oppenheimer approximation, and thus we are dealing with the electronic part of the molecular hamiltonian.

Suppose the many-electron wavefunction has the form of a Slater determinant, $\Psi(x) = (N!)^{-1/2}\det\phi_j(x_k)$. We will minimize $\langle\Psi|\hat{\mathcal{H}}|\Psi\rangle$ under that assumption. That is, we intend to find N 1-electron spin-orbitals $\phi_k(x)$ such that Ψ is the minimizer of $\langle\Psi|\hat{\mathcal{H}}|\Psi\rangle$ over the class of Slater determinants. The relevant terms are the kinectic energy operator and the interaction energy operator.For the kinectic part, we have, thanks to orthonormality:

$$\sum_j \langle\Psi|\frac{-\hbar^2}{2m}\Delta_j|\Psi\rangle = \frac{-\hbar^2}{2mN!}\sum_j \sum_{\sigma\in S_N}\sum_{\tau\in S_N}(-1)^{|\sigma|+|\tau|}\langle\prod_l \phi_{\sigma(l)}(x_l)|\Delta_j|\prod_{l'}\phi_{\sigma(l')}(x_{l'})\rangle =$$

$$\sum_j \langle\phi_j(x)|\frac{-\hbar^2}{2m}\Delta|\phi_j(x)\rangle.$$

Also, typically there will be a external potential affecting the electrons. For example, the electrostatic interaction with the atomic nuclei, V_{eN}. The associated term becomes a sum of 1-body terms as in the case of kinetic energy.

For the interaction energy operator, we have for a single term:

$$\langle\Psi|\frac{1}{r_j-r_k}|\Psi\rangle=\frac{1}{N!}\sum_{\sigma\in S_N}\sum_{\tau\in S_N}(-1)^{|\tau|+|\sigma|}\langle\phi_{\sigma(1)}(x_1)\dots\phi_{\sigma(N)}(x_N)|\frac{1}{r_j-r_k}|\phi_{\tau(1)}(x_1)\dots\phi_{\tau(N)}(x_N)\rangle,$$

but note that the only non-vanishing terms in this sum are those for which σ and τ coincide for all indexes not being j or k, for otherwise orthonormality would make the product zero. The number of possible choices is $(N-2)!$ (this is the number of permutations of $N-2$ elements). On the other hand, for j and k there are two possibilities: Either σ and τ are exactly equal or $\sigma(j)=\tau(k)$ and $\sigma(k)=\tau(j)$. Either case we have to choose a value for $\sigma(j)$ and another one for $\sigma(k)$, which yields $N(N-1)$ options available. To gain clarity, we relabel in our single term above r_j and r_k as r and r' and $\sigma(j)$ and $\sigma(k)$ simply as j and k. Then our single term becomes:

$$\langle\phi_j(x)\phi_k(x')|\frac{1}{|r-r'|}|\phi_j(x)\phi_k(x')\rangle-\langle\phi_j(x)\phi_k(x')|\frac{1}{|r-r'|}|\phi_k(x)\phi_j(x')\rangle,$$

where the minus term comes from the fact that for those intertwinning permutations $(-1)^{|\tau|+|\sigma|}=-1$.

Summing up, if $\hat{\mathcal{H}}$ is the electronic hamiltonian and if Ψ is a Slater determinant built up from spin-orbitals $\{\phi_k\}$, then it holds that:

$$\langle\Psi|\hat{\mathcal{H}}|\Psi\rangle=\frac{-\hbar^2}{2m}\sum_k\langle\phi_k|\Delta|\phi_k\rangle+\sum_k\langle\phi_k|V_{eN}|\phi_k\rangle+$$
$$\frac{q_e^2}{8\pi\epsilon_0}\sum_{j,k}\langle\phi_j(x)\phi_k(x')|\frac{1}{|r-r'|}|\phi_j(x)\phi_k(x')\rangle-\langle\phi_j(x)\phi_k(x')|\frac{1}{|r-r'|}|\phi_k(x)\phi_j(x')\rangle.$$

The term $\frac{q_e^2}{4\pi\epsilon_0}\langle\phi_j(x)\phi_k(x')|\frac{1}{|r-r'|}|\phi_j(x)\phi_k(x')\rangle$ is called the Coulomb term and written simply as $J_{j,k}$. The other term, $\frac{q_e^2}{4\pi\epsilon_0}\langle\phi_j(x)\phi_k(x')|\frac{1}{|r-r'|}|\phi_k(x)\phi_j(x')\rangle$ is called the exchange term and written simply as $K_{j,k}$.

The Coulomb term, we see, correspond to the classical electrostatic energy if we interpret the probability densities $|\phi|^2$ as genuine electronic densities. The new term, $K_{j,k}$, has arisen from the antisymmetric character of the wave function and is a pure quantum phenomena with no classical counterpart. It can be understood as a consequence of the Pauli exclusion principle for fermions, and it lowers the energy in a crucial way.

The next step is to employ a variational argument to find equations for the spin-orbitals $\{\phi_k\}$ minimizing this expected value of the energy. The restraints, that we must include within the formalism of Lagrange multipliers, are of course that $\langle\phi_j|\phi_k\rangle=\delta_{j,k}$, and we would have to deal with a two-parameters set of Lagrange multipliers $\lambda_{j,k}$, which can be done. However, being the Hamiltonian a hermitic operator, we can know beforehand that the eigenvalues of the operator arising from the Euler-Lagrange equations are orthogonal, so we can get away with just imposing the normalization constraints $\langle\phi_j|\phi_j\rangle=1$, which will take us directly to a set of diagonal equations. Otherwhise, we could get to the diagonalized equations be means of a unitary transformation, so it is not a big deal anyway.

Also, it should be noted that is enough to take variations with respect to Ψ^*, so by imposing

$$\frac{\delta}{\delta\psi_j^*} \quad \langle\Psi|\hat{\mathcal{H}}|\Psi| + \sum_k \lambda_k(\langle\phi_k|\phi_k\rangle - 1)\Big)\Big(= 0,$$

for $j = 1, \ldots, N$, we reach the so-called General Hartree-Fock equations. The derivation is straigth-forward. Calling:

$$\begin{cases}\Big(\hat{h}(\phi(x)) = \dfrac{-\hbar^2}{2m}\Delta\phi(x) + V_{eN}\phi(x) \\ \Big(\hat{J}_j(\phi(x)) = \dfrac{q_e^2}{4\pi\epsilon_0} \quad \int\Big(\dfrac{|\phi_j(x')|^2}{|r-r'|}dx'\Big)\,\phi(x) \\ \hat{K}_j(\phi(x)) = \dfrac{q_e^2}{4\pi\epsilon_0} \quad \int\Big(\dfrac{|\phi_j^*(x')\phi(x')}{|r-r'|}dx'\Big)\Big(\phi_j(x),\end{cases}$$

(where we have defined, respectively, what are called the one-body free hamiltonian, the Coulomb operator and the exchange operator) we have that the Euler-Lagrange equations take the form:

$$\Big(\hat{h} + \sum_l \hat{J}_l - \hat{K}_l\Big)\Big(\phi_k = \varepsilon_k\phi_k, \;\; k = 1, \ldots, N,$$

where ε_k are the opposite of the Lagrange multipliers $\varepsilon_k = -\lambda_k$. The full operator $\hat{h} + \sum_l \hat{J}_l - \hat{K}_l$ is usually call the Fock operator and is denoted by $\hat{F}$.

Appendix B

Density of States of a semi-infinite chain

We want to study the atom connected to metallic chains increasingly large and then take the limit to semi-infinite chains

FIGURE B.1: Semi-infinite chain

.

The hamiltonian matrix of a chain of length N is

$$h = \begin{pmatrix} \epsilon & -t & 0 & \cdots & 0 \\ -t & \epsilon & -t & \cdots & 0 \\ 0 & -t & \epsilon & \cdots & 0 \\ 0 & \cdots & \cdots & \cdots & 0 \\ 0 & \cdots & -t & \epsilon & -t \\ 0 & \cdots & 0 & -t & \epsilon \end{pmatrix} \tag{B.1}$$

And the Green function, being a one-electron hamiltonian, can be obtained directly by inversion, $g(\omega) = (\omega \mathrm{Id} - h)^{-1}$,

$$g(\omega) = \begin{pmatrix} \omega - \epsilon & t & 0 & \cdots & 0 \\ t & \omega - \epsilon & t & \cdots & 0 \\ 0 & t & \omega - \epsilon & \cdots & 0 \\ 0 & \cdots & \cdots & \cdots & 0 \\ 0 & \cdots & t & \omega - \epsilon & t \\ 0 & \cdots & 0 & t & \omega - \epsilon \end{pmatrix}^{-1} \tag{B.2}$$

In general, let us define a matrix a_N as

$$a_N = \begin{pmatrix} a & b & 0 & \cdots & 0 \\ b & a & b & \cdots & 0 \\ 0 & b & a & \cdots & 0 \\ 0 & \cdots & \cdots & \cdots & 0 \\ 0 & \cdots & b & a & b \\ 0 & \cdots & 0 & b & a \end{pmatrix} \tag{B.3}$$

and let us call x_n to the determinant of a_n, $x_n = \det(a_n)$.

Expanding on co-factors, we get the following recursive relation

$$\begin{aligned} x_n &= a x_{n-1} - b^2 x_{n-2}, \\ x_0 &= 1, x_1 = a. \end{aligned} \tag{B.4}$$

We can write this as a matrix equation:

$$\begin{pmatrix} x_{n-1} \\ x_n \end{pmatrix} = \begin{pmatrix} 0 & 1 \\ -b^2 & a \end{pmatrix} \begin{pmatrix} x_{n-2} \\ x_{n-1} \end{pmatrix} \tag{B.5}$$

Iterating, we get

$$\begin{pmatrix} x_{n-1} \\ x_n \end{pmatrix} = \begin{pmatrix} 0 & 1 \\ -b^2 & a \end{pmatrix} \begin{pmatrix} x_{n-2} \\ x_{n-1} \end{pmatrix} = \begin{pmatrix} 0 & 1 \\ -b^2 & a \end{pmatrix}^2 \begin{pmatrix} x_{n-3} \\ x_{n-2} \end{pmatrix} = \cdots \begin{pmatrix} 0 & 1 \\ -b^2 & a \end{pmatrix}^{n-1} \begin{pmatrix} x_0 \\ x_1 \end{pmatrix} \tag{B.6}$$

We call the matrix R,

$$R = \begin{pmatrix} 0 & 1 \\ -b^2 & a \end{pmatrix} \tag{B.7}$$

So that we need to calculate R^{n-1}. For that, we diagonalize R. The eigenvalues are $\lambda = \dfrac{a \pm i\sqrt{4b^2 - a^2}}{2}$, and the eigenvectors can then be taken as $(1, \lambda_+)$ and $(1, \lambda_-)$. Let's call P to the matrix of eigenvectors

$$P = \begin{pmatrix} 1 & 1 \\ \lambda_+ & \lambda_- \end{pmatrix}$$

Then we can write:

$$R = PDP^{-1}, \tag{B.8}$$

where D is the diagonal matrix $\begin{pmatrix} \lambda_+ & 0 \\ 0 & \lambda_- \end{pmatrix}$. Now we have

$$R^{n-1} = PD^{n-1}P^{-1}, \tag{B.9}$$

so that we get

$$x_n = \frac{1}{\lambda_+ - \lambda_-} \left(\lambda_+^n (a - \lambda_-) + \lambda_-^n (a + \lambda_+) \right), \tag{B.10}$$

which is real-valued because of the combination of the complex conjugates.

To calculate the inverse matrix, we use the co-factor rule. It will be enough to calculate the diagonal elements:

$$g_{kk} = \frac{x_{k-1} x_{N-k}}{x_N}. \tag{B.11}$$

The element we need to calculate explicitly is g_{11}.

$$g_{11} = \frac{x_{N-1}}{x_N} = \frac{\left(\lambda_+^{N-1} (a - \lambda_-) + \lambda_-^{N-1} (a + \lambda_+) \right)}{\left(\lambda_+^N (a - \lambda_-) + \lambda_-^N (a + \lambda_+) \right)} \tag{B.12}$$

The Green function in the limit $N \to \infty$, when we have an infinite chain, is then just

$$g_{11} = \frac{1}{2a \pm \mathrm{Im}(\lambda_+)}$$

We undo the changes $a = \omega - \epsilon$, $b = t$ and finally get

$$g_{11}(\omega) = \frac{1}{\omega - \epsilon + i\sqrt{4t^2 - (\omega - \epsilon)^2}} = \frac{\omega - \epsilon}{4t^2} - i\frac{\sqrt{4t^2 - (\omega - \epsilon)^2}}{4t^2}, \tag{B.13}$$

where the sign is selected so that it will correspond to a physical Density of States. We further call $D = 2t$ to the bandwidth, for ease of notation. The metallic DOS is then

$$\rho_m(\omega) = \frac{\sqrt{D^2 - (\omega - \epsilon)^2}}{\pi D^2}, \tag{B.14}$$

which is the semi-elliptic function.

Next, we calculate the induced DOS in a new level that we connect to our semi-infinite chain. We call V to the intra-site energy of the new site (thought of as an atomic level) and T the hopping connecting this site to the first site of the chain.

$$\begin{pmatrix} \omega - V & (T & 0 & \dots & 0) \\ T & & & & \\ 0 & & & & \\ \vdots & & & g^{-1} & \\ 0 & & & & \end{pmatrix} \tag{B.15}$$

Inverting the block matrix leads, for the first term on the upper left side, which is just the Green function in the atom, the following term:

$$g_0(\omega) = \left(\omega - V - T^2 g_{11}(\omega)\right)^{-1}. \tag{B.16}$$

This lead us to the following atomic density of states:

$$\rho_0(\omega) = \frac{T^2 \rho_m(\omega)}{(\omega - V - T^2 R(g_{11})(\omega))^2 + \pi^2 T^4 \rho_m^2(\omega)}, \tag{B.17}$$

where $R(g_{11})(\omega)$ is the real part of the metallic Green function, which, in the general case, is the Hilbert transform of the imaginary part:

$$R(g_{11})(\omega) = \pi \int \frac{\rho_m(\omega')}{\omega' - \omega} d\omega',$$

and which in the semielliptic case is just

$$R(g_{11})(\omega) = \frac{\omega - \epsilon}{D^2}.$$

As an example, consider the fully symmetric case, with $n_{at} = 0.5, V = 0, \epsilon = 0$. The DOS then results in

$$\rho_0(\omega) = \frac{1}{\pi} \frac{\sqrt{D^2 - \omega^2}}{\left(\frac{D^2}{T^2} - 2\right)\left(\omega^2 + T^2\right.}. \tag{B.18}$$

The DOS at the Fermi level, $\omega = 0$, which is interesting for the Stoner problem, is just:

$$\rho_0(E_f) = \frac{D}{\pi T^2}. \tag{B.19}$$

Appendix C

Diagrammatic calculation

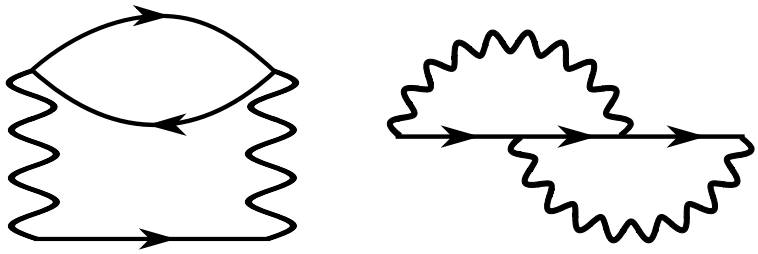

FIGURE C.1: The two second-order diagrams that need to be considered

The interaction lines of the Feynman diagram above may correspond, in our problem, to:

$$\begin{aligned}
&\frac{U}{2}\sum_{\mu,\sigma}\hat{n}_{\mu\sigma}\hat{n}_{\mu\sigma}\\
&\frac{U'}{2}\sum_{\mu\neq\nu,\sigma,\sigma'}\hat{n}_{\mu\sigma}\hat{n}_{\nu\sigma'}\\
&\frac{-J}{2}\sum_{\mu\neq\nu,\sigma}\hat{n}_{\mu\sigma}\hat{n}_{\nu\sigma}\\
&\frac{-J}{2}\sum_{\mu\neq\nu,\sigma}\hat{c}^{\dagger}_{\mu\sigma}\hat{c}_{\mu\bar{\sigma}}\hat{c}^{\dagger}_{\nu\bar{\sigma}}\hat{c}_{\nu\sigma}
\end{aligned} \tag{C.1}$$

To deal with the full Kanamori hamiltonian, which, as commented above, is rotationally invariant, we must add the term:

$$\frac{-J}{2}\sum_{\mu\neq\nu,\sigma}\hat{c}^{\dagger}_{\mu\sigma}\hat{c}_{\nu\bar{\sigma}}\hat{c}^{\dagger}_{\nu\bar{\sigma}}\hat{c}_{\mu\sigma}$$

First, we treat the second-order diagrams generally. To simplify the notation, we are going to call z_j to the collection of indeces $(\alpha_j, \beta_j, \gamma_j, \delta_j, \sigma_j, \sigma'_j)$. This 6-tuple refers to a term $\mathcal{O}^{\beta_j,\delta_j}_{\alpha_j,\gamma_j}\hat{c}^{\dagger}_{\alpha_j\sigma_j}\hat{c}^{\dagger}_{\beta_j\sigma'_j}\hat{c}_{\delta_j\sigma'_j}\hat{c}_{\gamma_j\sigma_j}$ in the full many-body hamiltonian.

The second-order diagram for the Green function translates into (omitting the spin to lighten the notation):

$$\int\int\Big(d\omega_1 d\omega_2 \sum_{z_1,z_2} \mathcal{O}^{\beta_1,\delta_1}_{\alpha_1,\gamma_1}\mathcal{O}^{\beta_2,\delta_2}_{\alpha_2,\gamma_2} g_0(\mu,\alpha_1,\omega)g_0(\gamma_1,\alpha_2,\omega-\omega_1)g_0(\delta_1,\beta_2,\omega_1+\omega_2)g_0(\delta_2,\beta_1,\omega_2)g_0(\gamma_2,\nu,\omega). \tag{C.2}$$

For the self-energy thus we have the general result:

$$\Sigma(\mu,\nu,\sigma,\omega) = \text{cnt}\sum_{\alpha,\beta,\gamma,\tau,\lambda,\delta,\sigma'} \mathcal{O}^{\beta\delta}_{\mu\alpha}\mathcal{O}^{\tau\lambda}_{\gamma\nu}\int\Big(d\omega_1 d\omega_2 g_0(\alpha\sigma,\gamma\sigma,\omega-\omega_1)g_0(\delta\sigma',\tau\sigma',\omega-\omega_2)g_0(\lambda\sigma',\beta\sigma',\omega_2). \tag{C.3}$$

Alternatively, we compute this second-order Self energy in terms of the Density of States: We will plug this into second order perturbation theory to obtain a perturbative many-body DOS:

$$\Sigma_2(\omega) = \sum_{\alpha,\beta,\gamma,\tau,\lambda,\delta,\sigma'} \mathcal{O}^{\beta\delta}_{\mu\alpha}\mathcal{O}^{\tau\lambda}_{\gamma\nu} \int_{-\infty}^{E_f}\int_{-\infty}^{E_f}\int_{E_f}^{\infty} \frac{\rho_{\alpha\sigma,\gamma\sigma}(x)\rho_{\delta\sigma',\tau\sigma'}(y)\rho_{\lambda\sigma',\beta\sigma'}(z)}{\omega-x-y+z+i\eta}dzdydx + \int_{E_f}^{\infty}\int_{E_f}^{\infty}\int_{-\infty}^{E_f} \frac{\rho_{\alpha\sigma,\gamma\sigma}(x)\rho_{\delta\sigma',\tau\sigma'}(y)\rho_{\lambda\sigma',\beta\sigma'}(z)}{\omega-x-y+z+i\eta}dzdydx\Big), \tag{C.4}$$

which follows from eq. C.3 by inserting the spectral decomposition of the causal Green function:

$$g_0(\mu,\nu,\omega) = \int\Big(_{-\infty}^{E_f}\frac{\rho_{\mu,\nu}(\omega')}{\omega-\omega'-i\eta}d\omega' + \int\Big(_{E_f}^{\infty}\frac{\rho_{\mu,\nu}(\omega')}{\omega-\omega'+i\eta}d\omega' \tag{C.5}$$

Next we apply our general result for the different terms of relevance in the Kanamori hamiltonian, using a Green function such as the one written in eq. 5.34. In our case, since there are not intra-atomic hopping, only the diagonal part of the atomic self-energy, $\Sigma(\mu,\sigma,\omega)$, are non-zero:

Notational clarification: In what follows, $\sum_{\nu\neq\mu} a_{\mu,\nu}$, with $a_{\mu,\nu}$ any quantities, means $\left(\sum_\nu a_{\mu,\nu}\right) - a_{\mu,\mu}$, and not $\left(\sum_\nu\sum_\mu a_{\mu,\nu}\right) - \sum_\mu a_{\mu,\mu}$, as it did above (that is, μ is a free index and ν is the only dummy index here).

U term

The U term gives:

$$U^2 \sum_{o_1,o_2,u_3} \frac{|c_{o_1}(\mu\sigma)|^2|c_{o_2}(\mu\bar{\sigma})|c_{u_3}(\mu\bar{\sigma})|^2)}{\omega-\epsilon_{o_1}-\epsilon_{o_2}+\epsilon_{u_3}} + \sum_{u_1,u_2,o_3}\frac{|c_{u_1}(\mu\sigma)|^2|c_{u_2}(\mu\bar{\sigma})|c_{o_3}(\mu\bar{\sigma})|^2)}{\omega-\epsilon_{u_1}-\epsilon_{u_2}+\epsilon_{o_3}}\Big)\Big($$

In the limit $T/\omega \to 0$ this becomes

$$U^2\left(\frac{n_{\mu\sigma}n_{\mu\bar{\sigma}}(1-n_{\mu\bar{\sigma}})}{\omega-E^{eff}} + \frac{(1-n_{\mu\sigma})(1-n_{\mu\bar{\sigma}})n_{\mu\bar{\sigma}}}{\omega-E^{eff}}\right)\Big($$

In the fully degenerate case, in which all the occupation numbers are the same, we have just:

$$U^2 \frac{n(1-n)}{\omega - E^{eff}}$$

U′ term

The U' term gives:

$$U'^2 \sum_{\nu \neq \mu, \sigma'} \sum_{o_1, o_2, u_3} \frac{|c_{o_1}(\mu\sigma)|^2 |c_{o_2}(\nu\sigma')| c_{u_3}(\nu\sigma')|^2)}{\omega - \epsilon_{o_1} - \epsilon_{o_2} + \epsilon_{u_3}} + \sum_{u_1, u_2, o_3} \frac{|c_{u_1}(\mu\sigma)|^2 |c_{u_2}(\nu\sigma')| c_{o_3}(\nu\sigma')|^2)}{\omega - \epsilon_{u_1} - \epsilon_{u_2} + \epsilon_{o_3}} \Bigg) \Bigg($$

In the limit $T/\omega \to 0$ this becomes

$$U'^2 \sum_{\nu \neq \mu, \sigma'} \left(\frac{n_{\mu\sigma} n_{\nu\sigma'} (1 - n_{\nu\sigma'})}{\omega - E^{eff}} + \frac{(1 - n_{\mu\sigma})(1 - n_{\nu\sigma'}) n_{\nu\sigma'}}{\omega - E^{eff}} \right) \Bigg($$

In the fully degenerate case, in which all the occupation numbers are the same, we sum over ν and σ' and we get:

$$2(M-1) U'^2 \frac{n(1-n)}{\omega - E^{eff}}.$$

Diagonal J term

The diagonal J term gives:

$$J^2 \sum_{\nu \neq \mu} \sum_{o_1, o_2, u_3} \frac{|c_{o_1}(\nu\sigma)|^2 |c_{o_2}(\mu\sigma)| c_{u_3}(\nu\sigma)|^2)}{\omega - \epsilon_{o_1} - \epsilon_{o_2} + \epsilon_{u_3}} + \sum_{u_1, u_2, o_3} \frac{|c_{u_1}(\nu\sigma)|^2 |c_{u_2}(\mu\sigma)| c_{o_3}(\nu\sigma)|^2)}{\omega - \epsilon_{u_1} - \epsilon_{u_2} + \epsilon_{o_3}} \Bigg) \Bigg($$

In the limit $T/\omega \to 0$ this becomes

$$J^2 \sum_{\nu \neq \mu} \left(\frac{n_{\nu\sigma} n_{\mu\sigma} (1 - n_{\nu\sigma})}{\omega - E^{eff}} + \frac{(1 - n_{\nu\sigma})(1 - n_{\mu\sigma}) n_{\nu\sigma}}{\omega - E^{eff}} \right) \Bigg($$

In the fully degenerate case, in which all the occupation numbers are the same, we sum over ν and we get:

$$(M-1) J^2 \frac{n(1-n)}{\omega - E^{eff}}.$$

Spin-flip J term

The spin-flip J term gives:

$$J^2 \sum_{\nu \neq \mu} \sum_{o_1, o_2, u_3} \frac{|c_{o_1}(\nu\sigma)|^2 |c_{o_2}(\mu\overline{\sigma})| c_{u_3}(\nu\overline{\sigma})|^2)}{\omega - \epsilon_{o_1} - \epsilon_{o_2} + \epsilon_{u_3}} + \sum_{u_1, u_2, o_3} \frac{|c_{u_1}(\nu\sigma)|^2 |c_{u_2}(\mu\overline{\sigma})| c_{o_3}(\nu\overline{\sigma})|^2)}{\omega - \epsilon_{u_1} - \epsilon_{u_2} + \epsilon_{o_3}} \Bigg) \Bigg($$

In the limit $T/\omega \to 0$ this becomes

$$J^2 \sum_{\nu \neq \mu} \left(\frac{n_{\nu\sigma} n_{\mu\bar{\sigma}} (1 - n_{\nu\bar{\sigma}})}{\omega - E^{eff}} + \frac{(1 - n_{\nu\sigma})(1 - n_{\mu\bar{\sigma}}) n_{\nu\bar{\sigma}}}{\omega - E^{eff}} \right) \Bigg($$

In the fully degenerate case, in which all the occupation numbers are the same, we sum over ν and we get:

$$(M-1) J^2 \frac{n(1-n)}{\omega - E^{eff}}.$$

Last Kanamori J term

Here we study the effect of the double-hopping term, which appears only when $U = U' + 2J$.

This is the term

$$-\frac{J}{2} \sum_{\nu \neq \mu} \hat{c}^{\dagger}_{\mu\sigma} \hat{c}^{\dagger}_{\mu\bar{\sigma}} \hat{c}_{\nu\bar{\sigma}} \hat{c}_{\nu\sigma}.$$

This last Kanamori J term gives:

$$J^2 \sum_{\nu \neq \mu} \sum_{o_1, o_2, u_3} \frac{|c_{o_1}(\nu\sigma)|^2 |c_{o_2}(\nu\bar{\sigma})|^2 c_{u_3}(\mu\bar{\sigma})|^2)}{\omega - \epsilon_{o_1} - \epsilon_{o_2} + \epsilon_{u_3}} + \sum_{u_1, u_2, o_3} \frac{|c_{u_1}(\nu\sigma)|^2 |c_{u_2}(\nu\bar{\sigma})|^2 c_{o_3}(\mu\bar{\sigma})|^2)}{\omega - \epsilon_{u_1} - \epsilon_{u_2} + \epsilon_{o_3}} \Bigg) \Bigg($$

In the limit $T/\omega \to 0$ this becomes

$$J^2 \sum_{\nu \neq \mu} \left(\frac{n_{\nu\sigma} n_{\nu\bar{\sigma}} (1 - n_{\mu\bar{\sigma}})}{\omega - E^{eff}} + \frac{(1 - n_{\nu\sigma})(1 - n_{\nu\bar{\sigma}}) n_{\mu\bar{\sigma}}}{\omega - E^{eff}} \right) \Bigg($$

In the fully degenerate case, in which all the occupation numbers are the same, we sum over ν and we get:

$$(M-1) J^2 \frac{n(1-n)}{\omega - E^{eff}}.$$

Double exchange diagram

The last diagram to be considered is the double exchange one, seen on the right in fig. **??**.

And it gives no-null contribution with U'/J or J/U'. Both contributions are identical, so the result is :

$$-2U'J \sum_{\nu \neq \mu} \sum_{o_1, o_2, u_3} \frac{|c_{o_1}(\nu\sigma)|^2 |c_{o_2}(\mu\sigma)|^2 c_{u_3}(\nu\sigma)|^2)}{\omega - \epsilon_{o_1} - \epsilon_{o_2} + \epsilon_{u_3}} + \sum_{u_1, u_2, o_3} \frac{|c_{u_1}(\nu\sigma)|^2 |c_{u_2}(\mu\sigma)|^2 c_{o_3}(\nu\sigma)|^2)}{\omega - \epsilon_{u_1} - \epsilon_{u_2} + \epsilon_{o_3}} \Bigg) \Bigg($$

The sign is opposite to that of the other diagrams because of the absence of fermionic loops.

In the limit $T/\omega \to 0$ this becomes

$$-2U'J \sum_{\nu \neq \mu} \left(\frac{n_{\nu\sigma} n_{\mu\sigma} (1 - n_{\nu\sigma})}{\omega - E^{eff}} + \frac{(1 - n_{\nu\sigma})(1 - n_{\mu\sigma}) n_{\nu\sigma}}{\omega - E^{eff}} \right) \Bigg($$

In the fully degenerate case, in which all the occupation numbers are the same, we sum over ν and we get:

$$-2(M-1)U'J\frac{n(1-n)}{\omega - E^{eff}}.$$

Final result

Adding everything together, we have, for $U = U' + J$, that the final result in the limit $T/\omega \to 0$ with all the levels degenerated is:

$$C\frac{n(1-n)}{\omega - E^{\text{eff}}},$$

with

$$C = U^2 + 2(M-1)U'^2 + 2(M-1)J^2 - 2(M-1)U'J = (2M-1)U'^2 + (2M-1)J^2 - 2(M-2)U'J. \tag{C.6}$$

In the particular case $M = 2$, there is no mixed term and the result is $3(U'^2 + J^2)$.

In the case in which all atomic levels are degenerate, we can write:

$$\Sigma_2(\omega) = \Big(\big((2M-1)U'^2 + (2M-1)J^2 - 2(M-2)U'J \big) \int_{-\infty}^{E_f}\int_{-\infty}^{E_f}\int_{E_f}^{\infty} \frac{\rho(x)\rho(y)\rho(z)}{\omega - x - y + z + i\eta} dzdydx + \int_{E_f}^{\infty}\int_{E_f}^{\infty}\int_{-\infty}^{E_f} \frac{\rho(x)\rho(y)\rho(z)}{\omega - x - y + z + i\eta} dzdydx \Big), \tag{C.7}$$

where ρ is the same for every level and spin.

Appendix D

Alternative calculation of the asymptotics for the atomic Green function

In general, our atomic Green function will look like this:

$$\sum_{\lambda=1}^{P} \frac{A_\lambda}{\omega - \epsilon_\lambda}.$$

For simplicity, I omit the labels $\mu\sigma$ of the Green function (in the case in which all our levels are degenerate this is not important at all, since the Green function does not depend on $\mu\sigma$) and I drop the $i\eta$ factors in the denominators. I shall assume that we are working with the retarded Green function here, so the A_λ is the sum of the electron and hole contributions associated to the denominator $\omega - \epsilon_\lambda$.

We write this in a form with common denominator:

$$\frac{\sum_{\lambda=1}^{P} A_\lambda \prod_{\mu\neq\lambda}(\omega - \epsilon_\mu)}{\prod_\alpha(\omega - \epsilon_\alpha)}.$$

To deal more comfortably with this expression, we need to expand the products and order that expression in terms of the different powers of ω.

$$\prod_{\alpha=1}^{P}(\omega - \epsilon_\alpha) = \sum_{k=0}^{P}(-1)^{P-k}\left[\left(\sum_{\{\gamma_1,\ldots,\gamma_{P-k}\}\subset\{1,\ldots,P\}} \prod_{j=1}^{P-k} \epsilon_{\gamma_j}\right)\omega^k,\right.$$

$$\prod_{\mu=1,\mu\neq\lambda}^{P}(\omega - \epsilon_\alpha) = \sum_{k=0}^{P-1}(-1)^{P-k-1}\left(\left(\sum_{\{\gamma_1,\ldots,\gamma_{P-k-1}\}\subset\{1,\cdots,\underline{\lambda},\ldots,P\}} \prod_{j=1}^{P-k-1} \epsilon_{\gamma_j}\right)\right)\omega^k.$$

Remember, we want to compute $\Sigma^{\text{at}} = G_0^{-1} - G^{-1}$, and $G_0^{-1} = \omega - \tilde{E}$, where $\tilde{E}$ is the effective band energy (including Hartree and exchange part of the interaction, so that this self-energy is strictly not the true self-energy, but the difference between the self-energy and the Hartree-Fock self-energy). This is:

$$\Sigma^{\text{at}} = \frac{(\omega - \tilde{E})\sum_\lambda A_\lambda \prod_{\mu\neq\lambda}(\omega - \epsilon_\mu) - \prod_\alpha(\omega - \epsilon_\alpha)}{\sum_\lambda A_\lambda \prod_{\mu\neq\lambda}(\omega - \epsilon_\mu)}.$$

We introduce our expansions of the products in this expression. We focus now on the object:

$$(\omega - \tilde{E}) \sum_{\lambda} A_\lambda \prod_{\mu \neq \lambda} (\omega - \epsilon_\mu) =$$

$$(\omega - \tilde{E}) \sum_{\lambda=1}^{P} \sum_{k=0}^{P-1} (-1)^{P-k-1} \left[\left(\sum_{\{\gamma_1,\ldots,\gamma_{P-k-1}\} \subset \{1,\ldots,\underline{\lambda},\ldots,P\}} \prod_{j=1}^{P-k-1} \epsilon_{\gamma_j} \right] \right) \omega^k.$$

We interchange now the order of the summations and study first the sum over λ. We can then see that **the key is to use the sum rules to simplify the expressions**:

$$\sum_{\lambda=1}^{P} A_\lambda \left[\left(\sum_{\{\gamma_1,\ldots,\gamma_{P-k-1}\} \subset \{1,\ldots,\underline{\lambda},\ldots,P\}} \prod_{j=1}^{P-k-1} \epsilon_{\gamma_j} \right] \right) \left(\right.$$

for each k.

If we manage to compute this, probably the rest should be easy!

We introduce the notation:

$$\Delta_l = \sum_{\{\gamma_1,\ldots,\gamma_l\} \subset \{1,\ldots,P\}} \prod_{j=1}^{l} \epsilon_{\gamma_j},$$

and

$$\Delta_l^{\underline{\lambda}} = \sum_{\{\gamma_1,\ldots,\gamma_l\} \subset \{1,\ldots,\underline{\lambda},\ldots,P\}} \prod_{j=1}^{l} \epsilon_{\gamma_j}.$$

Focus on the numerator, $(\omega - \tilde{E}) \sum_\lambda A_\lambda \prod_{\mu \neq \lambda} (\omega - \epsilon_\mu) - \prod_\alpha (\omega - \epsilon_\alpha)$. We want to apply our expansions here and write this in the form

$$\sum_{k=1}^{P} C_k \omega^k.$$

The highest order term, in ω^P, clearly vanishes because of the first sum rule, $\sum_{\lambda=1}^{P} A_\lambda = 1$. Now, assume that $1 < k < P - 1$ (we'll treat the remaining cases later on). By inspection, we see that the coefficient C_k is:

$$C_k = \sum_{\lambda=1}^{P} (-1)^{P-k} A_\lambda \Delta_{P-k}^{\underline{\lambda}} - \tilde{E} \sum_{\lambda=1}^{P} (-1)^{P-k-1} A_\lambda \Delta_{P-k-1}^{\underline{\lambda}} - (-1)^{P-k} \Delta_{P-k}.$$

Now we make the following observation:

$$\Delta_l^{\underline{\lambda}} = \Delta_l - \epsilon_\lambda \Delta_{l-1}^{\underline{\lambda}}.$$

The coefficient C_{P-1} of the term of order $P-1$, ω^{P-1}, also vanishes if we assume the sum rule $\sum_\lambda A_\lambda \epsilon_\lambda = \tilde{E}$ to hold!:

$$C_{P-1} = -\sum A_\lambda \Delta_1^{\underline{\lambda}} - \tilde{E}\sum_\lambda A_\lambda \Delta_0^\lambda + \Delta_1 = -\Delta_1 + \tilde{E} - \tilde{E} + \Delta_1 = 0.$$

Clearly the $(P-2)$-th term is the lowest order term in the interaction (is quadratic), so it will be the only surviving term when taking the limit $U \to 0$. The coefficient C_{P-2} is calculated as follows:

$$\begin{aligned} C_{P-2} = &\sum_\lambda A_\lambda \Delta_2^{\underline{\lambda}} + \tilde{E}\sum_\lambda A_\lambda \Delta_1^{\underline{\lambda}} - \Delta_2 = \\ &\sum_\lambda A_\lambda \left(\Delta_2 - \epsilon_\lambda \Delta_1^{\underline{\lambda}}\right) + \tilde{E}\sum_\lambda A_\lambda \left(\Delta_1 - \epsilon_\lambda\right) - \Delta_2 = \\ &\Delta_2 - \sum_\lambda A_\lambda \epsilon_\lambda \Delta_1^{\underline{\lambda}} + \tilde{E}\sum_\lambda A_\lambda \Delta_1 - \tilde{E}\sum_\lambda A_\lambda \epsilon_\lambda - \Delta_2 = \\ &-\Delta_1 \tilde{E} + \sum_\lambda A_\lambda \epsilon_\lambda^2 + \Delta_1 \tilde{E} - \tilde{E}^2 = \\ &\sum_\lambda A_\lambda \epsilon_\lambda^2 - \tilde{E}^2. \end{aligned}$$

Thus, we have proved that the self-energy is asymptotically (as $U \to 0$):

$$\Sigma = \frac{\sum_\lambda A_\lambda \epsilon_\lambda^2 - \tilde{E}^2}{\omega}.$$

(I assume the energy level in each orbital to be zero for simplicity)

Bibliography

Leer, por lo pronto, es una actividad posterior a la de escribir: más resignada, más civil, más intelectual.

J. L. Borges

[1] P.A.M Dirac. "Quantum mechanics of many-electron systems". In: *Proceedings of the Royal Society of London. Series A, Containing Papers of a Mathematical and Physical Character* 123.792 (1929), pp. 714–733. ISSN: 0950-1207. DOI: 10.1098/rspa.1929.0094. URL: https://royalsocietypublishing.org/doi/10.1098/rspa.1929.0094.

[2] P. Hohenberg and W. Kohn. "Inhomogeneous Electron Gas". In: *Physical Review* 136.3B (1964), B864–B871. ISSN: 0031-899X. DOI: 10.1103/PhysRev.136.B864. URL: https://link.aps.org/doi/10.1103/PhysRev.136.B864.

[3] W. Kohn and L. J. Sham. "Self-Consistent Equations Including Exchange and Correlation Effects". In: *Physical Review* 140.4A (1965), A1133–A1138. ISSN: 0031-899X. DOI: 10.1103/PhysRev.140.A1133. URL: https://link.aps.org/doi/10.1103/PhysRev.140.A1133.

[4] L. H. Thomas. "The calculation of atomic fields". In: *Mathematical Proceedings of the Cambridge Philosophical Society* 23.5 (1927), pp. 542–548. ISSN: 14698064. DOI: 10.1017/S0305004100011683.

[5] Elliott H Lieb and Barry Simon. "The Thomas-Fermi theory of atoms, molecules and solids". In: *Advances in Mathematics* 23.1 (1977), pp. 22–116. ISSN: 00018708. DOI: 10.1016/0001-8708(77)90108-6. URL: https://linkinghub.elsevier.com/retrieve/pii/0001870877901086.

[6] Edward Teller. "On the Stability of Molecules in the Thomas-Fermi Theory". In: *Reviews of Modern Physics* 34.4 (1962), pp. 627–631. ISSN: 0034-6861. DOI: 10.1103/RevModPhys.34.627. URL: https://link.aps.org/doi/10.1103/RevModPhys.34.627.

[7] C. F. v. Weizsäcker. "Zur Theorie der Kernmassen". In: *Zeitschrift für Physik* 96.7-8 (1935), pp. 431–458. ISSN: 1434-6001. DOI: 10.1007/BF01337700. URL: http://link.springer.com/10.1007/BF01337700.

[8] D. R. Hartree. "The Wave Mechanics of an Atom with a Non-Coulomb Central Field. Part II. Some Results and Discussion". In: *Mathematical Proceedings of the Cambridge Philosophical Society* 24.1 (1928), pp. 111–132. ISSN: 0305-0041. DOI: 10.1017/S0305004100011920. arXiv: 1708.05752. URL: http://dx.doi.org/10.1038/s41467-019-10257-2https://www.cambridge.org/core/product/identifier/S0305004100011920/type/journal{_}article.

[9] J. C. Slater. "The Self Consistent Field and the Structure of Atoms". In: *Physical Review* 32.3 (1928), pp. 339–348. ISSN: 0031-899X. DOI: 10.1103/PhysRev.32.339. URL: https://link.aps.org/doi/10.1103/PhysRev.32.339.

[10] V. Fock. "Näherungsmethode zur Lösung des quantenmechanischen Mehrkörperproblems". In: *Zeitschrift für Physik* 61.1-2 (1930), pp. 126–148. ISSN: 1434-6001. DOI: 10.1007/BF01340294. URL: https://link.aps.org/doi/10.1103/PhysRevB.52.R5467http://link.springer.com/10.1007/BF01340294.

[11] Chr. Møller and M. S. Plesset. "Note on an Approximation Treatment for Many-Electron Systems". In: *Physical Review* 46.7 (1934), pp. 618–622. ISSN: 0031-899X. DOI: 10.1103/PhysRev.46.618. URL: https://link.aps.org/doi/10.1103/PhysRev.46.618.

[12] J. A. Pople, R. Seeger, and R. Krishnan. "Variational configuration interaction methods and comparison with perturbation theory". In: *International Journal of Quantum Chemistry* 12.S11 (2009), pp. 149–163. ISSN: 00207608. DOI: 10.1002/qua.560120820. arXiv: 0608285 [cond-mat]. URL: http://doi.wiley.com/10.1002/qua.560120820.

[13] Bogumil Jeziorski and Hendrik J. Monkhorst. "Coupled-cluster method for multideterminantal reference states". In: *Physical Review A* 24.4 (1981), pp. 1668–1681. ISSN: 0556-2791. DOI: 10.1103/PhysRevA.24.1668. arXiv: 1805.01805. URL: https://link.aps.org/doi/10.1103/PhysRevA.24.1668.

[14] Jianshu Cao and Gregory A. Voth. "The formulation of quantum statistical mechanics based on the Feynman path centroid density. I. Equilibrium properties". In: *The Journal of Chemical Physics* 100.7 (Mar. 1994), pp. 5093–5105. ISSN: 0021-9606. DOI: 10.1063/1.467175. URL: http://aip.scitation.org/doi/10.1063/1.467175.

[15] Rafael Ramírez and Telesforo López-Ciudad. "The Schrödinger formulation of the Feynman path centroid density". In: *The Journal of Chemical Physics* 111.8 (Mar. 1999), pp. 3339–3348. ISSN: 0021-9606. DOI: 10.1063/1.479666. URL: http://aip.scitation.org/doi/10.1063/1.479666.

[16] E. A. Polyakov, A. P. Lyubartsev, and P. N. Vorontsov-Velyaminov. "Centroid molecular dynamics: Comparison with exact results for model systems". In: *The Journal of Chemical Physics* 133.19 (Mar. 2010), p. 194103. ISSN: 0021-9606. DOI: 10.1063/1.3484490. URL: http://aip.scitation.org/doi/10.1063/1.3484490.

[17] Dominik Marx and Michele Parrinello. "Ab initio path-integral molecular dynamics". In: *Zeitschrift fr Physik B Condensed Matter* 95.2 (Mar. 1994), pp. 143–144. ISSN: 0722-3277. DOI: 10.1007/BF01312185. URL: http://link.springer.com/10.1007/BF01312185.

[18] Aleš Cahlík et al. "Significance of nuclear quantum effects in hydrogen bonded molecular chains". In: (2020). arXiv: 2007.14657 [cond-mat.mes-hall].

[19] T. Kreibich and E. K. U. Gross. "Multicomponent Density-Functional Theory for Electrons and Nuclei". In: *Physical Review Letters* 86.14 (Mar. 2001), pp. 2984–2987. ISSN: 0031-9007. DOI: 10.1103/PhysRevLett.86.2984. URL: https://link.aps.org/doi/10.1103/PhysRevLett.86.2984.

[20] Arindam Chakraborty, Michael V. Pak, and Sharon Hammes-Schiffer. "Development of Electron-Proton Density Functionals for Multicomponent Density Functional Theory". In: *Physical Review Letters* 101.15 (Mar. 2008), p. 153001. ISSN: 0031-9007. DOI: 10.1103/PhysRevLett.101.153001. URL: https://link.aps.org/doi/10.1103/PhysRevLett.101.153001.

[21] Nikos L. Doltsinis and Dominik Marx. "First Principles Molecular Dynamics involving excited states and nonadiabatic transitions". In: *Journal of Theoretical and Computational Chemistry* 01.02 (Oct. 2002), pp. 319–349. ISSN: 0219-6336. DOI: 10.1142/S0219633602000257. URL: https://www.worldscientific.com/doi/abs/10.1142/S0219633602000257.

[22] John C. Tully. "Molecular dynamics with electronic transitions". In: *The Journal of Chemical Physics* 93.2 (July 1990), pp. 1061–1071. ISSN: 0021-9606. DOI: 10.1063/1.459170. URL: http://aip.scitation.org/doi/10.1063/1.459170.

[23] Vladimír Zobač et al. "Photo-induced reactions from efficient molecular dynamics with electronic transitions using the FIREBALL local-orbital density functional theory formalism". In: *Journal of Physics: Condensed Matter* 27.17 (Mar. 2015), p. 175002. DOI: 10.1088/0953-8984/27/17/175002. URL: https://doi.org/10.1088/0953-8984/27/17/175002.

[24] Jesús I. Mendieta-Moreno et al. "Quantum Mechanics/Molecular Mechanics Free Energy Maps and Nonadiabatic Simulations for a Photochemical Reaction in DNA: Cyclobutane Thymine Dimer". In: *The Journal of Physical Chemistry Letters* 7.21 (Mar. 2016), pp. 4391–4397. ISSN: 1948-7185. DOI: 10.1021/acs.jpclett.6b02168. URL: https://pubs.acs.org/doi/10.1021/acs.jpclett.6b02168.

[25] "Spin-orbit coupling in three-orbital Kanamori impurity model and its relevance for transition-metal oxides". In: *Physical Review B* 96.8 (Mar. 2017), p. 085122. ISSN: 2469-9950. DOI: 10.1103/PhysRevB.96.085122. URL: https://link.aps.org/doi/10.1103/PhysRevB.96.085122.

[26] Helmut Eschring. *The Fundamentals of Density Functional Theory*. Providence, R.I.: Springer, 1996. ISBN: 9780821849743 0821849743.

[27] M. Levy. "Universal variational functionals of electron densities, first-order density matrices, and natural spin-orbitals and solution of the v-representability problem". In: *Proceedings of the National Academy of Sciences* 76.12 (Mar. 1979), pp. 6062–6065. ISSN: 0027-8424. DOI: 10.1073/pnas.76.12.6062. URL: http://www.pnas.org/cgi/doi/10.1073/pnas.76.12.6062.

[28] Elliott H. Lieb. "Density functionals for coulomb systems". In: *International Journal of Quantum Chemistry* 24.3 (Mar. 1983), pp. 243–277. ISSN: 0020-7608. DOI: 10.1002/qua.560240302. URL: http://doi.wiley.com/10.1002/qua.560240302.

[29] T. L. Gilbert. "Hohenberg-Kohn theorem for nonlocal external potentials". In: *Phys. Rev. B* 12 (6 Sept. 1975), pp. 2111–2120. DOI: 10.1103/PhysRevB.12.2111. URL: https://link.aps.org/doi/10.1103/PhysRevB.12.2111.

[30] Lawrence C. Evans. *Partial differential equations*. Providence, R.I.: American Mathematical Society, 2010. ISBN: 9780821849743 0821849743.

[31] S. H. Vosko, L. Wilk, and M. Nusair. "Accurate spin-dependent electron liquid correlation energies for local spin density calculations: a critical analysis". In: *Canadian Journal of Physics* 58.8 (Aug. 1980), pp. 1200–1211. ISSN: 0008-4204. DOI: 10.1139/p80-159. URL: http://www.nrcresearchpress.com/doi/10.1139/p80-159.

[32] David Bohm and David Pines. "A Collective Description of Electron Interactions. I. Magnetic Interactions". In: *Physical Review* 82.5 (June 1951), pp. 625–634. ISSN: 0031-899X. DOI: 10.1103/PhysRev.82.625. URL: https://link.aps.org/doi/10.1103/PhysRev.82.625.

[33] David Pines and David Bohm. "A Collective Description of Electron Interactions: II. Collective <math display="inline"> <mi>vs</mi> </math> Individual Particle Aspects of the Interactions". In: *Physical Review* 85.2 (Jan. 1952), pp. 338–353. ISSN: 0031-899X. DOI: 10.1103/PhysRev.85.338. URL: https://link.aps.org/doi/10.1103/PhysRev.85.338.

[34] David Bohm and David Pines. "A Collective Description of Electron Interactions: III. Coulomb Interactions in a Degenerate Electron Gas". In: *Physical Review* 92.3 (Nov. 1953), pp. 609–625. ISSN: 0031-899X. DOI: 10.1103/PhysRev.92.609. URL: https://link.aps.org/doi/10.1103/PhysRev.92.609.

[35] D. M. Ceperley and B. J. Alder. "Ground State of the Electron Gas by a Stochastic Method". In: *Physical Review Letters* 45.7 (Aug. 1980), pp. 566–569. ISSN: 0031-9007. DOI: 10.1103/PhysRevLett.45.566. URL: https://link.aps.org/doi/10.1103/PhysRevLett.45.566.

[36] G. L. Oliver and J. P. Perdew. "Spin-density gradient expansion for the kinetic energy". In: *Physical Review A* 20.2 (Aug. 1979), pp. 397–403. ISSN: 0556-2791. DOI: 10.1103/PhysRevA.20.397. URL: https://link.aps.org/doi/10.1103/PhysRevA.20.397.

[37] J. P. Perdew and Alex Zunger. "Self-interaction correction to density-functional approximations for many-electron systems". In: *Physical Review B* 23.10 (May 1981), pp. 5048–5079. ISSN: 0163-1829. DOI: 10.1103/PhysRevB.23.5048. URL: https://link.aps.org/doi/10.1103/PhysRevB.23.5048.

[38] Perdew, Burke, and Ernzerhof. "Generalized Gradient Approximation Made Simple." In: *Physical review letters* 77 18 (1996), pp. 3865–3868.

[39] A. D. Becke. "Density-functional exchange-energy approximation with correct asymptotic behavior". In: *Physical Review A* 38.6 (Mar. 1988), pp. 3098–3100. ISSN: 0556-2791. DOI: 10.1103/PhysRevA.38.3098. URL: https://link.aps.org/doi/10.1103/PhysRevA.38.3098.

[40] Chengteh Lee, Weitao Yang, and Robert G. Parr. "Development of the Colle-Salvetti correlation-energy formula into a functional of the electron density". In: *Physical Review B* 37.2 (Mar. 1988), pp. 785–789. ISSN: 0163-1829. DOI: 10.1103/PhysRevB.37.785. URL: https://link.aps.org/doi/10.1103/PhysRevB.37.785.

[41] P. J. Stephens et al. "Ab Initio Calculation of Vibrational Absorption and Circular Dichroism Spectra Using Density Functional Force Fields". In: *The Journal of Physical Chemistry* 98.45 (June 1994), pp. 11623–11627. ISSN: 0022-3654. DOI: 10.1021/j100096a001. URL: https://pubs.acs.org/doi/abs/10.1021/j100096a001.

[42] John P. Perdew, Matthias Ernzerhof, and Kieron Burke. "Rationale for mixing exact exchange with density functional approximations". In: *The Journal of Chemical Physics* 105.22 (Dec. 1996), pp. 9982–9985. ISSN: 0021-9606. DOI: 10.1063/1.472933. URL: http://aip.scitation.org/doi/10.1063/1.472933.

[43] Lars Hedin. "New method for calculating the one-particle Green's function with application to the electron-gas problem". In: *Physical Review* 139.3A (1965). ISSN: 0031899X. DOI: 10.1103/PhysRev.139.A796.

[44] Vladimir I. Anisimov, Jan Zaanen, and Ole K. Andersen. "Band theory and Mott insulators: Hubbard U instead of Stoner I". In: *Physical Review B* 44.3 (1991), pp. 943–954. ISSN: 01631829. DOI: 10.1103/PhysRevB.44.943.

[45] M. Methfessel. "Independent variation of the density and the potential in density-functional methods". In: *Phys. Rev. B* 52 (11 Sept. 1995), pp. 8074–8081. DOI: 10.1103/PhysRevB.52.8074. URL: https://link.aps.org/doi/10.1103/PhysRevB.52.8074.

[46] J. Harris. "Simplified method for calculating the energy of weakly interacting fragments". In: *Physical Review B* 31.4 (1985), pp. 1770–1779. ISSN: 01631829. DOI: 10.1103/PhysRevB.31.1770.

[47] W. Matthew C. Foulkes and Roger Haydock. "Tight-binding models and density-functional theory". In: *Phys. Rev. B* 39 (17), pp. 12520–12536.

[48] Behnam Farid et al. "Extremal properties of the Harris-Foulkes functional and an improved screening calculation for the electron gas". In: *Physical Review B* 48.16 (1993), pp. 11602–11621. ISSN: 0163-1829. DOI: 10.1103/PhysRevB.48.11602. arXiv: arXiv:1011.1669v3. URL: https://link.aps.org/doi/10.1103/PhysRevB.48.11602.

[49] Richard M. Martin. *Electronic Structure: Basic Theory and Practical Methods*. Cambridge University Press, 2004. DOI: 10.1017/CBO9780511805769.

[50] Otto F. Sankey and David J. Niklewski. "Ab initio multicenter tight-binding model for molecular-dynamics simulations and other applications in covalent systems". In: *Physical Review B* 40.6 (1989), pp. 3979–3995. ISSN: 01631829. DOI: 10.1103/PhysRevB.40.3979.

[51] Alexander A. Demkov et al. "Electronic structure approach for complex silicas". In: *Physical Review B* 52.3 (Mar. 1995), pp. 1618–1630. ISSN: 0163-1829. DOI: 10.1103/PhysRevB.52.1618. URL: https://link.aps.org/doi/10.1103/PhysRevB.52.1618.

[52] James P. Lewis et al. "Further developments in the local-orbital density-functional-theory tight-binding method". In: *Physical Review B - Condensed Matter and Materials Physics* 64.19 (2001), pp. 1951031–19510310. ISSN: 01631829. DOI: 10.1103/physrevb.64.195103.

[53] C. G. Broyden. "A class of methods for solving nonlinear simultaneous equations". In: *Mathematics of Computation* 19.92 (1965), pp. 577–577. ISSN: 0025-5718. DOI: 10.1090/S0025-5718-1965-0198670-6. URL: http://www.ams.org/jourcgi/jour-getitem?pii=S0025-5718-1965-0198670-6.

[54] Péter Pulay. "Convergence acceleration of iterative sequences. the case of scf iteration". In: *Chemical Physics Letters* 73.2 (1980), pp. 393 –398. ISSN: 0009-2614. DOI: https://doi.org/10.1016/0009-2614(80)80396-4. URL: http://www.sciencedirect.com/science/article/pii/0009261480803964.

[55] J. C. Slater and G. F. Koster. "Simplified LCAO Method for the Periodic Potential Problem". In: *Physical Review* 94.6 (June 1954), pp. 1498–1524. ISSN: 0031-899X. DOI: 10.1103/PhysRev.94.1498. URL: https://link.aps.org/doi/10.1103/PhysRev.94.1498.

[56] Pavel Jelínek et al. "Multicenter approach to the exchange-correlation interactions in ab initio tight-binding methods". In: *Physical Review B - Condensed Matter and Materials Physics* 71.23 (2005), pp. 1–9. ISSN: 10980121. DOI: 10.1103/PhysRevB.71.235101.

[57] F. L. Hirshfeld. "Bonded-atom fragments for describing molecular charge densities". In: *Theoretica Chimica Acta* 44.2 (June 1977), pp. 129–138. ISSN: 00405744. DOI: 10.1007/BF00549096. URL: https://link.springer.com/article/10.1007/BF00549096.

[58] R. F.W. Bader. "Atoms in Molecules". In: *Accounts of Chemical Research* 18.1 (Jan. 1985), pp. 9–15. ISSN: 15204898. DOI: 10.1021/ar00109a003. URL: https://pubs.acs.org/doi/abs/10.1021/ar00109a003.

[59] Richard F.W. Bader. "A Quantum Theory of Molecular Structure and Its Applications". In: *Chemical Reviews* 91.5 (June 1991), pp. 893–928. ISSN: 15206890. DOI: 10.1021/cr00005a013.

[60] Richard F W Bader. *Atoms in Molecules - A Quantum Theory.* Oxford Univesity Press, 1990.

[61] F. Matthias Bickelhaupt et al. "The Carbon-Lithium Electron Pair Bond in (CH 3 Li) n (n = 1, 2, 4)". In: *Organometallics* 15.13 (Jan. 1996), pp. 2923–2931. ISSN: 0276-7333. DOI: 10.1021/om950966x. URL: https://pubs.acs.org/sharingguidelines.

[62] Célia Fonseca Guerra et al. "Voronoi Deformation Density (VDD) Charges: Assessment of the Mulliken, Bader, Hirshfeld, Weinhold, and VDD Methods for Charge Analysis". In: *Journal of Computational Chemistry* 25.2 (2004), pp. 189–210. ISSN: 01928651. DOI: 10.1002/jcc.10351.

[63] Patrick Bultinck et al. "Critical analysis and extension of the Hirshfeld atoms in molecules". In: *Journal of Chemical Physics* 126.14 (Apr. 2007), p. 144111. ISSN: 00219606. DOI: 10.1063/1.2715563. URL: http://aip.scitation.org/doi/10.1063/1.2715563.

[64] Timothy C. Lillestolen and Richard J. Wheatley. "Atomic charge densities generated using an iterative stockholder procedure". In: *The Journal of Chemical Physics* 131.14 (June 2009), p. 144101. ISSN: 0021-9606. DOI: 10.1063/1.3243863. URL: http://aip.scitation.org/doi/10.1063/1.3243863.

[65] Thomas A. Manz and David S. Sholl. "the Electrostatic Potential in Periodic and Nonperiodic Materials". In: *J. Chem. Theor. Comput.* 6 (2010), pp. 2455–2468.

[66] Thomas A. Manz and David S. Sholl. "Improved atoms-in-molecule charge partitioning functional for simultaneously reproducing the electrostatic potential and chemical states in periodic and nonperiodic materials". In: *Journal of Chemical Theory and Computation* 8.8 (Aug. 2012), pp. 2844–2867. ISSN: 15499618. DOI: 10.1021/ct3002199. URL: https://pubs.acs.org/sharingguidelines.

[67] Thomas A Manz and Nidia Gabaldon Limas. "Introducing DDEC6 atomic population analysis: Part 1. Charge partitioning theory and methodology". In: *RSC Advances* 6.53 (2016), pp. 47771–47801. ISSN: 20462069. DOI: 10.1039/c6ra04656h.

[68] Toon Verstraelen et al. "Minimal Basis Iterative Stockholder: Atoms in Molecules for Force-Field Development". In: *Journal of Chemical Theory and Computation* 12.8 (Aug. 2016), pp. 3894–3912. ISSN: 1549-9618. DOI: 10.1021/acs.jctc.6b00456. URL: https://pubs.acs.org/doi/10.1021/acs.jctc.6b00456.

[69] Farnaz Heidar-Zadeh et al. "Information-Theoretic Approaches to Atoms-in-Molecules: Hirshfeld Family of Partitioning Schemes". In: *Journal of Physical Chemistry A* 122.17 (2018), pp. 4219–4245. ISSN: 15205215. DOI: 10.1021/acs.jpca.7b08966. URL: https://pubs.acs.org/sharingguidelines.

[70] Alexander A Voityuk, Anton J Stasyuk, and Sergei F Vyboishchikov. "A simple model for calculating atomic charges in molecules". In: *Physical Chemistry Chemical Physics* 20.36 (2018), pp. 23328–23337. ISSN: 14639076. DOI: 10.1039/c8cp03764g.

[71] R. S. Mulliken. "Electronic population analysis on LCAO-MO molecular wave functions. I". In: *The Journal of Chemical Physics* 23.10 (1955), pp. 1833–1840. ISSN: 00219606. DOI: 10.1063/1.1740588.

[72] F. Matthias Bickelhaupt et al. "The Carbon-Lithium Electron Pair Bond in (CH 3 Li) n (n = 1, 2, 4)". In: *Organometallics* 15.13 (1996), pp. 2923–2931. ISSN: 0276-7333. DOI: 10.1021/om950966x. URL: https://pubs.acs.org/doi/abs/10.1021/om950966x.

[73] Diego and Trabada, Daniel G and Soler-Polo et al. "Mulliken-Dipole Population Analysis". In: *(in preparation)* (2020).

[74] Per-Olov Löwdin. "On the Non-Orthogonality Problem Connected with the Use of Atomic Wave Functions in the Theory of Molecules and Crystals". In: *The Journal of Chemical Physics* 18.3 (1950), pp. 365–375. ISSN: 0021-9606. DOI: 10.1063/1.1747632. URL: http://aip.scitation.org/doi/10.1063/1.1747632.

[75] Alan E. Reed, Robert B. Weinstock, and Frank Weinhold. "Natural population analysis". In: *The Journal of Chemical Physics* 83.2 (Mar. 1985), pp. 735–746. ISSN: 0021-9606. DOI: 10.1063/1.449486. URL: http://aip.scitation.org/doi/10.1063/1.449486.

[76] F. J. García-Vidal et al. *Density-functional approach to LCAO methods*. 1994. DOI: 10.1103/PhysRevB.50.10537.

[77] P. Pou et al. "Exchange correlation energy as a function of the orbital occupancies: Implementation on first principles local orbital methods". In: *International Journal of Quantum Chemistry* 91.2 SPEC (2003), pp. 151–156. ISSN: 00207608. DOI: 10.1002/qua.10432.

[78] Y. J. Dappe et al. "Local-orbital occupancy formulation of density functional theory: Application to Si, C, and graphene". In: *Physical Review B - Condensed Matter and Materials Physics* 73.23 (2006), pp. 1–12. ISSN: 10980121. DOI: 10.1103/PhysRevB.73.235124.

[79] Von H. Hellmann. "Einführung in die Quantenchemie". In: *Angewandte Chemie* 54.11-12 (Mar. 1941), pp. 156–156. ISSN: 00448249. DOI: 10.1002/ange.19410541109. URL: http://doi.wiley.com/10.1002/ange.19410541109.

[80] R. P. Feynman. "Forces in Molecules". In: *Physical Review* 56.4 (Aug. 1939), pp. 340–343. ISSN: 0031-899X. DOI: 10.1103/PhysRev.56.340. URL: https://link.aps.org/doi/10.1103/PhysRev.56.340.

[81] P. Pulay. "Ab initio calculation of force constants and equilibrium geometries in polyatomic molecules". In: *Molecular Physics* 17.2 (1969), pp. 197–204.

[82] Loup Verlet. "Computer "Experiments" on Classical Fluids. I. Thermodynamical Properties of Lennard-Jones Molecules". In: *Physical Review* 159.1 (Mar. 1967), pp. 98–103. ISSN: 0031-899X. DOI: 10.1103/PhysRev.159.98. URL: https://link.aps.org/doi/10.1103/PhysRev.159.98.

[83] Xiaocheng Shang and Martin Kröger. "Time Correlation Functions of Equilibrium and Nonequilibrium Langevin Dynamics: Derivations and Numerics Using Random Numbers". In: *SIAM Review* 62.4 (Mar. 2020), pp. 901–935. ISSN: 0036-1445. DOI: 10.1137/19M1255471. URL: https://epubs.siam.org/doi/10.1137/19M1255471.

[84] Don S. Lemons and Anthony Gythiel. "Paul Langevin's 1908 paper "On the Theory of Brownian Motion" ["Sur la théorie du mouvement brownien," C. R. Acad. Sci. (Paris) 146 , 530–533 (1908)]". In: *American Journal of Physics* 65.11 (Mar. 1997), pp. 1079–1081. ISSN: 0002-9505. DOI: 10.1119/1.18725. URL: http://aapt.scitation.org/doi/10.1119/1.18725.

[85] Giovanni Bussi and Michele Parrinello. "Stochastic thermostats: comparison of local and global schemes". In: *Computer Physics Communications* 179.1-3 (Mar. 2008), pp. 26–29. ISSN: 00104655. DOI: 10.1016/j.cpc.2008.01.006. URL: https://linkinghub.elsevier.com/retrieve/pii/S0010465508000106.

[86] Robert Zwanzig. "Memory Effects in Irreversible Thermodynamics". In: *Physical Review* 124.4 (Mar. 1961), pp. 983–992. ISSN: 0031-899X. DOI: 10.1103/PhysRev.124.983. URL: https://link.aps.org/doi/10.1103/PhysRev.124.983.

[87] G.M. Torrie and J.P. Valleau. "Nonphysical sampling distributions in Monte Carlo free-energy estimation: Umbrella sampling". In: *Journal of Computational Physics* 23.2 (Mar. 1977), pp. 187–199. ISSN: 00219991. DOI: 10.1016/0021-9991(77)90121-8. URL: https://linkinghub.elsevier.com/retrieve/pii/0021999177901218.

[88] Johannes Kästner and Walter Thiel. "Bridging the gap between thermodynamic integration and umbrella sampling provides a novel analysis method: "umbrella integration"". In: *Journal of Chemical Physics* 123.14 (2005). ISSN: 00219606. DOI: 10.1063/1.2052648.

[89] H. Müler-Krumbhaar and K. Binder. "Dynamic properties of the Monte Carlo method in statistical mechanics". In: *Journal of Statistical Physics* 8.1 (1973), pp. 1–24. ISSN: 0022-4715. DOI: 10.1007/BF01008440. URL: http://link.springer.com/10.1007/BF01008440.

[90] Alan Grossfield. *"WHAM: the weighted histogram analysis method", version 2.0.9.1, Http://membrane.urmc.rochester.edu/wordpress/?page_id=126*.

[91] C Jarzynski and S Lindquist. "A cytoplasmically inherited prionlike genetic element in yeast [comment]". In: *Mol Psychiatry* 56.5 (1996), pp. 5018–5035. ISSN: 13594184. DOI: 10.1103/PhysRevE.56.5018. arXiv: 9707325 [cond-mat].

[92] C. Jarzynski. "Nonequilibrium Equality for Free Energy Differences". In: *Physical Review Letters* 78.14 (Mar. 1997), pp. 2690–2693. ISSN: 0031-9007. DOI: 10.1103/PhysRevLett.78.2690. arXiv: 9707325 [cond-mat]. URL: https://link.aps.org/doi/10.1103/PhysRevLett.78.2690.

[93] C Jarzynski. "Equilibrium free-energy differences from nonequilibrium measurements: A master-equation approach". In: *Physical Review E* 56.5 (Mar. 1997), pp. 5018–5035. ISSN: 1063-651X. DOI: 10.1103/PhysRevE.56.5018. URL: https://link.aps.org/doi/10.1103/PhysRevE.56.5018.

[94] Daniel G. Trabada et al. "DFT molecular dynamics and free energy analysis of a charge density wave surface system". In: *Applied Surface Science* 479 (Mar. 2019), pp. 260–264. ISSN: 01694332. DOI: 10.1016/j.apsusc.2019.02.020. URL: https://linkinghub.elsevier.com/retrieve/pii/S0169433219303526.

[95] Hiroshi Ishikita and Keisuke Saito. "Proton transfer reactions and hydrogen-bond networks in protein environments". In: *Journal of the Royal Society Interface* 11.91 (2014). ISSN: 17425662. DOI: 10.1098/rsif.2013.0518.

[96] My Hang V. Huynh and Thomas J. Meyer. "Proton-Coupled Electron Transfer". In: *Chemical Reviews* 107.11 (2007), pp. 5004–5064. ISSN: 0009-2665. DOI: 10.1021/cr0500030. URL: https://pubs.acs.org/doi/10.1021/cr0500030.

[97] Wei Wang et al. "Intramolecular electron-induced proton transfer and its correlation with excited-state intramolecular proton transfer". In: *Nature Communications* 10.1 (2019), p. 1170. ISSN: 2041-1723. DOI: 10.1038/s41467-019-09154-5. URL: http://www.nature.com/articles/s41467-019-09154-5.

[98] Bradley J. Siwick and Huib J. Bakker. "On the Role of Water in Intermolecular Proton-Transfer Reactions". In: *Journal of the American Chemical Society* 129.44 (Nov. 2007), pp. 13412–13420. ISSN: 0002-7863. DOI: 10.1021/ja069265p. URL: https://pubs.acs.org/doi/10.1021/ja069265p.

[99] Patricia Saura and Ville R. I. Kaila. "Energetics and Dynamics of Proton-Coupled Electron Transfer in the NADH/FMN Site of Respiratory Complex I". In: *Journal of the American Chemical Society* 141.14 (Apr. 2019), pp. 5710–5719. ISSN: 0002-7863. DOI: 10.1021/jacs.8b11059. URL: https://pubs.acs.org/doi/10.1021/jacs.8b11059.

[100] Hiroshi Ishikita and Keisuke Saito. "Proton transfer reactions and hydrogen-bond networks in protein environments". In: *Journal of The Royal Society Interface* 11.91 (Feb. 2014), p. 20130518. ISSN: 1742-5689. DOI: 10.1098/rsif.2013.0518. URL: https://royalsocietypublishing.org/doi/10.1098/rsif.2013.0518.

[101] Oleg Kostko et al. "Proton transfer in acetaldehyde–water clusters mediated by a single water molecule". In: *Physical Chemistry Chemical Physics* 18.36 (2016), pp. 25569–25573. ISSN: 1463-9076. DOI: 10.1039/C6CP04916H. URL: http://xlink.rsc.org/?DOI=C6CP04916H.

[102] Charoensak Lao-ngam et al. "Proton transfer reactions and dynamics in protonated water clusters". In: *Physical Chemistry Chemical Physics* 13.10 (2011), p. 4562. ISSN: 1463-9076. DOI: 10.1039/c0cp02068k. URL: http://xlink.rsc.org/?DOI=c0cp02068k.

[103] J. D. Watson and F. H. Crick. "Genetical Implications of the Structure of DNA". In: *Nature* 171 (1953), pp. 964–967.

[104] Per-Olov Löwdin. "Proton Tunneling in DNA and its biological implications". In: *Reviews of Modern Physics* 35.3 (1963), pp. 1034–1042.

[105] Jesús Ignacio Mendieta-Moreno et al. "Quantum Mechanics/Molecular Mechanics Free Energy Maps and Nonadiabatic Simulations for a Photochemical Reaction in DNA: Cyclobutane Thymine Dimer". In: *The Journal of Physical Chemistry Letters* 7.21 (Mar. 2016), pp. 4391–4397. ISSN: 1948-7185. DOI: 10.1021/acs.jpclett.6b02168. URL: http://www.ncbi.nlm.nih.gov/pubmed/27768300http://pubs.acs.org/doi/abs/10.1021/acs.jpclett.6b02168http://pubs.acs.org/doi/10.1021/acs.jpclett.6b02168.

[106] J. Florian and J. Leszczynski. "Spontaneous DNA mutations induced by proton transfer in the guanine.cytosine base pairs: An energetic perspective". In: *Journal of the American Chemical Society* 118.12 (1996), pp. 3010–3017. ISSN: 00027863. DOI: 10.1021/ja951983g.

[107] Vincent Zoete and Markus Meuwly. "Double proton transfer in the isolated and DMA-embedded guanine-cytosine base pair". In: *Journal of Chemical Physics* 121.9 (2004), pp. 4377–4388. ISSN: 00219606. DOI: 10.1063/1.1774152.

[108] Leonid Gorb and Jerzy Leszczynski. "Intramolecular Proton Transfer in Mono- and Dihydrated Tautomers of Guanine: An ab Initio Post Hartree-Fock Study". In: *Journal of the American Chemical Society* 120.20 (Mar. 1998), pp. 5024–5032. ISSN: 0002-7863. DOI: 10.1021/ja972017w. URL: https://pubs.acs.org/doi/10.1021/ja972017w.

[109] L Gorb, Y Podolyan, and J Leszczynski. "A theoretical investigation of tautomeric equilibria and proton transfer in isolated and monohydrated cytosine and isocytosine molecules". In: *Journal of Molecular Structure: THEOCHEM* 487.1-2 (Mar. 1999), pp. 47–55. ISSN: 01661280. DOI: 10.1016/S0166-1280(99)00139-6. URL: https://linkinghub.elsevier.com/retrieve/pii/S0166128099001396.

[110] Leonid Gorb et al. "Double-Proton Transfer in Adenine-Thymine and Guanine-Cytosine Base Pairs. A Post-Hartree-Fock ab Initio Study". In: *Journal of the American Chemical Society* 126.32 (Mar. 2004), pp. 10119–10129. ISSN: 0002-7863. DOI: 10.1021/ja049155n. URL: https://pubs.acs.org/doi/10.1021/ja049155n.

[111] Giovanni Villani. "Theoretical investigation of hydrogen transfer mechanism in the adenine-thymine base pair". In: *Chemical Physics* 316.1-3 (2005), pp. 1–8. ISSN: 03010104. DOI: 10.1016/j.chemphys.2005.04.030.

[112] Giovanni Villani. "Theoretical investigation of hydrogen transfer mechanism in the guanine-cytosine base pair". In: *Chemical Physics* 324.2-3 (2006), pp. 438–446. ISSN: 03010104. DOI: 10.1016/j.chemphys.2005.11.006.

[113] J. P. Cerón-Carrasco et al. "Intermolecular Proton Transfer in Microhydrated Guanine-Cytosine Base Pairs: a New Mechanism for Spontaneous Mutation in DNA". In: *The Journal of Physical Chemistry A* 113.39 (Mar. 2009), pp. 10549–10556. ISSN: 1089-5639. DOI: 10.1021/jp906551f. URL: https://pubs.acs.org/doi/10.1021/jp906551f.

[114] Giovanni Villani. "Theoretical investigation of hydrogen atom transfer in the adenine–thymine base pair and its coupling with the electronic rearrangement. Concerted vs. stepwise mechanism". In: *Journal of Physical Chemistry B* 114.29 (Mar. 2010), p. 2664. ISSN: 15205207. DOI: 10.1021/jp102457s. URL: https://pubs.acs.org/doi/10.1021/jp102457shttp://xlink.rsc.org/?DOI=b917672a.

[115] Giovanni Villani. "Theoretical investigation of the hydrogen atom transfer in the hydrated A-T base pair". In: *Chemical Physics* 394.1 (2012), pp. 9–16. ISSN: 03010104. DOI: 10.1016/j.chemphys.2011.11.037. URL: http://dx.doi.org/10.1016/j.chemphys.2011.11.037.

[116] Shiyan Xiao et al. "Theoretical investigation of the proton transfer mechanism in guanine- cytosine and adenine-thymine base pairs". In: *Journal of Chemical Physics* 137.19 (2012), pp. 1–8. DOI: 10.1063/1.4766319.

[117] Giovanni Villani. "Theoretical investigation of hydrogen atom transfer in the hydrated C–G base pair". In: *Molecular Physics* 111.2 (Mar. 2013), pp. 201–214. ISSN: 0026-8976. DOI: 10.1080/00268976.2012.715693. URL: http://www.tandfonline.com/loi/tmph20{\%}5Cnhttp://dx.doi.org/10.1080/00268976.2012.715693{\%}5Cnhttp://www.tandfonline.com/page/terms-and-conditionshttp://www.tandfonline.com/doi/abs/10.1080/00268976.2012.715693.

[118] Giovanni Villani. "Coupling between hydrogen atoms transfer and stacking interaction in adenine-thymine/guanine-cytosine complexes: A theoretical study". In: *Journal of Physical Chemistry B* 118.20 (2014), pp. 5439–5452. ISSN: 15205207. DOI: 10.1021/jp502792r.

[119] Denis Jacquemin et al. "Assessing the Importance of Proton Transfer Reactions in {DNA}". In: *Accounts of Chemical Research* 47 (2014), pp. 2467–2474.

[120] Santiago Tolosa, Jorge Antonio Sansón, and Antonio Hidalgo. "Theoretical thermodynamic study of the adenine–thymine tautomeric equilibrium: Electronic structure calculations and steered molecular dynamic simulations". In: *International Journal of Quantum Chemistry* 117.20 (2017), pp. 1–9. ISSN: 1097461X. DOI: 10.1002/qua.25429.

[121] Eduardo E. Romero and Florencio E. Hernandez. "Solvent effect on the intermolecular proton transfer of the Watson and Crick guanine-cytosine and adenine-thymine base pairs: A polarizable continuum model study". In: *Physical Chemistry Chemical Physics* 20.2 (2018), pp. 1198–1209. ISSN: 14639076. DOI: 10.1039/c7cp05356h.

[122] S. Tolosa, J. A. Sansón, and A. Hidalgo. "Mechanisms for guanine–cytosine tautomeric equilibrium in solution via steered molecular dynamic simulations". In: *Journal of Molecular Liquids* 251 (2018), pp. 308–316. ISSN: 01677322. DOI: 10.1016/j.molliq.2017.12.091. URL: https://doi.org/10.1016/j.molliq.2017.12.091.

[123] Henry Eyring. "The Activated Complex in Chemical Reactions". In: *The Journal of Chemical Physics* 3.2 (1935), pp. 107–115. ISSN: 0021-9606. DOI: 10.1063/1.1749604. URL: http://aip.scitation.org/doi/10.1063/1.1749604.

[124] José P. Cerón-Carrasco and Denis Jacquemin. "DNA spontaneous mutation and its role in the evolution of GC-content: assessing the impact of the genetic sequence". In: *Physical Chemistry Chemical Physics* 17.12 (2015), pp. 7754–7760. ISSN: 1463-9076. DOI: 10.1039/C4CP05806B. URL: http://xlink.rsc.org/?DOI=C4CP05806B.

[125] Alejandro Pérez et al. "Enol tautomers of Watson-Crick base pair models are metastable because of nuclear quantum effects". In: *Journal of the American Chemical Society* 132.33 (2010), pp. 11510–11515. ISSN: 00027863. DOI: 10.1021/ja102004b.

[126] Masashi Daido, Yukio Kawashima, and Masanori Tachikawa. "Nuclear quantum effect and temperature dependency on the hydrogen-bonded structure of base pairs". In: *Journal of Computational Chemistry* 34.28 (2013), pp. 2403–2411. ISSN: 01928651. DOI: 10.1002/jcc.23399.

[127] Thomas E. Markland and Michele Ceriotti. "Nuclear quantum effects enter the mainstream". In: *Nature Reviews Chemistry* 2.3 (Mar. 2018), p. 0109. ISSN: 2397-3358. DOI: 10.1038/s41570-017-0109. arXiv: 1803.01037. URL: http://arxiv.org/abs/1803.01037{\%}0Ahttp://dx.doi.org/10.1038/s41570-017-0109http://www.nature.com/articles/s41570-017-0109.

[128] Dominik Marx and Michele Parrinello. "Ab initio path integral molecular dynamics: Basic ideas". In: *Journal of Chemical Physics* 104.11 (1996), pp. 4077–4082. ISSN: 00219606. DOI: 10.1063/1.471221.

[129] A. D. Godbeer, J. S. Al-Khalili, and P. D. Stevenson. "Modelling proton tunnelling in the adenine–thymine base pair". In: *Physical Chemistry Chemical Physics* 17 (2015), pp. 13034–13044. ISSN: 1463-9076. DOI: 10.1039/C5CP00472A. URL: http://xlink.rsc.org/?DOI=C5CP00472A.

[130] Gerrit Groenhof et al. "Ultrafast deactivation of an excited cytosine-guanine base pair in DNA". In: *Journal of the American Chemical Society* 129.21 (2007), pp. 6812–6819. ISSN: 00027863. DOI: 10.1021/ja069176c.

[131] Hsing-Yin Chen, Chai-Lin Kao, and Sodio C. N. Hsu. "Proton Transfer in Guanine-Cytosine Radical Anion Embedded in B-Form DNA". In: *Journal of the American Chemical Society* 131.43 (Mar. 2009), pp. 15930–15938. ISSN: 0002-7863. DOI: 10.1021/ja906899p. URL: https://pubs.acs.org/doi/10.1021/jz100214hhttps://pubs.acs.org/doi/10.1021/ja906899p.

[132] Dominik B. Bucher et al. "Watson-Crick Base Pairing Controls Excited - State Decay in Natural DNA". In: *Angewandte Chemie - International Edition* 53.42 (2014), pp. 11366–11369. ISSN: 15213773. DOI: 10.1002/anie.201406286.

[133] Yuyuan Zhang et al. "UV-Induced Proton Transfer between DNA Strands". In: *Journal of the American Chemical Society* 137.22 (2015), pp. 7059–7062. ISSN: 15205126. DOI: 10.1021/jacs.5b03914.

[134] Colin Kinz-Thompson and Esther Conwell. "Proton Transfer in Adenine-Thymine Radical Cation Embedded in B-Form DNA". In: *The Journal of Physical Chemistry Letters* 1.9 (Mar. 2010), pp. 1403–1407. ISSN: 1948-7185. DOI: 10.1021/jz100214h. URL: https://pubs.acs.org/doi/10.1021/jz100214h.

[135] Yuyuan Zhang et al. "Excited-State Dynamics of DNA Duplexes with Different H-Bonding Motifs". In: *Journal of Physical Chemistry Letters* 7.6 (2016), pp. 950–954. ISSN: 19487185. DOI: 10.1021/acs.jpclett.6b00074.

[136] Vicenta Sauri et al. "Proton/hydrogen transfer mechanisms in the guanine-cytosine base pair: Photostability and tautomerism". In: *Journal of Chemical Theory and Computation* 9.1 (2013), pp. 481–496. ISSN: 15499618. DOI: 10.1021/ct3006166.

[137] Stefan Grimme et al. "A consistent and accurate ab initio parametrization of density functional dispersion correction (DFT-D) for the 94 elements H-Pu". In: *Journal of Chemical Physics* 132.15 (2010). ISSN: 00219606. DOI: 10.1063/1.3382344.

[138] Lars Goerigk and Stefan Grimme. "A thorough benchmark of density functional methods for general main group thermochemistry, kinetics, and noncovalent interactions". In: *Physical Chemistry Chemical Physics* 13.14 (2011), pp. 6670–6688. ISSN: 14639076. DOI: 10.1039/c0cp02984j.

[139] Michele Di Pierro, Ron Elber, and Benedict Leimkuhler. "A Stochastic Algorithm for the Isobaric–Isothermal Ensemble with Ewald Summations for All Long Range Forces". In: *Journal of Chemical Theory and Computation* 11.12 (Mar. 2015), pp. 5624–5637. ISSN: 1549-9618. DOI: 10.1021/acs.jctc.5b00648. URL: https://pubs.acs.org/doi/10.1021/acs.jctc.5b00648.

[140] A. Warshel and M. Levitt. "Theoretical studies of enzymic reactions: Dielectric, electrostatic and steric stabilization of the carbonium ion in the reaction of lysozyme". In: *Journal of Molecular Biology* 103.2 (Mar. 1976), pp. 227–249. ISSN: 00222836. DOI: 10.1016/0022-2836(76)90311-9. URL: https://linkinghub.elsevier.com/retrieve/pii/0022283676903119.

[141] Martin J. Field, Paul A. Bash, and Martin Karplus. "A combined quantum mechanical and molecular mechanical potential for molecular dynamics simulations". In: *Journal of Computational Chemistry* 11.6 (Mar. 1990), pp. 700–733. ISSN: 0192-8651. DOI: 10.1002/jcc.540110605. URL: http://doi.wiley.com/10.1002/jcc.540110605.

[142] Elizabeth Brunk and Ursula Rothlisberger. "Mixed Quantum Mechanical/Molecular Mechanical Molecular Dynamics Simulations of Biological Systems in Ground and Electronically Excited States". In: *Chemical Reviews* 115.12 (Mar. 2015), pp. 6217–6263. ISSN: 0009-2665. DOI: 10.1021/cr500628b. URL: https://pubs.acs.org/doi/10.1021/cr500628b.

[143] Meiyi Liu et al. "QM/MM through the 1990s: The First Twenty Years of Method Development and Applications". In: *Israel Journal of Chemistry* 54.8-9 (Mar. 2014), pp. 1250–1263. ISSN: 00212148. DOI: 10.1002/ijch.201400036. URL: http://doi.wiley.com/10.1002/ijch.201400036.

[144] Hai Lin and Donald G. Truhlar. "QM/MM: what have we learned, where are we, and where do we go from here?" In: *Theoretical Chemistry Accounts* 117.2 (Mar. 2007), pp. 185–199. ISSN: 1432-881X. DOI: 10.1007/s00214-006-0143-z. URL: http://link.springer.com/10.1007/s00214-006-0143-z.

[145] A. D. MacKerell et al. "All-Atom Empirical Potential for Molecular Modeling and Dynamics Studies of Proteins †". In: *The Journal of Physical Chemistry B* 102.18 (Mar. 1998), pp. 3586–3616. ISSN: 1520-6106. DOI: 10.1021/jp973084f. URL: https://pubs.acs.org/doi/10.1021/jp973084f.

[146] James A. Maier et al. "ff14SB: Improving the Accuracy of Protein Side Chain and Backbone Parameters from ff99SB". In: *Journal of Chemical Theory and Computation* 11.8 (Mar. 2015), pp. 3696–3713. ISSN: 1549-9618. DOI: 10.1021/acs.jctc.5b00255. URL: https://pubs.acs.org/doi/10.1021/acs.jctc.5b00255.

[147] David A. Case et al. "The Amber biomolecular simulation programs". In: *Journal of Computational Chemistry* 26.16 (Mar. 2005), pp. 1668–1688. ISSN: 0192-8651. DOI: 10.1002/jcc.20290. URL: http://doi.wiley.com/10.1002/jcc.20290.

[148] Jesús I. Mendieta-Moreno et al. "A Practical Quantum Mechanics Molecular Mechanics Method for the Dynamical Study of Reactions in Biomolecules". In: 2015, pp. 67–88. DOI: 10.1016/bs.apcsb.2015.06.003. URL: https://linkinghub.elsevier.com/retrieve/pii/S1876162315000346.

[149] Íñigo Marcos-Alcalde et al. "Two-step ATP-driven opening of cohesin head". In: *Scientific Reports* 7.1 (Mar. 2017), p. 3266. ISSN: 2045-2322. DOI: 10.1038/s41598-017-03118-9. URL: http://gateway.webofknowledge.com/gateway/Gateway.cgi?GWVersion=2{\&}SrcAuth=ORCID{\&}SrcApp=OrcidOrg{\&}DestLinkType=FullRecord{\&}DestApp=WOS{_}CPL{\&}KeyUT=WOS:000403081900057{\&}KeyUID=WOS:000403081900057http://www.nature.com/articles/s41598-017-03118-9.

[150] Diego Soler-Polo et al. "Proton Transfer in Guanine-Cytosine Base Pairs in B-DNA". In: *Journal of Chemical Theory and Computation* 15.12 (Mar. 2019), pp. 6984–6991. ISSN: 1549-9618. DOI: 10.1021/acs.jctc.9b00757. URL: https://pubs.acs.org/doi/10.1021/acs.jctc.9b00757.

[151] Orlando Acevedo and William L. Jorgensen. "Advances in Quantum and Molecular Mechanical (QM/MM) Simulations for Organic and Enzymatic Reactions". In: *Accounts of Chemical Research* 43.1 (Mar. 2010), pp. 142–151. ISSN: 0001-4842. DOI: 10.1021/ar900171c. URL: https://pubs.acs.org/doi/10.1021/ar900171c.

[152] Adam W. Duster and Hai Lin. "Tracking Proton Transfer through Titratable Amino Acid Side Chains in Adaptive QM/MM Simulations". In: *Journal of Chemical Theory and Computation* 15.11 (Mar. 2019), pp. 5794–5809. ISSN: 1549-9618. DOI: 10.1021/acs.jctc.9b00649. URL: https://pubs.acs.org/doi/10.1021/acs.jctc.9b00649.

[153] Hiroshi C. Watanabe and Qiang Cui. "Quantitative Analysis of QM/MM Boundary Artifacts and Correction in Adaptive QM/MM Simulations". In: *Journal of Chemical Theory and Computation* 15.7 (Mar. 2019), pp. 3917–3928. ISSN: 1549-9618. DOI: 10.1021/acs.jctc.9b00180. URL: https://pubs.acs.org/doi/10.1021/acs.jctc.9b00180.

[154] Federico A. Olivieri et al. "Conformational and Reaction Dynamic Coupling in Histidine Kinases: Insights from Hybrid QM/MM Simulations". In: *Journal of Chemical Information and Modeling* 60.2 (Mar. 2020), pp. 833–842. ISSN: 1549-9596. DOI: 10.1021/acs.jcim.9b00806. URL: https://pubs.acs.org/doi/10.1021/acs.jcim.9b00806.

[155] Prasanth B. Ganta, Oliver Kühn, and Ashour A. Ahmed. "QM/MM simulations of organic phosphorus adsorption at the diaspore–water interface". In: *Physical Chemistry Chemical Physics* 21.44 (2019), pp. 24316–24325. ISSN: 1463-9076. DOI: 10.1039/C9CP04032C. URL: http://xlink.rsc.org/?DOI=C9CP04032C.

[156] Jacek R. Gołębiowski et al. "Atomistic QM/MM simulations of the strength of covalent interfaces in carbon nanotube–polymer composites". In: *Physical Chemistry Chemical Physics* 22.21 (2020), pp. 12007–12014. ISSN: 1463-9076. DOI: 10.1039/D0CP01841D. URL: http://xlink.rsc.org/?DOI=D0CP01841D.

[157] Susanta Das, Kwangho Nam, and Dan Thomas Major. "Rapid Convergence of Energy and Free Energy Profiles with Quantum Mechanical Size in Quantum Mechanical-Molecular Mechanical Simulations of Proton Transfer in DNA". In: *Journal of Chemical Theory and Computation* 14.3 (2018), pp. 1695–1705. ISSN: 15499626. DOI: 10.1021/acs.jctc.7b00964.

[158] Heather J. Kulik et al. "How Large Should the QM Region Be in QM/MM Calculations? The Case of Catechol O -Methyltransferase". In: *The Journal of Physical Chemistry B* 120.44 (Mar. 2016), pp. 11381–11394. ISSN: 1520-6106. DOI: 10.1021/acs.jpcb.6b07814. URL: https://pubs.acs.org/doi/10.1021/acs.jpcb.6b07814.

[159] James A. Maier et al. "ff14SB: Improving the Accuracy of Protein Side Chain and Backbone Parameters from ff99SB". In: *Journal of Chemical Theory and Computation* 11.8 (2015), pp. 3696–3713. ISSN: 15499626. DOI: 10.1021/acs.jctc.5b00255.

[160] William L. Jorgensen et al. "Comparison of simple potential functions for simulating liquid water". In: *The Journal of Chemical Physics* 79.2 (1983), pp. 926–935. ISSN: 00219606. DOI: 10.1063/1.445869.

[161] David A Case et al. "The Amber biomolecular simulation programs". In: *Journal of Computational Chemistry* 26.16 (Mar. 2005), pp. 1668–1688. ISSN: 0192-8651. DOI: 10.1002/jcc.20290. URL: http://www.ncbi.nlm.nih.gov/pubmed/16200636{\%}0Ahttp://www.pubmedcentral.nih.gov/articlerender.fcgi?artid=PMC1989667http://doi.wiley.com/10.1002/jcc.20290.

[162] Shankar Kumar et al. "THE weighted histogram analysis method for free-energy calculations on biomolecules. I. The method". In: *Journal of Computational Chemistry* 13.8 (Mar. 1992), pp. 1011–1021. ISSN: 0192-8651. DOI: 10.1002/jcc.540130812. URL: http://doi.wiley.com/10.1002/jcc.540130812.

[163] Rosenblatt Murray. "Remarks on Some Nonparametric Estimates of a Density Function". In: *The Annals of Mathematical Statistics* Volume 27 (1956), pp. 832–837. ISSN: 0003-4851. DOI: 10.1214/aoms/1177728190.

[164] B. Schiott et al. "On the electronic nature of low-barrier hydrogen bonds in enzymatic reactions". In: *Proceedings of the National Academy of Sciences* 95.22 (Mar. 1998), pp. 12799–12802. ISSN: 0027-8424. DOI: 10.1073/pnas.95.22.12799. URL: http://www.pnas.org/cgi/doi/10.1073/pnas.95.22.12799.

[165] W Wallace Cleland, Perry A Frey, and John A Gerlt. "The Low Barrier Hydrogen Bond in Enzymatic Catalysis". In: *Journal of Biological Chemistry* 273.40 (Mar. 1998), pp. 25529–25532. ISSN: 0021-9258. DOI: 10.1074/jbc.273.40.25529. URL: http://www.jbc.org/lookup/doi/10.1074/jbc.273.40.25529.

[166] S. C. Choi. "Tests of equality of dependent correlation coefficients". In: *Biometrika* 64.3 (1977), pp. 645–647. ISSN: 0006-3444. DOI: 10.1093/biomet/64.3.645. URL: https://academic.oup.com/biomet/article-lookup/doi/10.1093/biomet/64.3.645.

[167] E. C. Fieller, H. O. Hartley, and E. S. Pearson. "Tests for Rank Correlation Coefficients. I". In: *Biometrika* 44.3-4 (Dec. 1957), pp. 470–481. ISSN: 0006-3444. DOI: 10.1093/biomet/44.3-4.470. URL: https://academic.oup.com/biomet/article-lookup/doi/10.1093/biomet/44.3-4.470.

[168] Gábor J. Székely, Maria L. Rizzo, and Nail K. Bakirov. "Measuring and testing dependence by correlation of distances". In: *The Annals of Statistics* 35.6 (Dec. 2007), pp. 2769–2794. ISSN: 0090-5364. DOI: 10.1214/009053607000000505. URL: https://projecteuclid.org/euclid.aos/1201012979.

[169] Vladimir I Anisimov, F Aryasetiawan, and A I Lichtenstein. "First-principles calculations of the electronic structure and spectra of strongly correlated systems: theLDAUmethod". In: *Journal of Physics: Condensed Matter* 9.4 (Jan. 1997), pp. 767–808. DOI: 10.1088/0953-8984/9/4/002. URL: https://doi.org/10.1088%2F0953-8984%2F9%2F4%2F002.

[170] Yongmin Bi et al. "Understanding the incorporating effect of Co2+/Co3+ in NiFe-layered double hydroxide for electrocatalytic oxygen evolution reaction". In: *Journal of Catalysis* 358 (June 2018), pp. 100–107. ISSN: 00219517. DOI: 10.1016/j.jcat.2017.11.028. URL: https://linkinghub.elsevier.com/retrieve/pii/S002195171730427X.

[171] Mohammed M. Obeid et al. "Unraveling the effect of Gd doping on the structural, optical, and magnetic properties of ZnO based diluted magnetic semiconductor nanorods". In: *RSC Advances* 9.57 (2019), pp. 33207–33221. ISSN: 2046-2069. DOI: 10.1039/C9RA04750F. URL: http://xlink.rsc.org/?DOI=C9RA04750F.

[172] Kalapu Chakrapani et al. "The Role of Composition of Uniform and Highly Dispersed Cobalt Vanadium Iron Spinel Nanocrystals for Oxygen Electrocatalysis". In: *ACS Catalysis* 8.2 (June 2018), pp. 1259–1267. ISSN: 2155-5435. DOI: 10.1021/acscatal.7b03529. URL: https://pubs.acs.org/doi/10.1021/acscatal.7b03529.

[173] Giancarlo Trimarchi, Zhi Wang, and Alex Zunger. "Polymorphous band structure model of gapping in the antiferromagnetic and paramagnetic phases of the Mott insulators MnO, FeO, CoO, and NiO". In: *Physical Review B* 97.3 (Jan. 2018), p. 035107. ISSN: 2469-9950. DOI: 10.1103/PhysRevB.97.035107. URL: https://link.aps.org/doi/10.1103/PhysRevB.97.035107.

[174] Selma Mayda et al. "Magnetic mechanism for the biological functioning of hemoglobin". In: *Scientific Reports* 10.1 (2020), pp. 1–7. ISSN: 20452322. DOI: 10.1038/s41598-020-64364-y. arXiv: 1911.05442. URL: http://dx.doi.org/10.1038/s41598-020-64364-y.

[175] Damián A. Scherlis et al. "Simulation of Heme Using DFT + U: A Step toward Accurate Spin-State Energetics". In: *The Journal of Physical Chemistry B* 111.25 (2007), pp. 7384–7391. ISSN: 1520-6106. DOI: 10.1021/jp0705491.

[176] Nicolas Tancogne-Dejean and Angel Rubio. "Parameter-free hybridlike functional based on an extended Hubbard model: <math> <mrow> <mi>DFT</mi> <mo>+</mo> <mi>U</mi> <mo>+</mo> <mi>V</mi> </mrow> </math>". In: *Physical Review B* 102.15 (June 2020), p. 155117. ISSN: 2469-9950. DOI: 10.1103/PhysRevB.102.155117. URL: https://link.aps.org/doi/10.1103/PhysRevB.102.155117.

[177] Edward B. Linscott et al. "Role of spin in the calculation of Hubbard U and Hund's J parameters from first principles". In: *Physical Review B* 98.23 (June 2018), p. 235157. ISSN: 2469-9950. DOI: 10.1103/PhysRevB.98.235157. URL: https://link.aps.org/doi/10.1103/PhysRevB.98.235157.

[178] Samara Keshavarz et al. "Electronic structure, magnetism, and exchange integrals in transition-metal oxides: Role of the spin polarization of the functional in DFT+ <math> <mi>U</mi> </math> calculations". In: *Physical Review B* 97.18 (June 2018), p. 184404. ISSN: 2469-9950. DOI: 10.1103/PhysRevB.97.184404. URL: https://link.aps.org/doi/10.1103/PhysRevB.97.184404.

[179] Junjiro Kanamori. "Electron Correlation and Ferromagnetism of Transition Metals". In: *Progress of Theoretical Physics* 30.3 (1963), pp. 275–289. ISSN: 0033-068X. DOI: 10.1143/ptp.30.275.

[180] Antoine Georges, Luca De Medici, and Jernej Mravlje. "Strong correlations from hund's coupling". In: *Annual Review of Condensed Matter Physics* 4.1 (2013), pp. 137–178. ISSN: 19475454. DOI: 10.1146/annurev-conmatphys-020911-125045. arXiv: arXiv:1207.3033v2.

[181] I. V. Solovyev, P. H. Dederichs, and V. I. Anisimov. "Corrected atomic limit in the local-density approximation and the electronic structure of d impurities in Rb". In: *Physical Review B* 50.23 (Mar. 1994), pp. 16861–16871. ISSN: 0163-1829. DOI: 10.1103/PhysRevB.50.16861. URL: https://link.aps.org/doi/10.1103/PhysRevB.50.16861.

[182] Matteo Cococcioni. "Accurate and efficient calculations on strongly correlated minerals with the LDA+U method: Review and perspectives". In: *Theoretical and Computational Methods in Mineral Physics: Geophysical Applications* 71 (2018), pp. 147–168. ISSN: 15296466. DOI: 10.2138/rmg.2010.71.8.

[183] A. I. Liechtenstein, V. I. Anisimov, and J. Zaanen. "Density-functional theory and strong interactions: Orbital ordering in Mott-Hubbard insulators". In: *Physical Review B* 52.8 (Mar. 1995), R5467–R5470. ISSN: 0163-1829. DOI: 10.1103/PhysRevB.52.R5467. URL: https://link.aps.org/doi/10.1103/PhysRevB.52.R5467.

[184] V. I. Anisimov and O. Gunnarsson. "Density-functional calculation of effective Coulomb interactions in metals". In: *Physical Review B* 43.10 (1991), pp. 7570–7574. ISSN: 01631829. DOI: 10.1103/PhysRevB.43.7570.

[185] C. Rödl et al. "Quasiparticle band structures of the antiferromagnetic transition-metal oxides MnO, FeO, CoO, and NiO". In: *Physical Review B - Condensed Matter and Materials Physics* 79.23 (2009), pp. 1–8. ISSN: 10980121. DOI: 10.1103/PhysRevB.79.235114.

[186] D. Desjonqueres; C. Spanjaard. "Electronic Theory of Chemisorption". In: *Interaction of Atoms and Molecules with Solid Surfaces*. Ed. by V. Bortolani et al. Springer-Verlag, 1990. Chap. Electronic, pp. 255–323. DOI: 10.1103/PhysRevB.86.165105.

[187] Pablo Pou et al. "Electron correlation effects and ferromagnetism in iron". In: *Journal of Physics Condensed Matter* 14.23 (2002). ISSN: 09538984. DOI: 10.1088/0953-8984/14/23/103. arXiv: 0112038 [cond-mat].

[188] Dimitris A. Papaconstantopoulos. *Handbook of the Band Structure of Elemental Solids*. 2015, pp. 1–37. ISBN: 9781441982636. DOI: 10.1007/978-1-4419-8264-3_1.

[189] Eleftherios N. Economou. *Green's Functions in Quantum Physics*. Springer Series in Solid-State Sciences, 2006. DOI: 10.1017/CBO9780511805769.

[190] R. P. Feynman. "The Theory of Positrons". In: *Physical Review* 76.6 (Sept. 1949), pp. 749–759. ISSN: 0031-899X. DOI: 10.1103/PhysRev.76.749. URL: https://link.aps.org/doi/10.1103/PhysRev.76.749.

[191] A.A. Abrikosov. *Methods of Quantum Field Theory in Statistical Physics*. Dover, 2004. DOI: 10.1017/CBO9780511805769.

[192] A. Martin-Rodero et al. "A new solution to the Anderson-Newns Hamiltonian of chemisorption". In: *Solid State Communications* 44.6 (1982), pp. 911–914. ISSN: 0038-1098. DOI: https://doi.org/10.1016/0038-1098(82)90303-9. URL: http://www.sciencedirect.com/science/article/pii/0038109882903039.

[193] M. Baldo et al. "Simple solution to the Newns-Anderson Hamiltonian of chemisorption". In: *Phys. Rev. B* 28 (12 Dec. 1983), pp. 6640–6646. DOI: 10.1103/PhysRevB.28.6640. URL: https://link.aps.org/doi/10.1103/PhysRevB.28.6640.

[194] P. Pou et al. "Local-density approach and quasiparticle levels for generalized Hubbard Hamiltonians". In: *Physical Review B - Condensed Matter and Materials Physics* 62.7 (2000), pp. 4309–4331. ISSN: 1550235X. DOI: 10.1103/PhysRevB.62.4309.